DOE/ER/61029--2

DE91 004085

FIELD EVALUATION AND HEALTH ASSESSMENT OF AIR CLEANERS IN REMOVING RADON DECAY PRODUCTS IN DOMESTIC ENVIRONMENTS

CHIH-SHAN LI

B.S., National Taiwan University, 1985
M.S., National Taiwan University, 1987

THESIS

Submitted in partial fulfillment of the requirements
for the degree of Doctor of Philosophy in
Environmental Engineering in Civil Engineering
in the Graduate College of the
University of Illinois at Urbana-Champaign, 1990

ABSTRACT

FIELD EVALUATION AND HEALTH ASSESSMENT OF AIR CLEANERS IN REMOVING RADON DECAY PRODUCTS IN DOMESTIC ENVIRONMENTS

Chih-Shan Li, Ph.D.
Department of Civil Engineering
University of Illinois at Urbana-Champaign, 1990
Philip K. Hopke, Advisor

The United States Environmental Protection Agency suggested in 1988 that the possibility for high radon concentration exits in some houses. The inhalation and deposition of radon decay products in human lungs are recognized as producing a significant health risk. Air cleaners are one of the mitigative methods that remove radon decay products rather than radon itself. Currently, there are still uncertainties about the health benefit of air cleaners. Therefore, a better understanding of how air cleaners influence the behavior of radon decay products is needed.

In this study, field evaluations of two types of air cleaners were conducted in three single-family houses. The measurements included radon concentration, particle number concentration, and concentration and size distribution of radon decay products. The influence on the behavior of radon decay products by various indoor particles both with and without the air cleaning systems was investigated. A room model was used to calculate the changes in the aerosol parameters caused by the operation of the air cleaners. Using the James dosimetric models (1989 and 1990), the changes in the hourly bronchial dose rate per Bq m^{-3} radon for men, women, and children can be estimated for various domestic environments.

The size distribution of radon decay products was bimodal under typical conditions. With particles produced from candle burning and vacuuming, an increase (20%) in the activity of radon decay products in the 1.5 - 50 nm size range was observed. Aerosols generated from cigarette smoldering and cooking are larger particles which shifted most of radon decay products to the "attached" mode. With the air filtration system operating, the size distribution of radon decay products has a major mode in the "unattached" fraction. During the particle generation period, the changes in the size distribution of radon decay products both with and without the air cleaners were very similar, with respect to the ^{218}Po "unattached" fraction and the size range of the "attached" mode.

The reductions in PAEC per Bq m^{-3} radon varied from 30% to 85% with the air filtration

system and 25% - 40% with the electronic air cleaner in use. The reductions in the hourly dose rate per Bq m^{-3} radon varied from 20% to 50% with the air filtration system and 10% to 25% for the electronic air cleaner. Both air cleaners, in a few cases, did increase the hourly dose rate. From this study, it is suggested that the air filtration system can be used when radon concentration is below 666 Bq m^{-3} in the house. If radon concentration is below 450 Bq m^{-3} indoors, the electronic air cleaner is recommended for use to reduce the radon risk.

ACKNOWLEDGMENTS

I would like to express my sincerest gratitude to my thesis advisor, Dr. Philip K. Hopke, for his support throughout my doctoral research. His scientific insights, guidance, encouragement toward research have been so profound to me in the course of this study.

I thank Drs. Shao-Lee Soo, Mark Rood, Susan Larson, Sheldon Landsberger, my thesis committee, for their time and helpful comments and suggestions. I would like to express my appreciation to K. Gadsby, Richard Gafgen, Cathy Reynold, Drs. A. Cavallo, and R. Socolow of the Center for Energy and Environmental Studies at Princeton University, Dr. Keng Tu of the Environmental Measurement Laboratory of the U.S. Department of Energy, Dr. Richard Roth of Amway Corporation, Dr. B. Leaderer of School of Medicine at Yale University for their help during my field measurements, and my dear friends Steve and Helen Chen for permitting me to perform field evaluations in their lovely home. I gratefully acknowledge the support by the New Jersey Department of Environmental Protection through contract J89-62 and by the U.S. Department of Energy through Grant No. DE FG02 89ER60876.

A special recognition goes to all the members of the Hopke group at the University of Illinois and Clarkson University whom I worked with, especially Dr. Mukund Ramamurthi for his great help. I also want to thank my American friend, John Barley at the University of Illinois for his great friendship and help in improving my English and understanding American society.

To my parents, younger sister, and youngest brother, I would like to express my deepest appreciation for their faith and encouragement through the years. I am really lucky to have a great family. Finally, I am extremely grateful to my wonderful husband, Rong-Hwa. He sacrificed his former position in Switzerland to come here as my best companion. He helped me out in every field measurement and always encourages me to do the best.

Praise God. You crown the year with your bounty, and your carts overflow with abundance.

TABLE OF CONTENTS

LIST OF TABLES

LIST OF FIGURES

ABBREVIATIONS

ach	air change per hour
AECB	Atomic Energy Control Board of Canada
AMAD	activity median aerodynamic diameter
AMD	activity median diameter
AMDD	activity median diffusion diameter
ASC-GSA	automatic semi-continuous-Graded Screen Array
Bq	becquerel
Bq m^{-3}	becquerels per cubic meter
BEIR	Biological Effects of Ionizing Radiations
^{214}Bi	bismuth-214
CEES	Center for Environmental and Energy Studies
Ci	curie
CNC	condensation nucleus counter
CRM	continuous radon monitor
DB	diffusion battery
DOP	dioctyl phthalate
EPA	Environmental Protection Agency
EML	Environmental Measurement Laboratory
ESP	electrostatic precipitatior
F	equilibrium factor
fp	"unattached" fraction
Gy	Gray
HEPA	high efficiency particulate air
HP	Harley-Pasternack
JB	James-Birchall
JE	Jacobi-Eisfeld
lcd	lung cancer deaths
ICRP	International Commission on Radiological Protection
OECD	Organization for Economic Cooperation and Development
^{214}Pb	lead-214
NCRP	National Council on Radiological Protection
pCi	picocurie
pCi/l	picocuries per liter
^{218}Po	polonium-218
PAEC	Potential Alpha Energy Concentration
RRDM	Residual Radon Daughter Monitor
Sv	Sivert
WL	Working Level
WLM	Working Level Month

CHAPTER 1
INTRODUCTION

The United States Federal officials issued a national health advisory on radon in September 1988. It suggested for the first time that every house in the United States be tested for this radioactive gas. Screening surveys by the Environmental Protection Agency (EPA) suggested that high levels of indoor radon might be more widespread than had been previously thought (EPA, 1988). The EPA screening surveys entailed sampling the air in more than 20,000 homes in seventeen states including ten states in 1987, and seven states in 1988 (EPA, 1988). More than 25 percent of the homes tested were found to have radon levels above 148 Bq m^{-3} (EPA guideline, 1986). More than 45 percent of the houses tested in Minnesota and 60 percent tested in North Dakota were found to have screening levels over 148 Bq m^{-3}. There are still some controversies about the interpretation of these measurements and the suggested guidance level for remediation. However, the results of the screening survey did indicate the possibility of high enough radon concentrations in some houses to represent a significant public health threat.

Radon-222, an inert gas, belongs to the U-238 series of natural radionuclide that decays to stable Pb-206 through 8 alpha-ray and 6 beta-ray transitions. The Rn-222 decay chain is shown in Figure 1. The first four radon decay products, polonium-218 (^{218}Po, RaA), lead-214 (^{214}Pb, RaB), bismuth-214 (^{214}Bi, RaC), and polonium-214 (^{214}Po, RaC'), are referred as the short-lived radon decay products because each has a half-life less than 30 minutes. Lead-210 with a half-life of 22.3 years is the effective end decay product of the radon series. Its low specific activity effectively terminates the radon decay chain, and thus is unimportant for most practical human exposure considerations.

The radon decay products rather than radon itself are the active species responsible for the health hazard. The main reason is that the radon decay products can be deposited on the lining of the respiratory tract before releasing ionizing radiation during their decay. It has become recognized that inhalation and lung deposition of radon decay products produce adverse health effects. The prolonged exposure periods indoors could then make indoor radon a potential hazard. The National Council on Radiological Protection (NCRP) estimated that 5,000-20,000 lung cancer deaths occur per year because of prolonged indoor radon exposure (NCRP, 1984). Another estimation of lung cancer death among residents of single-family homes was conducted by Lubin and Boice (1989). Single-family houses constitute approximately 70% of the U.S.

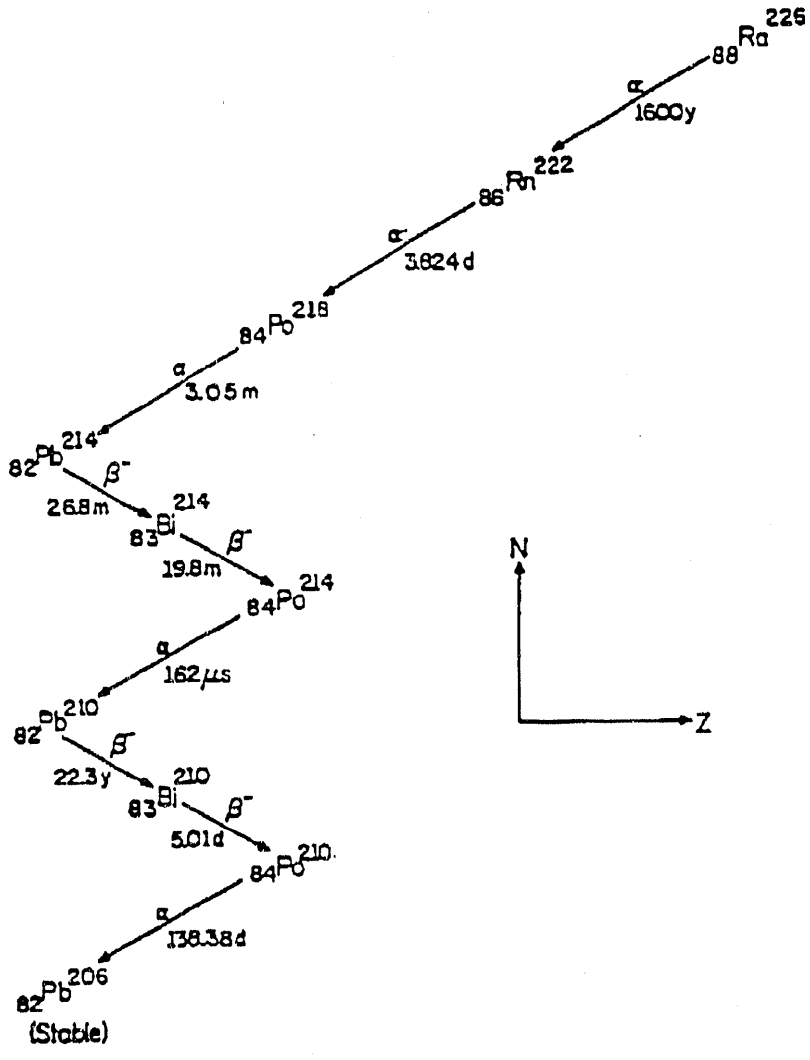

Figure 1. Decay chain for the formation and decay of ^{222}Rn.

houses (Nero et al., 1986). The calculation was made assuming the log-normal distribution of radon concentrations in the homes (Nero et al., 1986) and the risk model developed by the National Academy of Sciences' Biological Effects of Ionizing Radiations (BEIV) IV Committee (BEIV IV, 1988). The predictions showed that approximately 14% of lung cancer deaths (about 13,300 deaths per year) may be due to indoor radon exposure. These estimated risks are similar for males and females and for smokers and nonsmokers. However, higher baseline risks of lung cancer cause much larger radon-attributable cancers among males and smokers. Recently, the

EPA estimated that 20,000 deaths occur annually from radon-induced lung cancer (EPA, 1989). This "new" estimate was obtained by using revised risk coefficients from the underground miner studies in both the International Commission on Radiological Protection 50 (ICRP 50) and BEIR IV risk estimates. For constant lifetime exposure, 360 lung cancer deaths (lcd) per 10^6 Working Level Month (WLM) is the central estimate of risk if the general population is exposed to an average of 0.25 WLM/year. (The WLM is a unit of cumulative exposure and is discussed in Chapter 2.)

Radon is present in indoor air primarily because of soil gas entering a building driven by a pressure difference between the interior of the building and the surrounding soil. In some limited cases, radon is emanated from building materials. Generally, the pathway for radon entry into the house is pressure driven flow of soil gas through cracks in the foundation, sump pumps, drains, and fittings. The infiltration rate is controlled by pressure, temperature conditions within and outside the house, the permeability of the soil and emissivity of radon from the soil grains (Hubbard et al., 1988). The natural outdoor radon concentration averages between 2.59 and 7.4 Bq m^{-3} (NCRP, 1984). Radon concentrations in closed areas can reach levels from 37 to 7,400 Bq m^{-3} (EPA, 1986). Therefore, effective methods of mitigating the indoor radon risks must be developed and thoroughly evaluated.

Controlling radon decay products in houses may be divided into three principal categories: (1) prevent its infiltration (basement pressurization, basement sealing, sub-slab depressurized, choice of building materials), (2) dilute it inside the house (air-to-air heat exchanger, ventilation), and (3) use air cleaning systems for direct removal (filtration, mixing fan, electric field methods, radon adsorption, and ion generator). Categories (1) and (2) can remove or prevent radon gas from entering the houses. The long term stability and reliability of radon mitigation systems are still uncertain. Since the radon health hazard is associated with the radon decay products, it may be more appropriate to remove the radon decay products rather than radon itself. At this time, EPA (1987) does not endorse the use of air cleaners as a method of reducing radon decay products in indoor air because this technology has not been adequately demonstrated to be effective in reducing the health risks associated with radon. Under some circumstances, air cleaning systems have been suggested to increase risk (Rudnick et al., 1983). However, there are still considerable uncertainties about the risk assessment of air cleaners. Thus, a better understanding of how air cleaners affect the behavior of radon decay products is needed.

There are two major objectives of this research. The first one is to field test a

semi-continuous measurement system to determine the concentration and activity size distribution of radon decay products. This measurement system involved a combination of computer-controlled, multiple wire screen sampler/detector units and the use of the radioactive properties of radon decay products attached to the indoor particles. The second objective is to utilize the tested measurement system in homes with the air cleaners. The effect of the air cleaning systems on activity size distribution and concentration of radon decay products can be evaluated with different indoor activities. Therefore, the resulting dose to the occupants of the house can be fully assessed.

Chapter 2 is an introduction to the radioactive and aerosol behavior of radon decay products. The terms characterizing radioactive behavior such as working level, potential alpha energy concentration, equilibrium factor, and "unattached" fraction are defined. Chapter 2 also contains a description of a room model for indoor air quality. To understand the aerodynamic behavior of radon decay products in the house, the uniformly mixed room model (Porstendörfer et al., 1978) is used to estimate the attachment rate and deposition velocity of radon decay products. The room model is also used in Chapter 6 to evaluate the influence of air cleaning system on the attachment rate and deposition velocity of radon decay products.

Chapter 3 is a discussion of the development of lung dosimetric models and the estimation of the bronchial dose from the radon exposure. Traditionally, the lung dose model has been only a very simple equation based on separating the radon decay products into "unattached" and "attached" fractions (James et al., 1980). There has been no variable size dependence in these lung models. Recent studies have suggested that the activity size plays an important role in the dose estimation (James, 1989, personal communication). The relationships (dose conversion factors) between the size of radon decay products and dose per unit exposure for epithelial cells, bronchial basal-cell nuclei, bronchial secretory-cell nuclei were developed by James (1989 and 1990, personal communication). James calculated different relationships for adult male, adult female, and children during rest, sleep, light activity, and heavy activity. These dose conversion coefficients will be used in this study to provide a more accurate dose estimation.

Chapter 4 is a review of the evaluations of the air cleaning systems in previously reported studies. Evaluations of air filtration systems, electrostatic precipitators, ion generators, ceiling fans, and electric fields are reviewed. The exposure and dose changes caused by the air cleaners were assessed in most of the studies. However, there are two problems with these earlier investigations. The first one is that the systems used for activity size measurements were not able

to determine the full size distribution of radon decay products. The second problem is that the dose estimations were made using the simple lung dose models. Thus, it is important to determine the full activity size distribution of radon decay products as well as calculate bronchial dose using the dose conversion factors.

Chapter 5 describes the methodology to conduct this study. The characteristics of three single-family houses are presented. The measurement system (Ramamurthi, 1989) used to determine the concentration and activity size distribution of radon decay products is briefly described. The measurement system is a Graded Screen Array (GSA) system (non-conventional wire screen diffusion battery). The alpha spectroscopic detection and analysis system are detailed. The characteristics of two air cleaners (air filtration system and electronic air cleaner) evaluated are also described in Chapter 5. The experimental setup in each home including the time sequence of measurement and particle generation is detailed. Aerosols were generated by running a shower, burning a candle, cooking, smoldering cigarettes, vacuuming, opening doors, and clothes washing and drying. The calculation of aerosol parameters of radon decay products and hourly bronchial dose rate per radon concentration in this study is also briefly described. By assuming the occupancy factor, the yearly bronchial dose can be also estimated.

Chapter 6 presents and discusses the results of field sampling in three single-family homes both with and without air cleaning systems. The influences on the behaviors of radon decay products by different types of indoor particles were discussed. The changes in measured exposure and bronchial dose by air cleaning systems as calculated with the James dosimetric model are presented for each environmental situation. The changes of attachment rate and deposition velocity of radon decay products induced by air cleaners are also evaluated.

Chapter 7 presents the conclusions and recommendations of this study. The influences on the behaviors by the indoor particles and the air cleaners are summarized. The suggestions to reduce the radon risk are also discussed.

CHAPTER 2

RADIOACTIVE AND AEROSOL BEHAVIOR OF RADON DECAY PRODUCTS

2.1 Introduction

The amount of radioactivity is described in units of disintegrations per unit time or activity rather than as the mass of the contaminant. The activity is the number of decay events per unit time and is calculated as follows

$$A = \lambda N \tag{1}$$

where λ is the probability of decay of the nucleus of a particular atom in a unit time ($\lambda = 0.693/T_{1/2}$, $T_{1/2}$ is the half-life of the isotope) and N is the total number of the atoms present in the sample. The S.I. unit of activity is the becquerel (Bq). A becquerel is the quantity of radioactive material in which one atom is transformed per second. However, in the case of radon, it is common practice in the United States to use picocuries (pCi). A picocuries is 10^{-12} curies (Ci) or 3.7×10^{-2} disintegrations per second. Since the interest is in the amount of activity per unit volume, the proper units are becquerels per cubic meter (Bq m^{-3}) or picocuries per liter (pCi/l). A concentration of 37 Bq m^{-3} is equal to 1 pCi/l.

If all the decay products formed by the decay of radon remain in the air, then there would also be equal activities of ^{218}Po, ^{214}Pb, etc. Such a mixture is said to be in secular equilibrium. The quantitative relationship between isotopes in secular equilibrium may be derived in the following manner for the general case

$$A \xrightarrow{\lambda_A} B \xrightarrow{\lambda_B} C$$

where the half-life of isotope A is very much greater than that of isotope B. The decay constant of A, λ_A, is therefore much smaller than λ_B, the decay constant of isotope B. The product of the decay probability times the number of atoms can be equal for A and B ($\lambda_A N_A = \lambda_B N_B$) because the larger λ_B compensates for the smaller N_B. From the monitoring of uranium mines, the amount of activity equal to that of ^{218}Po, ^{214}Pb, and ^{214}Bi in secular equilibrium at a concentration of 100 pCi/l of each isotope is called one working level (WL). Thus, a 10 pCi/l (370 Bq m^{-3}) equilibrium mixture represents 0.1 WL. The WL is a measure of the total potential alpha energy of the short-lived decay products and thus of the total radiological exposure. The cumulative exposure to such activity can be expressed as the amount of activity in WL multiplied by time. In the past analysis of occupational exposure by miners, this cumulative exposure was given in WLM

by assuming 170 hours in a working month and is calculated as

$$Cumulative\ Exposure\ (WLM) = \sum_{i=1}^{n} (WL_i)(\frac{t_i}{170})$$

The occupancy factor should be considered in determining cumulative exposure to indoor air. The occupancy factor is the mean residence time spent indoors. The ICRP Task Group (ICRP 87) recommends the following mean annual residence probabilities: 6000 hours in home, 1500 hours indoors elsewhere and 1000 hours outdoors, which implies an indoor occupancy factor around 0.86. From the survey conducted in United Kingdom dwellings (Wrixon *et al.*, 1988), the average occupancy factor is about 0.77 over the whole year and 0.97 for housewives, infants, and the elderly.

Another way to express the total activity of all of radon decay products is as the Potential Alpha Energy Concentration (PAEC) in the air and is expressed as MeV/m^3 or WL (Hopke, 1987). One WL of 100 pCi/l (3,700 Bq m^{-3}) in equilibrium deposits 1.3×10^5 MeV/l.

$$\begin{aligned} PAEC(MEV/m^3) &= (3.69)(10^3)C1 + (4.01)(10^4)C2 + (5.82)(10^4)C3 \\ PAEC(WL) &= (0.00103)I1 + (0.00507)I2 + (0.00373)I3 \end{aligned} \qquad (3)$$

where C1, C2, and C3 in Bq m^{-3} and I1, I2, and I3 in pCi/l are the activity concentrations of ^{218}Po, ^{214}Pb, and ^{214}Bi, respectively (Hopke, 1986). Because the decay products deposit on surfaces such as walls, ceilings, and furniture, the decay product activity is less than the radon activity. The term characterizing the airborne concentration of PAEC as a fraction of the radon activity is equilibrium factor (F). F is defined as the ratio of radon decay products activities to radon by

$$F = \frac{(100)\ WL}{A_0} = 0.103a1 + 0.507a2 + 0.373a3 \qquad (4)$$

where a1, a2, and a3 are the relative activities of the three radon decay products (relative to radon, A_0) (Hopke, 1986). Swedjemark (1983) found that for low air exchange rates (< 0.3 hr^{-1}), F averages 0.51 (typical range 0.28 - 0.74). For an average air exchange rate between 0.3 hr^{-1} and 0.6 hr^{-1}, F is about 0.43 (typical range 0.21 - 0.66) and for high air exchange rate (> 0.6 hr^{-1}), F is about 0.33 (typical range 0.21 - 0.47). Swedjemark's work was done in 225 dwellings in Sweden.

Another study of the relationship between the equilibrium factor, F, and aerosol sources was conducted by Porstendörfer *et al.* (1987). The results indicated that the mean value of F in houses without aerosol sources was 0.3 ± 0.1. The equilibrium factor increased to 0.5 with additional aerosol particles (cigarette smoke and candle) in the room air. The equilibrium factor in Swedish houses (Jonassen and Jensen, 1989) was 0.51 in a house inhabited by smokers and 0.46 in eight non-smoker's houses.

Following the decay of Rn-222, the decay products exist as highly diffusive clusters in the air for a period of time depending on the availability of surfaces including airborne particles and walls for attachment (Hopke, 1989). The samplers commonly used in the measurement of the size of radon decay products include high volume cascade impactors, medium volume cascade impactors, and screen diffusion batteries. Measurements of the size distribution of radon decay products were made using high volume screen diffusion batteries (Reineking and Porstendörfer, 1986). In closed rooms without additional aerosol sources, a bimodal distribution (shown in Figure 2) for Po-218 (1 nm and 300 nm) and an unimodal distribution (shown in Figure 2) for Pb-214/Po-214 (300 nm) were observed. Trimodal and bimodal size distributions for Po-218 (0.8 nm, 30 nm, 200 nm) and Pb-214/Po-214 (50 nm, 200 nm) shown in Figure 3 were obtained in a closed room with additional aerosol sources. Traditionally, a distinction is made in the state of the airborne decay products based on their apparent attachment to aerosol particles. The "unattached" fraction (ultrafine mode, 0.5-5 nm) refers to those decay products existing as ions, molecules, or small clusters. The "attached" fraction (accumulation mode, 0.1 - 0.4 μm) is regarded as those radionuclides attached to ambient particles. The "unattached" fraction f_p of the total potential alpha energy of the radon decay products mixture is described as

$$f_p = \frac{C_{eq}^{(u)}}{C_{eq}} \tag{5}$$

where $C_{eq} = 0.103\ C_1 + 0.507\ C_2 + 0.373\ C_3$, C_j with j = 1, 2, 3 being the activity concentration of radon decay products. The superscript u defines the "unattached" fraction. Typically most of the "unattached" activity is Po-218. Measurements of the "unattached" fraction in the domestic environment (Reineking *et al.*, 1985 and Vanmarcke *et al.*, 1987) showed that f_p is between 0.05 and 0.15 without any aerosol sources in the room. It will decrease below 0.05 in the presence of aerosol sources (cigarette smoke, cooking, stove heating). However, Jonassen and

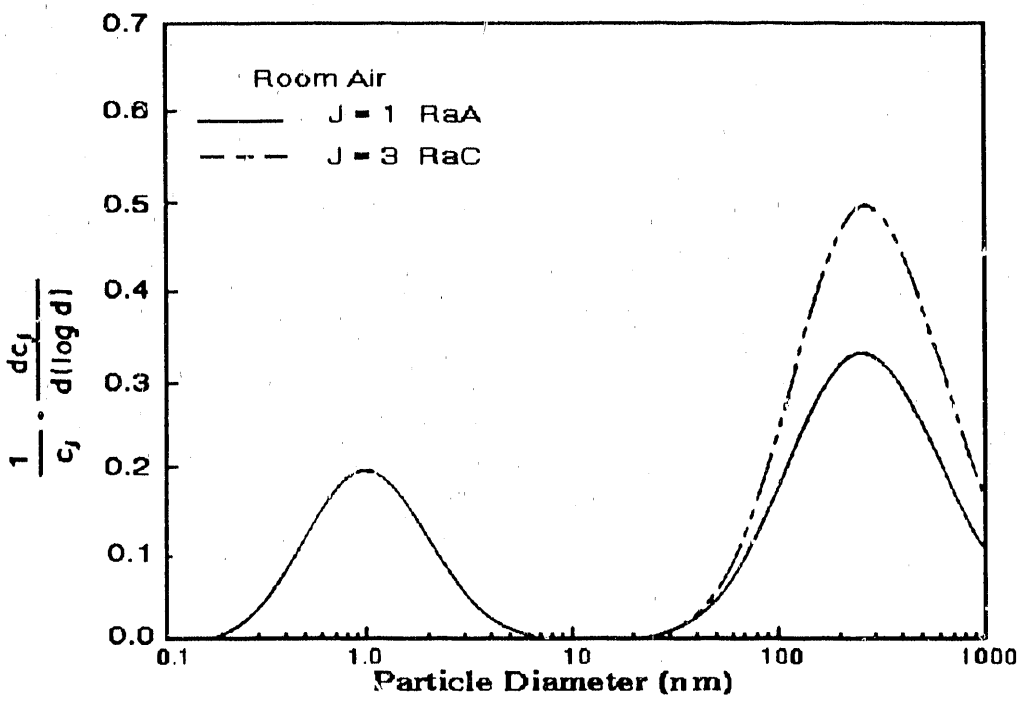

Figure 2 Typical activity size distribution of ^{218}Po and $^{214}Pb/^{214}Po$ measured in a closed room without aerosol sources. Reprinted with permission from J. Aerosol Sci.

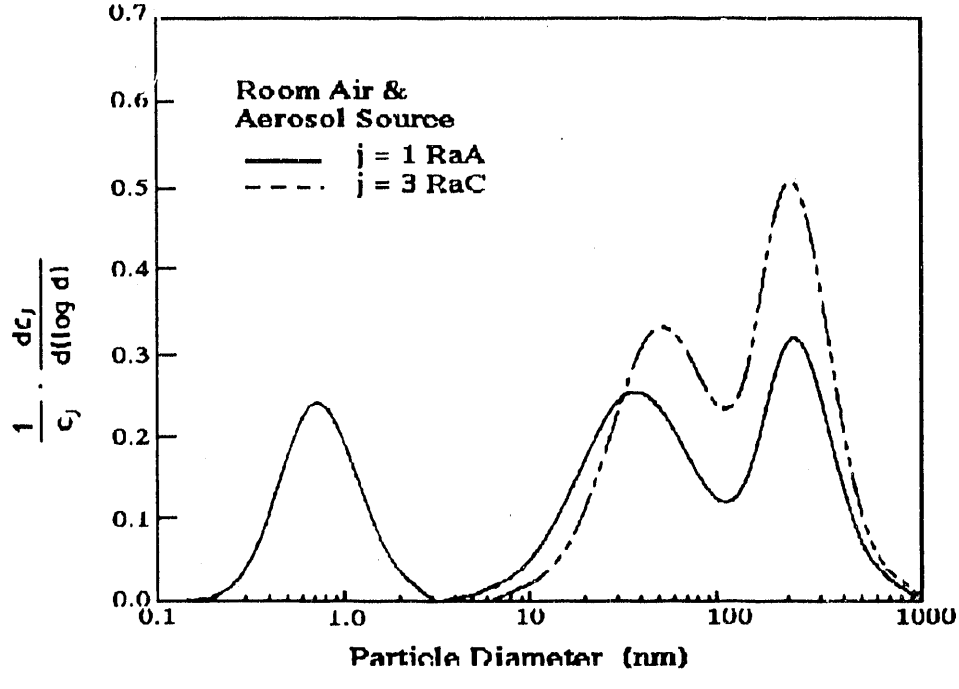

Figure 3 Typical activity size distribution of ^{218}Po and $^{214}Pb/^{214}Po$ measured in a closed room with an additional aerosol source (electrical motor). Reprinted with permission from J. Aerosol Sci.

Jensen (1989) found that $f_p = 0.01$ for a house inhabited by smokers and $f_p = 0.04$ for eight non-smokers' houses.

2.2 Room Model

A simple model of a room based on a well-mixed, flow through reactor mass balance is denoted as a "room model". The room model (Porstendörfer *et al.*, 1978) is used to estimate the degree of equilibrium between radon and its decay products, wall deposition, ventilation, and the partition of the radon decay products between "attached" and "unattached" fraction in the dwellings. The basic processes influencing the activity balance of radon and radon decay products in houses are presented in Figure 4. The governing parameters are ventilation rate, attachment of diffusive airborne decay products to atmospheric particles, deposition (plateout) of "unattached" and "attached" decay products on the macroscopic surfaces, and recoil factors. The air cleaning system investigated in this study can be regarded as a sink to collect both "unattached" and "attached" radon decay products in domestic environments. The influence of air cleaners on aerodynamic behavior of radon decay products will be discussed later in Chapter 6. The differential equation for the concentration of the "unattached" ($C_i^{j(u)}$) and "attached" ($C_i^{j(a)}$)jth decay products in indoor air can be written (Porstendörfer *et al.*, 1978):

$$C_i^o = \frac{(e + \nu C_o^o)}{(\lambda_o + \nu)} \tag{6}$$

$$\frac{\partial C_i^{j(u)}}{\partial t} = \nu C_o^{j(u)} + \lambda_j C_i^{j-1(u)} + r_{(j-1)}\lambda_j C_i^{j-1(a)} - (\nu + \lambda_j + X + q^{(u)})C_i^{j(u)} \tag{7}$$

$$\frac{\partial C_i^{j(a)}}{\partial t} = \nu C_o^{j(a)} + \lambda_j(1 - r_{j-1})C_i^{j-1(a)} + XC_i^{j(u)} - (\nu + \lambda_j + q^{(a)})C_i^{j(a)} \tag{8}$$

The superscript "o" stands for radon gas itself. $C_o^{j(u)}$ and $C_o^{j(a)}$ are the concentrations of the jth (j) decay products from outdoor (o) and $C_i^{j(u)}$ and $C_i^{j(a)}$ are the concentrations of the "unattached" (u) and "attached" (a) fractions in indoor (i). $q^{(u)}$ and $q^{(a)}$ are deposition rates of the "unattached" and "attached" fractions in the room and are calculated using equation (9) below. The assumptions

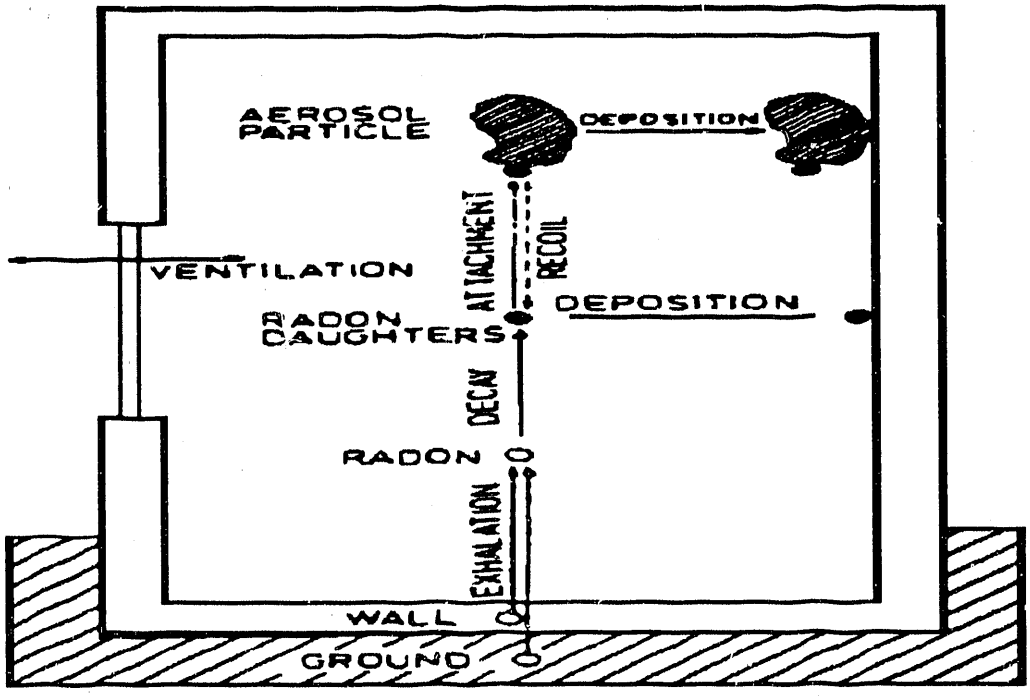

Figure 4. The basic processes influencing the activity balance of radon and radon decay products. Reprinted with permission from American Chemical Society.

used in equations 6, 7, and 8 are (1) a constant radon emanation, e, with a homogeneous activity distribution, (2) the incoming air is assumed to be filtered, so the "unattached" fraction is zero.

$$q^{(u)} = v_d^{(u)}(S/V)$$
$$q^{(a)} = v_d^{(a)}(S/V) \qquad (9)$$

The parameters are individually discussed below:

(1) Ventilation Rate (v)

If air leaves a room of a volume V at the rate Q and is replaced at the same rate by clean air, a fraction Q/V (v = Q/V) of the room's airborne contaminants is removed per unit time.

(2) Attachment Rate (X)

The radon decay products attach to all surfaces including the surface of airborne particles. The typical particle size found in residences is between 0.1 and 0.2 μm (George and Breslin, 1980). The attachment rate, X, is calculated from the number distribution $N(d_p)$ as follows:

$$X = \int_o^\infty B(d_p)N(d_p)dd_p \tag{10}$$

$$N_{act}(d_p) = \alpha B(d_p)N(d_p) \tag{11}$$

$$B(d_p) = \frac{(2\pi Dd_p)}{\frac{8D}{vd_p} + \frac{1}{H}} \tag{12}$$

$$H = (1 + \frac{2\Delta}{d_p}) \tag{13}$$

where $N_{act}(d_p)$ is the number of Rn decay products attached to particles of size d_p, α is a proportionality factor, $B(d_p)$ is the attachment coefficient depending on nuclide diffusion coefficient, condensation nuclei particle size and other factors, D is diffusion coefficient of the "unattached" decay products, v is mean thermal velocity of "unattached" decay products, and Δ is the approximate mean free path of the "unattached" decay products

The simplified form of the average attachment rate is

$$X = \beta(d)Z(d) = \beta Z \tag{14}$$

where β is the average attachment coefficient and Z is particle number concentration.

The value of β that is commonly used in the modeling the aerodynamic behavior of radon decay products is 5×10^{-3} cm^3h^{-1} (Porstendörfer and Mercer, 1978). The particle concentration, Z, is typically between 2,000 and 20,000 particles cm^{-3} indoors for low ventilation rates ($v < 0.3$ h^{-1}). For $v > 1$ h^{-1}, the nuclei concentration (10^4 - 10^5 particles cm^{-3}) indoors is about the same as outside (Porstendörfer, 1984). Therefore, the attachment rate of decay products in room air typically ranges from 10 to 50 h^{-1}. Using equation (14) by the calculated attachment rate and measured particle number concentration for every condition, the average attachment coefficient can be obtained. From the relationship between the attachment coefficient of atoms and ions and particle size (Porstendörfer *et al.*, 1979) shown in Figure 5, the average attachment diameter can be estimated.

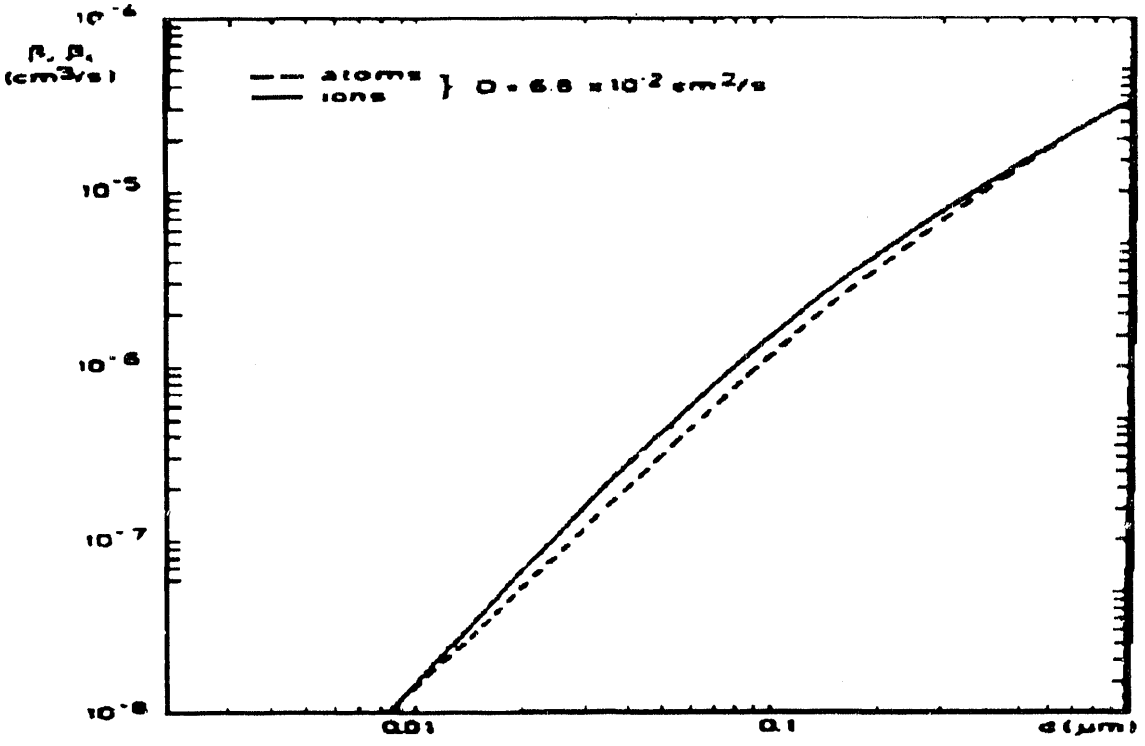

Figure 5. The influence of the particle size on the attachment coefficient of atoms and ions (taken from Porstendörfer and Mercer, 1978 and used with permission).

(3) Deposition Velocity (v_d)

There are losses of the decay products from their deposition on environmental surfaces (walls, floors, furniture, and the people in the room). Several mechanisms lead to the deposition of ion clusters on surfaces such as diffusion, electrophoresis (the attraction of charged clusters by static charge on the walls), thermophoresis and photophoresis (forces induced by temperature gradients across the particles). For submicron particles and clusters (such as radon decay products), diffusion and electrophoresis are the major deposition mechanisms. The degree of plate-out is dependent on environmental conditions including aerosol concentration, air moisture, the presence of trace gases, and the properties of the surface of the material (Bigu, 1987). If C is the airborne concentration of radon decay products and S is the surface area available for deposition, then the rate of removal is Cv_dS where v_d is the deposition velocity of the radionuclide. The average deposition velocities (Porstendörfer, 1984) for the "unattached" and the "attached" radon decay products are estimated to be 2 mhr^{-1} and 0.02 mhr^{-1}, respectively. Porstendörfer made the measurements for aerosol deposition in a turbulent atmosphere. The deposition velocity of the "unattached" fraction is much higher than that of the "attached" fraction

because of its higher diffusivity. The deposition (plateout) rates of radon decay products in a domestic environment (Porstendörfer, 1987) with a low ventilation rate varied among 20 and 100 hr^{-1} ("unattached") and 0.1 and 0.4 hr^{-1} ("attached"), respectively.

(4) Recoil Factor (r)

The recoil factor, r, is the probability of desorption of an attached radioactive atom from the particle surface as a consequence of an α or β decay. Mercer (1976) calculated a r value of 0.83 for Po-218. The recoil factor for the β-decay is only between 0.01 and 0.02 and thus is negligible. In the room model, the recoil factors are set as $r_1 = 0.83$ and $r_2, r_3 = 0$.

The steady-state solutions of equations 7 and 8 give

$$C_i^{j(u)} = \frac{\nu C_o^{j(u)} + \lambda_j C_i^{j-1(u)} + r_{j-1}\lambda_j C_i^{j-1(a)}}{\nu + \lambda_j + X + q^{(u)}} \tag{15}$$

$$C_i^{j(a)} = \frac{\nu C_o^{j(a)} + \lambda_j (1 - r_{j-1}) C_i^{j-1(a)} + X C_i^{j(u)}}{(\nu + \lambda_j + q^{(a)})} \tag{16}$$

with $C_i^{o(u)} = C_i^o$, $C_i^{o(a)} = 0$, $C_o^{j(u)} = 0$, j = 1, 2, 3.

It has been assumed that the deposition rate $q^{(u)}$ and $q^{(a)}$ are of the order of 30 h^{-1} and 0.2 h^{-1} ($q^{(u)} >> q^{(a)}$). The attachment rate X could be calculated by means of the measured ratio $C_i^{1(a)} / C_i^{1(u)}$:

$$X = \left(\frac{C_i^{1(a)}}{C_i^{1(u)}}\right)(\lambda_1 + \nu + q^{(a)}) = \left(\frac{C_i^{1(a)}}{C_i^{1(u)}}\right)(\lambda_1 + \nu) \tag{17}$$

with $(\lambda_1 + \nu) >> q^{(a)}$.

The deposition rate $q^{(u)}$ can be calculated from the activity concentration of the "unattached" fraction of ^{218}Po and radon activity concentration with X :

$$q^{(u)} = \lambda_1 \left(\frac{C_i^o}{C_i^{1(u)}}\right) - \nu - \lambda_1 - X \tag{18}$$

From the concentrations and the full size distribution (0.5 nm - 300 nm) of radon decay products, the degree of equilibrium and the "unattached" fraction can be estimated. In this research, the changes in plate-out rate caused by alteration of the particle and activity size distributions will be assessed. The changes in attachment rates and average attachment diameter with the particle number reduction induced by the air cleaners will be also evaluated.

CHAPTER 3
LUNG DOSIMETRIC MODELS

3.1 Introduction

The risk of lung cancer from radon exposure in homes can be estimated by assessing the dose of radiation to the lung. It is very difficult to directly measure the regional dose to lung tissue from inhalation of radon decay products. The alternative approach to dose assessments is to develop dosimetric models that simulate the sequence of inhalation, deposition, clearance, decay of the radon decay products, and dose to the cells at risk within the respiratory airways. The parameters (Nuclear Energy Agency, 1983) included in the lung model are morphological lung characteristics (age dependence), breathing rate (occupational exposure, domestic exposure, age dependence, annual intake), deposition in the respiratory tract ("unattached" fraction, "attached" aerosol, effect of breathing rate, age dependence), retention in the respiratory tract (mucociliary transport, age dependence of ciliary clearance, compartment models, age dependence of uptake to the blood), and tissue dosimetric characteristics (target tissues, depth distribution of basal cells). The following sections will describe how these parameters effect nasal and tracheobronchial deposition. The deposition behavior of radon decay products in the respiratory tract depends on the activity size distribution of radon decay products, the breathing rate, and the airway dimensions. The major effect of air cleaning systems on radon decay products is the alteration of the activity size distribution and the particle concentration. Therefore, the change of bronchial dose from air cleaning is mainly the result of changing the amounts of radon decay products deposited in the respiratory tract. The dose conversion coefficients for three most commonly used lung models will be listed. The newest lung models (James 1989 and 1990, personal communication) with relationship between monodisperse radon decay products size and dose per unit exposure also will be discussed in this chapter. The James lung models will be used for dose calculations in Chapter 6.

3.2 Parameters in Lung Models

Several geometric lung models have been developed by Findeisen (1935), Weibel (1963), Olson *et al.* (1970), Hansen and Ampaya (1975), and Yeh and Schum (1980). The comparison of these models was described very well by Yu and Diu (1982). Although these geometric lung models have very similar arrangements, the number of structures and airway dimensions differ considerably. The reason for these differences is each research group used different lung casts

and different airway identification schemes. The Yeh and Schum lung model (1980) and Weibel lung model (1963) have been most widely used in the bronchial dose estimation. For the retention in the respiratory tract, a compartment model is typically used to simulate the mucociliary clearance. Also, it is necessary to consider the additional possibility of absorption of contaminates through the epithelium and elimination by the bloodstream. The comparisons of ICRP (1979), Harley-Pasternack (HP, 1972, 1982), Jacobi-Eisfeld (JE, 1980), and James-Birchall (JB, 1982) clearance models was discussed by James (1984). The tissue dosimetric models assume the location of target cells below the epithelial and the thickness of the epithelium (James, 1988) as shown in Table 1. The concern is that alpha decay from radon and its decay products has a short range. Table 2 details the range in the tissue of alpha particles emitted by radon and its decay products. The HP model considered only basal cells lying at 22 μm below the surface in thinner epithelium. The JB model incorporates the probability distribution of target cell depths reported by Gastineau *et al.* (1972).

Table 1 Normal distribution of epithelial thickness (μm).

Airway classification (approx. generation)	Mean	SD
Main bronchi	80	6
Lobar bronchi	50	12
Segmental bronchi	50	18
Transitional bronchi	20	5
Bronchiole	15	5

Table 2 Ranges in tissue of alpha particles emitted by radon and its decay products.

Nuclide	Energy (MeV)	Range (μm)
^{222}Rn(Rn)	5.49	41
^{218}Po(RaA)	6.00	48
^{214}Po(RaC')	7.69	71

3.3 Deposition in the Respiratory Tract

3.3.1 Nasal Penetration

The upper airways can limit exposure to respiratory tissues because inhaled radon decay products deposit in the nasal cavity. A study by George and Breslin (1969) suggested that 50% - 72% of the "unattached" decay products inhaled through the nose were deposited there. However, a recent study of deposition of ultrafine aerosols in a human nasal cast was conducted by Cheng *et al.* (1988). The results showed that turbulent diffusion was the dominant removal mechanism. At the same time, deposition efficiency increased with decreasing particle size between 4.6 nm and 200 nm as well as with decreasing flow rates between 4 and 50 l/min. The deposition data were well represented by the theoretical equation based on the model for the turbulent diffusion deposition in a circular straight pipe:

$$\eta = 1 - \exp(-40.3\ Q^{-1/8} D^{2/3}) \tag{19}$$

where η : inspiratory deposition efficiency

Q : flow rate comparable to breathing rate (l/min)

D : diffusion coefficient comparable to particle size (cm^2/sec) (Ramamurthi and Hopke, 1989)

From the extrapolation of the previous data to the size of "unattached" radon decay products (about 1 nm), the deposition efficiency is predicted to be greater than 90% as shown in Figure 6 (Hopke *et al.*, 1990). Strong (personal communication, 1989) from National Radiological Protection Board (NRPB) of the United Kingdom found that the nasal deposition in a different half nasal cast followed a collection efficiency equation of $\eta = 1 - \exp(-16\ Q^{-1/8}\ D^{2/3})$. Recently, additional data has led to an empirical nasal penetration equation developed by Cheng (1989), $\eta = 1 - \exp(-12.3\ Q^{-1/8}\ D^{1/2})$. This equation is based on several nasal and oral casts built from magnetic resonance images of healthy adults. Most recently, James *et al.* (1989) has reanalyzed the human nasal penetration data of Breslin and George (1969) and obtained the nasal deposition efficiency as $\eta = 1 - \exp(-12.5\ Q^{-1/8}\ D^{2/3})$. The newest nasal filtration efficiencies of the adult and child from Strong and Swift (1989, personal communication) is $\eta = 1 - \exp(-7.7\ Q^{-1/8}\ D^{1/2})$. Thus, there is some uncertainty regarding the nasal penetration of the smallest sized radioactive particles. It would appear, however, that there is somewhat higher nasal deposition than has been typically incorporated into previous dosimetric models.

For larger particle sizes ($d_p \geq 200$ nm), Yu and coworkers (Yu *et al.*, 1981; Yu and Diu,

1982) derived an empirical nasal inspiratory deposition efficiency relationship .

$$\eta = -0.014 + 0.023 \log(\rho d_p^2 Q/g\mu m^2 sec^{-1}) \quad for\ \rho\ d_p^2 Q < 337 g\mu m^2 sec^{-1}$$
$$\eta = -0.959 + 0.397 \log(\rho d_p^2 Q/g\mu m^2 sec^{-1}) \quad for\ \rho\ d_p^2 Q > 337 g\mu m^2 sec^{-1} \qquad (20)$$

where ρ is the particle mass density (g cm^{-3}), d_p the particle diameter (μm), Q the air flow rate (cm^3 sec^{-1}), and μ is gas viscosity (1.83×10^{-4} g cm s^{-1} for air at 293 K).

3.3.2 Tracheobronchial Deposition

The geometrical parameters (airway segment diameters, lengths, branching angles, and angles of inclination to gravity), breathing rate and pattern, and particle sizes are the considerations for determining the tracheobronchial deposition (within tracheobronchial generations 0 - 16). The tracheobronchial deposition was estimated by assuming that the airflow pattern is laminar. The deposition fraction F_d for laminar flow may be estimated from the Gormley-Kennedy (1949) equation for the penetration of diffusing particles through a cylindrical tube as formulated by Ingham (1975):

$$F_p = 1-[0.819 \exp(-14.63\Delta) + 0.097 \exp(-89.22\Delta) + 0.0325 \exp(-228\Delta) + 0.0509 \exp(-125.9\Delta^{2/3}) \qquad (21)$$

where $\Delta = \pi$ D L/(4 Q)

D = particles diffusion coefficient (cm^2/sec)

L = tube length (cm)

Q = mean flow rate through the tube (cm^3/sec)

The calculation of particle collection in the tracheobronchial region (within generations 0 - 16) using equation (21) is made by using lung model parameters (diameter and length of each generation) given by James (1988) and Yeh and Schum (1980). However, the deposition for the six airway generations just beyond the trachea has been measured to be about twice the value calculated by equation (21) because of nonuniform particle deposition (Cohen, 1987). Using equation (21) with the correction factor of two derived from Cohen's results, the collection efficiency within tracheobronchial region can be estimated at an average inspiration/expiration flow rate of 30 l/m. This efficiency curve is shown in Figure 7 (Hopke *et al.*, 1990).

For larger particles ($d_p \geq 200$ nm), impaction and sedimentation mechanisms dominate the

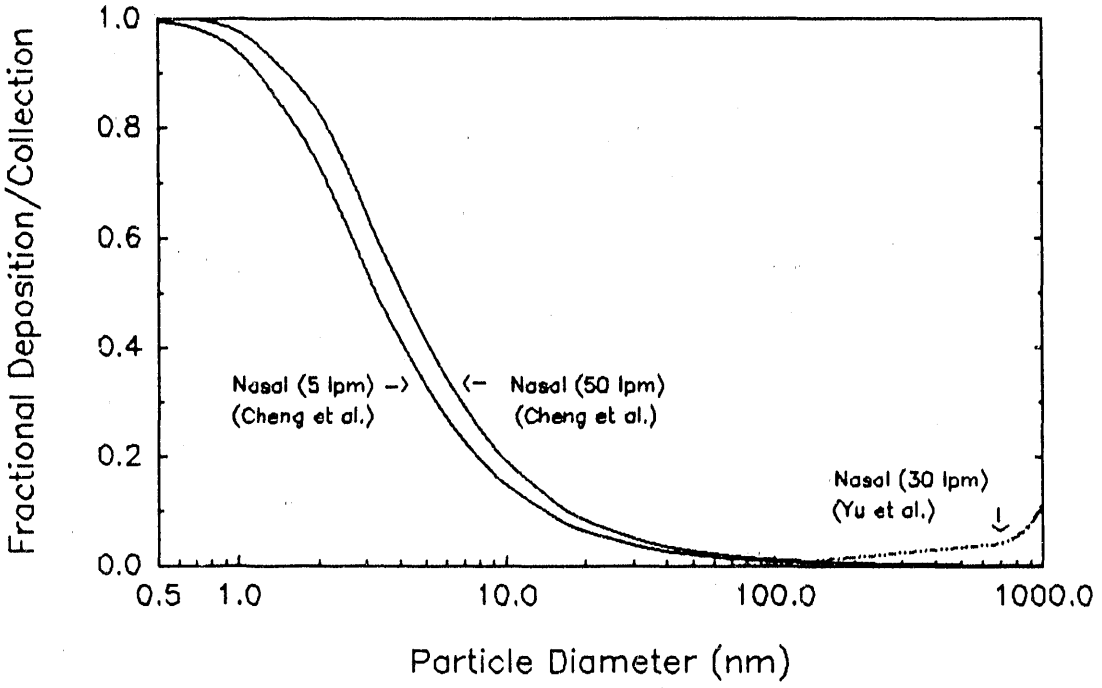

Figure 6 Fractional collection of particles in the nasal cavity as modeled by equation (19) (Hopke *et al.*, 1990)

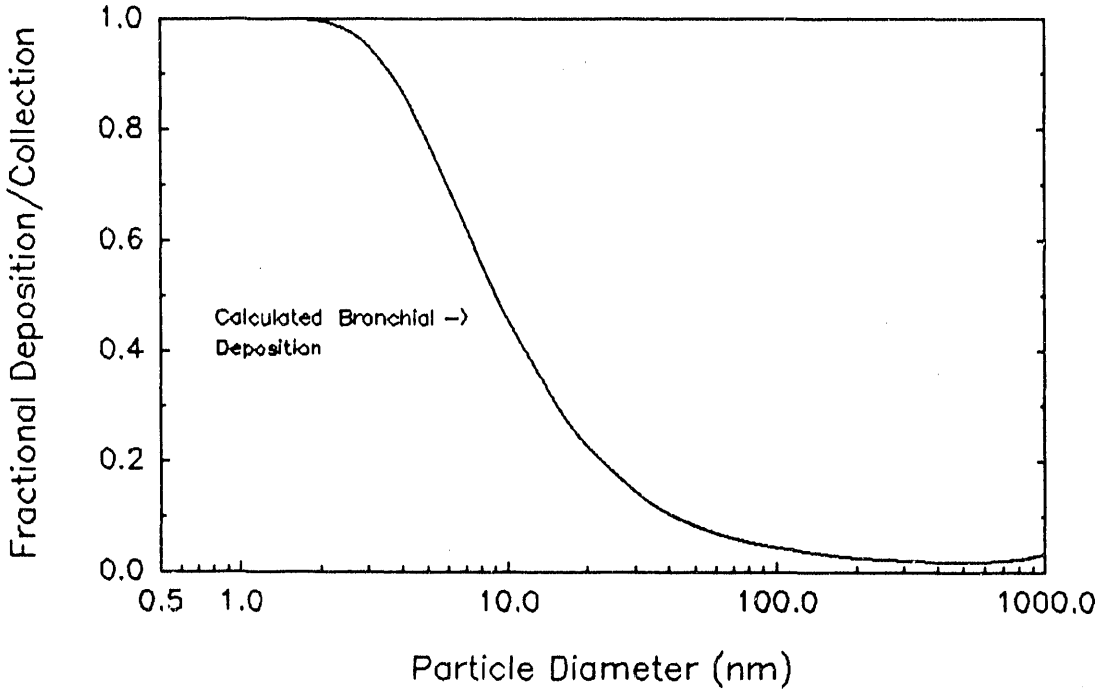

Figure 7 Fractional deposition in the tracheobronchial region (generation 1-16) at 30 l min^{-1} (Hopke *et al.*, 1990).

particle deposition per airway generation. For impaction, $\eta = 0.768\ \theta(St)$, where $St = \rho d_p^2 u/(9\mu d)$ and $\theta = L/(4d)$ is the bend angle; ρ is the mass density of the particle; d_p is the diameter of the particle; u is the mean flow velocity; μ is the air viscosity; d is the diameter of the airway; and L is the length of the airway. For sedimentation, $\eta = 2/\pi\ (2e(1-e^{2/3})^{1/2} - e^{1/3}\ (1-e^{2/3})^{1/2} + \sin^{-1} e^{1/3})$, where $e = 3u_s L \sin\varnothing/(4u_s d)$, in which u_s is the settling velocity of the particle, and $\varnothing = \pi/4$ is the angle of inclination of the airway to the vertical.

3.4 Commonly Used Simple Lung Dosimetric Models

Several dosimetric models have been developed for the evaluation of the absorbed dose, averaged over all sensitive cells in the bronchial regions of the lung, per unit exposure to potential alpha energy. These lung dosimetric models are the James-Birchall-model (James, *et al.*, 1980), Jacobi-Eisfeld-model (1980), and Harley-Pasternak model (1972 and 1982). The dose discussed here is assumed to have been received by the basal cells in the bronchial epithelium according to different groups of individuals exposure to the atmosphere studied.

The dose D can be expressed generally as

$$D = Rt(A'faRa + B'fbRb + C'fcRc + A(1-fa)Ra + B(1-fb)Rb + C(1-fc)Rc) \qquad (22)$$

where Ra, Rb, Rc are the activity concentrations of ^{218}Po, ^{214}Pb and ^{214}Bi, r is the breathing rate characteristic of the group considered, t is the exposure time, fa, fb, and fc are the "unattached" fraction of the radon decay products, and A', B', C', A, B and C in Table 3 are the constants characteristic for the model, the group of the exposed individuals, and the aerosol size distribution used. The assumption is made that the average number particle diameter is 0.1 μm. The radon decay products concentrations are expressed in Bq m^{-3}. The dose is expressed in grays (Gy) for the constants of the JB and JE models. Gy is the unit of radiation dose, D, expressed in terms of absorbed energy per unit mass of tissue (1 Gy = 1 J/kg). However, the HP model only considers ^{218}Po to be "unattached". Thus, B' and C' are zero. The radon decay products concentrations are expressed as Bq m^{-3}, then the dose is given in mrad/year, where 1 mrad/year = 10^{-5} Gy/year.

The other to estimate dose is to use the mean bronchial dose equivalent conversion factor. This conversion factor (mSv/WLM) is 92 + 180 f_p for Jacobi-Eisfeld model (1980), 70 + 795 f_p for Harley-Pasternack model (1982), and 66 + 1370 f_p for James-Birchall (James *et al.*, 1980), where f_p is "unattached" fraction of potential alpha energy concentration. Sv (Sieverts) is the unit

Table 3 Dose conversion coefficients for the three most commonly used dosimetric models for radon decay products (The values of the coefficients in the table should be multiplied by 10^{-9}).

(a) James-Birchall-model (1981)

	A'	B'	C'	A	B	C	R(m3/h)
infant, 1 year	192	573	0	19.3	80.7	64.2	0.084
child, 6 years	54.2	198	0	4.1	17.7	13.7	0.38
child, 10 years	32.3	126	0	2.5	11.2	8.6	0.45
adults	14.0	62.6	0	1.4	6.4	5.0	0.45
adults	14.9	66.5	0	1.1	5.3	4.0	0.75
adults	15.0	67.0	0	0.9	4.2	3.2	1.2

(b) Jacobi-Eisfeld-model (1980)

	A'	B'	C'	A	B	C	R(m3/h)
infant, 1 year	0	0	0	15.6	83.4	56.4	0.084
child, 6 years	6.14	9.48	33.0	3.12	16.8	11.5	0.38
child, 10 years	4.26	7.28	24.2	1.93	10.6	7.37	0.45
adults	1.28	2.50	8.50	1.05	6.02	4.30	0.45
adults	2.36	5.32	16.0	0.74	4.28	3.03	0.75
adults	3.14	7.69	21.4	0.60	3.46	2.44	1.20

(c) Harley-Pasternak-model (1972, 1982)

	A	A	B	C
female adults, light activity	22.2	0.78	4.32	3.78
male adults, light activity	26.5	0.78	4.32	3.78
adults, resting	8.64	0.59	3.24	2.70
children, light activity	63.8	1.62	7.02	7.56
children, resting	14.6	1.08	4.59	4.86

of radiation dose equivalent, H, considering both physical and biological factors. For alpha rays, H (Sv) = 20 × D (Gy). The assumptions for these conversion factors include a reference aerodynamic median activity diameter (AMAD) of 0.15 μm for the "attached" decay products, a diffusion coefficient of 0.05 cm^2/s for "unattached" decay products, and an adult mean breathing rate of 0.75 m^3/h. These three models differ in various respects including the mathematical treatment of aerosol deposition, the clearance of deposited activity, the various geometrical models of lung dimensions, and the assumed location of target cells below the epithelial surface (James, 1984).

The models described above only divide the radon decay products into "unattached" and

"attached" fraction, and therefore no detailed size dependence of dose was taken into consideration. The health risk estimation corresponding to these different models show considerable differences. These differences resulted from the way in which the models treated the effectiveness of the various sizes of airborne activity in delivering dose to the tissue.

The recent dose estimates by James (James *et al.*, 1989) take particle size and recent nasal deposition results into consideration. This "updated" James model considered new research data on filtration efficiencies of the nose and mouth and the thickness of bronchial epithelium. The nasal deposition equation used in the James' model is $\eta = 1 - \exp(-12.5\ Q^{-1/8}\ D^{2/3})$. The dose conversion coefficients for different activity median diffusion diameter (AMDD) in the range of 0.6 nm - 700 nm are shown in Table 4. Table 4 shows that the dose per unit exposure is strongly dependent on the activity median diameter especially for particle diameters smaller than 10 nm. In this model, the "unattached" fraction activity is treated as a sequence of monodisperse mode each with fixed diffusion coefficients. The dose for 10 nm and larger particles is based on the deposition of a lognormal size distribution ($\sigma_g = 2$) centered at an aerodynamic median diameter 2 times its value in the air. The increase in size is due to hygroscopic growth. The value of 2 was in part based on the results of Tu and Knutson (1984). However, information on the hygroscopicity of indoor airborne particles is currently unavailable. The reference dose conversion coefficient for "unattached" WL, assumed to be 0.9 nm AMDD, is 92 mGy/WLM. The AMDD of the "attached" WL in room air was assumed as 150 nm. The reference dose conversion coefficient for the "attached" WL, assumed to be 300 nm AMDD after humid growth doubling in the respiratory tract, is 3.6 mGy/WLM. However, the Activity Median Aerodynamic Diameter (AMAD) of "attached" decay products depends on the environment. The AMAD was found to be 110 nm in the kitchen with cooking and 150 nm in the living room during summer for English rural dwellings (Strong, 1988).

Table IV Dose Conversion Coefficients (Mean Doses to the Bronchial Epithelium Cells from Exposure to 1 WLM).

AMDD, nm	ξET,[a] %	Dose Conversion Coefficient, mGy/WLM: Man (b)	Man (c)	Woman (c)	Child(c) Age 10 yr.	Child(c) Age 6 yr.	Infant(c) Age 2 yr.
0.6	80	70	77	70	88	93	100
0.8	70	86	104	97	119	126	136
0.9	66	92	113	106	130	138	148
1.0	63	97	122	115	141	149	160
1.5	48	112	147	141	170	180	194
2.0	37	115	154	150	179	190	206
3.0	34	111	148	146	173	185	201
4.0	17	102	134	133	157	168	185
5.0	13	93	120	120	140	151	167
7.0	9	77	97	98	114	123	137
10	5	60	74	75	87	95	106
15	3	43	53	53	61	67	75
20	2	33	41	42	47	52	59
30	1.3	23	28	29	32	36	41
40	0.9	18	22	22	25	27	31
50	0.7	14.5	17.5	17.9	20.1	22.1	25.3
70	0.5	10.8	12.7	13.0	14.5	16.1	18.5
100	0.3	7.9	9.0	9.2	10.3	11.4	13.2
150	0.2	5.6	6.1	6.2	7.0	7.8	9.0
200	0.1	4.5	4.7	4.8	5.4	6.0	6.9
300	---	3.6	3.4	3.5	3.9	4.3	5.0
400	---	3.3	2.9	3.0	3.4	3.7	4.3
500	---	3.3	2.9	2.8	3.3	3.6	4.1
600	---	3.6	3.0	2.9	3.4	3.7	4.3
700	---	4.1	3.4	3.1	3.7	4.0	4.7

(a) Extrathoracic filtration efficiency (%).
(b) Reference" values calculated using the probabilities of deposition in bronchial airways given by Egan et al. (1989).
(c) "Comparative" values calculated using deposition probabilities based on James (1988).

3.5 Dose per Unit Exposure for Monodisperse Activity

The particle size to which the decay products are attached are important factors in dose estimation. The relationships between monodisperse size of radon decay products and dose per unit exposure was developed by James (1989, 1990, personal communication). These two models were used for the dose estimates in this study. The dosimetric calculations account for characteristics of bronchial tissues at risk, characteristics of target cells, morphometry of mucous, influence of smoking and disease, and influence of age. The parameters in the James' dosimetric model are : (1) the particle sources and size distribution of the "unattached" and "attached" fraction of radon decay products in domestic environment, (2) the penetration efficiency of the nose and mouth for radon decay products (accounting for the influence of exercise and age independence), (3) aerosol deposition behavior in the bronchial tree (accounting for the dependence on aerosol size distribution, influence of exercise, age dependence, influence of smoking and disease), (4) retention in the respiratory tract, (5) the location of the sensitive target cells (accounting for the influence of smoking and disease, age dependence), and (6) the morphometry and cellular composition of bronchial epithelium (Nuclear Energy Agency, 1983). The differences between 1989 and 1990 models include the target cells and nasal penetration equations. In the 1989 model, the target cell include the bronchial (from generation 1 to generation 8) and bronchiolar epithelium (from generation 9 to generation 16). In the 1990 model, the target cells were only considered to be the bronchial epithelium containing basal cells and secretory cells. This change is due to the observation that only in this part of trachebronchi were lung cancers found in the underground miner populations.

3.5.1 Nasal Penetration

The nasal penetration equation contained in the 1989 model and used for the calculation of dose per unit exposure is $\eta = 1 - \exp(-12.5\ Q^{-1/8}\ D^{1/2})$ for particles smaller than 200 nm (Cheng *et al.*, 1989). For the 1990 model, the nasal equation is $\eta = 1 - \exp(-7.7\ Q^{-1/8}\ D^{1/2})$ (Strong and Swift, 1989, personal communication). For particles larger than 200 nm, equation (17) is used. The diffusion coefficient is calculated from Einstein-Cunningham equations fitted to kinetic theory (Ramamurthi and Hopke, 1989) and can be written :

$$d_p^* = d_p(1 + 3\ \exp(-2.2x10^7 d_p)) \qquad (23)$$

$$C = 1 + \lambda [2.514 + 0.8 \exp (- 0.55 d_p^*/\lambda)]/d_p^* \quad (24)$$

$$D = kTC/(3\pi\mu d_p) \quad (25)$$

where d_p is particle diameter (cm), D is diffusivity ($cm^2\ s^{-1}$), C is Cunningham correction factor, μ is viscosity of air (1.83×10^{-4} g cm sec^{-1}), T is temperature (K), k is Boltzman's constant, and λ is the mean free path of the gas (0.646×10^{-5} cm at 298 K and 1 atm).

3.5.2 Aerosol Deposition in the Respiratory Tract

A particular model that describes aerosol transport and deposition used in James' lung models was developed by Egan and Nixon (1985, 1989). The mechanisms for deposition include Brownian diffusion, gravitational settling, and inertial impaction. Aerosol transport and deposition within the lung airways is represented by

$$\frac{\partial(A_T C)}{\partial T} = - \frac{\partial(A_A \mu C)}{\partial X} + \frac{\partial}{\partial X}(A_A D \frac{\partial C}{\partial X}) - L \quad (26)$$

where A_A is the cross-sectional area for aerosol transport, summed over all airways at distance x from the origin of the trachea. A_T represents the total-sectional area which, in the lung periphery, includes the additional volume associated with alveoli. The aerosol concentration, C, is governed by the mean convective flow velocity of the aerosol, u, the effective axial diffusion coefficient of the aerosol, D, and the deposition rate of the aerosol per unit length, L, of aerosols. All variables are functions of time, T, and distance, X. The details of the calculation of A_A, A_T, u, D, L, and concentration over different volumetric flowrates and tidal volumes are given by Egan and Nixon (1985, 1989).

3.5.3 Retention in the Respiratory Tract

The model of mucous clearance and partial uptake of radon decay products by epithelial tissue used in the James' lung models was developed by James and Birchall (James, 1988). The description and transfer of radon decay products in each bronchial generation were detailed by the Nuclear Energy Agency (1983). It is assumed that about 10% of deposited decay products enter a rapid absorption pathway with a half-time of biological retention in the mucosa of about 15 min.

There are two kinds of protracted retention mechanisms at bronchial surface for about 30 % of deposited decay products. The first one is rapid transfer with retention in epithelial tissue (epithelial retention). The second one is slow transfer through the mucous sol (mucous retention) followed by rapid absorption into the blood.

3.5.4 The Location of Sensitive Target Cells and Morphometric Data

In 1989 James' model, the morphometry of bronchial epithelium and target cells are adopted from the paper of Bowden and Baldwin (1989) and Mercer *et al.* (1989). Both groups of researchers have conducted comprehensive measurements of the thickness of epithelial tissue in the human bronchi and bronchioles and of the distance of basal and secretory cell nuclei from the epithelial surface. It is assumed that the critical carcinogenic doses are those averaged over the whole population of secretory and basal cell nuclei in the bronchi, and secretory cell nuclei in the bronchiole. The basal cells are distributed in the bronchi over a range of depths, with an average value of approximately 50 μm. Secretory cell nuclei were assumed to occur at all depths, from the epithelial surface through the full thickness of the epithelium. The lining layer of mucus was assumed to be 14 μm thick in the bronchi and 10 μm in the bronchiole (Bowden and Baldwin, 1989, Mercer *et al.*, 1989). In 1990 James' model, the target cell is bronchial epithelium including bronchial basal cell nuclei and bronchial secretory-cell nuclei. Because of the different dose conversion coefficient (nGy per disintegrations/cm^2) for secretory cell nuclei and basal cell nuclei in the bronchial epithelium, the dose per unit exposure for these two kinds of cells are significantly different.

From the assumptions described above, the particle size versus dose per unit exposure in the 1989 model for adult males, adult females, and children, ages 10 and 5, are shown in Figures 8 and 9. The breathing flowrates for sleep (M_s), rest (M_r), light work (M_l), and heavy work (M_h) of adult males are 250, 300, 833, and 1667 cm^{3}s^{-1}, respectively. For adult females, the breathing flowrates at rest (F_r) and exercise (F_e) are 215 and 700 cm^{3}s^{-1}, respectively. The breathing flowrates for children age 10, at rest ($C10_r$) and exercise ($C10_e$) are 210 and 617 cm^{3}s^{-1}, respectively; these are 175 ($C5_r$) and 317 ($C5_e$) cm^{3}s^{-1}, respectively for children age 5. The dose per unit exposure in the 1990 James' model for basal-cell nuclide (B_l, B_h) and secretory-cell nuclide (S_l, S_h) of adult males are shown in Figure 10. The lower breathing flowrate for each cell is 125 cm^{3}s^{-1} (B_l, S_l), while the higher breathing flowrate (B_h, S_h) is 833 cm^{3}s^{-1}. The conversion factor coefficients used in this research were from the 1989 and 1990 James' models as shown in

Table 5. The dose in this study was calculated by the size distributions of PAEC and total PAEC taken from the field measurements and is discussed in Chapter 5.

In the domestic environment, air cleaning systems can remove most of the particles and radon decay products. By measuring the concentration and activity size distribution of radon decay products with air cleaners, the effects of air cleaners on radon decay products behavior and radioactive dose can be evaluated.

Table 5 Dose conversion coefficients (mGy/WLM) of monodisperse radon decay products size from James 1989 and 1990 models.

d_p	M_s	$_{+r}$	M_l	M_h	F_r	F_e	$C10_r$	$C10_e$	$C5_r$	$C5_e$	B_l	B_h	S_l	S_h
0.9	43.2	53.5	154	297	41.7	148	48.2	150	55.1	101	46	240	79	390
2.8	67.8	80.4	181	297	67.5	180	77	184	90	144	49	175	86	317
8.9	43.5	49.4	89.5	127	44.2	91	49.6	94	60	83.8	29	80	50	133
28.1	16.5	18.1	29.7	29.8	19.2	34.3	20.8	35.5	23.9	32.3	8.9	22.7	14	40
88.9	6.5	7.0	10.8	14.2	7.4	12.2	7.9	12.6	9.0	11.8	3.5	11.4	6	15.5
281.	2.4	2.6	4.1	6.3	2.6	4.3	2.8	4.5	3.4	4.3	1.9	2.6	3	8.2

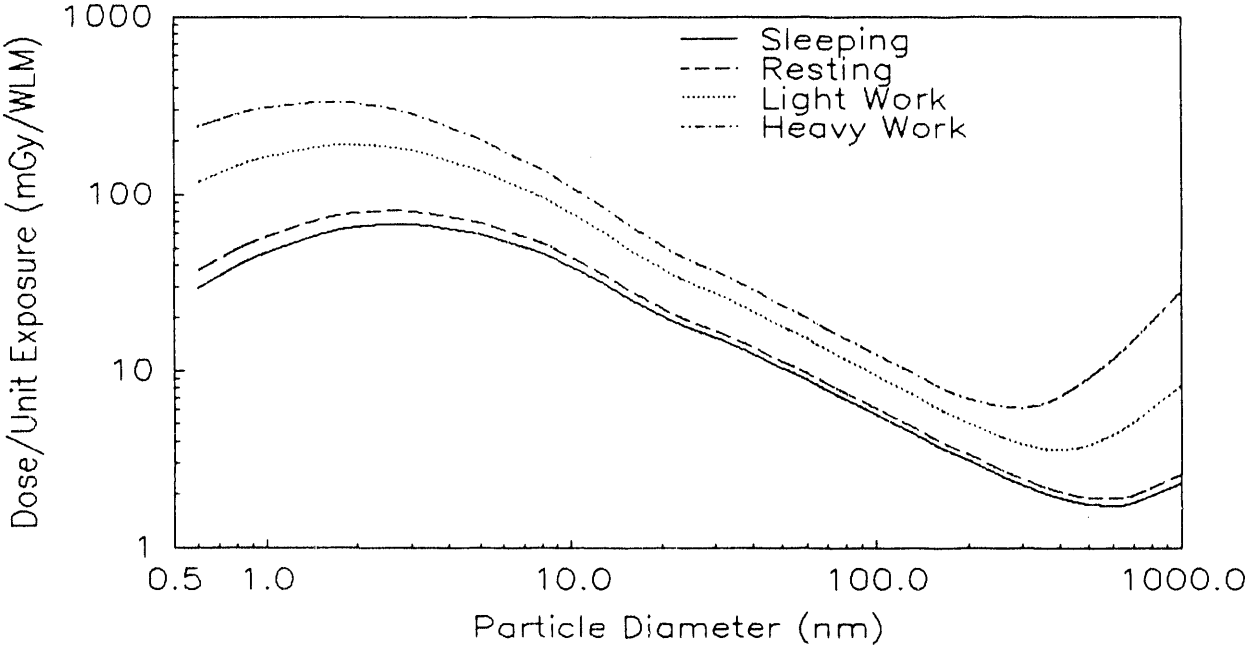

Figure 8 Dose to bronchial epithelial cells as functions of radon progeny size for adult male (James, 1989).

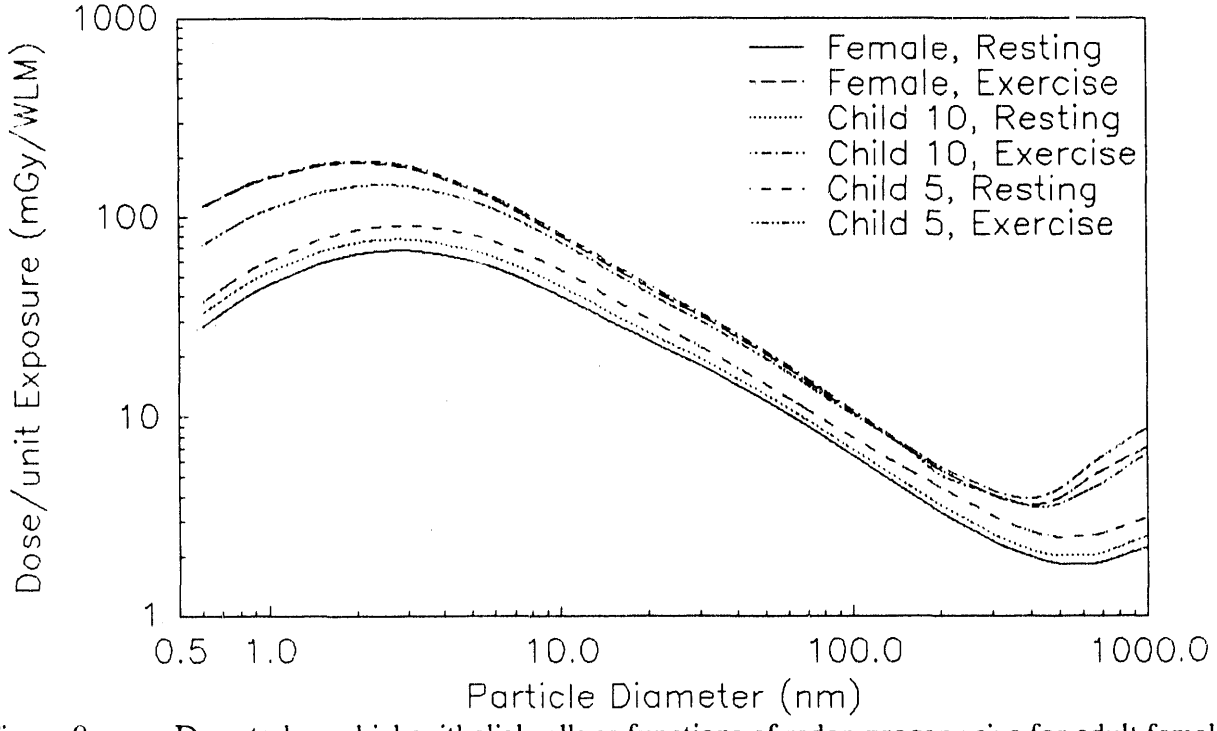

Figure 9 Dose to bronchial epithelial cells as functions of radon progeny size for adult female, child at age of 10 and 5 (James, 1989).

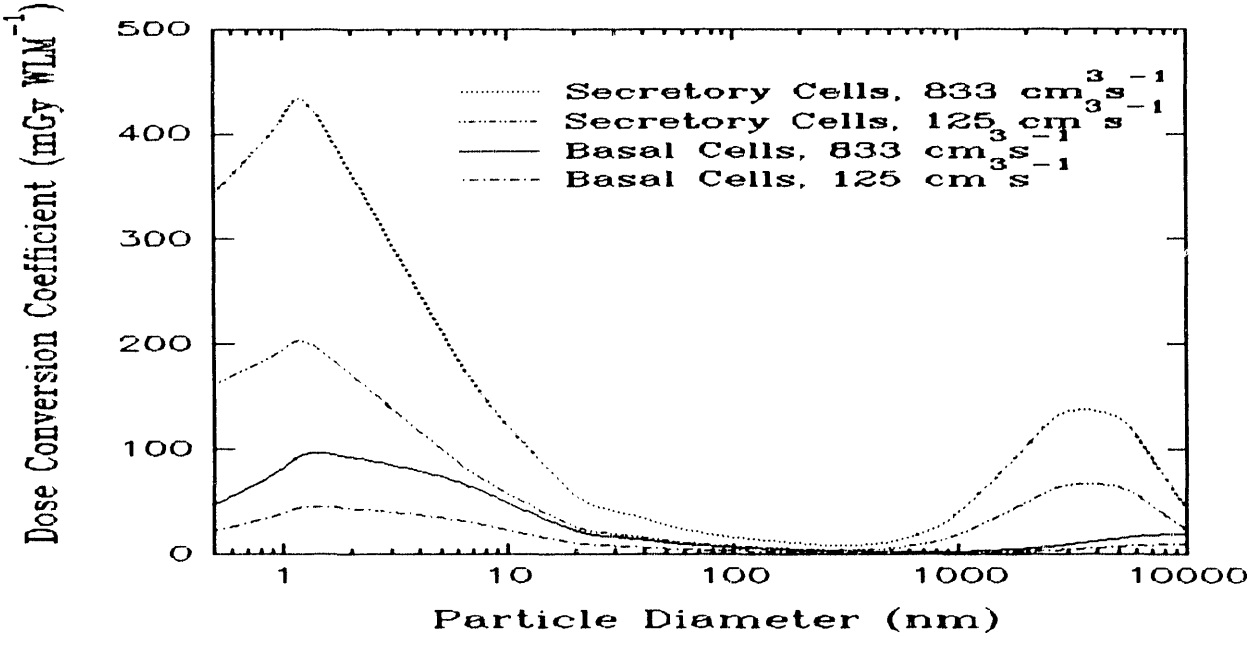

Figure 10 Dose to bronchial basal and secretory cells as functions of radon progeny size for adult male (James, 1990)

CHAPTER 4
CONTROL TECHNIQUES

4.1 Radon Control

Although the primary causes of lung cancer are the radon decay products, radon control is still an important way to reduce exposure to radon decay products. If radon is prevented from entering the structure, then the decay products cannot be formed in the house. General methods to prevent radon infiltration into houses (especially in basements and crawlspaces) include sub-slab and wall depressurization with and without sealing, subslab pressurization, basement pressurization, heat recovery ventilators, and basement sealing. An evaluation of these methods in seven single-story houses was performed by Hubbard *et al.* (1989, personal communication). The radon concentrations were originally in the range of 12,950 Bq m^{-3} (350 pCi/l). Each method had significantly different efficiencies for radon reduction. The reduction of radon concentration strongly depends on the characteristics of the houses (specific leakage area, soil permeation, etc.). It is a case-by-case control methodology. The most efficient method is generally sub-slab depressurization. However, this method can not effectively reduce radon level in all houses. Even with sub-slab ventilation, the radon concentration may still be higher than 148 Bq m^{-3} (4 pCi/l) in the basement and the living area. Also, it may be important to provide immediate relief from high exposure once a house has been identified and while radon controls are being put in place. Hence, there are needs for alternative control strategies to reduce exposure and dose to acceptable levels.

4.2 Radon Decay Products Control

The air cleaning systems that have been used to remove radon decay products in the domestic environments include filtration, mixing fans, ventilation systems, ion generators, and electrostatic precipitatiors (ESP). These air cleaning systems have been evaluated by other researchers by operating the air cleaning system under different concentrations and size distributions of particles, radon concentrations, ventilation rates, filtration rates, and measuring the activities and other variables needed to calculate the bronchial dose. This Chapter will describe studies of air cleaners previously reported in the literature.

Lethimaeki *et al.* (1984) evaluated an air cleaning system containing both a low efficiency mechanical filter and an ESP. The measurements of the concentrations of radon decay products were carried out in a room of a relatively new one-family house, with a total volume of

approximately 250 m^3. The indoor air was circulated at 1 to 2 air changes per hour. The highest radon concentration was measured to be about 800 Bq m^{-3} (22 pCi/l) depending on the ventilation rate. Two WL monitors were used to measure the concentration of radon decay products. One used a filter (Millipore FALP 04700, pore size 1.0 mm supported by a Gelman A/E 61631 glass fiber filter) for collection of the total airborne decay products ("attached" and "unattached"). The other one used a wire mesh screen (J. Keskinen, 1989, personal communication) for the collection of "unattached" decay products. The screen wire diameter was 0.04 mm. The mesh number was 120 cm^{-1}. The face velocity was 10 cm s^{-1} for those experiments reported by Lehtimaeki *et al.* (1984) and 5 cm s^{-1} for the Rajala *et al.* (1985; 1986) experiments.

With recirculation off, the equilibrium factor, F, was between 0.4 and 1.0. With a low efficiency filter and recirculation, F was between 0.15 and 0.50. F had a value around 0.4, when the ESP was operated. The ESP was found to produce observable condensation nuclei when no other particle sources were present. The ozone produced by the corona discharge of ESP probably has a substantial effect on the production of these submicron particles. Therefore, the radon decay products attached to the precipitator-produced condensation nuclei lead to an increase in total airborne activity. This additional attachment also resulted in smaller wall deposition of radon decay products (Lehtimaeki *et al.*, 1984). No WL and dose reduction were evaluated.

Rajala *et al.* (1985 and 1986) performed another experiments in a 28 m^3 test chamber equipped with a recirculation system including a high-efficiency mechanical filter. The two air cleaners studied were a high efficiency particulate air (HEPA) filter and an ESP. Both had air flowrates of four equivalent room volumes per hour. The radon concentration was between 5,000 and 10,000 Bq m^{-3} (135 pCi/l and 270 pCi/l). Aerosols containing 0.1 mm monodisperse dioctyl phthalate (DOP) particles were added to the chamber. The systems to measure the concentrations of radon decay products (total and "unattached" fraction) were the same as described above. Both the HEPA filter and the ESP were found to decrease the equilibrium factor from 0.8 to 0.1 and to increase the "unattached" fraction of radon decay products from 0.05 to 0.10.

The effect of two cleaners to human health risk was estimated by the use of several simple dosimetric models such as the James-Birchall (JB) (James *et al.*, 1980; James, 1984), Jacobi-Eisfeld (JE) (1980), and Harley-Pasternack (HP) (1972, 1982) models. In a few cases, the bronchial dose increased when the air cleaners were operated. The results showed large differences in the

estimated doses, especially with the air cleaner on. The main reason is that each dosimetric lung model uses different assumptions about the influence of "unattached" decay products on the bronchial dose (Rajala *et al.*, 1985). Jacobi-Eisfeld assumed rapid solubilization of the "unattached" activity, so that its effective dose is substantially decreased.

Hinds *et al.* (1982, 1983) and Rudnick *et al.* (1983) conducted evaluations of control devices including a box fan, a ceiling fan, an ESP, and a filter in a 78 m^3 (6 x 4 x 3.5 meters) experimental chamber with an interior surface area of 122 m^2. The air exchange rate ranged from 0.2 to 0.8 h^{-1}. The number mean diameter of the aerosol particles was between 0.1 and 0.2 mm, with a concentration range of 12 to 83 mg/m^3. Radon decay products were collected on Millipore AA membrane filters. The "unattached" fraction was determined by a diffusion battery (DB) that removed the "unattached" decay products while "attached" decay products reached the exit filter. The DB was a parallel plate type with 42 channels, each 32 x 0.38 x 150 mm long with a flow rate of 28.3 lpm. It gave greater than 98% collection of particles with diffusion coefficients greater than 0.004 cm^2/s and less than 10% collection of particles 20 nm and larger. Two groups of researchers defined "unattached" radon decay products to have diffusion coefficients in the range of 0.005 to 0.1 cm^2/s. Such a definition will include much more of the activity size distribution than would be determined by a conventional single screen "unattached" fraction measurement system. Thus, the "unattached" fractions are overestimated in these experiments. Since the models used for dose estimation assign a high dose per unit exposure to this activity, the overestimation of the "unattached" fraction could misrepresent the effectiveness of air cleaning.

The characteristics of air treatment devices investigated by Hinds *et al.* (1983) are given in Table 6. The WL reduction was 67% for the box fan, 60% for the ceiling fan, 75% for the ESP, and 92% for the filter. However, the reduction in the "unattached" decay products concentration is much smaller than that in WL when using the fans and ESP. For the filter unit, 80% of residual activity was "unattached". No significant reduction in ^{218}Po concentration, although there were substantial reductions in ^{214}Pb and ^{214}Bi concentrations.

Maher and coworkers (Maher, 1985; Maher *et al.* 1987) evaluated an ESP, a high efficiency filter, a negative ion generator, a positive ion generator, a negative ion generator with ceiling fan, and a positive ion generator with ceiling fan. The radon decay products were collected on an 0.8 mm pore cellulose acetate membrane filter. The activity size distribution of radon decay products was characterized with a screen-type diffusion battery. Two identical 47-mm closed-faced filter holders (with 0.8 mm diameter pore size membrane filters) were used to sample

Table 6: Characteristics of air cleaning systems examined by Hinds *et al.* (1983).

Air Treatment Device	Flowrate (m^3/s)	Power Consumption (W)	Collection Efficiency for 0.1 μm particles(%)
Box Fan[a]	2.6	185	0
Ceiling Fan[b]	3.3	155	0
ESP[c]	0.11	110	70
Filter[d]	0.11	-	>99.9

[a]Hunter Model 11077, 51 cm
[b]Hunter Model 22306-75, 130 cm
[c]Sears Model 156.73300
[d]Fabricated from nuclear grade HEPA filter

radon decay products. One filter was positioned in front of the diffusion battery. The other was used to collect the activity penetrating various stages of diffusion battery with an 11 stage, 400 mesh, 5.0 cm diameter. The diffusion battery and a Pollak condensation nuclei counter were used to determine particle size distribution.

The activity distributions showed a distinct bimodal appearance with minor and major modes with 2 nm and 100 nm, respectively. The minor mode was assumed to be "unattached" fraction. The size distribution of the minor mode had a considerable spread that covered the range from 1 nm to 6 nm. The "unattached" fraction was assumed for particles with a diffusion coefficient larger than 0.005 cm^2/s. This definition again represents an overestimation of the magnitude of the "unattached" fraction. No activity size distribution data of radon decay products were provided. The AMAD was reported to be between 0.04 mm and 0.17 mm.

The characteristics of the air cleaning systems evaluated by Maher *et al.* (1987) are as following. The filtration unit includes a pleated, high-efficiency, hospital-grade filter and a variable-speed blower within a cabinet. The ESP combines a charging and a collection stage with an activated charcoal bed to remove ozone generated in the charging area. A conventional, 0.13-m diameter, four-bladed ceiling fan, mounted with blades located 0.5 m below the center of the ceiling was tested alone. The combination of an ion generator suspended 0.5 m beneath the ceiling fan was also tested. The fan was operated at a rotational speed of 200/min. The ion generator produced either positive or negative ions at current outputs of 1.2 and 1.4 mA. All of

the devices decreased the radon decay products concentrations and PAEC by up to 50% as shown in Figure 11. However, some devices did increase the "unattached" fraction even to seven times as shown in Figure 12. However, it must be remembered that these "unattached" fraction values are systematically biased above their true values. Using the conversion factors of the HP, JE, and JB lung model, the high-efficiency filter yielded up to a twofold increase in the bronchial dose. The ESP and negative ion generator also increased the bronchial dose at low ventilation rates shown in Figure 13. Figure 14 showed the relative bronchial dose by "updated" James model (James *et al.*, 1989) with the following dose conversion coefficients: 115 mGy/WLM (2 nm) for "unattached" WL and 4.5 mGy/WLM (200 nm) for "attached" WL. Most of air treatment methods reduced bronchial dose, except for the HEPA filter, where the estimated dose increased by 130% at 0.5 h^{-1} filtration rate.

The best treatment method found by Maher was a combination of nonuniform positive space charge generated by an ion generator with enhanced convection from a fan. This systempreferentially removed the "unattached" decay products and the smallest particles because of their high electrical mobility, charge, and susceptibility to turbulent plateout. This system did give a reduction in the WL by about 95% and in the bronchial dose reduction ranging from 68%

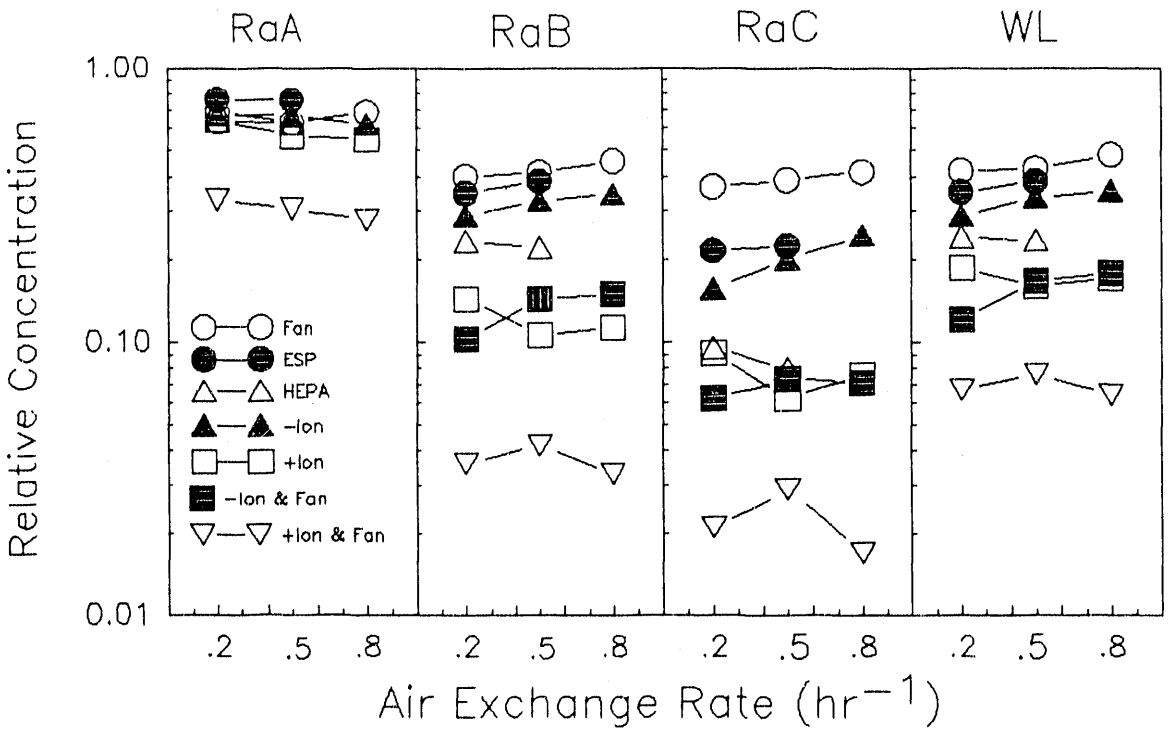

Figure 11 Relative total concentrations of radon progeny and WL after the application of air cleaners. Graph drawn from data from Maher (1985).

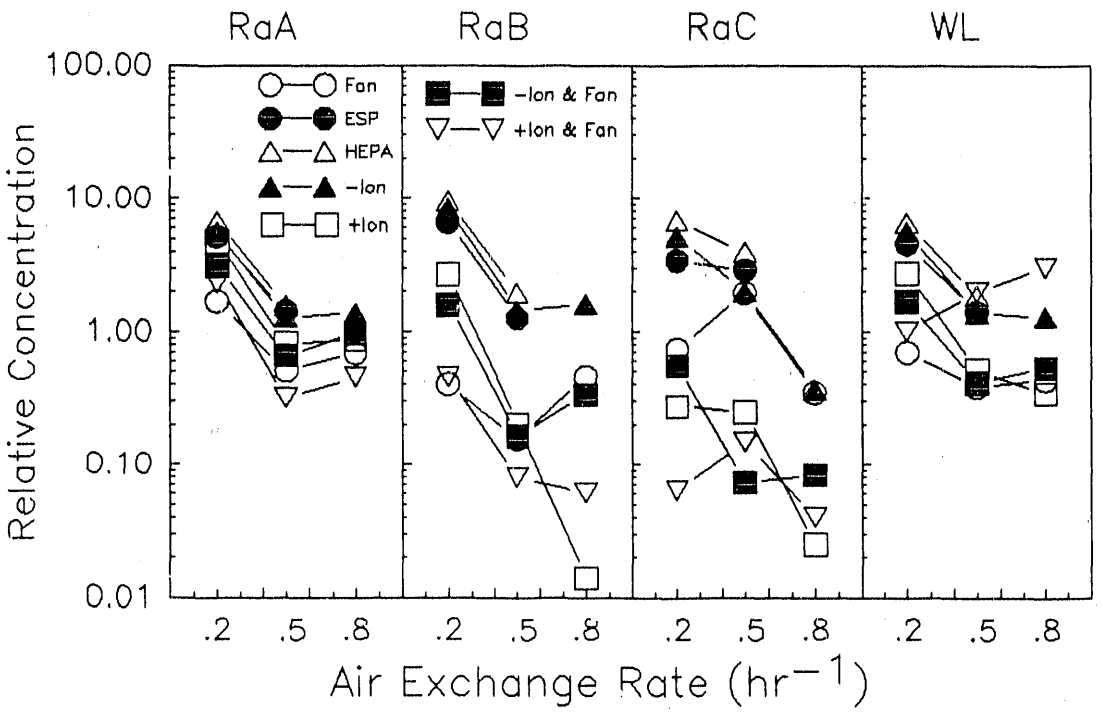

Figure 12 Relative concentrations of "unattached" radon progeny and working levels after the application of air cleaners. Graphs drawn from data taken from Maher (1985).

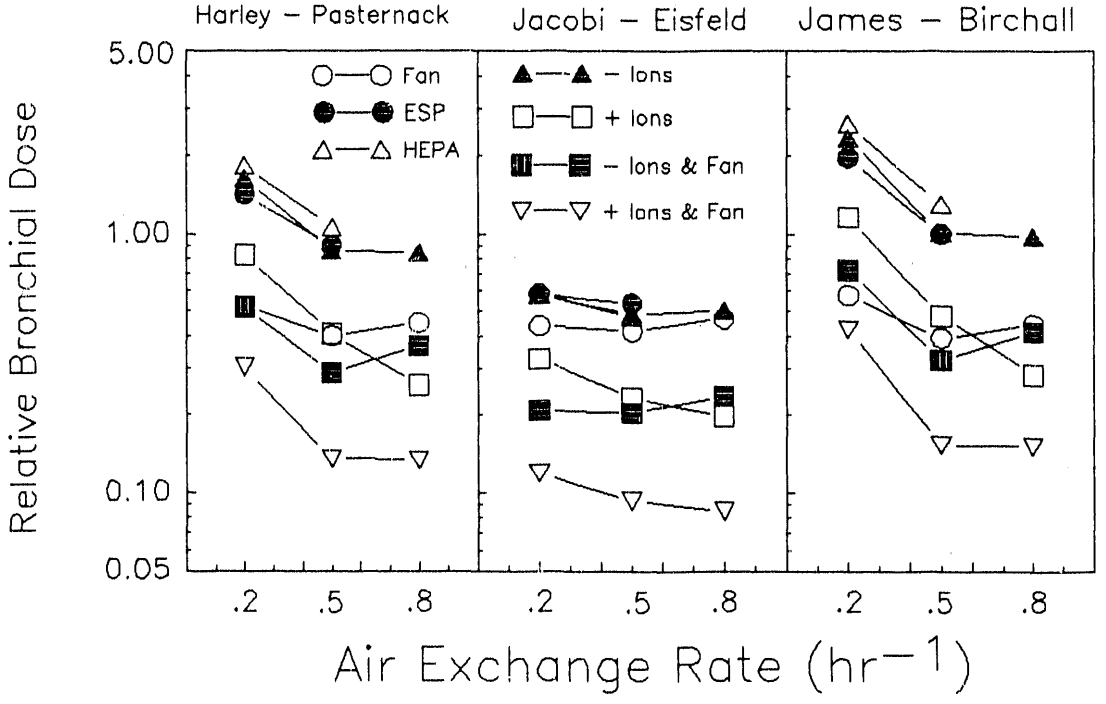

Figure 13 Relative bronchial dose for air after cleaning as a function of air exchange rate. Figure drawn from data given in Maher (1985).

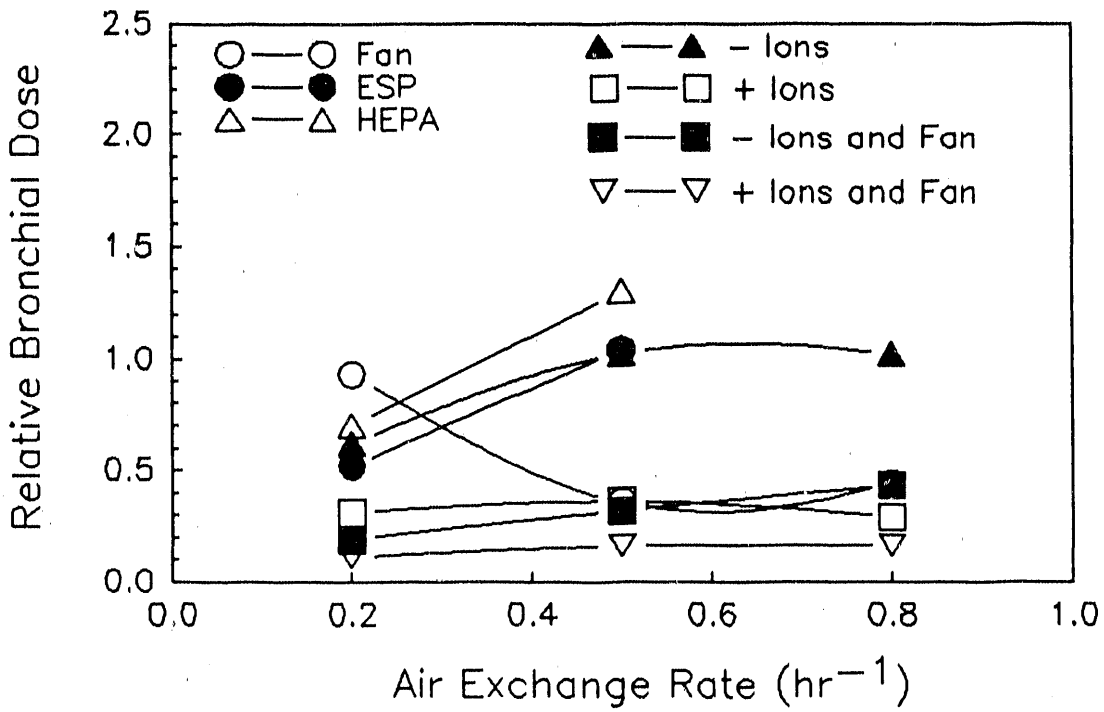

Figure 14 Relative bronchial dose for air cleaning experiments of Maher (1985) using James 1989 dosimetric model.

to 87%, depending on the ventilation rate.

The ion generator system has been commercialized for radon decay product removal, and the unit incorporated filtration as well. The unit had been independently tested by Jonassen and Jensen (1988a). In a 150 m^3 room with aerosol concentration of 15,000 to 20,000 cm^{-3}, and a radon concentration of 1,000 Bq m^{-3} (27 pCi/l), they found that with the positive ion generator on, the PAEC was reduced by a factor of about 4. They also found that the dose as calculated with all three of the earlier dose models and averaged over all age and sex categories was reduced to about 45% of the initial values independent of the use of the filtration unit. When only the filtration system was on and the ion generator was off, the PAEC was reduced by about a factor of 2 and the dose to 65% of the initial value. They reported essentially no effect on the PAEC by the use of the negative ion generator.

Bigu (1983) and Bigu and Grenier (1984) has also shown reductions in the PAEC of both radon and thoron decay products in a relatively small chamber (3 m^3), when using a negative ion generator and a mixing fan. However, no estimation of the effect on the dose were made and the data presented were insufficient to permit the calculations to be performed.

Jonassen (1982) evaluated a filtering system in an experimental chamber with a volume of

324 m^3 and a surface area of 360 m^2. The average radon concentration was found to be approximately 185 - 370 Bq m^{-3} (5 - 10 pCi/l), with values as high as 925 - 1,110 Bq m^{-3} (25 - 30 pCi/l). The "unattached" decay products concentrations were determined by using a fine wire mesh. The membrane filter was used for measuring the total concentrations of radon decay products. The collection efficiency of this wire mesh is greater than 90% for 5 nm particle (Jonassen, personal communication, 1989). The filtering system was installed in the room, consisting of a fan behind a fine filter. The experiments were conducted under conditions of different filtration rates (0.5 - 2 air changes per hour) and aerosol concentrations (10^6 particles cm^{-3}, 3 - 5 x 10^2 particles cm^{-3}, 1 - 5 x 10^2 particles cm^{-3}). Air changes per hour (ach) stands for the rate of the air circulated through the filter. The results indicated the total potential alpha energy concentration and the equilibrium factor, F, effectively decreased with increasing filtration rates and decreasing aerosol loadings. However, the "unattached" fraction of airborne ^{218}Po was found to be less than 1% at the high aerosol concentration (10^{12} particles m^{-3}). At the medium concentration (3 - 5 x 10^{10} particles m^{-3}), f_p is about 25% - 20% and about 80% at the low aerosol concentration (1 - 5 x 10^8 particles m^{-3}). The dose to the basal cells of the epithelium of the bronchi decreased with increasing filtration rate and aerosol concentration, according to the early HP lung model (1972). The more recent HP model (Harley and Pasternack, 1982) would suggest somewhat less dose reduction than the earlier model, but would still suggest that there is always a reduction in dose for realistic initial aerosol concentrations.

Jonassen (1983) evaluated an electric field in a basement room with the volume of 153 m^3 (6 m x 7.3 m x 3.5 m). At a height of approximately 1.7 m above the floor a 15-m long copper wire (diameter 2 mm) was strung along three of the walls at the distance of about 1 m from the wall. The applied field strength is an important consideration for insuring complete collection of ions. The radon concentration was about 185 - 370 Bq m^{-3}. The radon decay products were collected on the membrane filters. No "unattached" decay products measurements were made. The results indicating that, at moderate radon activities (lower than 370 Bq m^{-3}) and low condensation nucleus concentration, the working level may be reduced by a factor of 2 - 3 by applying a few thousand volts to the wire. However, safety considerations makes this control method impractical for residential use. The maximum reductions for equilibrium factor and PAEC by electric field were 87%. The corresponding reductions in doses by HP model were 50% (Jonassen, 1983; Jonassen and Mclaughlin, 1984; Jonassen and Jensen, 1988c).

A series of experiments studying the radon decay products removal effectiveness of

mechanical and electro-filters were performed in an unventilated basement room with average radon concentration about 400 - 500 Bq m^{-3} by Jonassen (1984). The particle concentration was in the range of 50,000 - 150,000 cm^{-3} with a median particle diameter about 0.05 mm. The aerosols were generated by gas burners. The room air was passed through mechanical or electro-filters with filtration rates up to three per hour. The results indicated that the total PAEC and the equilibrium factor, F, effectively decreased by a factor of 4-6 with increasing filtration rates by a factor of two and decreasing aerosol concentrations by a factor of 10. The dose estimate calculated using the 1982-HP model showed that the effect of filtration on the dose depends strongly on the type of individual exposed and upon the model used. When filtration rate was around three per hour, the dose decreased by a factor from two to six (Jonassen, 1982, 1985, 1988a&b).

Another test conducted by Jonassen (1984) was an evaluation of a metal disc (47 mm diameter) on the top of a 2 m high stand placed in the middle of the experimental room. The aerosol particle concentration was between 10^3 and 10^4 cm^{-3} with no filtration. A negative voltage was applied to the disc. The activity measured was not the total activity collected on the disc, but only the activity deposited on the upper surface of the disc. The decay products concentration reduction was up to 70% depending on the applied voltage (5 - 15 KV).

Jonassen and Jensen (1988c) evaluated four different types of filters, three air-exchange rates, and two ionizers in a 120 m^3 room with radon concentration in the range 50 - 6,000 Bq m^{-3}. The radon decay products concentration and "unattached" fraction were determined by alpha spectroscopy of membrane filter and wire screens. The ionizers are very small units (25 cm x 25 cm x 12 cm) mounted about 1 m below the ceiling.

All of the air treatment devices reduced the exposure to 20 - 40% of the value in untreated air. If a combination of two methods was used, the exposure reduction was 80 to 90%. The most effective method found by Jonassen (1984) was the combination of filtration and ionization devices. This system can produce exposure reductions to 10 - 20% as well as a dose reduction of 50% as estimated using 1972-HP model.

Jonassen and Jensen (1987) also conducted field studies to investigate effectiveness of filtration for removing radon decay products in nine Swedish houses. The radon concentrations were in the range of 250 to 3,500 Bq m^{-3}. All four of the filters were electrofilters with different filtration rates. The experimental procedures included the effect of the filter on the room in which the filter is situated (the primary room) and the effect of the filter on a room next to the

room which the filter is located (the secondary room). No activity size distribution measurements were performed. No activity median aerodynamic diameter information was provided. The dose estimation was calculated by "updated" James' model with the reference values (0.9 nm for "unattached" WL and 150 nm for "attached" WL). The calculation showed that the dose was three times that in the untreated air because of the increase in the "unattached" fraction. The effect of filters on secondary room is sometimes significant as that on primary room. The dose reduction still can reach 40% in some cases.

In the most recent report of tests of a filtration unit, James *et al.* (1989) reported the study of a commercial filtration unit that has been placed in a 24 m^3 test chamber to which polydisperse particles had been added. Initial particle concentrations ranged from 3,000 to 4,800 cm^{-3}. "Unattached" fractions were measured using a single screen system similar to that described by George (1972). They observed reductions in the PAEC of 60% to 90% with the unit in continuous operation. They found that the efficiency of the filtration unit for reducing dose would vary with room conditions and that continuous operation would decrease dose by 10% to 60% based on the James model (James *et al.*, 1989). The dose reduction will be greatest for high initial particle concentrations. Air treatment will be less effective in reducing dose in poorly ventilated rooms if the initial particle concentration is low. This result is similar to that reported by Jonassen (1983). Finally, it is emphasized that these results are only applicable to this particular air cleaning system and do not necessarily reflect the behavior of any other system.

Abu-Jarad and Fremlin (1982) installed a mixing fan in an ordinary room to understand the removal mechanics of radon decay products. Their results showed that the fan can plate out from 17% to 84% radon decay products activity in the room in an inverse relationship with the particle concentration (10^2, 10^4, and 10^5 cm^{-3}). The number of radon decay products deposited per unit area on the two sides of the blades of the fan are more than those plated out per unit area on the surface of the walls. However, the total surface area of the fan blades is only 0.2% of the surface area of the walls. Therefore, more than 99% of the plateout activity was found on the walls and less than 1% on the fan blades (Abu-Jarad and Sextro, 1988).

Nazaroff *et al.* (1981) evaluated a mechanical ventilation system with heat recovery as an energy-efficient control technique in houses. This unit provides fresh outside air to the living space while exhausting an equal amount of indoor air to the outside. The radon concentration was consistently greater 740 Bq m^{-3}. Radon decay products concentrations were measured by the Residential Radon Daughter Monitor (RRDM) developed at Lawrence Berkeley Laboratory

(Nazaroff, 1980). At ventilation rates of 0.6 air change per hour and higher, radon decay products levels dropped below the 0.02 WL value as an indoor guideline level of Atomic Energy Control Board of Canada (AECB, 1979). The variations in radon concentration at a given ventilation rate are much smaller than the variations that occur when the ventilation rate is changed.

4.3 Discussion

The above investigations demonstrated that the air cleaning systems can effectively remove radon decay products from indoor air. At the same time, particles are removed from the air. As a result, the "unattached" fraction increases and may be more effective in depositing their radiation dose to the lung tissue. The dose reductions are therefore always smaller than the PAEC reductions. In some cases, it is estimated that the dose can increase even with lower airborne radioactivity concentrations.

There are two major problems in these previous investigations. The first one is that the measurement systems were not able to determine the full size distribution of radon decay products, especially smaller than 10 nm in diameter. The second problem is that the dose estimates are made based on very simple lung models. Only estimates of the "unattached" fractions were made. At the same time, some of these measurements include a larger portion of the size distribution than is generally accepted as "unattached". In many of the reported studies, the methods of size measurement of radon decay products and the study of the results are not clearly stated. The determinations of "unattached" fraction in previous measurements are not consistent with each other or with the dosimetric models, especially regarding specification of the diffusion coefficient. Because of the importance of particle size in relating exposure to dose, it becomes difficult to have a full assessment of the reported air cleaning systems' effectiveness. The health risk estimations have been made with different dose models, and thus considerable differences in the resulting dose estimates have been obtained. The important factor for these discrepancies is that all these three models (HP, JE, and JB) had higher dose factors for "unattached" than for "attached" decay products. Recent investigations showed that the dose conversion factor is strongly dependent on the actual activity size. The separation of "unattached" and "attached" fractions is insufficient to provide accurate dose estimation. Therefore, further research is needed to measure the concentration and the full activity size distribution of the radon decay products where air cleaner devices are employed.

CHAPTER 5
METHODOLOGY

5.1 Introduction

This chapter describes the protocol for the field measurements taken in three single-family houses located in Springfield, PA, Princeton, NJ, and Northford, CT. The descriptions of each house are given below.

Radon concentration, condensation nuclei count, and activity-weighted size distribution of radon-decay products were measured in each house. A continuous radon monitor (CRM) was used to determine radon concentration. The particle number concentration was measured by using a condensation nucleus counter (CNC). The semi-continuous screen diffusion battery system (Ramamurthi, 1989) was used to measure the concentration and activity-weighted size distribution of radon decay products. The characteristics of these measurement systems will be described.

Two types of air cleaners each based on a different particle removal principle were evaluated. The first device is a room-type air filtration system. The second one is an electronic air cleaner which collects particles by using an electric field. The characteristics of the air cleaners are described in detail.

The influence on the behaviors of radon decay products by various indoor particle sources was investigated. Aerosols were generated by running water in a shower, washing and drying clothes, burning a candle, smoldering a cigarette, vacuuming, opening a door, and cooking. The time sequences of measurements and particle generation are also listed.

The room model (Porstendörfer *et al.*, 1978) was used to calculate the changes in several aerosol parameters of radon decay products such as the attachment rate, the deposition rate of the "unattached" fraction, and the average attachment diameter. Using James dose models (James, personal communication, 1989, 1990), the estimated bronchial doses can be made. The calculation of both aerosol parameters, hourly dose rate, and yearly bronchial dose are presented.

5.2 House Characteristics

5.2.1 House in Springfield, PA

The house in Springfield, PA is located about twenty miles from Philadelphia. The house consists of a living room, a dining room, and a kitchen on the first floor, two bedrooms, a bathroom, and a study on the second floor, and an unfinished basement. Typical radon

concentration in the basement was in the range of 74 - 148 Bq m^{-3} and around 56 - 111 Bq m^{-3} on the first floor.

The sampling location was in the basement. The basement had a volume of approximately 75 m^3 (5.5 m × 5.5 m × 2.5 m). A washing machine, clothes dryer and heating system are located in the basement. The heating system is an oil furnace with an electronic air cleaner and humidifier. In the absence of the room filtration unit operating in the basement, the particle concentration was always above 100,000 cm^{-3}. In addition, the particle concentration in the larger bedroom was on the order of 150,000 cm^{-3} with a particle concentration of 120,000 cm^{-3} in the other bedroom. At the same time, the outdoor particle concentration was 30,000 cm^{-3}. In order to identify the particle source, the oil-fired furnace was turned off (temperature set at 7°C) for about four hours. The particle concentration in the basement then decreased to 20,000 - 30,000 cm^{-3}, a more typical indoor particle number concentration. Subsequently, the nozzle of the oil furnace was changed. No effect of this change was observed on the particle concentration. Therefore, it appears there is a problem with leaks from the furnace combustion zone to the house, although a furnace repair technician could not identify a problem.

5.2.2 House in Princeton, NJ

The house near the Princeton University campus in Princeton, NJ is a one-story residence with a living room, dining room, kitchen, study, two bedrooms, two bathrooms, and a basement. An oil furnace is used for heat, and a gas stove is used for cooking. The first floor plan of the house is shown in Figure 15. The measurements in this house were in collaboration with Princeton University's Center for Energy and Environmental Studies (CEES). The CEES group has made a study of ventilation, radon entry pathways, and interzonal transport within this house. They instrumented the house for the measurement of radon and several physical parameters. The continuously monitored physical parameters are : (1) the basement, bedroom, and subslab radon concentrations; (2) the pressure differences across the southern basement/outside interface, basement/subslab, basement/upstairs, and the eastern basement/outside interface; and (3) the temperatures in the basement, upstairs, outside, and soil. Radon concentration on the first floor could reach 7,400 Bq m^{-3}. A subslab fan system was operating in the basement as a way of reducing the indoor radon concentration. The particle concentration in the kitchen was always in the range of 80,000 - 100,000 cm^{-3} because of the gas stove's pilot lights. In the living room and dining room, the particle concentration was around 9,000 - 13,000 cm^{-3}. The particle

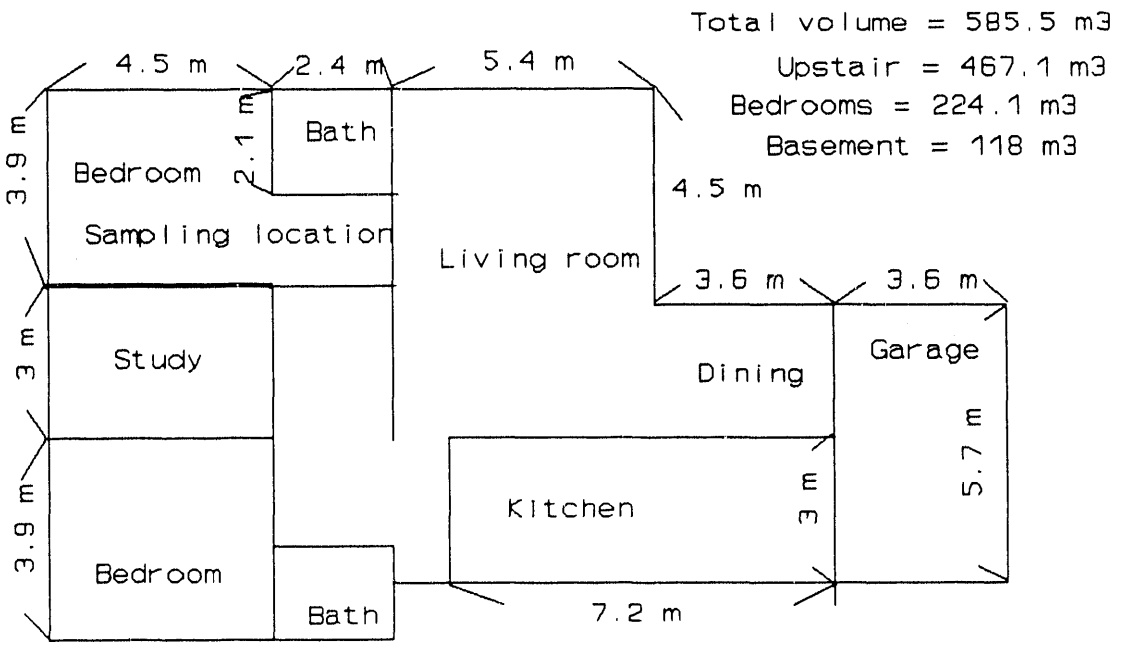

Figure 15 Princeton house first floor plan.

concentration of 5,500 - 10,000 cm^{-3} was observed in the two bedrooms when the bedroom doors were open.

5.2.3 House in Northford, CT

The single-family house in Northford, CT is located twenty-five miles north of New Haven. The house is a one-story residence comprised of a living room, dining room, kitchen, two bedrooms, a study, a bathroom, and a basement. The living room, dining room, and kitchen are connected together as one open space. The first floor plan of the house is shown in Figure 16. An electric stove is used for cooking. The heating system is an oil furnace. During the winter, the occupants sometimes burn wood in a fireplace as an auxiliary heat source. None of the occupants smoke. Radon concentration on the first floor was in the range of 37 - 240 Bq m^{-3} and between 111 and 370 Bq m^{-3} in the basement. The typical particle concentrations were below 10,000 cm^{-3} in the basement and 4,000 cm^{-3} on the first floor. During the sampling period, the fireplace was not used and the door to the basement was always closed. The thermostat was set at 18° C.

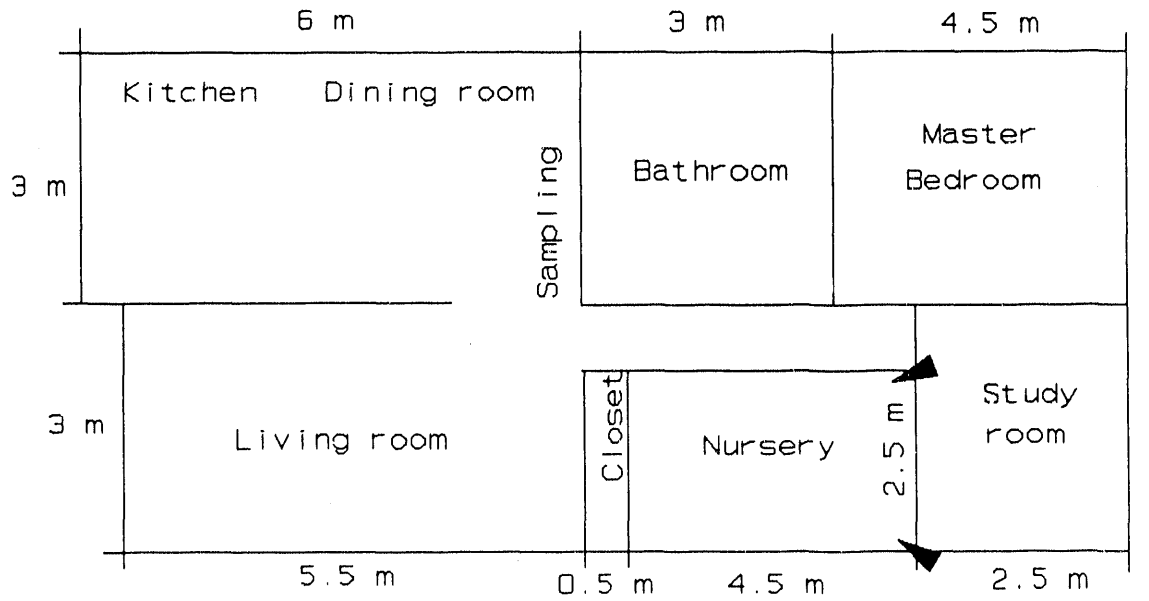

Figure 16 Northford house first floor plan.

5.3 Measurement Systems

5.3.1 Measurements of Radon and Particle Concentrations

Radon concentration was monitored constantly during the experiments with a CRM. The CRM was designed and built by Lawrence Berkeley Laboratory (Nazaroff *et al.*, 1981). The CRM includes a scintillation cell, a photomultiplier tube, and a high voltage power supply. Each CRM used in this study was calibrated in a radon chamber (Gadsby, 1990, personal communication) to obtain calibration equation for radon concentration calculation. The general form of the calibration equation is ax + b, where a and b are calibrated constants with x representing alpha counts per minute. A CNC made by Gardner Associates, Inc. was used to measure particle number concentration. The CNC is designed to measure particles by condensation of water vapor on the surfaces of the particles to produce optically detectable droplets of several micrometer diameters. Therefore, the droplets can be determined by photometric measurements by the scattering of light by the droplets in a chamber of fixed volume. A standard technique for producing supersaturation of water vapor in CNC is to humidify the sample to near saturation followed by a rapid adiabatic expansion to lower the temperature below the dew point. Once supersatured, the excess water vapor proceeds to condense upon any particles present. This CNC can detect particles larger than 10 nm and smaller than 10 μm.

5.3.2 Concentration and Size Distribution Measurements of Radon Decay Products

The conventional method to measure the "unattached" fraction of radon decay products in ambient and mine atmospheres utilizes single wire screen systems (James *et al.*, 1972; Thomas and Hinchliffe, 1972; George, 1972). James found that 200 mesh wire gauze collected airborne "unattached" ^{218}Po with an efficiency of more than 98%, at 10 lpm air-sampling rate through an area of 14 cm^2. Thomas and Hinchliffe evaluated the efficiency of four wire screens (different screen mesh size, opening/cm, screen wire diameter) in filtering ^{218}Po aerosol at air velocities from 5 to 50 cm s^{-1}. The efficiencies of about 5% - 95% were obtained. George showed that a reasonable collection efficiency for "unattached" radon decay products can be obtained by a proper combination of mesh size and air velocity. Particles of approximately 50 nm and 100 nm were used to determine the collection efficiency of particles by screens. The combined result of zero collection of condensation nuclei and appreciable efficiency for ^{218}Po atoms was taken as confirmation that 60-mesh screen had the best performance. However, the "unattached" fraction is in reality an ultrafine cluster mode in the 0.5 - 5 nm size range. It is evident that the collection efficiencies versus particle diameter characteristics of wire screens do not provide a distinct separation of the "attached" and "unattached" fraction (Ramamurthi and Hopke, 1989). The development of an alternative measurement system to capably determine the full size distribution of radon decay products was needed.

Ramamurthi (1989) developed a Graded Screen Array (GSA) system (non-conventional wire screen diffusion batteries) to determine both the concentration and size distribution of radon decay products from 0.5 nm to 500 nm. The original design and conceptual framework of this system were presented by Hopke (1986) and Kulju *et al.*(1986). The measurement system involves the use of a combination of a number of sampler-detector units similar to that shown in Figure 17. The screen was wrapped around the sampler covering the slit except for the one sampler that is left open for measuring the total concentration of radon decay products. The operation of the system involves the sampling of air simultaneously through all the units at independent flow rates (parallel operation). Each sampler-detector unit is thus an independent stage. Every stage separates the airborne activity based on atmospheric diffusion coefficient, which is related to the particle size. The upper section of each sampler-detector unit consists of an ORTEC Model DIAD II ruggedized with a 450 mm^2 surface barrier alpha detector (EG & G ORTEC, Oak Ridge, TN) sealed into an aluminum block. The detectors in the sampler/detector units are connected to a single IBM PC based multichannel analyzer through a multiplexer.

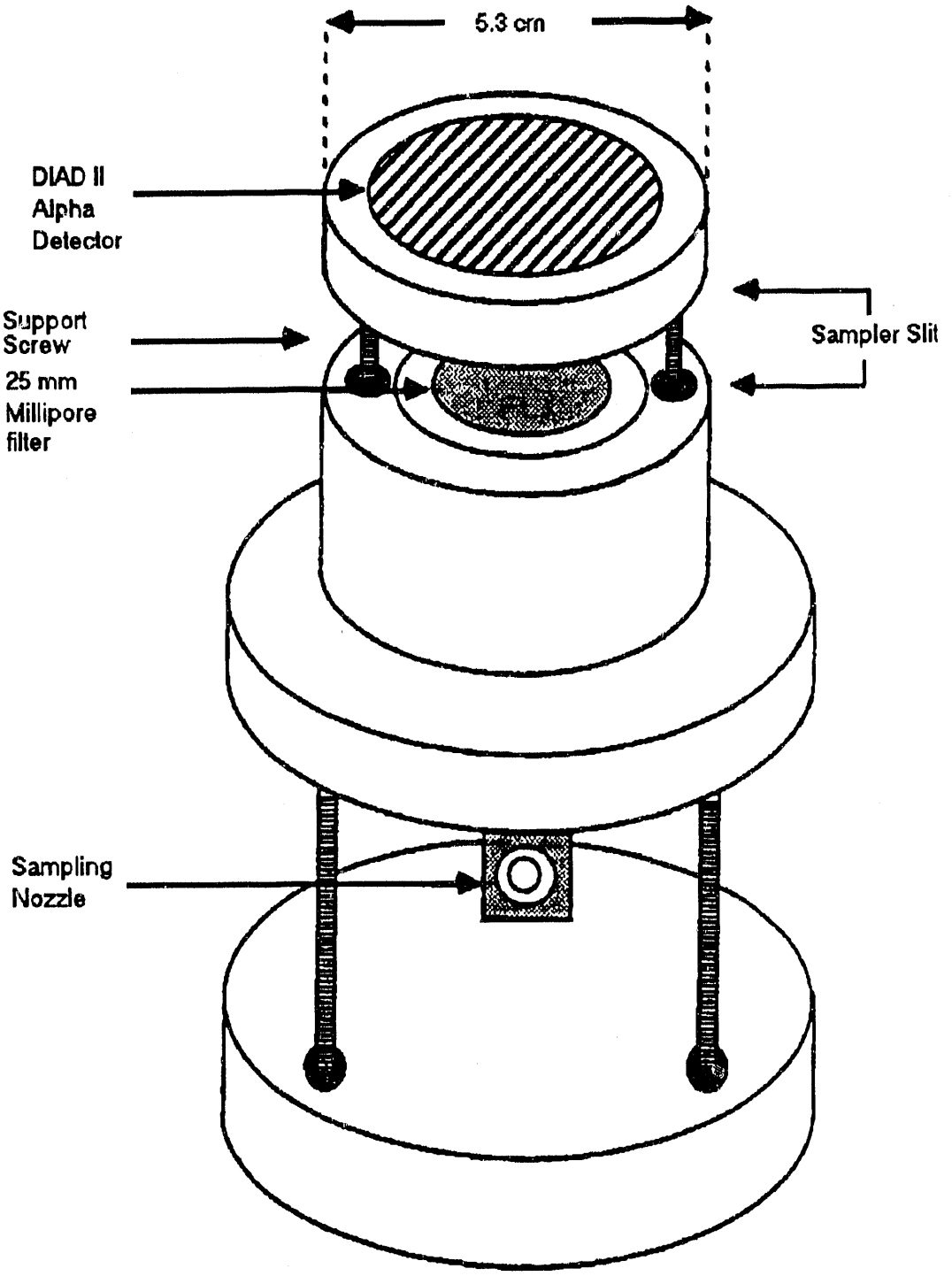

Figure 17 Sampler-detector unit in the measurement system.

Figure 18 is a schematic diagram of the various components of the measurement system. A

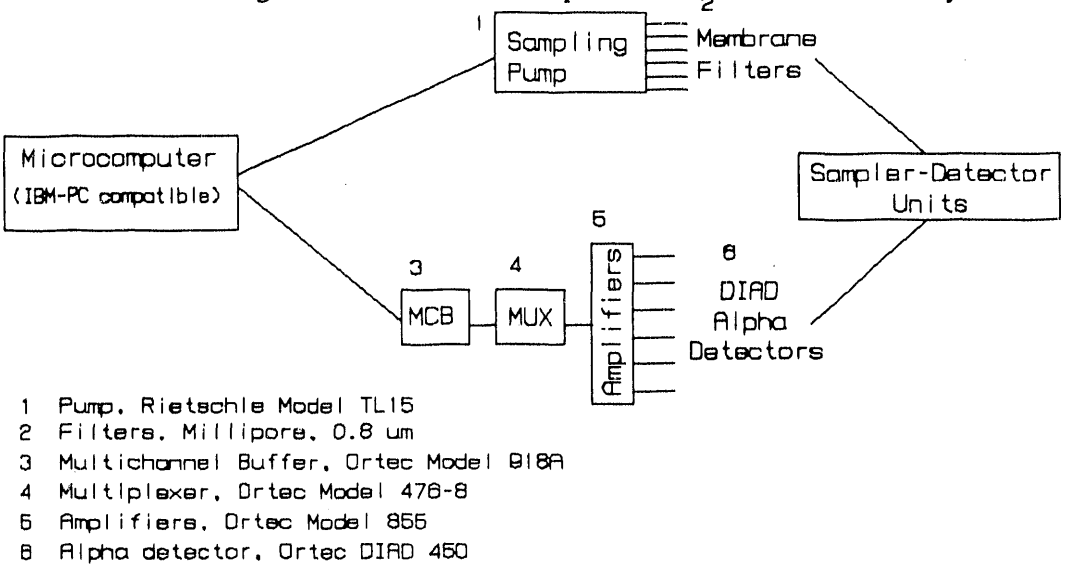

Figure 18 Schematic representation of the various components of the measurement system.

dedicated microcomputer controls acquisition of the alpha spectra, operation of the sampling pump, sample time sequencing, and data analysis. The IBM PC-based analysis system allows the determination of the concentrations of ^{218}Po, ^{214}Pb and ^{214}Bi (or ^{214}Po) that penetrate to the filter in each sampler-detector unit using alpha spectroscopy with counting while sampling.

The sequence of optimum sampling and counting intervals depends on several

Table 7 Sequence of steps involved in a typical measurement using the ASC-GSA system.

Time(min)	Event
0	Pump ON MCA Acquisition Start - First alpha spectrum
15	Pump OFF MCA Acquisition End First alpha spectrum saved
35	MCA Acquisition Start - Second alpha spectrum
75	MCA Acquisition End Second alpha spectrum saved
75	Start next sample

Table 8 Optimum wire screen combinations and sampler-detector design and operating parameters for the six stages in the ASC-GSA system.

Unit	Sampler Slit Width (cm)	Sampler Diameter (cm)	Screen Mesh	Dp_{50} (0.5-350nm) (nm)
1	0.5	5.3	-	-
2	0.5	5.3	145	1.0
3	0.5	5.3	145x3	3.5
4	0.5	5.3	400x12	13.5
5	1.0	12.5	635x7	40.0
6	1.0	12.5	635x20	98.0

Sampling Flow Rate = 15 lpm (each unit)
Detector-Filter separation = 0.8 cm (each unit)

environmental factors, including the fluctuations in radon activity levels and the degree of disequilibrium between the various decay products. A typical sampling sequence is utilized to determinate the concentration and size distribution of decay products for radon concentration in the range of 185 - 1,850 Bq m^{-3}. This time sequence (0-15, 0-15, 15-35, 35-75) refers to a 15-minute sampling interval during which the first ^{218}Po and ^{214}Po counting interval from 0 - 15 minutes is acquired followed by a 20-minute delay period and a second ^{214}Po counting interval between 35 - 75 minutes. For radon concentration below 185 Bq m^{-3}, the sequence (0-30, 0-30, 30-50, 50-90) can yield sufficient measurement sensitivity. The sequence of the steps in the measurement procedure is shown in Table 7 (Ramamurthi, 1989). The sequence yields a nominal detection limit of 3.7 Bq m^{-3} for ^{218}Po, ^{214}Pb and ^{214}Bi, and 0.05 mWL for PAEC at a 25% (one σ) uncertainty level.

The alpha counts from ^{218}Po and ^{214}Po in the two counting intervals are used to calculate concentrations of radon decay products penetrating into each unit. Given knowledge of the penetration characteristics of each GSA stage and the measured detection efficiency of each sampler, the activity size distributions can then be calculated from the observed stage activities using the reconstruction algorithms described by Ramamurthi and Hopke (1989). The observed concentrations of ^{218}Po, ^{214}Pb, and ^{214}Bi activity penetrating into each sampler will allow the reconstruction of the corresponding activity-weighted size distributions using the Expectation-Maximization algorithm (Maher and Laird, 1985). The penetration characteristics of five stages with screen are calculated using the Cheng-Yeh penetration theory since the wire screen

parameters used in these samplers are identical to those of Yeh *et al.* (1982). The determination of optimum sampler-detector design and operating parameters (sampler diameter, slit width, detector-filter distance, and sampling flow rate) were determined by experimental testing of a prototype sampler-detector unit in a 2.43 m^3 radon-aerosol chamber and theoretical studies described by Ramamurthi (1989) and Ramamurthi *et al.*(1990). Table 8 summarizes the wire screen combinations and sampler-detector design and operating parameters for the six stages in the automatic semi-continuous GSA (ASC-GSA) system. The number of stage (six) and stage progression was based on the conclusions of the simulation study (Ramamurthi and Hopke, 1990). The number and width of the size intervals used in the reconstruction process were dictated by considerations of size distribution accuracy and stability. An optimum number of six inferred size intervals in geometric progression within the 0.5 - 500 nm size range was selected. The mid-point diameters of size range 0.50 - 1.5, 1.5 - 5.00, 5.00 - 15.0, 15.0 - 50.00, 50.00 -150.0, and 150.0 - 500.00 nm are 0.9, 2.8, 8.9, 28.1, 88.9, and 281.2 nm, respectively. This progression of size intervals provides sufficiently large differences in the penetrability through the various stages. Therefore, it results in sufficient size resolution in the inferred activity distribution. An upper size limit of 500 nm was imposed on the inferred size distribution to prevent from collection by impaction and interception of larger particles. Typically, indoor air does not have large numbers of particles larger than 500 nm (Reineking and Porstendörfer, 1986), therefore the fraction of radioactivity within this size range could be neglected.

For each activity size distribution presented in this study, the radon concentration, the particle number concentration, and the concentrations of three decay products with the associated measurement errors are listed along with the figure. The ^{218}Po distribution is plotted as a histogram to illustrate the inferred nature of the distribution. The ^{214}Po and ^{214}Bi distributions are shown by curves connecting the mid-point diameter values. A Monte Carlo type stability analysis was performed for each of size distributions. This analysis makes an estimate of the stability of the inferred solutions with respect to errors in the input penetration data. Ten sets of data were generated from each sequence of decay products penetrations by superposing a degree of random error in the data. Each measured decay products concentration is regarded to be normally distributed with a standard error equal to the estimated measurement error. The ten size distributions obtained from the reconstruction algorithms for each measured sequence of penetrations were combined to yield average size interval fractions and variances shown by error bars in each interval fraction. "Unattached" fraction in this study is regarded over the range of 0.5

to 1.5 nm size range. The whole aerosol size range can be divided into four modes. The "cluster" mode is in the 0.5 -10 nm size range. The "nucleation" mode is between 10 nm and 100 nm. For the "accumulation" mode, the size range is 100 nm - 500 nm. Particles larger than 500 nm are considered to be in the "coarse" mode.

Since the technology for making these size measurements is still evolving, there are no final protocols for routine measurements. Thus, one of the purposes of the field trials was to test the initial protocol suggested by Ramamurthi (1989). Distributed standards to test the accuracy and precision of the measurements are not available. Therefore, intercomparison with other expert groups is the only way to corroborate the measurements of size distribution of radon decay products. Quality assurance for airborne alpha energy concentration of this measurement system is being obtained by intercomparison with the group in the Environmental Measurements Laboratory (EML). EML is 1 of 4 OECD (Organization for Economic Cooperation and Development) radon measurement reference laboratories in the world and the designated reference laboratory for the Department of Energy's Radon Research Program. This ASC-GSA system for size distributions has been intercompared with other designs of U.S. Bureau of Mines and the Department of Energy's EML (Holub and Knutson, 1987), the Australian Radiation Laboratory (Solomon, 1988), the National Radiation Protection Board of the United Kingdom (Strong, 1988), and the University of Göttingen (Reineking and Porstendörfer, 1986) in late April 1989. The results provided confidence in radon decay products measurement proficiency and reliability of this system. In September 1989, a one-week sampling experiment (Ramamurthi and Hopke, 1990) was conducted in a house in the Princeton area to perform additional testing of the system at high radon concentration (1,750 Bq m^{-3}) and at low concentration (111 Bq m^{-3}, resulting from heavy rain). These measurements were in collaboration with CEES at Princeton University. The CEES group has considerable expertise in ventilation, radon entry pathways, and interzone transport within houses. They have instrumented several houses for the measurements of radon and physical parameters (e.g, temperature, pressure). The results showed a reasonable representation of the state of the radioactive aerosol being examined.

5.4 Characteristics of the Air Cleaners

Two types of air cleaners investigated in this study are an air filtration system and an electronic air cleaner. The characteristics of these two air cleaning system will be discussed below.

5.4.1 Air Filtration System

The air filtration system used in this work was called a Pureflow Air Treatment System manufactured by the Amway Corporation, Ada, Michigan. It is a multi-stage filtering system containing a total of five separate filters : (1) a flexible, foam pre-filter which traps hair, lint, and large dust particles, (2&3) two activated carbon filters that contain two pounds each of proprietary blends of a variety of specially treated activated carbons, supported uniformly in honeycomb beds covered with white filter media and encased in a high quality aluminum frame, (4) a final carbon filter which is composed of activated carbon bonded to a non-woven substrate, and (5) a high efficiency particulate air (HEPA) filter that is designed to maximize filter efficiency, eliminate leaks and reduce the possibility of breakage. This HEPA filter contains the same filtering material used in many hospital surgical suite air filtration system and industry "clean rooms". Figures 19 and 20 show the filter installation inside of the air filtration system. The pre-filter (B) and activated carbon filters (C, D) are installed at the back of the system. The third carbon filter (J) and the HEPA filter (I) are placed in the front of the air filtration system. The system's microcomputer allows the programming up to four different sets of ON-OFF times and fan speeds for automatic operation. There are four fan speeds, 1.13, 2.26, 3.40, and 4.25 m^3 min^{-1}.

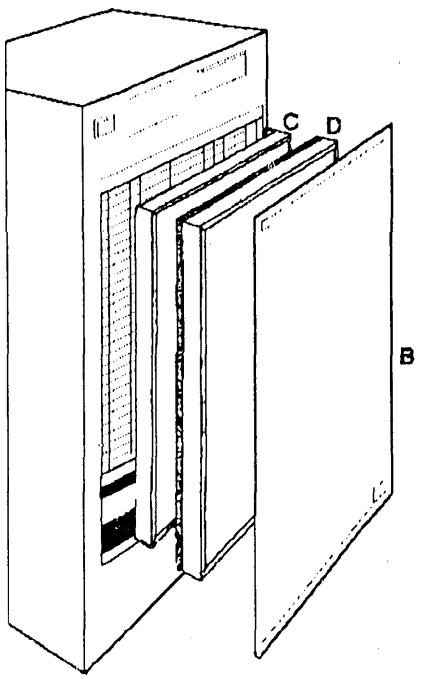

Figure 19 The back cabinet of the air filtration system. B: Prefilter; C and D are activated carbon filters.

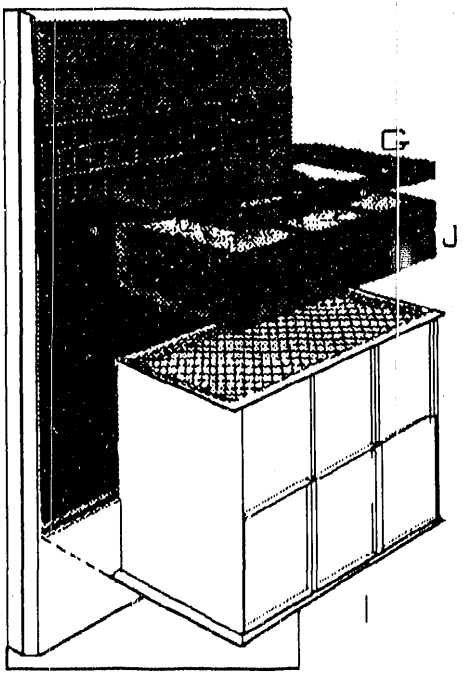

Figure 20 The front cabinet of the air filtration system. I: HEPA; J: Final carbon filter.

The air filtration system can give maximum particle removal efficiency when operating at the highest speed (4.25 m^3 min^{-1}). The fan speeds of air filtration system are calibrated by the Amway company and were not calibrated in this study. The Amway calibration showed small fluctuations (about 5%) of fan speeds for the unit tested. No collection efficiency of particle with in the 0.5 nm - 500 nm size range was conducted in this work. When placing the air filtration system in a room, the back of the cabinet requires at least a three- inch spacing from a wall. Also the unit must be clear of any objects that could restrict the intake of air. System maintenance requires that the filters be changed after approximately six months of operation. Replacement times may vary depending on environmental conditions. In the absence of exposure to high concentrations of organic such as painting supplies, insecticides or pesticides, it is recommended that the two activated carbon filters located inside the back of the cabinet be replaced at least every six months. Depending on conditions some filters may have to be replaced more frequently than every six months. During this study, no filters of the air filtration system were changed. No collection efficiency tests for gaseous contaminants that could have been collected by the air filtration system presented.

5.4.2 Electronic Air Cleaner

The electronic air cleaner is a positive voltage ESP made by the Honeywell Company, Golden Valley, MN. This portable air cleaner includes one electronic cell (46.6 cm × 31.7 cm, including the charging and collection sections), three propeller fan speeds (4.53, 7.50, and 9.34 m^3 min^{-1}), one activated carbon filter (32.4 cm × 41.0 cm), two prefilter screens (32.7 cm × 41.3 cm), and a high voltage power supply. The components of this cleaner are as shown in Figure 21. During normal operation air is drawn into the electronic air cleaner through the prefilter screen at the rear of the unit. The internal fan then pulls the air through the electronic cell and the activated charcoal filter, discharging the air through the front of the cabinet. The prefilter screens out the larger airborne particles. Airborne particles are then carried into the electronic cell where they pass through a powerful electric field established between a series of electrodes and ionizing wires. In passing through this field, the particles become electrically charged. When entering the collector section of the electronic cell, the particles enter a second electric field established between a series of parallel metal plates. Every other plate is a high positive potential while the alternate plates are at ground potential. The charged particles are attracted to the ground plates of the collector and attach to the plate until they are washed off in the cleaning cycling. Odors are removed by the activated charcoal filter before clean air is discharged. The air cleaning process is summarized as shown in Figure 22. The time period between cell washing varies with the applications and the way the air cleaner is used. The recommendations from the Honeywell company for the typical applications are (1) one to two months in an office, (2) once a month in a meeting room, and (3) every one to three months in a home. The electronic air cleaner was used as supplied by the Honeywell company. No flow calibration and collection efficiency measurements of this air cleaning system was performed in this study. The collection section of the electronic air cleaner was not washed in this work because the operating period of time was not long enough (one week).

5.5 Experimental Setup

5.5.1 House in Springfield, PA

An initial field trial of the air filtration system was performed in a two-story single-family house in Springfield, PA. The electronic air cleaner was not yet available for these studies. Therefore, the results are presented only for the influence on radon decay products by the air filtration system. The goals of this field study were to check the measurement system and make

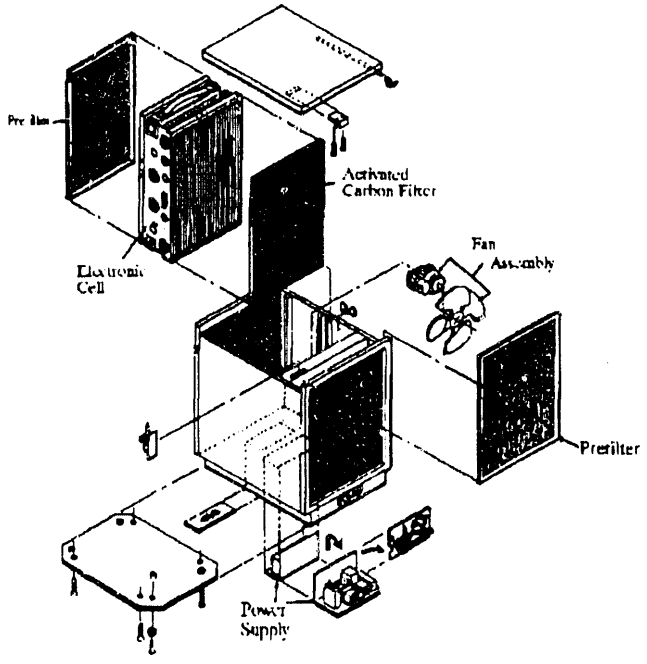

Figure 21 The components of the electronic air cleaner.

an initial comparison of activity size distributions both with and without the air filtration system. Radon concentration was below 185 Bq m^{-3} in the house and radon level in the basement was higher than that on the first floor. In order to obtain more accurate results from the measurement system, activity size distributions of radon decay products were measured in the basement over the period of a week (12/12/89-12/19/89). At the same time, the characteristic of radon decay products in the basement can be made. Because the radon concentration was below 185 Bq m^{-3}, the concentration and size distribution of radon decay products were measured with a sequence (0-30, 0-30, 30-50, 50-90). A total of 20 measurements were made during the seven day period with and without the air filtration system operating. In addition, the clothes dryer was operated at a specific time for thirsty minutes during this period. During the measurements, the windows and the door from the basement to the upstairs were closed and the thermostat was set at 18° C (65° F). No note was made as to whether the heating system was on during the sampling period. The air filtration system was placed in the middle of the basement, and the fan speed was kept at 4.24 m^3 min^{-1}.

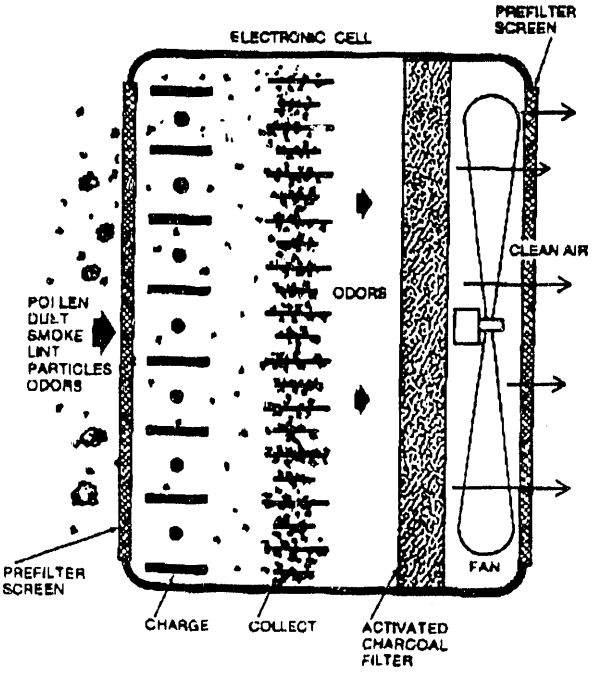

Figure 2? The air cleaning process of the electronic air cleaner.

5.5.2 House in Princeton, NJ

In order to understand the behavior of radon decay products in the indoor environment, activity size distributions were measured in the living room and the master bedroom over a two-week period (1/16-1/31/90). The house was unoccupied during the measurements, thus the Princeton house can be regarded as an experimental home. Since people spend approximately eight hours per day in the bedroom, the primary sampling location was chosen to be in the master bedroom which adjoins one of the bathrooms. More than one hundred measurements were made in the bedroom, and only four measurements were taken in the living room. A sequence (0-15, 0-15, 15-35, 35-75) was used to determine the concentration and size distribution of radon decay products because radon concentrations were in the range of 185 - 1,850 Bq m^{-3}.

The goals of this study are (1) to understand the typical behavior of radon decay products in the domestic environment, and (2) to compare the difference in concentration and size distributions of radon decay products both with and without the air filtration running while each type of particle was generated. The air filtration system was operated with a constant speed of 4.24 m^3 min^{-1}. During these measurements, the electronic air cleaner was not yet available. Aerosols were produced from running water in a shower, burning a candle, smoldering a cigarette, vacuuming, cooking, and opening the bedroom door. Measurements of size distributions were

made during the active particle generation period and over time after the aerosol production stopped. No determination of ventilation rate was made during the measurements. The thermostat on the first floor was set at 18° C (65° F) and no note was made about when the heating system was operated or off. The time sequence of particle generation and measurement is as following:

Running Water in a Shower

Warm water used for a shower was run in a shower for 20 minutes in the master bedroom with the bedroom door closed (0-20 minutes from experiment start). Measurements were made in the master bedroom during the water running interval (0 - 15 minutes from the experiment start), 55 minutes after the end of the water running interval (75 - 90 minutes from the experiment start), and 130 minutes after the end of the water running interval (150 - 165 minutes from the experiment start).

Burning a Candle

A candle burned for 20 minutes in the master bedroom with the closed bedroom door (0 - 20 minutes from the experiment start). Measurements were made in the master bedroom during the candle burning interval (0 - 15 minutes from the experiment start), 55 minutes after the end of the burning interval (75 - 90 minutes from the experiment start), and 130 minutes after the end of the burning interval (150 - 165 minutes from the experiment start).

Smoldering a Cigarette

Two cigarettes were burnt consecutively for a total of 20 minutes in the master bedroom with the bedroom door closed (0 - 20 minutes). The cigarette produced only sidestream smoke. The measurements were made in the master bedroom 5 minutes after lighting the cigarette (5 - 20 minutes), 60 minutes after the end of the burn interval (80 - 95 minutes from the experiment start), and 135 minutes after the end of the burn interval (155 - 170 minutes from the experiment start).

Vacuuming

A vacuum cleaner was operated in the master bedroom for 20 minutes with closed bedroom door (0-20 minutes). Measurements were made in the master bedroom 5 minutes after

vacuuming began (5 - 20 minutes), 60 minutes after the end of the vacuuming period (80 - 95 minutes after the experiment start), and 135 minutes after the end of the vacuuming period (155 - 170 minutes after the experiment start).

Cooking

A steak was pan fried for 20 minutes (0-20 minutes) using the gas stove in the kitchen. The master bedroom door was open for this experiment. Measurements in the master bedroom were made 5 minutes after cooking started (5-20 minutes), 60 minutes after the end of the cooking interval (80-95 minutes after the experiment start), and 135 minutes after the end of the cooking interval (155-170 minutes after the experiment start).

5.5.3 House in Northford, CT

Activity size distributions were measured over a three-week period (3/21/90-4/12/90). The sampling location was chosen in the middle of the three-room open space (6.0 m × 6.0 m × 2.5 m). The two air cleaners (air filtration system and electronic air cleaner) were installed in one corner of the living room. For the first week (3/21/90-3/27/90), the room-type air filtration system was operated for the entire week with a flowrate of 4.28 m^3 min^{-1}. During the second week (3/28/90-4/4/90), the background conditions without any air cleaner were measured without any air cleaner running. During the third week (4/5/90-4/12/90), the electronic air cleaner was operated at 4.67 m^3 min^{-1} for the whole week. Because the electronic air cleaner has the potential of producing ozone (Rajala *et al.*, 1986), a continuous ozone monitor was used to measure the ozone concentration in the house. A sequence (0-30, 0-30, 30-50, 50-90) was used to determine the concentrations and size distributions of radon decay products because radon concentration was below 185 Bq m^{-3}. Particles were generated from cooking, vacuuming, washing and drying clothes, and by opening the outside doors. During most of the measurements, the housewife and a ten-month old baby boy stayed at home. The occupants lived in the way they would usually live. The timing of each kind of particle generation was different for each week. The time intervals for sampling the background condition, generating particles, and making the follow-up measurements were not the same with and without the air cleaners operating. Therefore, the realistic indoor situations both with and without the air cleaners could be understood. The summary of the field tests performed in three houses is shown in Table 9.

Table 9 Summary of the field test in three homes with and without the air cleaners (AFS : air filtration system, EAC : electronic air cleaner)

Condition	Air Cleaner	Springfield	Princeton	Northford
Background	No	Yes	Yes	Yes
Candle Burning	No	No	Yes	Yes
Cigarette Smoldering	No	No	Yes	No
Vacuuming	No	No	Yes	Yes
Cooking	No	No	Yes	Yes
Clothes Washing & Drying	No	Yes	No	Yes
Opening the bedroom door	No	No	Yes	No
Background	AFS	Yes	Yes	Yes
Candle Burning	AFS	No	Yes	No
Cigarette Smoldering	AFS	No	Yes	No
Vacuuming	AFS	No	Yes	Yes
Cooking	AFS	No	Yes	Yes
Clothes Washing & Drying	AFS	No	No	No
Opening the bedroom door	AFS	No	Yes	No
Background	EAC	No	No	Yes
Vacuuming	EAC	No	No	Yes
Cooking	EAC	No	No	Yes
Clothes Washing & Drying	EAC	No	No	Yes
Opening the Outside Door	EAC	No	No	Yes

5.6 Calculation of Aerodynamic Parameters of radon decay products and Bronchial Dose

5.6.1 Aerodynamic Parameters of radon decay products

Measured concentrations and size distributions of radon decay products can be made to calculate the aerodynamic parameters, the attachment rate, the average attachment diameter, and the deposition rate of "unattached" fraction. The attachment rate can be estimated by equation (17) with a λ_1 of 13.6 hr^{-1}, the ventilation rate, and the "unattached" and "attached" concentrations of ^{218}Po. No ventilation rate determination was performed in this study. The ventilation rate used in the room model for all three houses was assumed to be 0.2 hr^{-1}. This value was chosen because the infiltration rate into the Princeton house was measured by the CEES group and found to be approximately 0.3 hr^{-1} with the interior doors open and all of the windows closed. Since the bedroom door and all of the windows were closed in the Princeton house during this study, a value of 0.2 hr^{-1} was assumed. In general, the normal ventilation rate in the house is in the range of 0.2 - 0.5 hr^{-1} and λ_1 is much larger than ventilation rate. Therefore, the assumption of a ventilation rate does not influence the value of the aerodynamic parameters very much.

From calculated attachment rate and measured particle number concentration, the average attachment coefficient can be estimated by equation (14). The average attachment diameter can be obtained by the relationship between attachment coefficient and particle size shown in Figure 5. The deposition rate of the "unattached" fraction can be evaluated by equation (18) using the calculated attachment rate, the radon concentration, and the "unattached" concentration of ^{218}Po.

5.6.2 Hourly Bronchial Dose

PAEC in every size range can be obtained from the measured total PAEC and the PAEC size distribution. PAEC in every size interval is multiplied by the dose conversion factor as shown in Table 5 at the mid-point of every size interval to estimate the dose in every size interval. Summing up these doses in each size interval and dividing 170 hours (a working month) and the radon concentration, the hourly dose rate per Bq m^{-3} radon can be estimated.

5.6.3 Yearly Bronchial Dose

By assuming the indoor occupancy factor for male, female, and children, the yearly bronchial dose can be estimated with a reasonable assumption of indoor activities. To sum all the individual hourly dose rate per Bq m^{-3} radon multiplied by the exposure time for each indoor activity, the yearly bronchial dose per Bq m^{-3} radon can be calculated.

The average occupancy factor is chosen from the survey conducted in the United Kingdom (Wrixon, *et al.*, 1988). The occupancy factor is 0.77 over the whole year and 0.97 for housewives. The assumptions made for the calculation of yearly bronchial dose are as following :

(1) breathing rate for males is chosen when he is resting
(2) breathing rate for females is chosen when she is resting
(3) breathing rate for children age 10 is chosen when he is resting
(4) breathing rate for children age 5 is chosen when he is resting
(5) occupancy factor is 0.77 for males, 0.85 for children age 10, and 0.97 for females and children age 5
(6) one hour cooking every day
(7) one hour vacuuming every week
(8) the other indoor activities were neglected

CHAPTER 6
RESULTS AND DISCUSSION

6.1 Introduction

This chapter describes the results of field studies performed in three single-family houses located in Springfield, PA, Princeton, NJ, and Northford, CT. The radon concentration, particle number concentration, and activity-weighted size distribution of radon decay products were measured in these three homes. The CRM and CNC (discussed in Chapter 5) were used to determine radon concentration and particle number concentration, respectively. The ASC-GSA measurement system (described in Chapter 5) was used to determine the concentration and activity-weighted size distribution of radon decay products.

The influence on the behavior of radon decay products by various indoor particle sources both with and without the air cleaning systems was investigated. Aerosols were generated by water running in a shower, clothes washing and drying, candle burning, cigarette smoldering, vacuuming, opening a door, and cooking. Measurements of radon concentration, particle number concentration, and activity-weighted size distribution of radon decay products were made during the particle generating period. In addition, the evolution of the resulting size distribution of radon decay products both with and without the air cleaners was measured over the course of time.

The room model (Porstendöerfer *et al.*, 1978) discussed in Chapter 2 was used to calculate the changes in aerosol parameters caused by the operation of the air cleaners. These parameters are the particle attachment rate, the deposition rate of the "unattached" fraction, and the average attachment diameter. Using the James dosimetric models (1989, 1990), the bronchial doses were calculated from the measured PAEC and activity size distribution of radon decay products. The hourly dose rates per Bq m^{-3} radon for various kinds of particle generation were calculated for men, women, and children at different levels of occupant activity. The estimated yearly dose rates per Bq m^{-3} radon are also presented. The changes in PAEC and dose with the use of each air cleaning system were made for various domestic environments.

6.2 Background Conditions without the Air Cleaners

6.2.1 Basement Measurements in the Springfield House

The particle number concentration was in the range of 50,000 - 100,000 cm^{-3} in the basement of the Springfield house. This high particle number concentration was due to the oil

furnace. For comparison, the measurements taken by Ramamurthi and Hopke (1989) in another basement showed that the particle number concentrations were only 2,000 - 8,000 cm^{-3}. In that study, the low particle count could be explained by the lack of windows or major opening to the outside (a typical basement condition).

Figure 23 presents the size distributions of radon decay products in the basement of the Springfield house. The ^{218}Po size distribution showed that 10% of the activity was in the smallest inferred size interval with a mid-point diameter of 0.9 nm (D= 0.045 cm^2/sec). The "unattached" fraction of PAEC was 0.05 and the equilibrium factor, F, was around 0.13 - 0.19. However, approximately 50% of ^{218}Po activity in the 0.5 - 1.5 nm size range was observed in the basement study by Ramamurthi and Hopke (1989) with particle concentration of 3,200 cm^{-3}. Because a large amount of particles exited in the basement of the Springfield house, the "unattached" fractions of ^{218}Po and PAEC were much smaller compared with that of the typical domestic environments. The corresponding ^{214}Pb and ^{214}Bi distributions showed almost no activity exited in the 0.9 nm size range. This result may reflect the fact that the longer lifetime of these decay products permits a greater fraction of their activity to become attached to the indoor particles. The activity of all three distributions (^{218}Po, ^{214}Pb, and ^{214}Bi) in the 1.5 - 5 nm size range was approximately 15%. This significant 1.5 - 5 nm mode was observed through the experiments in the Springfield house and was thought to be due to the combustion particles generated from the oil-furnace. The "attached" mode of all three decay products peaked in the 50 - 150 nm size range. This "attached" mode may be due to outdoor particles penetrating into the basement. In summary, a bimodal size distribution was observed for the three decay products in the 1.5 - 5 nm size range and the "attached" mode. The attachment rate was around 45 hr^{-1} with the average attachment diameter around 33 nm. The deposition rate of "unattached" fraction was from 40 hr^{-1} to 55 hr^{-1}.

6.2.2 Living Room Measurements in the Princeton House

The particle concentration in the living room of the Princeton house ranged from 9,000 to 11,000 cm^{-3}. Strong (1989) found significantly different particle number concentrations in the living rooms of the rural and urban homes, 5,000 cm^{-3} and 15,000 cm^{-3}, respectively. This difference may be due to the different ambient particle concentrations, especially caused by heavy traffic or industries in the urban area. The Princeton house is located in suburban area near the

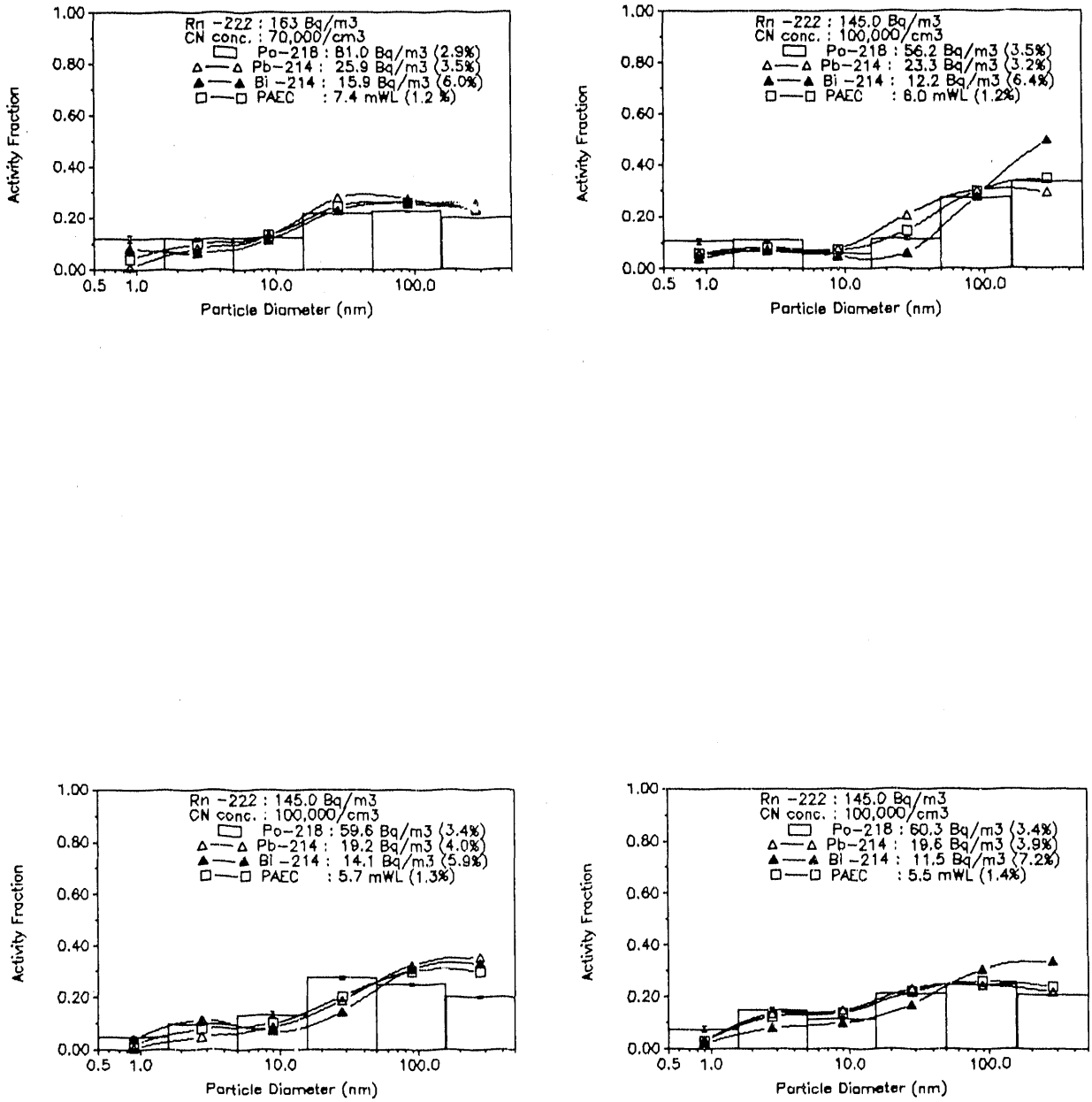

Figure 23 ^{218}Po, ^{214}Pb, and $^{214}Bi/^{214}Po$ activity size distributions measured under typical conditions in the basement.

Princeton University's campus. The particle concentration obtained was comparable with Strong's urban results.

Figure 24 presents the typical activity size distributions of radon decay products in the living room of the Princeton house. The fraction of ^{218}Po in the 0.9 nm size range was 30%, with insignificant activity in the 1.5 - 15 nm size range. More than one third of ^{218}Po activity was found in the "cluster" mode. The remaining activity was attached to indoor particles larger than 50 nm. The corresponding ^{214}Pb and ^{214}Bi distributions showed that less than 10% activity was observed in the smallest size range. For all three distributions, the "attached" mode peaked in the 150 - 500 nm size range. As a whole, a bimodal activity size distribution was observed for ^{218}Po in the 0.5 - 1.5 nm and 150 - 500 nm size ranges. Unimodal distributions were found for ^{214}Pb and ^{214}Bi in the 150 - 500 nm size range. During these background measurements, no additional indoor particles were generated. The "attached" mode of radon decay products may be related to the outdoor particles penetrating the house. Similar activity size distributions of bimodal for ^{218}Po (1 nm, 300 nm) and unimodal for ^{214}Pb and ^{214}Bi (300 nm) were observed previously by Reineking and Porstendoerfer (1986). Their experiments were performed in a closed room, and no measurements of particle number concentration were made.

The "unattached" fractions of ^{218}Po and PAEC were 0.3 and 0.1 in the Princeton house, respectively. Strong (1989) conducted several measurements in the living room during summer and winter at the urban and rural areas in United Kingdom. The "unattached" fraction was approximately 20% with AMD of 2 nm in the rural area and of 3.5 nm in the urban area. The AMD of "attached" mode was in the range of 110 - 150 nm.

6.2.3 Bedroom Measurements in the Princeton House

6.2.3.1 Bedroom Door Closed

With the bedroom door closed, the particle concentration in the bedroom of the Princeton house was relatively low, in the range of 2,500 - 3,000 cm^{-3}. The results of size distributions of radon decay products are as shown in Figure 25. Most of ^{218}Po activity (70%) was in the 0.9 nm size range. Because of low particle concentrations in the bedroom, the "unattached" fractions in the bedroom were larger than that in the living room. The activity of ^{214}Pb and ^{214}Bi in the smallest size range was only 20%. For all three distributions, little activity was observed in the 1.5 - 15 nm size range. The remaining activity of all three decay products was in the 15 - 500 nm size range. The "unattached" fraction of ^{218}Po and PAEC was in the range of 0.5 - 0.7 and

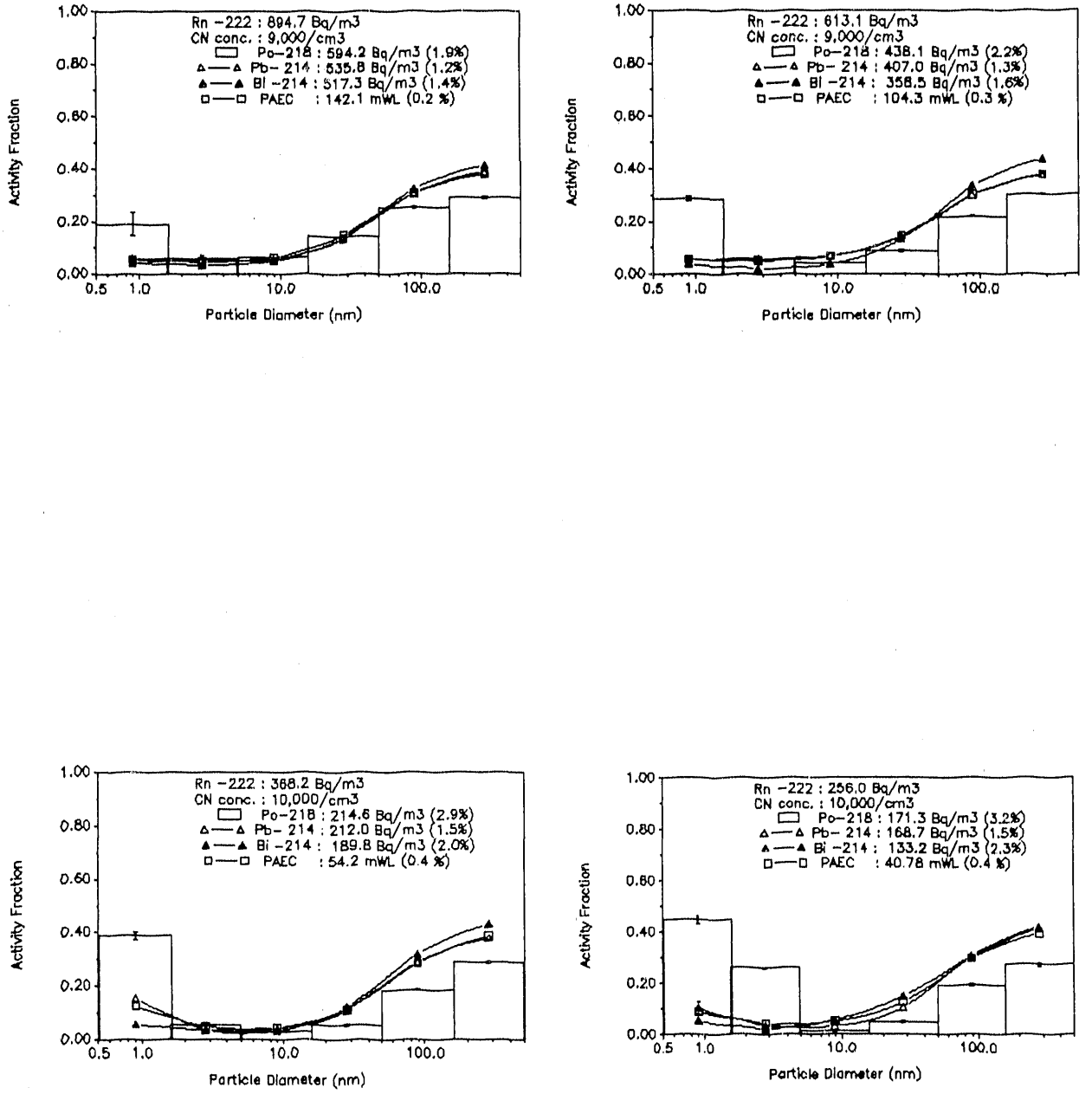

Figure 24 ^{218}Po, ^{214}Pb, and $^{214}Bi/^{214}Po$ activity size distributions measured under typical conditions in the living room area.

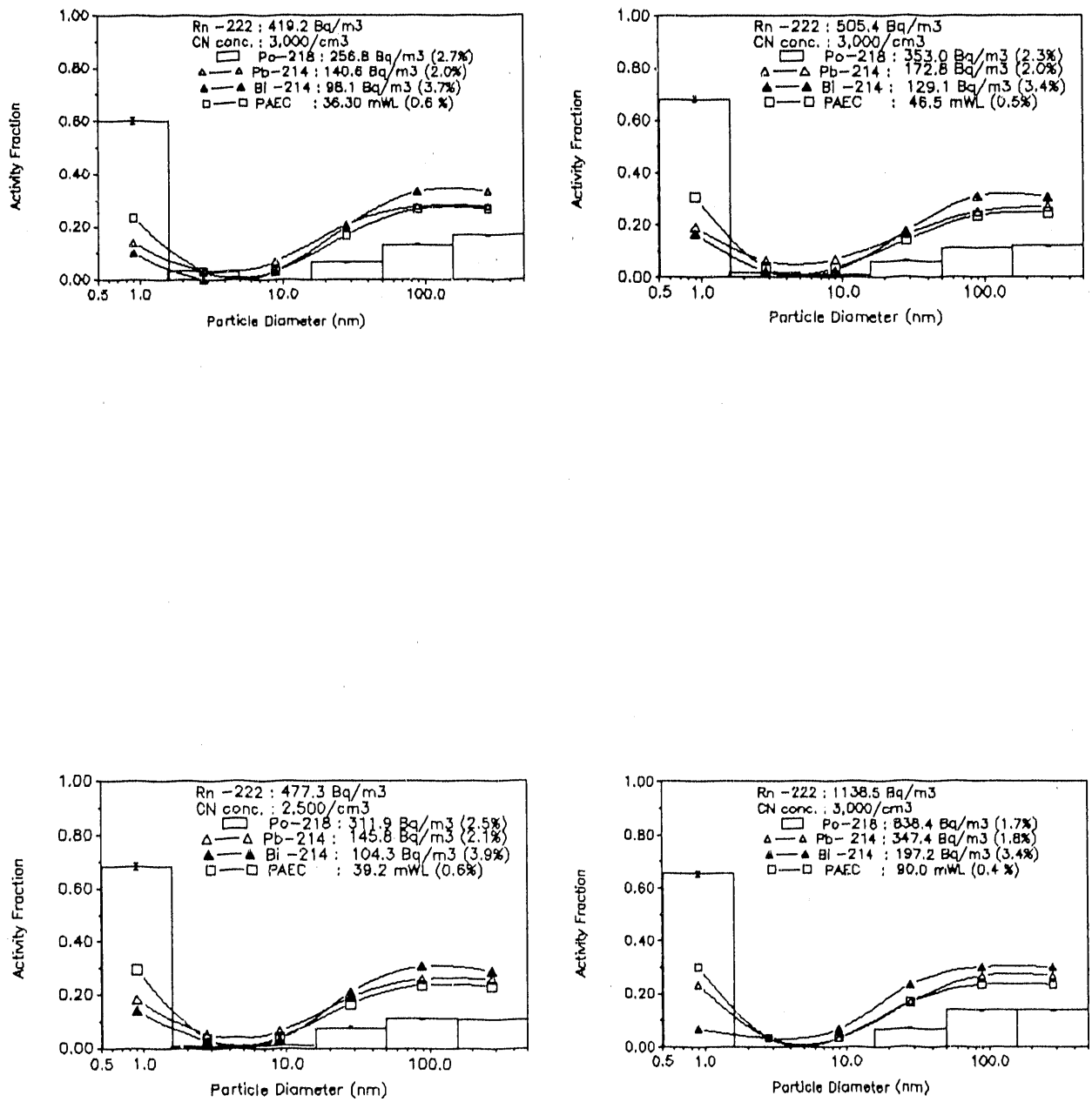

Figure 25 ^{218}Po, ^{214}Pb, and $^{214}Bi/^{214}Po$ activity size distributions measured under typical conditions in the bedroom with the door closed.

from 0.2 to 0.4, respectively. The equilibrium factor, F, was in the range of 0.3 - 0.5; a similar value (average 0.3) to that reported by Porstendöerfer *et al.* (1987), and by Wicke and Porstendöerfer (1982) in low ventilated rooms. The attachment rate in this study was between 6 and 14 hr^{-1}. The average attachment diameter was in the range of 50 - 90 nm. The deposition rate of "unattached" fraction was approximately 4 - 12 hr^{-1}.

6.2.3.2 Bedroom Door Open

By opening the bedroom door, the particle concentration in the bedroom increased to 7,000 - 10,000 cm^{-3}. The particle number concentration was higher with the door open than with the door closed because of the increased influence of the outdoor particles and the gas pilot light in the kitchen. The size distributions of radon decay products are presented in Figure 26. The ^{218}Po activity slightly increased in the smallest size range compared to the situations with the bedroom door closed. The "unattached" fraction of ^{218}Po and PAEC was in the range of 0.70 - 0.83 and ranged from 0.35 to 0.40, respectively. The equilibrium factor, F, was in the range of 0.43 - 0.54 and was much higher than that with the bedroom door closed because of the higher particle concentrations. The activity (20%) of ^{214}Pb and ^{214}Bi in the 0.5 - 1.5 nm size range was still much less than that of ^{218}Po. No activity in the 1.5 - 15 nm size range was observed for all three size distributions. The "attached" mode of all three decay products peaked at 28 nm. For the ^{214}Pb and ^{214}Bi size distributions, the only difference between having the door open and closed was in the size of the "attached" mode. Strong (1989) conducted field measurements in a bedroom at a rural area and found the particle number concentration of 5,000 cm^{-3}. The "unattached" fraction in Strong's study was smaller (17%) than that observed in this study (35% - 40%). No experimental setup was described in Strong's paper in terms of closing or opening bedroom door or the size of the bedroom. In this present study, the lower attachment rate (4 hr^{-1}) and average attachment diameter (30 nm) may be related to small particles generated from gas stove's pilot lights. The deposition rate of "unattached" fraction was 1.5 - 3 hr^{-1}.

6.2.4 Living Room Measurements in the Northford House

Under the typical conditions, the particle concentration in the living room of the Northford house was between 2,500 cm^{-3} and 4,000 cm^{-3}. The lowest particle concentration observed, 1,000 cm^{-3}, was found in the very early morning. The Northford house is located in a suburban area with very light traffic. The size distributions of all three decay products are

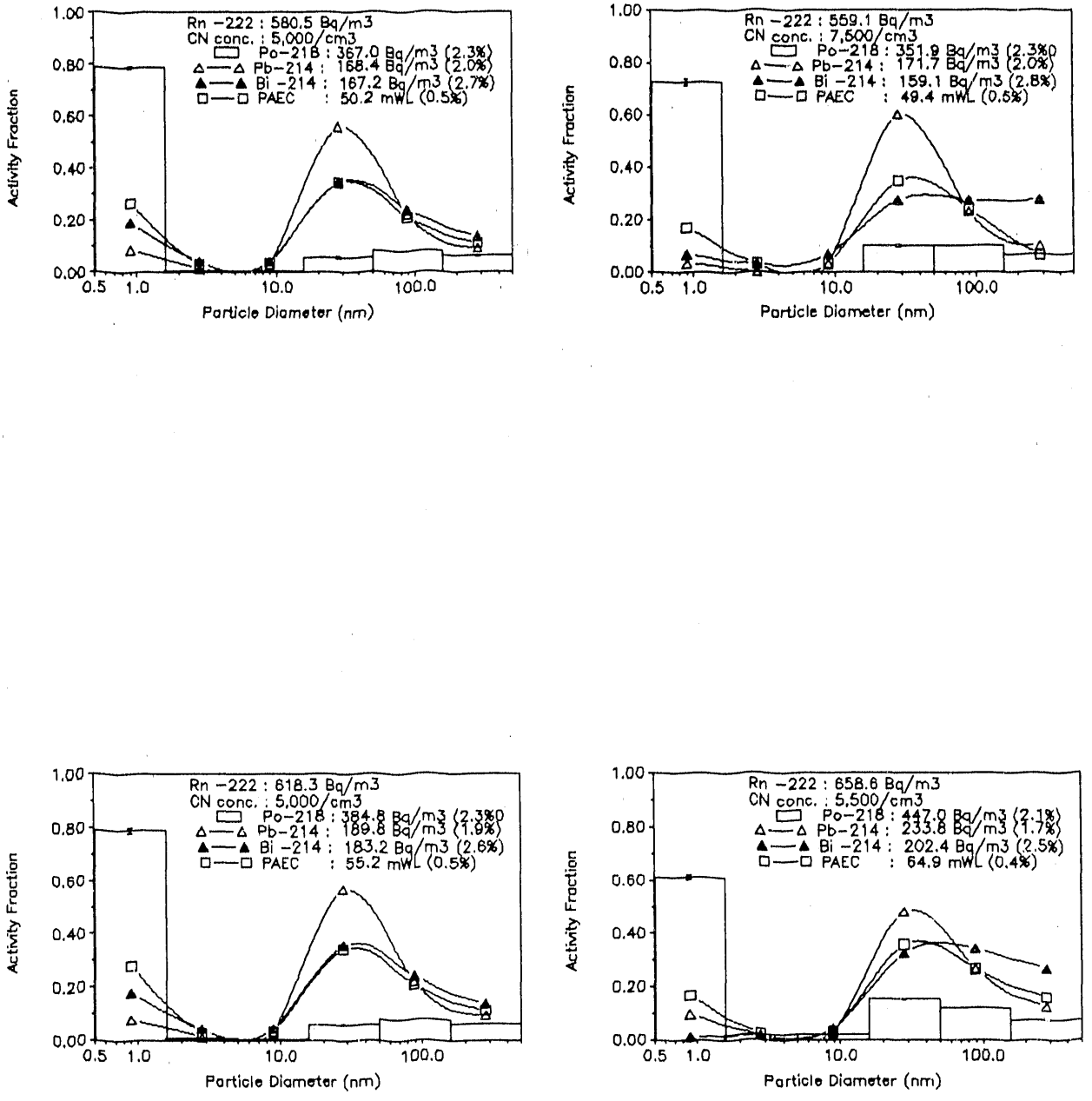

Figure 26 ^{218}Po, ^{214}Pb, and $^{214}Bi/^{214}Po$ activity size distributions measured under typical conditions in the bedroom with door open.

presented in Figure 27. A bimodal size distribution was observed for ^{218}Po with the major mode (60%) in the highly diffusive "unattached" fraction. The "unattached" fraction PAEC ranged from from 0.25 to 0.45. The equilibrium factor, F, was in the range from 0.18 to 0.22. The ^{218}Po distribution revealed very little activity in the 1.5 - 15 nm size range. The remaining ^{218}Po activity (40%) was attached to particles larger than 15 nm. Approximately 30% activity of ^{214}Pb and ^{214}Bi was spread evenly over 0.5 - 15 nm size range. The "attached" mode of ^{214}Pb and ^{214}Bi peaked in the 50 - 500 nm size range. These background size distributions are similar to those obtained in the master bedroom of the Princeton house with the bedroom door closed. Both had similar particle concentrations. This result may have been due to the fact that the measurements in the Northfod house were made with all of the windows and the outside doors closed. Therefore, the ventilation and infiltration rates of this house may be low. In order to use the room model, a ventilation rate of 0.2 hr^{-1} will be assumed. The size distributions of radon decay products may be explained by either the presence of condensables leading to the formation of ultrafine particles or a source of small primary particles in the house. The attachment rate was about 4 - 20 hr^{-1} with the 55 nm particle attachment diameter. The deposition rate of "unattached" fraction ranged from 40 to 70 hr^{-1}. The summary of the aerosol parameters of radon decay products is presented in Table 10.

6.2.5 Conclusion

The variation in the particle number concentrations in indoor environments ranging from 3,000 cm^{-3} to 10,000 cm^{-3} may be related to the location of the houses. A bimodal size distribution was observed for all three decay products (^{218}Po, ^{214}Pb and ^{214}Bi) in the typical conditions (without any air cleaner operating). For ^{218}Po size distributions, the major mode was in the 0.5 - 1.5 nm size range and a minor mode occurred in the "attached" size range. For ^{214}Pb and ^{214}Bi, a bimodal size distribution was observed to have a major mode in 50 - 500 nm size range and a minor mode in the "cluster" fraction. In a few cases, a unimodal size distribution was found for ^{214}Pb and ^{214}Bi because of the presence of higher particle number concentrations. The relatively lower "unattached" fraction and 1.5 - 5 nm mode observed in the basement the Springfield house was mainly because of the apparently faulty oil furnace. The "unattached" fraction of ^{218}Po and PAEC varied from 0.3 to 0.6 and 0.1 to 0.3, respectively, depending on the environments. The equilibrium factor, F, was in the range of 0.20 to 0.30. The attachment rate was in the range of 4 - 20 hr^{-1} with average attachment diameter of 50 nm. The deposition rate

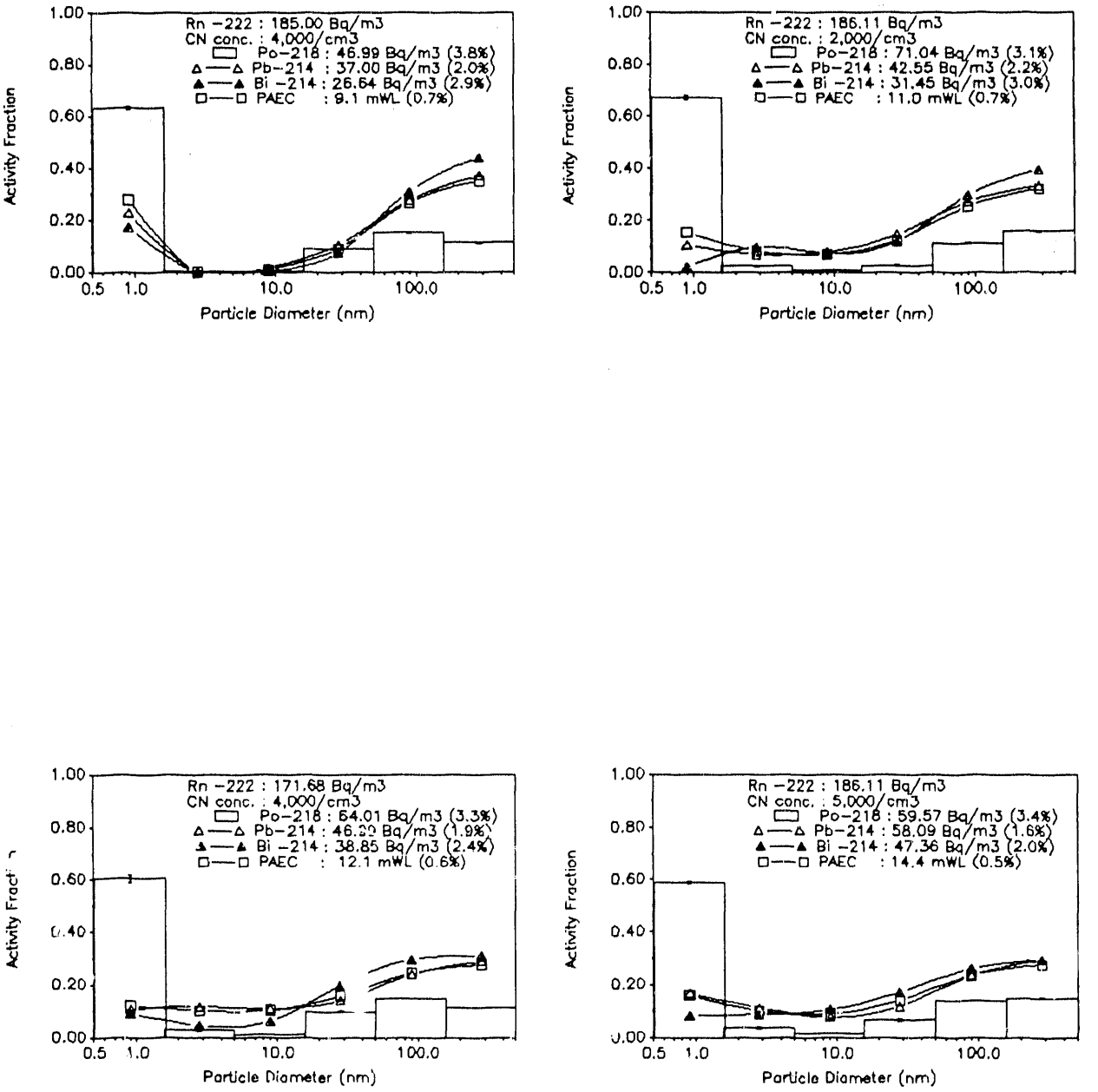

Figure 27 ^{218}Po, ^{214}Pb, and ^{214}Bi/^{214}Po activity size distributions without the air cleaners.

Table 10 The measurements and calculation of X, d, $q^{(u)}$ and dose for background conditions in Northford house.

Aerosol Source Cleaner	Co (Bq/m^3)	Z ($10^3 cm^{-3}$)	f_1	f_p	F	PAEC (mWL)	X (hr^{-1})	d (nm)	$q^{(u)}$ (hr^{-1})	Dose($\mu Gyhr^{-1}/Bq/m^3$) M(s,r) M(l,h)	F(r,e)	C10(r,e) C5(r,e)	M(l,h) Basal	M(l,h) Secretory
(1) Without air cleaner														
off	227.5	1.5	0.625	0.326	0.133	8.2	8.1	90	41.8	4.7,5.5 13.4,23.8	4.6,13.3	5.3,13.6 6.1,10.1	4,17.8	6.9,29.6
off	186.1	2	0.695	0.235	0.218	11.0	6.0	60	30.9	6.8,8.0 18.2,31	7.0,18.3	7.8,18.6 9.1,14.4	5.4,21.9	9.3,37
off	171.7	4	0.631	0.222	0.261	12.1	7.9	55	35.3	8.8,10.4 22.6,37.5	9.1,22.8	10,23.3 11.9,18.5	6.7,25.7	11.5,43.6
off	186.1	5	0.628	0.259	0.286	14.4	8.0	50	45	10.0,11.8 26.6,45.1	10.3,26.7	11.5,27.3 13.5,21.2	7.9,31.6	13.6,53.3
(2) With air filtration system														
on	61.1	1.5	0.830	0.473	0.139	2.3	2.8	50	26.5	5.1,6.2 17,32.4	5.1,16.5	5.7,16.8 6.5,11.6	5.2,25.8	8.8,42.2
on	64.8	1	0.843	0.380	0.143	2.5	2.5	60	25.9	4.9,6.0 15.3,28.0	4.9,15.1	5.7,15.3 6.5,11.1	4.6,21.6	7.9,35.6
on	58.1	5.5	0.693	0.309	0.159	2.5	6.0	35	35.5	5.0,6.0 14.9,26.8	5.0,14.8	5.7,14.9 6.7,11.0	4.5,20.1	7.7,34
on	67.7	2	0.831	0.407	0.158	2.9	2.7	45	31.2	5.9,7.1 18.3,33.7	5.9,18	6.8,18.3 7.8,13.1	5.5,26.0	9.5,42.8
(3) With electronic air cleaner														
on	156.5	4	0.597	0.273	0.179	7.6	9	60	46	5.9,6.9 16.3,28.2	6.0,16.3	6.7,16.6 7.9,12.7	4.8,20.4	8.3,34.2
on	156.9	4	0.609	0.276	0.229	9.7	8.7	60	61 22.2,37.6	8.3,9.7	8.4,22.2 11.0,17.5	9.5,22.7	6.5,26.5	11.3,44.6
on	155.4	2.5	0.683	0.321	0.190	8.0	6.3	65	58	6.4,7.6 13.4,33.3	6.4,18.5	7.3,18.7 8.4,13.8	5.6,25.0	9.6,41.6
on	166.9	4.5	0.679	0.292	0.157	7.1	6.4	45	69	5.0,5.9 14.3,25.3	4.9,14.1	5.6,14.3 6.5,10.7	4.3,18.9	7.3,31.4

of "unattached" fraction was approximately 3 - 12 hr^{-1}.

6.3 Influence of Additional Particle Generation on Background Conditions without the Air Cleaners

6.3.1 Running Water in a Shower

No significant effect on the size distributions of radon decay products by running water in a shower in the Princeton house was observed (Figure 28). The particle concentration remained the same at 5,000 cm^{-3}. Since running the water in the shower without the air filtration system operating produced no observable effect on the size distributions of radon decay products, no similar experiments with the air filtration system were performed.

6.3.2 Candle Burning in the Princeton House

During the candle burning period, the average particle concentration increased from 3,000 cm^{-3} to 80,000 cm^{-3} as shown in Figures 29 and 30. By the second measurement, the particle concentration reached steady state at approximately 3,000 cm^{-3}. During candle burning, this significant quantity of particles decreased the activity of ^{218}Po in the smallest size range (from 75% to 50%). At the same time, the "unattached" fraction of PAEC was also moderately decreased from 0.35 to 0.25 and the equilibrium factor, F, increased from 0.32 to 0.38. However, no significant change on ^{214}Pb and ^{214}Bi in this size range was observed. There was 15% activity in the 1.5 - 15 nm size range for ^{218}Po, but very little ^{214}Pb and ^{214}Bi activity in this size range. The increase in the activity of ^{218}Po in this size range was due to the attachment of ^{218}Po to particles generated from candle burning. The "attached" mode of all three distributions peaked in the 50 - 500 nm size range for all conditions. These results suggested that burning a candle produces very small particles with diameters smaller than 100 nm. The average attachment diameter changed from 50 nm to 15 nm during candle burning; a similar value (22 nm) as that reported by Reineking et al. (1985), and to 70 nm 55 and 130 minutes after the end of candle burning. At the same time, a low average attachment coefficient and attachment diameter were observed as shown in Table 11. The attachment rate increased from 5 hr^{-1} to 10 hr^{-1} during candle burning, and to 8 hr^{-1} 55 and 130 minutes after the end of candle burning. The deposition rate of "unattached" fraction increased from 10 hr^{-1} to 20 hr^{-1} 55 and 130 minutes after candle burning discontinued. The size distributions of the second and third measurements returned to that of the background condition gradually. This result was due to the fact that the small size particles

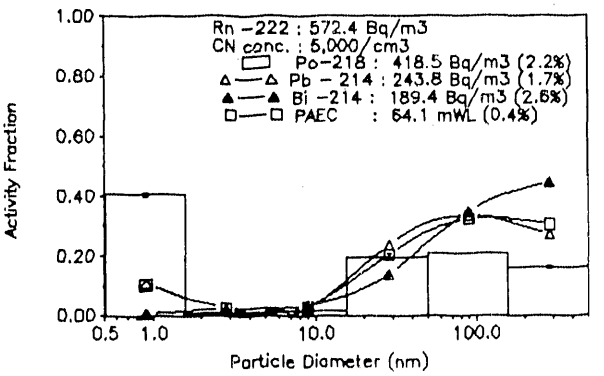

A: Background

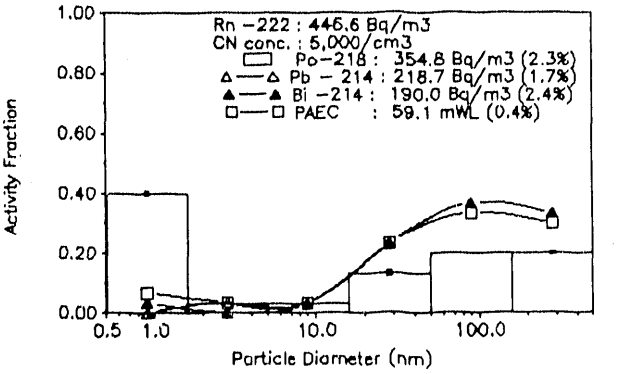

B: During Running water in a shower

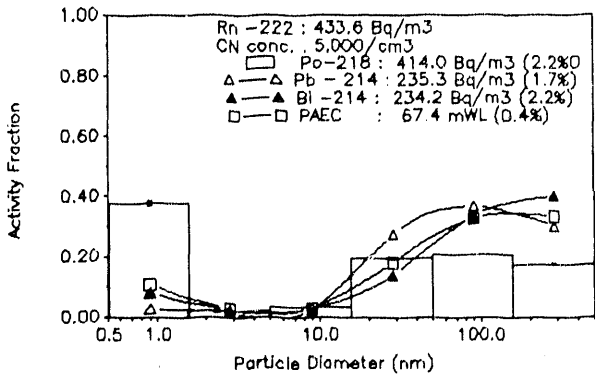

C: after 55 minutes

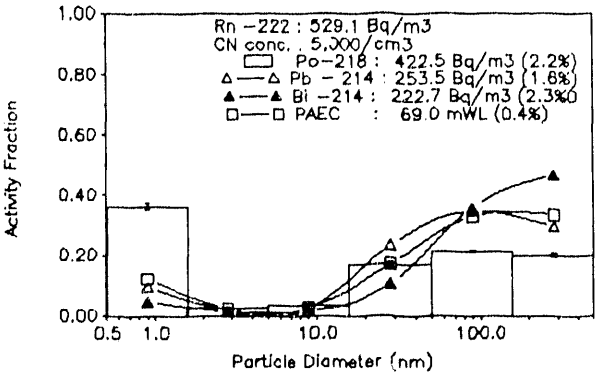

D: after 130 minutes

Figure 28 ^{218}Po, ^{214}Pb and $^{214}Bi/^{214}Po$ activity size distributions measured while running water in the shower in the bedroom without air filtration system.

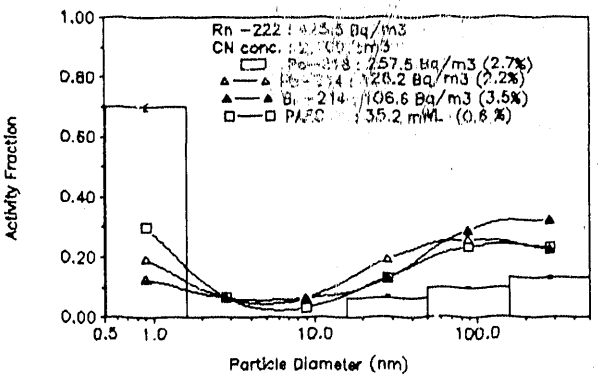

A: Background

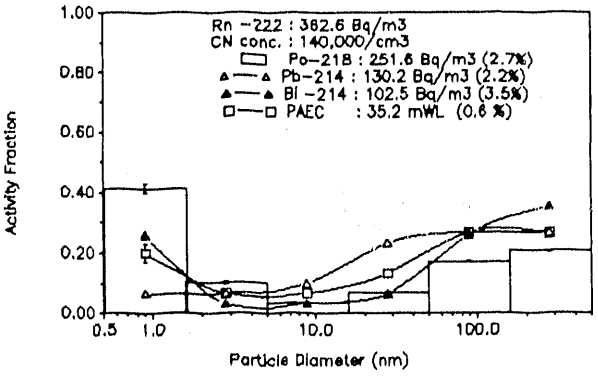

B: During candle burning

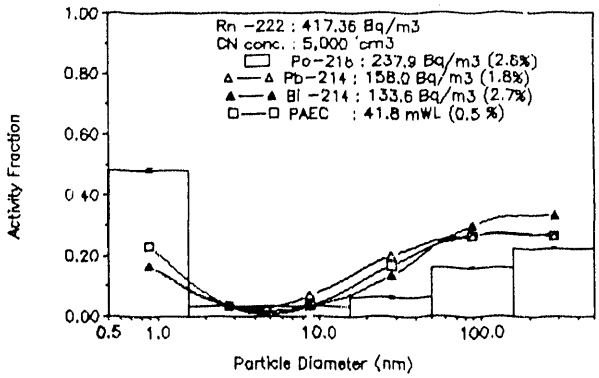

C: after 55 minutes

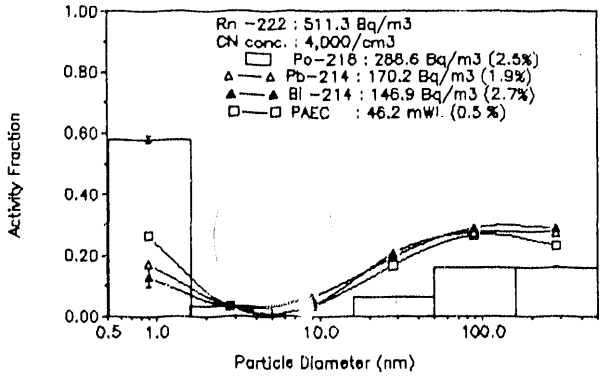

D: after 130 minutes

Figure 29 ^{218}Po, ^{214}Pb and $^{214}Bi/^{214}Po$ activity size distributions measured under aerosol generated from candle burning in the bedroom without air filtration system. (a)

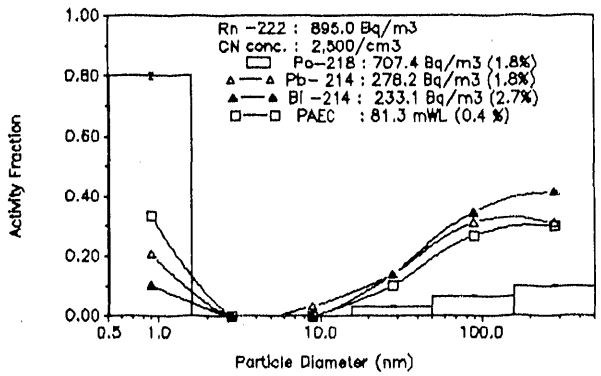

A: Background

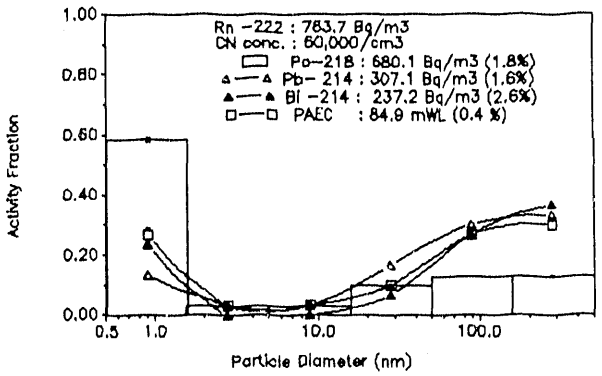

B: During candle burning

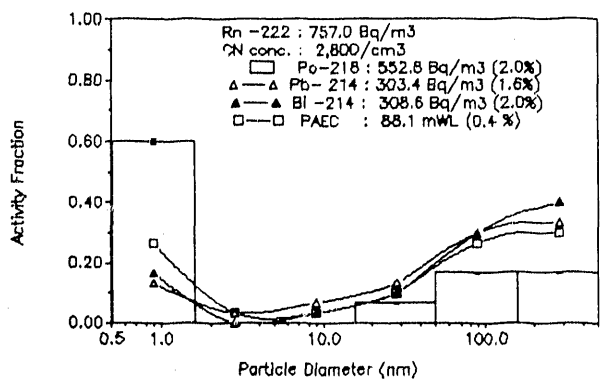

C: after 55 minutes

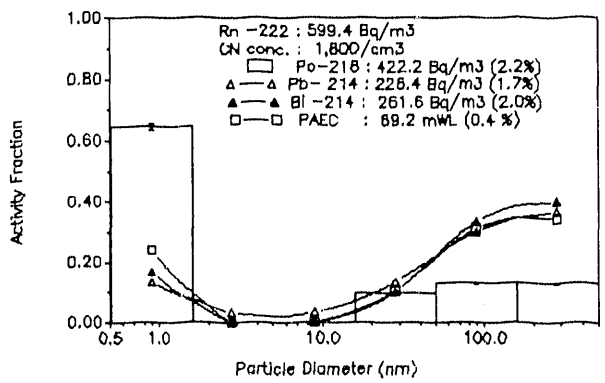

D: after 130 minutes

Figure 30 ^{218}Po, ^{214}Pb, and $^{214}Bi/^{214}Po$ activity size distributions measured under aerosol generated from candle burning in the bedroom without air filtration system. (b)

Table 11 The measurements and calculation of X, d, $q^{(u)}$ and dose with candle burning in Princeton house.

Aerosol Source Cleaner	Co (Bq/m^3) ($10^3 cm^{-3}$)	Z	f_1	f_p	F	PAEC (mWL)	X (hr^1)	d (nm)	$q^{(u)}$ (hr^{-1})	Dose($\mu Gyhr^{-1}/Bq/m^3$) M(s,r) M(l,h)	F(r,e)	C10(r,e) C5(r,e)	M(l,h) Basal	M(l,h) Secretory
(1)off (background)	425.5	2.7	0.7	0.367	0.306	35.2	6	52	12	11.3,13.5 33.4,60.0	11.3,33.0	12.9,33.6 14.9,24.7	10.0,45.0	17.0,74.7
off (during candle burning)	362.6	140	0.517	0.267	0.359	35.2	13	15	11	11.8,13.9 32.5,56.3	12,32.4	13.5,33 15.7,25.2	9.7,41	16.7,68.4
off (after 55 minutes)	417.4	5	0.516	0.266	0.370	41.8	13	70	19	11.1,13.1 31.7,56.1	11.3,31.6	12.8,32.2 14.8,24	9.6,42.3	16.3,70
off (after 130 minutes)	511.34	4	0.614	0.3	0.334	46.2	8.5	60	17	10.8,12.8 31.3,55.9	10.9,31.1	12.4,31.7 14.3,23.4	9.4,42.5	16.1,70
(2)off (cleaner off for 4 hours)	895.03	2.5	0.800	0.333	0.336	81.3	3.39	45	4.38	9.9,11.9 31.2,58.0	9.9,30.6	11.3,31.0 12.9,22.0	9.5,46.0	16.1,75.0
off (cleaner off for 5 hours, during candle burning)	783.7	60	0.613	0.300	0.401	84.9	8.57	16	3.2	12.3,14.7 36.4,65.5	12.4,36.0	14.1,36.6 16.2,26.9	11.0,50.0	18.8,82.6
off (after 55 minutes)	757.0	2.8	0.6	0.3	0.431	88.1	9.0	75	8.1	13.2,15.8 39.1,70.4	13.3,38.7	15.1,39.4 17.4,28.9	4.2,14.3	7.2,24.5
off (after 130 minutes)	599.4	1.8	0.645	0.241	0.427	69.2	7.47	80	8.59	10.2,12.1 30.5,55.8	10.3,30.2	11.7,30.7 13.4,22.3	9.3,43.9	15.9,71.8

produced from candle burning yielded a lower attachment rate and a higher deposition rate. In the present experiments, the particle number concentration increased to 10^5 cm^{-3} with a relatively small attachment rate of 10 hr^{-1}. These results were compatible to those reported by Reineking and Porstendoerfer (1989). They showed that the attachment rate can be as high as 100 h^{-1} when the particle concentration is 10^6 cm^{-3} as the result of candle burning. In general, the attachment rate is proportional to the particle number concentration for the same size of particles.

6.3.3 Cigarette Smoldering in the Princeton House

A particle con .entration of 100,000 cm^{-3} was observed in the master bedroom of the Princeton house while the cigarettes were smoldering. The particle concentration declined to 10,000 cm^{-3} 135 minutes after the end of cigarette smoldering. It appears that the particles produced from cigarette smoldering were typically in the larger size range of the accumulation mode (Stoute et al., 1984). In the presence of these larger particles, a dramatic decrease in the activity in the 0.5 - 1.5 nm size range was observed for ^{218}Po (from 60% to 8%) and for ^{214}Pb and ^{214}Bi (from 10% to zero) as shown in Figures 31 and 32. No activity of any of the three decay products was found in the 1.5 - 15 nm size range. All three size distributions became unimodal in the 50 - 500 nm size range, with little activity in the "cluster" mode. All three distributions remained the same for long periods of the time. The equilibrium factor, F, reached 0.55 while the "unattached" fraction of PAEC remained unchanged below 0.10. This result was due to the fact that the particles generated from cigarette smoldering have a higher attachment rate than those from candle burning. The attachment rate as presented in Table 12 increased from 8 hr^{-1} to 110 hr^{-1} during the particle generation period, to 120 hr^{-1} 60 minutes after the end of cigarette smoldering, and to 60 hr^{-1} 135 minute after cigarette smoldering stopped. With the particle number concentration on the order of 10^5 cm^{-3} because of cigarette smoldering, the attachment rate reached 100 hr^{-1}. Reineking and Porstendoerfer (1989) found the attachment rate reached 1,000 h^{-1} with a cigarette smoldering particle concentration of 4×10^5 cm^{-3}. The average diameter decreased from 60 nm to 50 nm during the particle gereration period, and to 120 nm; a value (160 nm) similar to that reported by Reineking et al. (1985), 60 and 135 minutes after the end of cigarette smoldering. The deposition rate of "unattached" fraction increased from 16 hr^{-1} to 30 hr^{-1}.

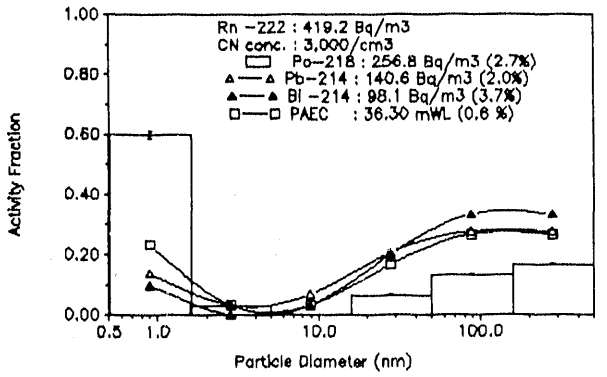

A: Background

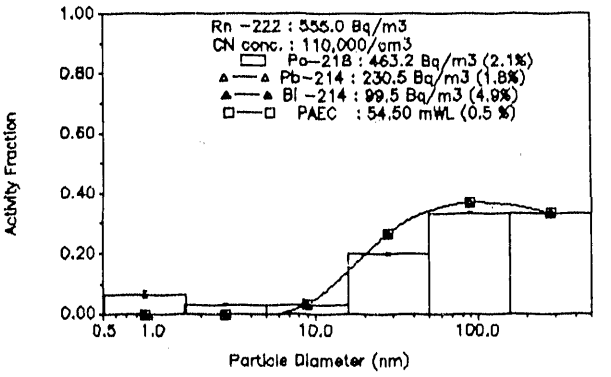

B: During cigarette smoke

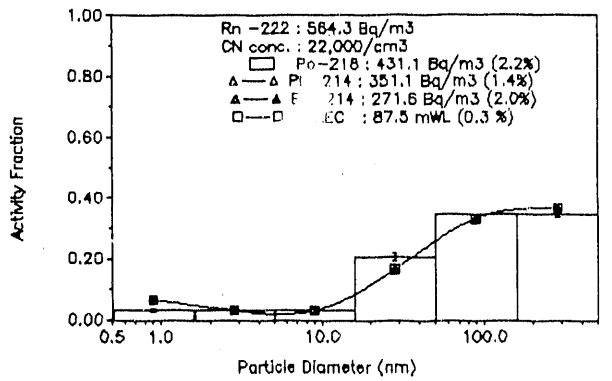

C: after 60 minutes

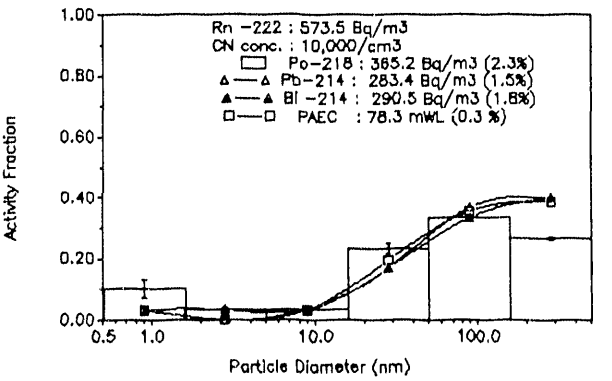

D: after 135 minutes

Figure 31 ^{218}Po, ^{214}Pb, and $^{214}Bi/^{214}Po$ activity size distributions measured under aerosol generated from cigarette smoke in the bedroom without air filtration system. (a)

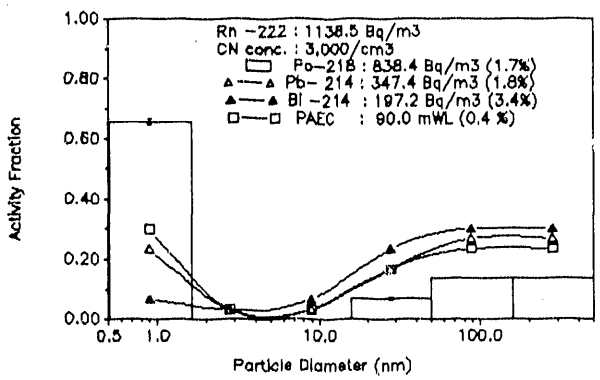

A: Background

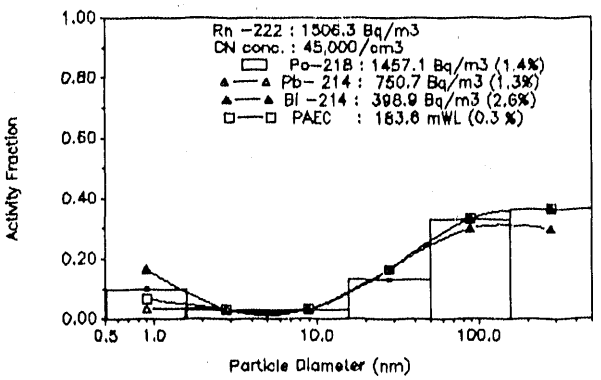

B: During cigarette smoldering

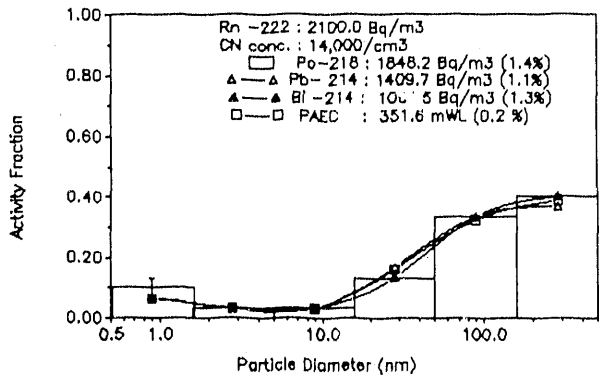

C: after 60 minutes

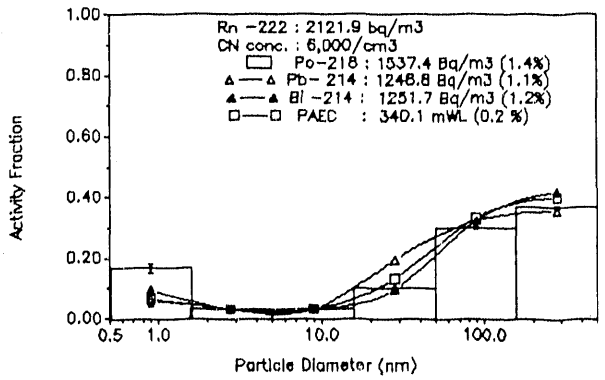

D: after 135 minutes

Figure 32 ^{218}Po, ^{214}Pb, and $^{214}Bi/^{214}Po$ activity size distributions measured under aerosol generated from cigarette smoke in the bedroom without air filtration system. (b)

Table 12 The measurements and calculation of X, d, $q^{(u)}$ and dose with cigarette smoidering in Princeton House.

Aerosol Source Cleaner	Co (Bq/m^3; (10^3cm^{-3})	Z	f_1	f_p	F	PAEC (mWL)	X (hr^1)	d (nm)	$q^{(u)}$ (hr^{-1})	Dose($\mu Gyhr^{-1}/Bq/m^3$) M(s,r) M(l,h)	F(r,e)	C10(r,e) C5(r,e)	M(l,h) Basal	M(l,h) Secretory
(1)off (background)	419.2	3	0.633	0.266	0.32	36.3	8	70	13	9.6,11.4 27.4,48.5	9.8,27.3	11.1,27.8 12.8,20.8	8.3,36.9	14.2,61
off (during cigarette smoke)	555.0	110	0.1	0	0.363	54.5	122	40	25	5.2,5.7 9.4,12.8	5.9,10.4	6.4,10.8 7.4,10.0	3.0,7.9	4.9,13.6
off (after 60 minutes)	564.3	22	0.068	0.1	0.574	87.5	186	110	58	11.3,12.9 26.8,43.4	11.9,27.6	13.2,28.3 15.4,23.0	8.2,30.0	13.9,51.0
off (after 135 minutes)	573.5	10	0.133	0.032	0.505	78.3	88	120	56	7.4,8.3 15.3,23.1	8.1,16.3	8.9,16.8 10.3,14.5	4.9,15.8	8.1,26.6
(2)off	505.4	3	0.7	0.344	0.340	46.5	5.81	54	8.1	11.7,13.9 35,63.2	11.8,34.5	13.4,35.1 15.4,25.7	10.5,48.5	18.0,80.0
off	477.3	2.5	0.714	0.333	0.304	39.2	5.43	60	9.8	10.4,12.4 30.7,55.3	10.5,30.4	11.9,31.0 13.7,22.7	9.2,42.3	15.7,69.6
off (background)	1138.5	3	0.655	0.333	0.292	90.0	7.14	62	7.2	10.1,12.0 29.9,53.7	10.2,29.5	11.5,30.1 13.3,22.1	8.9,41.1	15.3,67.6
off (during the cigarette smoke)	1506.3	45	0.133	0.1	0.451	183	88.5	54	2.09	8.9,10.1 21.0,34.1	9.4,21.6	10.4,22.2 12.1,18.1	6.5,23.7	10.9,40.0
off (after 60 minutes)	2099.8	14	0.133	0.096	0.620	351	88.7	95	12.4	11.8,13.6 27.9,45.3	12.5,28.9	13.9,29.6 16.2,24.1	22.5,81.0	39.0,143.0
off (after 135 minutes)	2121.9	6	0.2	0.1	0.593	340	54.3	130	24.6	11.2,12.9 26.8,43.8	11.8,27.5	13.1,28.2 15.3,22.9	8.3,30.5	14.0,51.6

6.3.4 Vacuuming

6.3.4.1 Princeton House

During the vacuuming period, the particle number concentration reached 90,000 cm^{-3} then decreased to 4,000 cm^{-3}, 135 minutes after the end of vacuuming. The significant additional mode of ^{218}Po in 15 - 100 nm size range was found because of the attachment of ^{218}Po to the small particles produced from vacuuming. The particles generated from vacuuming are smaller than 100 nm, similar to those produced from candle burning. These results are shown in Figures 33 and 34 were similar to that observed by Reineking and Porstendoerfer (1986). They found an additional mode in the size range of 20 - 80 nm formed by the particles generated from an electrical motor. In the two sets of vacuuming experiments, a significant difference in the particle concentration during the particle generation period caused a variation in the size distirbution of radon decay products. For the case with particle concentration of 15,000 cm^{-3}, a moderate activity decrease in the 0.9 nm size range was observed for ^{218}Po (about 40%) and for ^{214}Pb and ^{214}Bi (about 10%). The "unattached" fraction of ^{218}Po decreased from 0.70 to 0.35 (during the particle generation period), to 0.56 (60 minutes after the end of vacuuming), and to 0.67 (135 minutes after the end of vacuuming). The "unattached" fraction of PAEC changed from 0.45 to 0.16 (during the particle generation period), to 0.30 (60 minutes after vacuuming was discontiuning), and to 0.30 (135 minutes after the end of vacuuming). The equilibrium factor, F, increased from 0.24 to 0.26 (during the particle generation period), to 0.34 (60 minutes after the end of vacuuming), and to 0.28 (135 minutes after vacuuming stopped). The average attachment diameter of these small particles was smaller and thus, a lower attachment rate was observed. The three size distributions of radon decay products returned to those of the background condition gradually 60 and 135 minutes after vacuuming was discontinued. The average attachment diameter decreased from 59 nm to 38 nm during the particle generation period; a value (26 nm) similar to that reported by Reineking et al. (1985), and to 64 nm 60 and 135 minutes after the end of vacuuming. In this study, the particle number concentration can reach 10^5 cm^{-3} with a relatively low attachment rate of 50 hr^{-1}. The deposition rate of "unattached" fraction increased from 5 hr^{-1} to 30 hr^{-1} as shown in Table 13.

6.3.4.2 Northford House

The vacuum cleaner was on for 12 minutes in the living room of the Northford house. During the vacuuming period, the particle concentration increased from 1,500 cm^{-3} to 25,000 cm^{-3}.

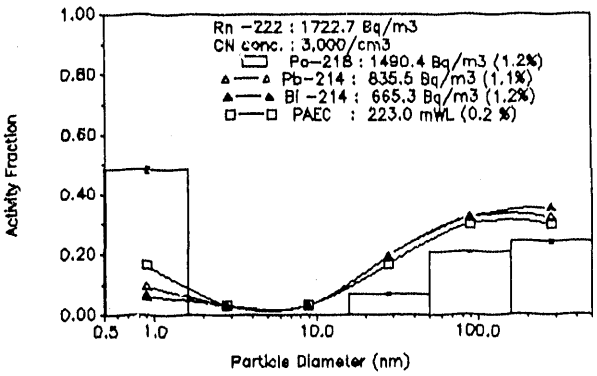

A: Background

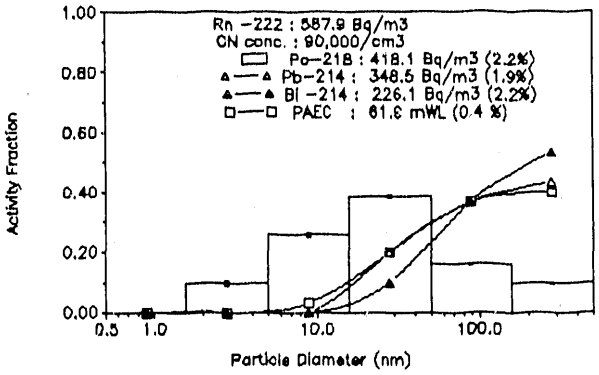

B: During the vacuuming

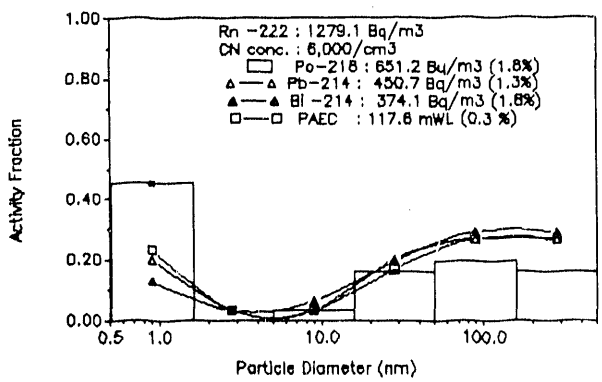

C: after 60 minutes

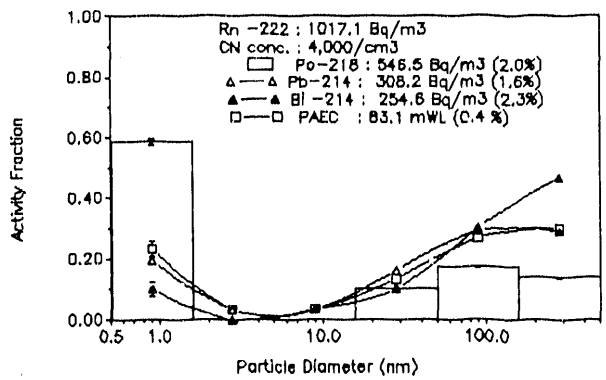

D: after 135 minutes

Figure 33 ^{218}Po, ^{214}Pb and $^{214}Bi/^{214}Po$ activity size distributions measured under aerosol generated from vacuuming in the bedroom without air filtration system. (a)

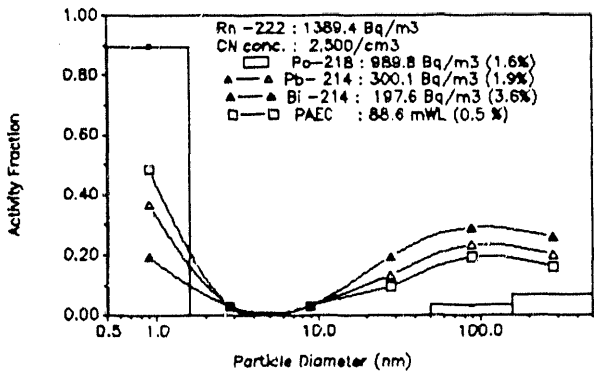

A: Background

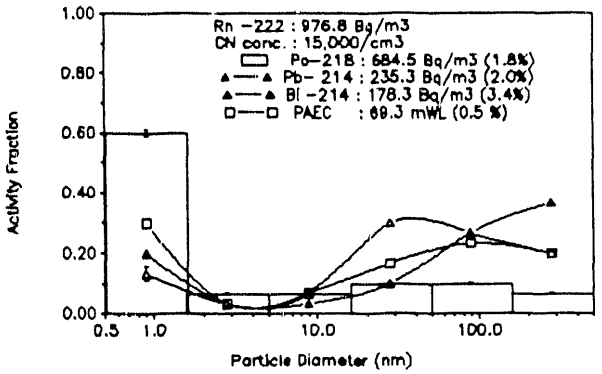

B: During the vacuuming

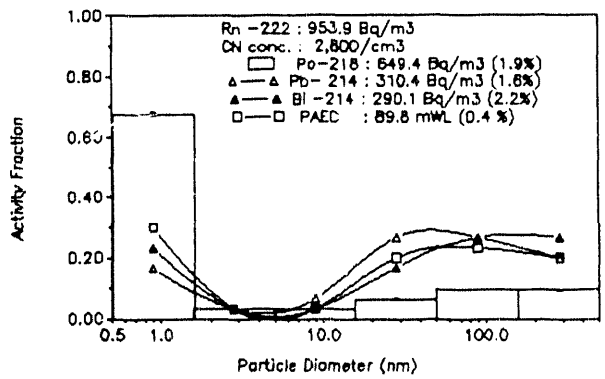

C: after 60 minutes

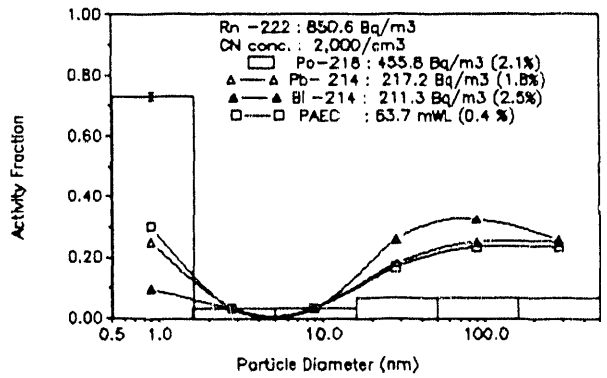

D: after 135 minutes

Figure 34 ^{218}Po, ^{214}Pb and $^{214}Bi/^{214}Po$ activity size distributions measured under aerosol generated from vacuuming in the bedroom without air filtration system. (b)

Table 13 The measurements and calculation of X, d, $q^{(u)}$ and dose with vacuuming in Princeton House.

Aerosol Source Cleaner	Co (Bq/m^3)	Z ($10^3 cm^{-3}$)	f_1	f_p	F	PAEC (mWL)	X (hr^1)	d (nm)	$q^{(u)}$ (hr^{-1})	Dose($\mu Gyhr^{-1}/Bq/m^3$) M(s,r) M(l,h)	F(r,e)	C10(r,e) C5(r,e)	M(l,h) Basal	M(l,h) Secretory
(1)off	898.3	3	0.483	0.2	0.527	128	14.5	90	1.5	13.7,16.0 37.0,64.0	14.1,37.2	15.8,38 18.4,29.1	11.2,47.4	19,78.7
off (background)	1722.7	3	0.483	0.2	0.479	223	14.5	90	4.1	12.4,14.6 33.6,58.1	12.8,33.8	14.4,34.5 16.7,26.4	10.2,43.0	17.3,71.4
off (during the vacuuming)	587.9	90	0.097	0	0.389	61.9	126	50	54	4.9,5.4 9.0,12.4	5.6,9.9	6.1,10.4 7.1,9.5	2.9,10.4	4.9,13.3
off (after 60 minutes)	1279.1	6	0.452	0.266	0.340	117	16	70	28	10.2,12.1 29.1,51.4	10.4,29	11.7,29.6 13.5,22.0	8.8,38.9	14.9,64.2
off (after 135 minutes)	1017.1	4	0.586	0.266	0.302	83.1	10	63	19	8.8,10.4 25.5,45.1	8.9,25.3	10.1,25.7 11.7,19.1	7.7,34.2	13.1,56.5
(2)off (cleaner off for 4 hours)	1389.4	2.5	0.897	0.516	0.236	88.6	1.55	28	5.99	10.3,12.6 33.3,61.8	10.3,32.5	11.8,33 13.5,23.4	9.9,48.4	17.1,79.3
off (cleaner off 5 hours, during the vacuuming)	976.8	15	0.667	0.333	0.263	69.3	6.77	26	12.2	9.5,11.4 27.7,49.4	9.6,27.5	10.9,28.1 12.6,20.8	8.4,37.6	14.2,62
off (after 60 minutes)	953.9	2.8	0.709	0.333	0.348	89.8	5.82	57	8.87	12.2,14.5 35.6,63.9	12.4,35.4	13.9,36 16,26.5	10.7,48.7	18.2,80
off (after 135 minutes)	850.5	2	0.766	0.333	0.277	63.7	4.14	58	15.1	9.4,11.3 28.0,50.4	9.5,27.7	10.8,28.2 12.5,20.7	8.3,38.4	14.3,63.4

The results of the size distributions of radon decay products are presented in Figure 35. A decrease in the activity of 0.9 nm size range was observed for ^{218}Po (from 75% to 45%) and ^{214}Pb (from 30% to 20%) during the vacuuming period. The "unattached" fraction of PAEC was approximately 0.20 and the equilibrium factor, F, was 0.32. For all three size distirbuions , the activity increase (15%) in the 1.5 - 50 nm size range was observed. This result reconfirms that vacuuming is a source of primary fine particles. As shown in Table 14, the average attachment diameter was 30 nm during the active particle generation, and to 45 nm 130 minutes after the vacuuming was off. The "attached" mode of all three distributions peaked in the 50 - 500 nm size range. The size distributions of radon decay products returned to those of the background shapes 130 minutes after the vacuuming stopped. The trend in the size distribution change corresponded with the measurements taken in Princeton house. The only major difference was in the degree of the decrease in the ^{218}Po cluster fraction which depends on the individual environment. The size distributions of ^{214}Pb and ^{214}Bi were in good agreement with those of the samples taken from the Princeton house. The deposition rate of "unattached" fraction was 40 hr^{-1}, which was compatible with that obtained from the Princeton house.

6.3.5. Cooking

6.3.5.1 Princeton House

During cooking in the kitchen, the particle number concentrations were found to be 250,000 cm^{-3} and 30,000 cm^{-3} in the kitchen and the bedroom of the Princeton house, respectively. The activity size distributions of radon decay products in the bedroom are presented in Figures 36 and 37. Only 10% activity of all three size distributions was in the 0.9 nm size range. The "unattached" fraction of PAEC was 0.15 with the equilibrium factor, F, of 0.50. All three size distributions in the bedroom were bimodal, with a major mode in the "attached" size range (80%). A significant increase in "attached" fraction larger than 20 nm was observed in the bedroom. The possible reasons are : (1) frying steak may produce larger particles; and (2) the small particles produced from cooking in the kitchen deposit and/or coagulate as they were transported to the bedroom. The average attachment diameter increased from 25 nm to 50 nm during the particle generation period, to 80 nm 60 and 135 minutes after the end of cooking. Reinking et al. (1985) reported a 74 nm attachment diameter for particles produced from tiled stove and cooking aerosols. Tu and Knutson (1988) conducted the measurements of particle size distribution in two residential dwellings. They found that the size ranges are different for cooking soup and frying

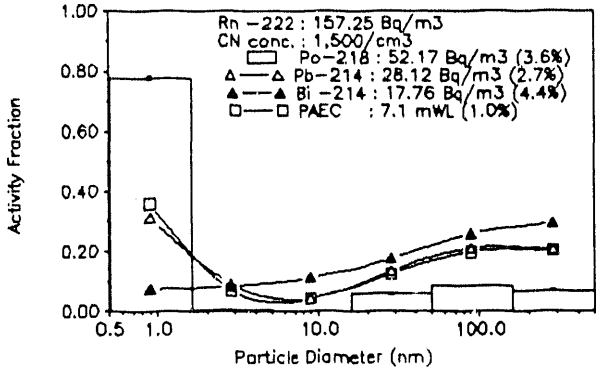

A: Background

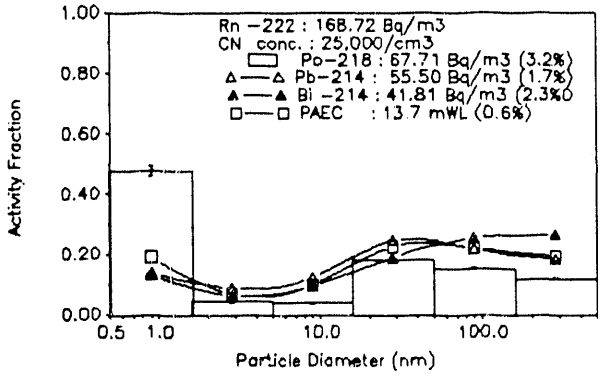

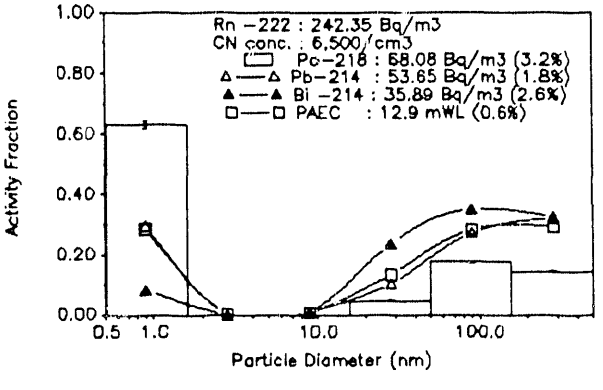

B: During the vacuuming

C: 130 minutes after vacuuming

Figure 35 ^{218}Po, ^{214}Pb, and $^{214}Bi/^{214}Po$ activity size distributions measured with aerosols generated from vacuuming.

Table 14 The measurements and calculation of X, d, $q^{(u)}$ and dose with vacuuming in Northford house.

Aerosol Source Cleaner	Co (Bq/m^3)	Z ($10^3 cm^{-3}$)	f_1	f_p	F	PAEC (mWL)	X (hr^{-1})	d (nm)	$q^{(u)}$ (hr^{-1})	Dose($\mu Gyhr^{-1}/Bq/m^3$) M(s,r) M(l,h)	F(r,e)	C10(r,e) C5(r,e)	M(l,h) Basal	M(l,h) Secretory
(1)Without air cleaner														
off (background)	157.3	1.5	0.781	0.431	0.167	7.1	3.8	65	34.2	6.9,8.3 20.9,37.8	6.9,20.6	7.9,21 9.1,15.3	6.2,28.6	10.7,47.4
off (during the vacuuming)	168.7	25	0.521	0.261	0.323	13.7	12.5	30	37.9	11,12.9 29.1,49.4	11.2,29.2	12.6,30 14.7,23.1	8.7,35.4	14.9,59.2
off (130 minutes after vacuuming)	242.4	6.5	0.631	0.286	0.197	12.9	7.9	45	53.9	5.4,6.5 16.5,30.3	5.5,16.4	6.3,16.6 7.2,12	5,23.8	8.6,38.9
(2)With air filtration system														
on (background)	232.7	1	0.746	0.310	0.094	5.9	4.6	80	52.3	3.4,4.1 9.5,16.5	3.5,9.5	3.9,9.7 4.6,7.3	2.8,11.9	4.9,20
on (background)	159.1	1.5	0.871	0.508	0.116	5.0	2.0	45	32.6	5.0,6.1 16,29.7	4.9,15.7	5.6,15.9 6.5,11.2	4.8,23	8.2,37.9
on (10 minutes after vacuuming)	180.9	22.5	0.597	0.315	0.139	6.8	9.2	28	47.5	6.4,7.5 16.5,27.4	6.5,16.5	7.3,16.9 8.5,13.3	4.9,18.6	8.4,31.7
on (100 minutes after vacuuming)	205.7	9	0.505	0.290	0.089	5.0	13.3	48	129	3.6,4.3 9.5,16	3.7,9.6	4.2,9.8 4.9,7.6	2.8,11.1	4.8,18.8
(3)With electronic air cleaner														
on (background)	41.44	1.5	0.629	0.293	0.107	1.2	8	90	137	3.1,3.8 9.4,17.1	3.1,9.2	3.6,9.4 4.1,7.0	2.9,9.4	4.8,21.5
on (background)	100.3	3	0.675	0.246	0.077	2.1	6.5	60	142	2.4,2.8 6.5,11.2	2.5,6.5	2.8,6.7 3.2,5.1	1.9,7.9	3.3,13.4
on (during the vacuuming)	80.6	12	0.301	0.180	0.459	5.1	31	45	104	6.9,8.1 17.5,29	7.3,17.9	8.2,18.2 9.4,14.5	5.2,20.5	8.9,34.2
on (100 minutes after vacuuming)	56.2	4	0.398	0.195	0.349	5.3	20	80	46	10.1,11.9 26.5,45	10.5,26.9	11.9,27.6 13.7,21.3	8,32.7	13.7,54.4

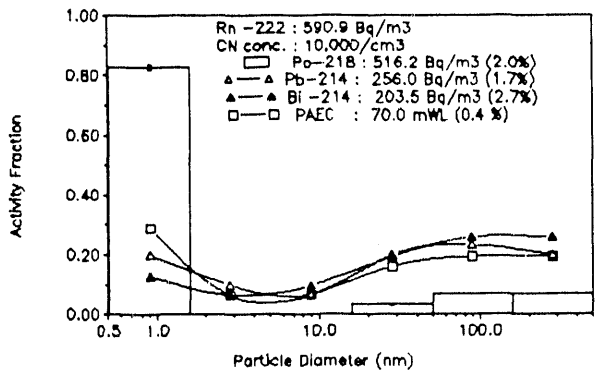

A: Background

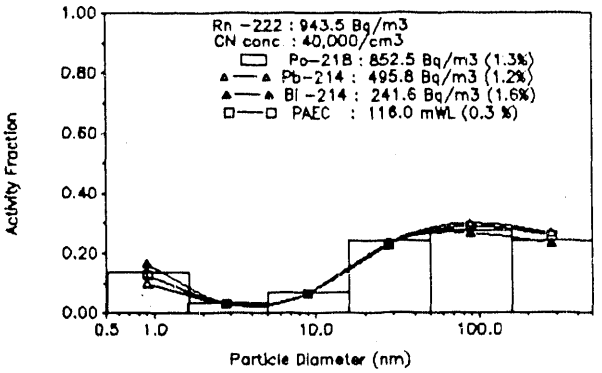

B: During the cooking

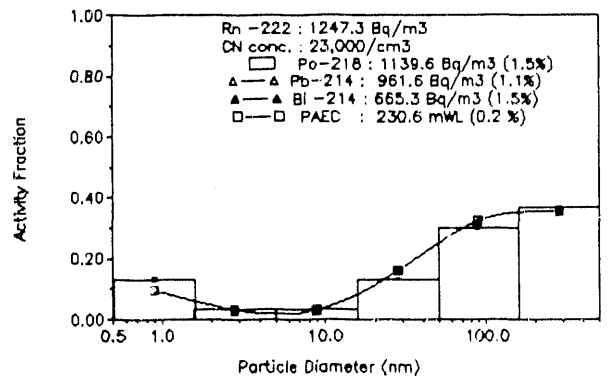

C: after 60 minutes

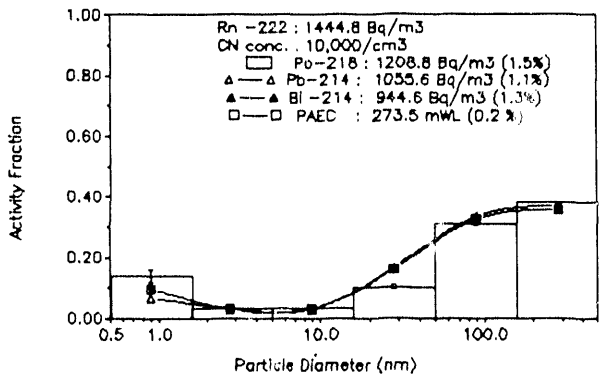

D: after 135 minutes

Figure 36 ^{218}Po, ^{214}Pb, and $^{214}Bi/^{214}Po$ activity size distributions measured under aerosol generated from cooking in the kitchen without air filtration system. (a)

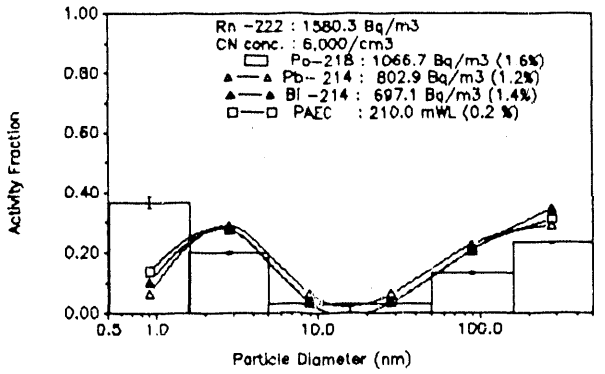

A: Background

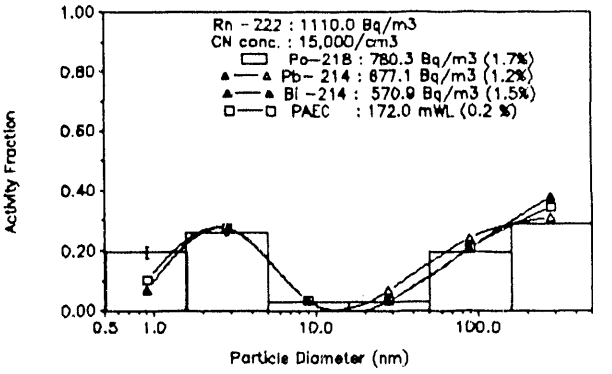

B: During the cooking

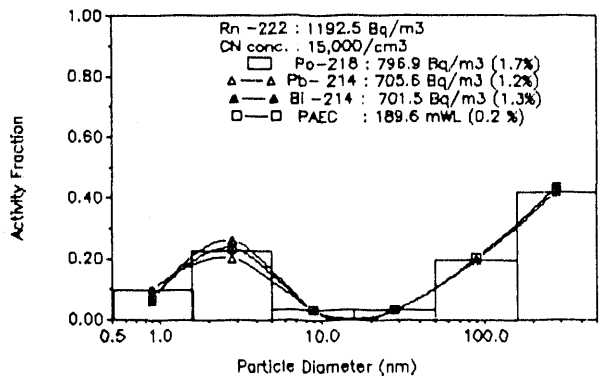

C: after 60 minutes

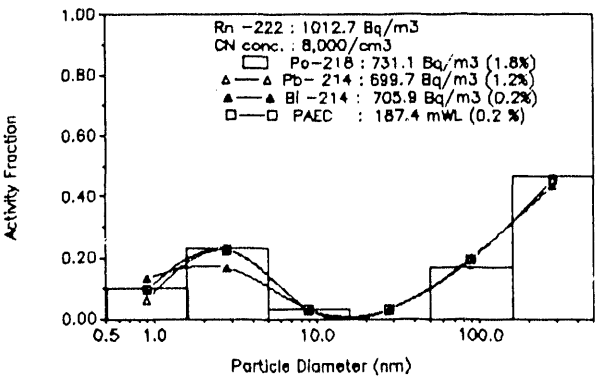

D: after 135 minutes

Figure 37 ^{218}Po, ^{214}Pb, and $^{214}Bi/^{214}Po$ activity size distributions measured under aerosol generated from cooking in the kitchen without air filtration system. (b)

meat and eggs. The soup particles produced using a gas stove are smaller in size, with a mean diameter of 14 nm, than particles from frying food, with a mean diameter of 54 nm. Tu and Knutson's investigation is in general agreement with the activity size distributions obtained in the bedroom with frying a steak in the kitchen. The larger particles observed in the bedroom from cooking had higher attachment rate as aerosols fromcigarette smoldering. Therefore, the size distributions of three decay products remained the same for longer periods of time. Table 15 summarizes the influence of cooking on the aerosol parameters of radon decay products. The attachment rate increased from 6 hr^{-1} to 40 hr^{-1} during the particle generation period, and to 48 hr^{-1} after 60 and 135 minute samples. The size distributions of three decay products remained the same for longer periods of time. The deposition rate of "unattached" fraction increased from 5 hr^{-1} to 12 hr^{-1}.

However, Strong (1988) found a quite different size distribution of radon decay products because of the cooking in the kitchen. Strong's results showed that the activity size distribution was trimodal (1.5 nm, 11 nm, 130 nm) before the cooking and bimodal (11 nm, 110 nm) during the cooking. During the cooking, the smallest mode (1.5 nm) disappeared, and this activity became associated with the 11 nm size range. In the same house, Strong (1989) made measurements in the living room while cooking in the adjacent kitchen. A trimodal size distribution of radon decay products was observed, with the additional mode occurring at 6 nm size range. This 6 nm mode may be due to the growth of aerosols from vapors generated during the cooking. In Strong's paper, no specific information was provided about the cooking process or what kind of food was cooked. Ramamurthi and Hopke (1990) also conducted several measurements in another kitchen. They found an approximately 10 nm mode when the gas burners were going. This small size range mode observed in the kitchen may be related to gas combustion of the gas burners.

For one set of experiments, all three size distributions of radon decay products were bimodal, with the major mode (70 %) in the 15 - 500 nm size range. The minor mode (20%) of three size distributions was in the 0.9 nm size range. For the other set of experiments, a minor mode of all three size distributions was in the 1.5 - 5 nm size range. This mode was more likely to be related to particles generated from the oil-furnace or some other unknown particle source. However, the same trend toward larger particles was observed by shifting most (60%) of radon decay products to the "attached" mode.

Table 15 The measurements and calculation of X, d, $q^{(u)}$ and dose with cooking in Princeton House.

Aerosol Source Cleaner	Co (Bq/m^3)	Z ($10^3 cm^{-3}$)	f_1	f_p	F	PAEC (mWL)	X (hr^1)	d (nm)	$q^{(u)}$ (hr^{-1})	Dose($\mu Gyhr^{-1}/Bq/m^3$) M(s,r) M(l,h)	F(r,e)	C10(r,e) C5(r,e)	M(l,h) Basal	M(l,h) Secretory
(1)off	146.9	7	0.7	0.387	0.547	22	5.8	35	3	22.5,26.5 66.0,117.0	22.5,65.3	25.9,66.7 30.0,49.0	19.7,87.8	33.3,145
off	243.83	9	0.793	0.4	0.508	33	3.5	25	1.8	21.3,25.4 62.3,111.0	21.3,61.5	24,62.7 27.9,46.3	18.5,83.7	32.0,138.0
off	429.2	10	0.827	0.367	0.432	50	2.8	20	1.6	17.0,20.0 49.6,88.0	17.2,49.0	19.6,50.0 22.6,37.0	14.9,65.7	25.4,109.0
off (background)	590.89	10	0.827	0.357	0.438	70	2.8	20	2.2	16.7,20.0 48.6,86.0	16.7,48.1	19.1,48.9 22.0,36.0	14.5,64.3	24.9,106
off (during the cooking)	943.5	40	0.176	0.161	0.455	116	65	50	7.3	12.1,14.1 30.6,51.0	12.6,31.2	14.1,32.0 16.4,25.2	9.3,36.7	15.8,61.2
off (after 60 minutes)	1247.3	23	0.166	0.129	0.684	230	68	72	6.6	14.5,16.7 36.2,60.4	15.1,37.0	17.0,38.0 19.7,30.0	11.0,43.1	18.8,72.4
off (after 135 minutes)	1444.8	10	0.172	0.129	0.700	273	70	100	15	14.9,17.2 37.1,61.9	15.6,37.9	17.4,38.8 20.2,30.8	11.4,44.0	19.2,74.0
(2)off (cleaner off 4 hours, background)	1580.3	6	0.567	0.414	0.492	210	10.3	51	11.2	22.5,26.7 61.6,104.0	22.5,61.3	25.6,62.6 29.9,48.0	17.5,68.8	30.5,119
off (cleaner off 5 hours, during the cooking)	1110.0	15	0.452	0.388	0.574	172	16.4	38	12.2	25.0,29.5 67.0,112.3	25.0,67.0	28.4,68.4 33.2,53.0	19.1,72.7	33.2,127
off (after 60 minutes)	1192.5	15	0.323	0.300	0.588	189	28.4	53	20.1	21.6,25.3 56.5,93.6	21.7,56.4	24.6,57.8 28.8,45.3	16.2,59.5	28,105
off (after 135 minutes)	1012.69	8	[illegible]33	0.323	0.685	187	27	80	15	25.9,30.5 69.4,116.0	26.0,69.0	29.4,70.7 34.5,54.8	19.8,75.7	34.5,133

6.3.5.2 Northford House

The family are of oriental origin. Generally speaking, the typical dinner meal in the Northford house consists of fried food and a soup. Dinner preparation time was typically from 16:00 to 18:00 and was the occasion of intermittent frying. An electric stove was used for cooking. It was anticipated that a lower number of particles are produced by an electric stove than by a gas stove. Figure 38 presents the influence of cooking on the size distribututions of radon decay products. During the first 10-minute cooking period, the particle concentration increased from 6,500 cm^{-3} to 15,000 cm^{-3}. The "unattached" fraction of ^{218}Po and PAEC decreased to 0.25 and 0.10. After the second frying and soup warming period lasting for 35 minutes, the particle concentration reached to 90,000 cm^{-3}. After 80 minutes when the second cooking stopped, the particle concentration declined to 8,000 cm^{-3}. During the second cooking period, the activity of three size distributions in the 0.9 nm size range of all three distributions decreased to approximately 10%. An increase (10%) in the 1.5 - 15 nm size range was observed for all three radon decay products. Most of the activity (75%) of all three decay products was distributed in the 50 - 500 nm size range. The equilibrium factor, F, was 0.35. The "attached" fraction was significantly increased by the particles larger than 20 nm. At the same time, the size distributions of radon decay products stayed constant for long periods of time. This constancy may be due to the larger particles produced from cooking remaining suspended for longer time and the higher attachment rate for activity to this size range. A similar phenomenon was observed previously in the Princeton house. The average attachment diameter as shown in Table 16 was 50 nm during the active cooking period, and 100 nm by the second measurement. The attachment rate was from 20 to 100 hr^{-1}. The deposition rate of "unattached" fraction was from 50 hr^{-1} to 150 hr^{-1}.

6.3.6 Clothes Washing and Drying

6.3.6.1 Springfield House

A test was conducted to evaluate the influence of a clothes dryer on the behavior of radon decay products in the basement of the Springfield house. Figure 39 shows a comparison of the typical distributions, with the air filtration system operating for 4 hours, followed by a four-hour period without the air filtration system. Immediately following the last four hour period without the air filtration system operating, the clothes dryer was operated for 30 minutes while the air filtration system was turned off. In comparison with the background conditions, the

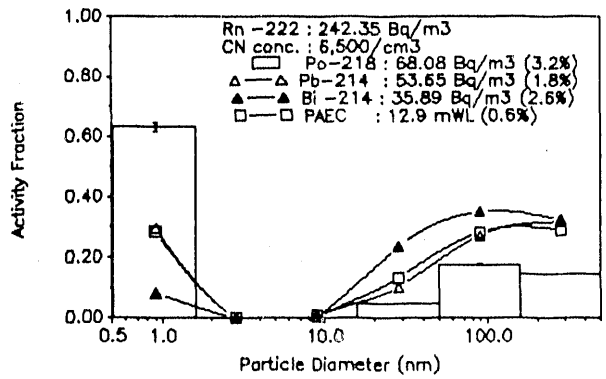

A: Background

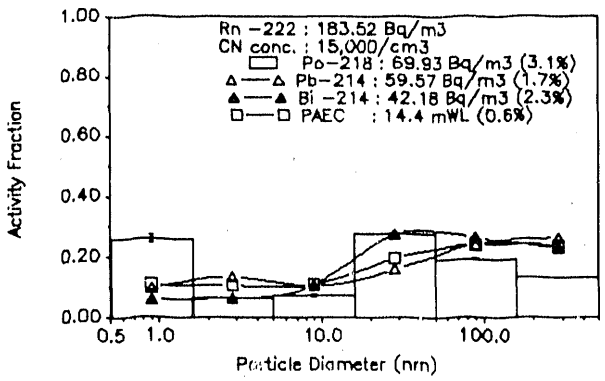

B: During the first cooking

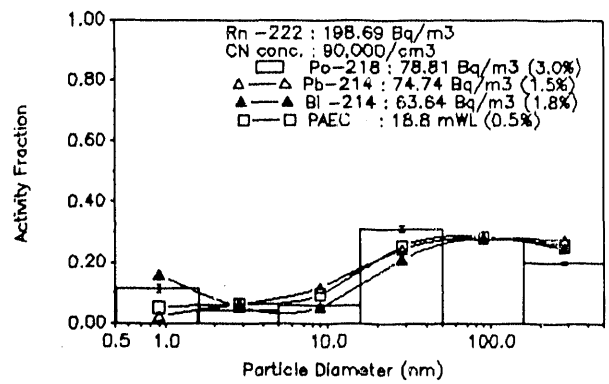

C: During the second cooking

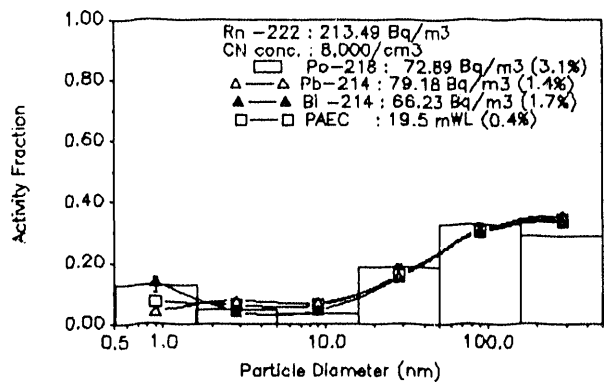

D: 80 minutes after cooking

Figure 38 ^{218}Po, ^{214}Pb, and $^{214}Bi/^{214}Po$ activity size distributions measured under aerosols generated from cooking.

Table 16 The measurements and calculation of X, d, $q^{(u)}$ and dose with cooking in Northford house.

Aerosol Source Cleaner	Co (Bq/m^3) (10^3cm^{-3})	Z	f_1	f_p	F	PAEC (mWL)	X (hr^1)	d (nm)	$q^{(u)}$ (hr^{-1})	Dose($\mu Gyhr^{-1}/Bq/m^3$) M(s,r) M(l,h)	F(r,e)	C10(r,e) C5(r,e)	M(l,h) Basal	M(l,h) Secretory
(1)Without air cleaner														
off	242.4	6.5	0.631	0.286	0.197	12.9	7.9	35	53.9	5.4,6.5	5.5,16.4	6.3,16.7	5,23.8	8.6,39.0
(background)										16.5,30.3		7.2,12.0		
off	183.5	15	0.322	0.216	0.290	14.4	29	50	66.8	10.2,11.9	10.5,25.9	11.8,26.5	7.6,28.4	13.0,48.3
(during the first cooking)										25.6,42.0		13.8,21.1		
off	198.7	90	0.157	0.113	0.350	18.8	73	50	128	9.5,10.9	10.0,22.5	11.2,23.2	6.6,26.2	12,44.6
(during the second cooking)										21.8,34.1		13.0,19.2		
2027	213.5	8	0.171	0.133	0.338	19.5	66	120	150	8.2,9.5	8.6,20.3	9.6,20.8	6.0,21.9	10.2,37.2
(80 minutes after cooking)										19.8,32.2		11.1,16.8		
(2)With air filtration system														
on	103.6	2	0.738	0.453	0.132	3.7	4.8	65	48.4	5.5,6.7	5.6,16.8	6.4,17.0	5.1,23.6	8.7,38.9
(background)										17,30.9		7.3,12.3		
on	51.1	4	0.673	0.326	0.200	2.8	6.6	50	27.1	7.4,8.8	7.4,20.7	8.4,21.1	6.3,26.2	10.6,44
(cooking started)										20.7,36.4		9.8,15.8		
on	70.7	10	0.446	0.241	0.204	3.9	17	55	42.9	7.9,9.2	8.2,20.1	9.2.20.6	5.8,21.6	10,36.9
(9 minutes before cooking finished)										19.8,32.3		10.7,16.4		
on	73.3	3.5	0.643	0.376	0.156	3.1	7.5	60	36.1	6.4,7.6	6.4,18.0	7.4,18.4	5.3,22.2	9.1,37.6
(115 minutes after cooking)										18.1,31.5		8.6,13.9		
(3)With electronic air cleaner														
on	56.2	4	0.398	0.195	0.349	5.3	20	80	46	10.1,11.9	10.5,26.8	11.9,27.6	8.0,32.7	13.7,54.4
(background)										26.5,45.0		13.7,21.3		
on	59.94	20	0.364	0.238	0.389	6.3	24	40	33	9.3,11.2	9.5,27.5	10.7,28.0	8.5,39.7	14.5,65
(cooking started)										28.2,50.7		12.3,20.0		
on	56.2	30	0.115	0.121	0.664	10.1	104	75	47	13.2,15.1	13.7,33.6	15.3,34.5	10.3,41.3	17.3,68.5
(40 minutes after cooking)										33.0,55.9		17.6,27.2		
on	220.52	15	0.277	0.158	0.186	11.1	35	65	190	4.1,4.8	4.3,11.0	4.8,11.2	3.3,14.1	5.7,23.3
(140 minutes after cooking)										10.8,18.8		5.5,8.6		

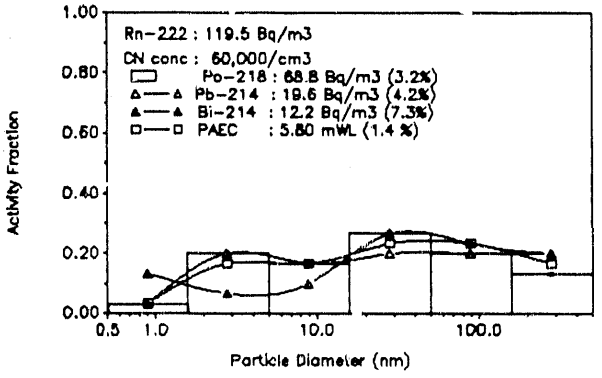

A: Background

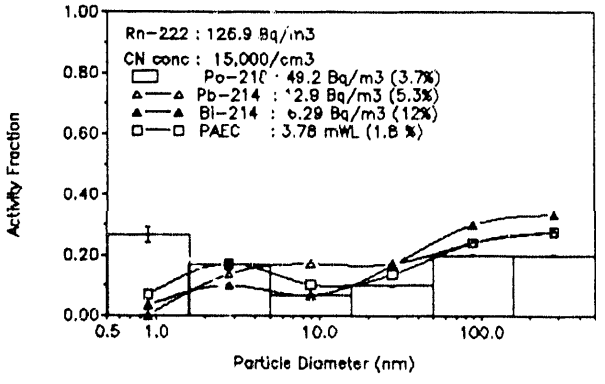

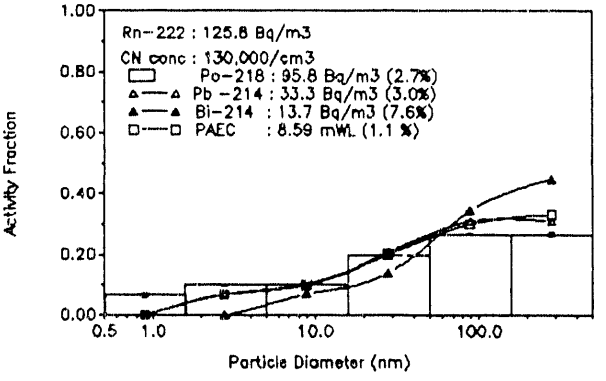

B: cleaner on for 4 hours

C: clothes dryer, cleaner off for 4 hours

Figure 39 ^{218}Po, ^{214}Pb, and $^{214}Bi/^{214}Po$ activity size distributions measured under aerosol generated from clothes dryer in the basement with air filtration system.

particle concentration increased from 100,000 cm^{-3} to 130,000 cm^{-3}. The activity of the ^{218}Po in the 0.9 nm size range was 7%, with a significant decrease in the 1.5 - 5 nm size range (from 20% to 10%). For all three decay products, most of the activity (70%) remained in the 15 - 500 nm size range. However, this result is a combination effect of the clothes dryer operating and no operating air filtration system. It is difficult to determine the effect on radon decay products of just the clothes dryer operating alone from this measurement. The single effect from the clothes drying operating will be evaluated in the Northford, CT house.

6.3.6.2 Northford House

The influence of the washing machine and clothes dryer on the behavior of radon decay products was evaluated in the living room of the Northford house. The results of size distributions of radon decay products are as shown in Figure 40. The washing machine and clothes dryer are brand new appliances and operated for an hour each. The particle concentration increased from 5,000 cm^{-3} to 10,000 cm^{-3}. However, an insignificant change was observed for all three decay products. The increase in particle concentration may be due to unknown particle sources.

6.3.7 Conclusion

The influence of indoor particles on the behavior of radon decay products was investigated in the domestic environments. Because of a large number of particles produced from indoor activities, different degrees of decrease in the "unattached" fraction of PAEC and increase in both equilibrium factor and total PAEC were observed. In the presence of additional aerosol sources, such as cigarette smoke and cooking, the "unattached" fraction was as low as 0.07. At the same time, the equilibrium factor could reach 0.50. Aerosols produced by candle burning and vacuuming decreased the "unattached" fraction of PAEC only moderately. This result was due to the difference in particle size distribution for these two groups of indoor particles. The "unattached" fraction is more dependent on the attachment rate (size and number of particles) than on the particle number concentration alone. No influence on radon decay products by running water in a shower, clothes washing, and clothes drying was observed.

Larger particles generated from cigarette smoke and cooking dramatically shift most of the radon decay products to the "attached" mode (15 - 500 nm). With regard to the higher attachment rate, all three size distributions were stable for long periods of time after aerosol

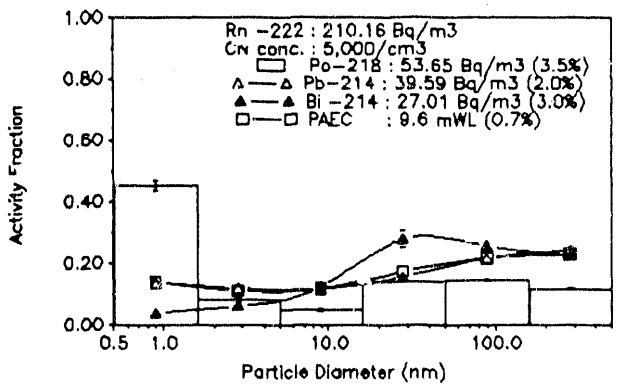

A: Background

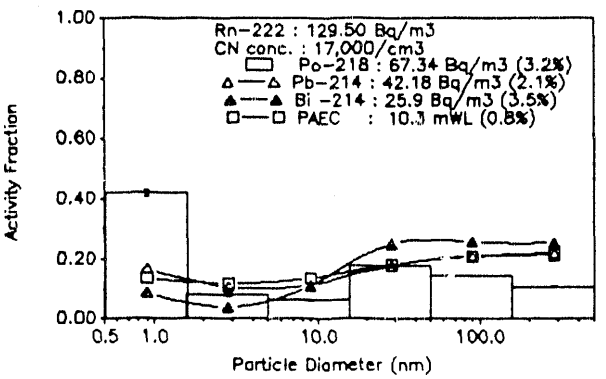

B: During clothes washing

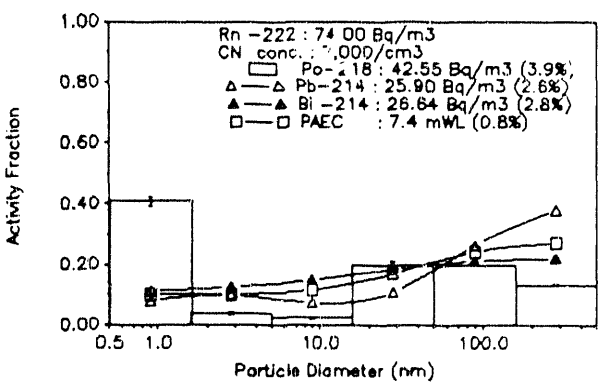

C: 30 minutes after clothes drying

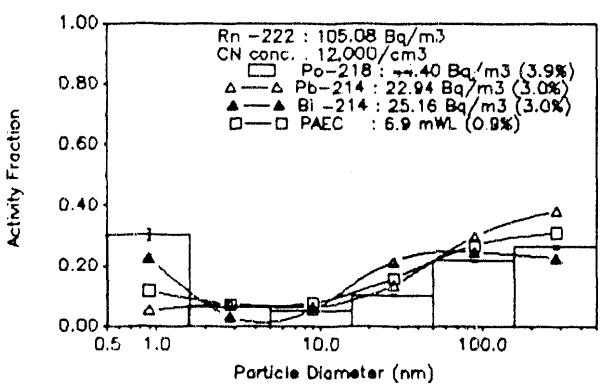

D: 120 minutes after clothes drying

Figure 40 ^{218}Po, ^{214}Pb, and $^{214}Bi/^{214}Po$ activity size distributions measured under aerosols generated from clothes washing and drying.

generation. The attachment rate was 50 - 120 hr^{-1} with an average attachment diameter of 120 nm. On the other hand, aerosols produced from candle burning and vacuuming were much smaller, with an average attachment diameter of 15 nm. The attachment rate ranged from 10 to 60 hr^{-1}. These particles did decrease the "unattached" fraction, especially during the period of active aerosol generation. However, the size distributions of radon decay products returned to those of the background condition within 150 minutes after the end of particle generation. This result was due to the fact that the particles had a higher deposition rate and a lower attachment rate. With additional particles present, the hourly dose rate per Bq m^{-3} radon changed insignificanly. At the same time, the PAEC substantially increased and the "unattached" fraction of PAEC decreased.

6.4 Background Conditions with the Air Filtration System

6.4.1 Basement Measurements in the Springfield House

With the air filtration system in use, the particle number concentration in the basement of the Springfield house was in the range of 15,000 - 40,000 cm^{-3}. Figures 41 and 42 present the change of activity size distributions of radon decay products with the air filtration system operating. The activity of ^{218}Po increased from 7% to 25% in the 0.9 nm size range having a diffusivity similar to the classical "unattached" fraction with insignificant change occurring in the 1.5 - 5 nm size range. The "unattached" fraction of ^{218}Po and PAEC was from 0.28 to 0.44 and 0.14 to 0.24, respectively. The corresponding ^{214}Pb and ^{214}Bi distributions indicated insignificant activity exited in the 0.5 - 1.5 nm size interval with 15% of the activity occurred in the 1.5 - 5 nm size range. The equilibrium factor, F, decreased to 0.09 - 0.12 because of the reduction in the particle number concentration. A bimodal size distribution was observed for ^{218}Po in the 0.9 nm and 89 nm size ranges and for ^{214}Pb and ^{214}Bi in the 2.8 nm and 89 nm size ranges. Because of the particles generated by the combustion of the oil furnace, the "unattached" fraction of PAEC in the basement was much lower than that of the typical condition with the air filtration system running. The differences in the size distributions of radon decay products between the background level and the level achieved with the air filtration system operating were primarily related to a 50% reduction in particle number concentration. In general, air cleaning systems reduce the concentration of radon decay products and PAEC by three mechanisms. The first is the direct collection of "unattached" and "attached" radon decay products by the air cleaning systems. The second is the enhancement of deposition of radon decay products to the room surfaces created by the air cleaning system's air circulation. The final mechanism is the

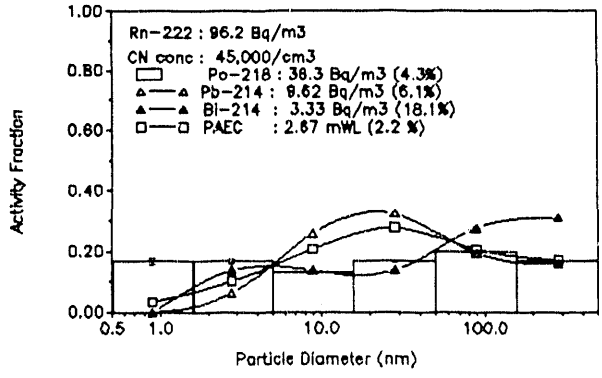

A: cleaner on for 4 hours

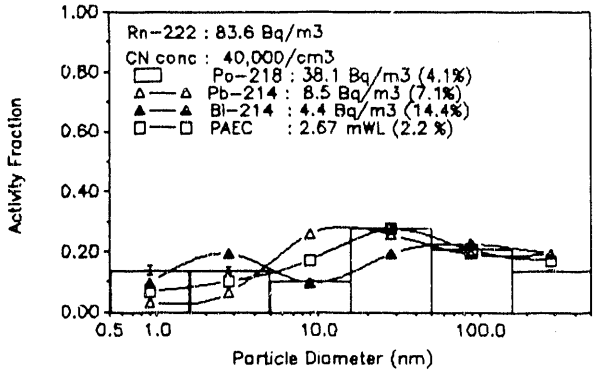

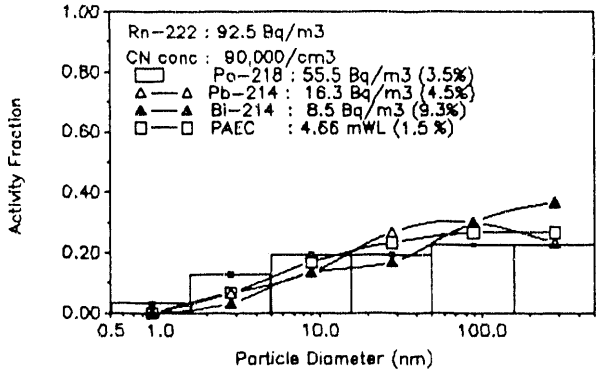

B: cleaner on for 7 hours

C: cleaner off for 4.5 hours

Figure 41 ^{218}Po, ^{214}Pb, and $^{214}Bi/^{214}Po$ activity size distributions measured under typical conditions in the basement with air filtration system. (a)

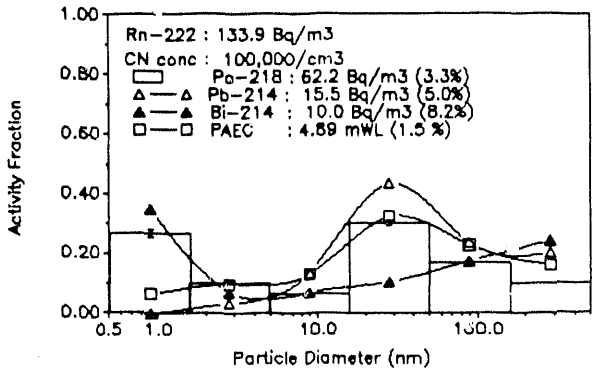

A: Background

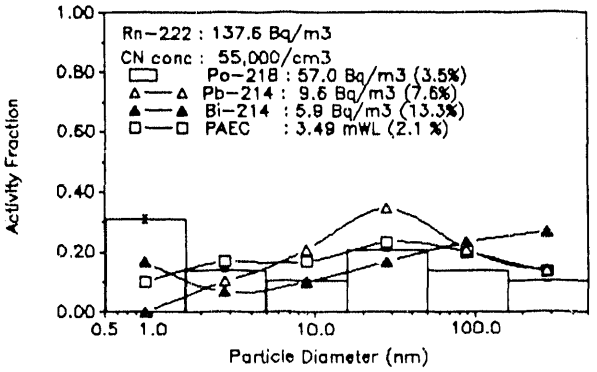

B: cleaner on for 2.5 hours

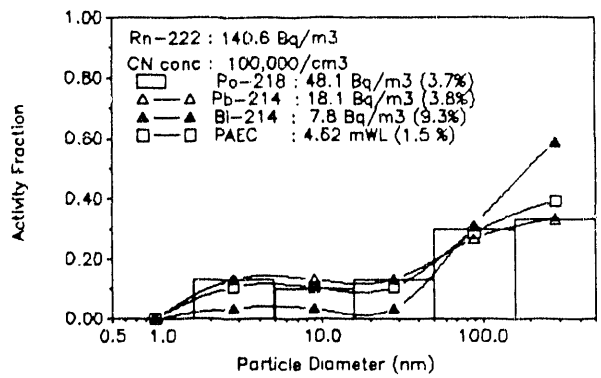

C: cleaner off for 2.5 hours

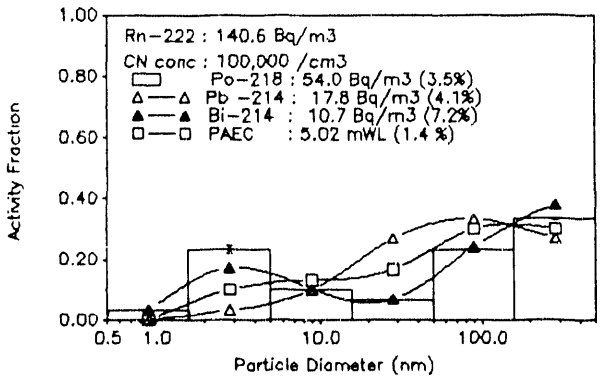

D: cleaner off for 6.5 hours

Figure 42 Po-218, Pb-214, and Bi-214/Po-214 activity size distributions measured under typical conditions in the basement with air filtration system. (b)

shift in average size to the smaller particles. The plateout rate then increases because of the higher diffusivity of these smaller particles. For the air filtration system, the PAEC reduction is mainly due to the direct capture of radon decay products. With the air filtration system in use, the attachment rate decreased to 25 hr^{-1} with smaller attachment diameter of 27 nm. The deposition rate of "unattached" fraction was in the range of 40 hr^{-1} to 65 hr^{-1} as shown in Table 17.

The increase in the "unattached" fraction of ^{214}Pb and ^{214}Bi was not as large as that of ^{218}Po by the air filtration system. The reductions of ^{218}Po, ^{214}Pb, ^{214}Bi concentration, and PAEC per Bq m^{-3} radon were approximately 23%, 41%, 48%, and 37%, respectively, compared with those in the background conditions without the air filtration system. The "unattached" fraction of PAEC increased from 10% to 20% due to particle removal by the air filtration system. The dose conversion factor of the "unattached" fraction (0.9 nm size range) is much larger compared with that of the "attached" mode. Approximately 20% of dose reduction resulted from the 10% increase in the "unattached" fraction of PAEC and 37% reduction of PAEC. The hourly dose rate per Bq m^{-3} radon was reduced with the air filtration system operating in the basement. The average reductions in hourly dose rate per Bq m^{-3} radon (dose reductions) for males at sleep, rest, light work, and heavy work were 28%, 26%, 22%, and 19%, respectively; for females at rest and exercise, the dose reductions were 28% and 24%, respectively; for children ages 10 at rest and exercise, the dose reductions were 27% and 24%, respectively; for children ages 5 at rest and exercise, the dose reductions were 28% and 25%, respectively. For bronchial basal cell, the average reductions in hourly dose rate per Bq m^{-3} radon for adult males at flowrates of 125 cm^3 s^{-1} and 833 cm^3 s^{-1} were 21% and 16%, respectively; for secretory cell nuclei, the dose reductions for adult males at flowrates of 125 cm^3 s^{-1} and 833 cm^3 s^{-1} were 22% and 16%, respectively.

6.4.2 Bedroom Measurements in the Princeton House

6.4.2.1 Bedroom Door Closed

With the bedroom door closed and the air filtration system on, the particle concentration in the bedroom of the Princeton house decreased from 3,000 cm^{-3} to 1,500 - 2,000 cm^{-3}. The size distributions of radon decay products are presented in Figure 43. For all three distributions of radon decay products, a large increase in the activity in the 0.9 nm size range was observed. The activities of ^{218}Po, ^{214}Pb, and ^{214}Bi in this size range were 95%, 80%, and 50%, respectively. The larger increase in the "unattached" fraction of ^{218}Po is due to the short half life of ^{218}Po. The

Table 17 The measurements and calculation of X, d, $q^{(u)}$ and dose in Springfield house.

Aerosol Source Cleaner	Co (Bq/m^3)	Z ($10^3 cm^{-3}$)	f_1	f_p	F	PAEC (mWL)	X (hr^1)	d (nm)	$q^{(u)}$	Dose($\mu Gy hr^{-1}/Bq/m^3$) M(s,r) (hr^{-1}) M(l,h)	F(r,e) M(l,h)	C10(r,e) C5(r,e)	M(l,h) Basal	M(l,h) Secretory
(1)off (background)	119.5	60	0.233	0.200	0.181	5.8	45	33	41	7.4,8.5 17.2,26.9	7.6,17.7	8.5,18.1 16.7,14.9	5.1,16.8	8.7,29.2
on (cleaner on for 4 hours)	126.9	15	0.434	0.241	0.110	3.78	17	40	48	4.2,4.8 10.4,16.8	4.3,10.5	4.8,10.7 5.6,8.6	3.0,10.8	5.2,18.8
off (during clothes dryer, cleaner off for 4 hours)	125.8	100	0.167	0.067	0.253	8.60	68	12	24	6,6.8 12.7,18.9	6.4,13.4	7.1,13.8 8.3,11.8	3.9,11.4	6.6,20.1
(2) on (cleaner on for 4 hours)	96.2	45	0.324	0.134	0.102	2.67	27	28	65	3.9,4.5 8.8,13.6	4.1,9.1	4.6,9.3 5.4,7.9	2.7,8.6	4.6,14.8
on (cleaner on for 7 hours)	83.62	40	0.276	0.172	0.118	2.67	35	34	57	4.5,5.1 10.6,16.7	4.7,10.9	5.3,11.1 6.2,9.2	3.2,10.9	5.4,18.7
off (cleaner off for 4.5 hours)	92.5	90	0.161	0.067	0.185	4.66	71	33	54	5.4,6.1 11.3,16.8	5.7,11.9	6.3,12.2 7.5,10.6	3.4,10.2	5.9,17.6
(3)off (background)	133.9	100	0.367	0.161	0.135	4.89	23	19	41	4.8,5.5 11.2,17.6	5.0,11.6	5.6,11.8 6.5,9.8	3.4,11.5	5.7,19.7
on (cleaner on for 2.5 hours)	137.6	55	0.448	0.267	0.094	3.49	17	22	42	4.2,4.9 10.5,17.0	4.4,10.6	4.9,10.9 5.7,8.8	3.1,11.1	5.3,19.1
off (cleaner off for 2.5 hours)	140.6	100	0.133	0.107	0.135	4.62	88	34	76	3.2,3.6 7.1,10.8	3.3,7.3	3.7,6.5 4.3,6.3	2.1,6.5	3.6,11.6

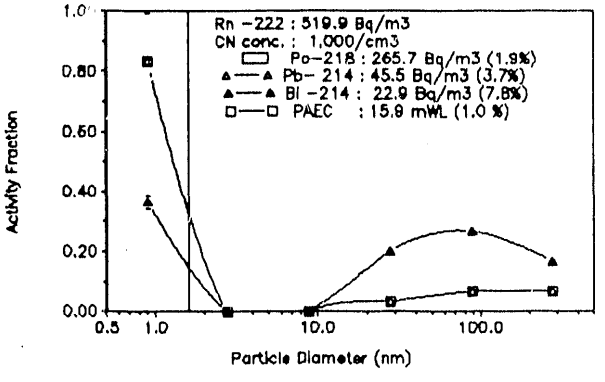

A: cleaner on for 2 hours

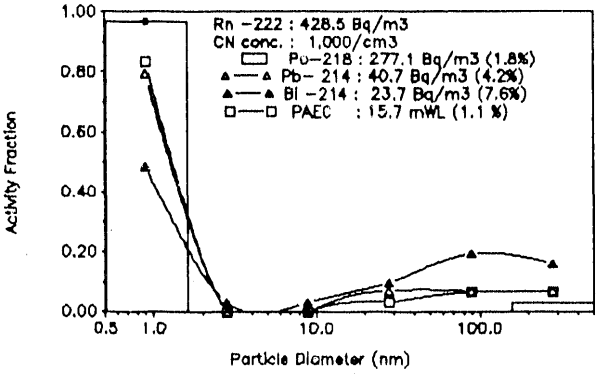

B: cleaner on for 4 hours

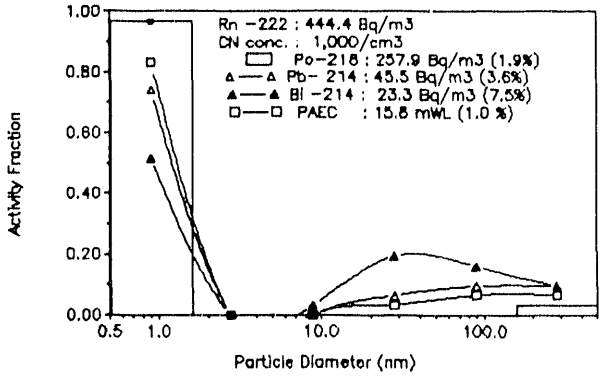

C: cleaner on for 6 hours

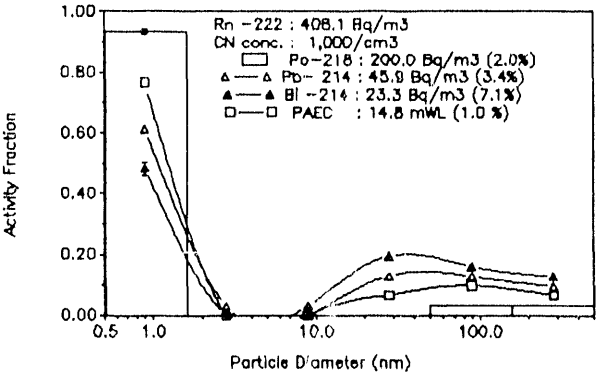

D: cleaner on for 8 hours

Figure 43 ^{218}Po, ^{214}Pb, and $^{214}Bi/^{214}Po$ activity size distributions measured under closing bedroom door with air filtration system.

"unattached" fraction of PAEC was from 0.67 to 0.83 and the equilibrium factor, F, reduced to the range of 0.10 - 0.16. No activity was found in the 1.5 - 15 nm size range for any of the three size distributions. Less than 20% of the activity of all three decay products was in the "attached" mode. At the same time, the attachment rate decreased to 0.4 - 2.0 hr^{-1} with the 20 - 30 nm average attachment diameter. The deposition rate of "unattached" fraction increased to approximately 8 - 16 hr^{-1}. These results indicated that the air filtration system effectively removed most of the particles in the bedroom. However, the particle removal does not produce a comparable removal of the "unattached" radon decay products. Therefore, the newly-formed radon decay products have fewer particles to which they can attach. This substantial increase in the "unattached" fraction by using the air filtration system agrees with the evaluations of HEPA filters done by Hinds (1983) and Maher (1985). They found that 80% of the residual activity was "unattached" with the filter units.

The reduction in PAEC per Bq m^{-3} radon was 55% with 40% increase in the "unattached" fraction of PAEC compared with the background condition. The reductions in hourly dose rate per Bq m^{-3} radon (dose reductions) for males at sleep, rest, light work, and heavy work were only 29%, 26%, 15%, and 10%, respectively; for females at rest and exercise, the dose reductions were 31% and 17%, respectively; for children age 10 at rest and exercise, the dose reductions were 30% and 18%, respectively; for children age 5 at rest and exercise, the dose reductions were 31% and 24%, respectively. For bronchial basal nuclei cell, the average dose reductions for adult males at flowrates of 125 cm^3 s^{-1} and 833 cm^3 s^{-1} were 16% and 5%, respectively; for secretory cell, the dose reductions for adult males at flowrates of 125 cm^3 s^{-1} and 833 cm^3 s^{-1} were 15% and 5%, respectively. The average dose reduction was 20%.

6.4.2.2 Bedroom Door Open

When the bedroom door was open and the air filtration system operating, the particle concentration in the bedroom of the Princeton house reduced to 6,000 - 7,000 cm^{-3} from 10,000 cm^{-3}. The results of the size distributions of radon decay products are shown in Figure 44. The "cluster" fraction of ^{218}Po was still high (90%), but slightly lower than with the bedroom door closed and the air filtration system operating. This result can be explained by the higher ventilation rate with the bedroom door open. As the air filtration system created air circulation, the particles continued entering the bedroom. The radon decay products became attached to particles entering the bedroom. The "unattached" fractions of ^{218}Po and PAEC were between 0.87 and 0.93 and ranged from 0.58 to 0.63, respectively. The fraction of ^{214}Pb and ^{214}Bi in the 0.9 nm size range was about 25% and 18%,

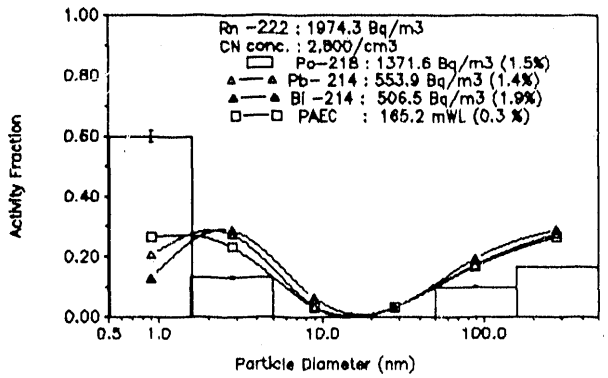

A: 135 minutes after cooking, on 10 hours

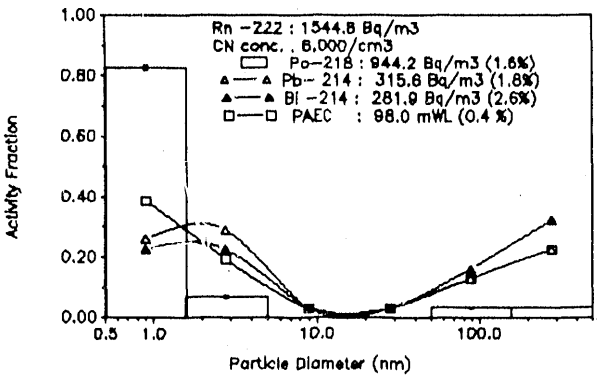

B: cleaner on for 12 hours

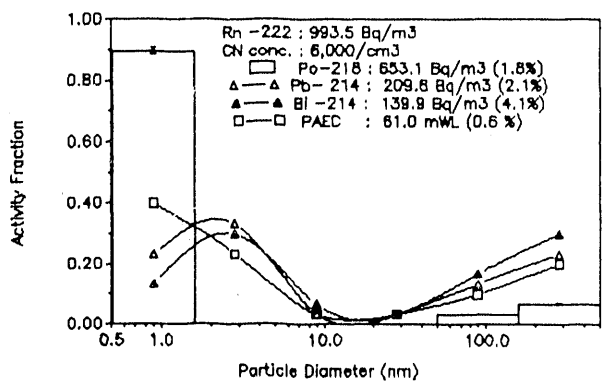

C: cleaner on for 15 hours

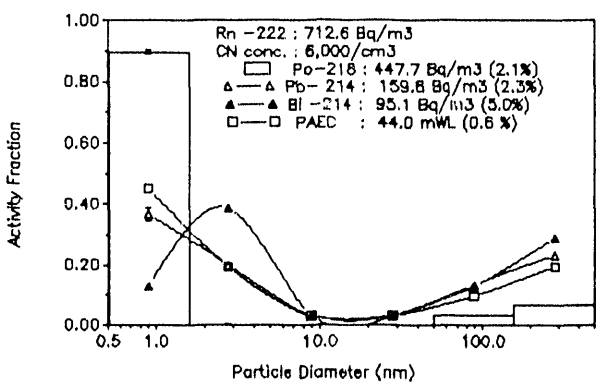

D: cleaner on for 17 hours

Figure 44. ^{218}Po, ^{214}Pb, and $^{214}Bi/^{214}Po$ activity size distributions measured under opening bedroom door with air filtration system.

respectively. No activity was observed in the 1.5 - 5 nm size range for ^{218}Po, but 30% was observed for ^{214}Pb and ^{214}Bi. In summary, a bimodal size distribution was observed for all three decay products with a major mode (80%) in the 0.5 - 5 nm size range and a minor mode (20%) in the 50 - 500 nm size range. The equilibrium factor, F, decreased from 0.50 to 0.23. The decreases in the attachment rate (from 4 hr^{-1} to 2 hr^{-1}) and average attachment diameter (from 30 nm to 24 nm) were observed compared with the background conditions without the air filtration system. The deposition rate of " unattached" fraction increased from 3 hr^{-1} to 7 hr^{-1}.

The reduction in PAEC per Bq m^{-3} radon was 45% and the "unattached" fraction of PAEC increased 20% compared to the condition without the air filtration system. The reductions in hourly dose rate per Bq m^{-3} radon (dose reductions) for males at sleep, rest, light work, and heavy work were 23%, 22%, 18%, and 17%, respectively; for females at rest and exercise, the dose reductions were 25% and 19%, respectively; for children age 10 at rest and exercise, the dose reductions were 24% and 19%, respectively; for children age 5 at rest and exercise, the dose reductions were 25% and 22%, respectively. For bronchial basal cell, the dose reductions for adult males at flowrates of 125 cm^3 s^{-1} and 833 cm^3 s^{-1} were 20% and 16%, respectively; for secretory cell, the dose reductions for adult males at flowrates of 125 cm^3s^{-1} and 833 cm^3 s^{-1} were 18%, and 15%, respectively. The average dose reduction was 20%.

6.4.3 Living Room Measurements in the Northford House

With the air filtration system operating, the particle concentrations in the living room of the Northford house were in the range of 1,000 cm^{-3} to 2,500 cm^{-3}. The size distributions of radon decay products are as shown in Figure 45. The fraction of ^{218}Po in the smallest size range was always more than 70%. The fraction of ^{214}Pb and ^{214}Bi in the 0.9 nm size range was approximately 40% and 5%, respectively. All three size distributions appeared to have very little activity in 1.5 - 15 nm size range, with the remaining activity attached to indoor particles larger than 50 nm. The "unattached" fraction of ^{218}Po and PAEC ranged from 0.60 to 0.80 and from 0.40 to 0.55, respectively. The equilibrium factor, F, decreased to 0.08 - 0.14 from 0.20. The activity distributions obtained in the Northford house are in general agreement, both with respect to the ^{218}Po cluster fraction (80%) and the size range of "attached" activity (20%), with those measured in the Princeton house when the air filtration system was operating. A smaller attachment rate in the range of 3 to 10 $hr^{-1}$was obtained with the average particle attachment diameter of 55 nm. A significant increase in the deposition rate of "unattached" fraction was observed in the range of 25 to 100 hr^{-1} as shown in Table 10.

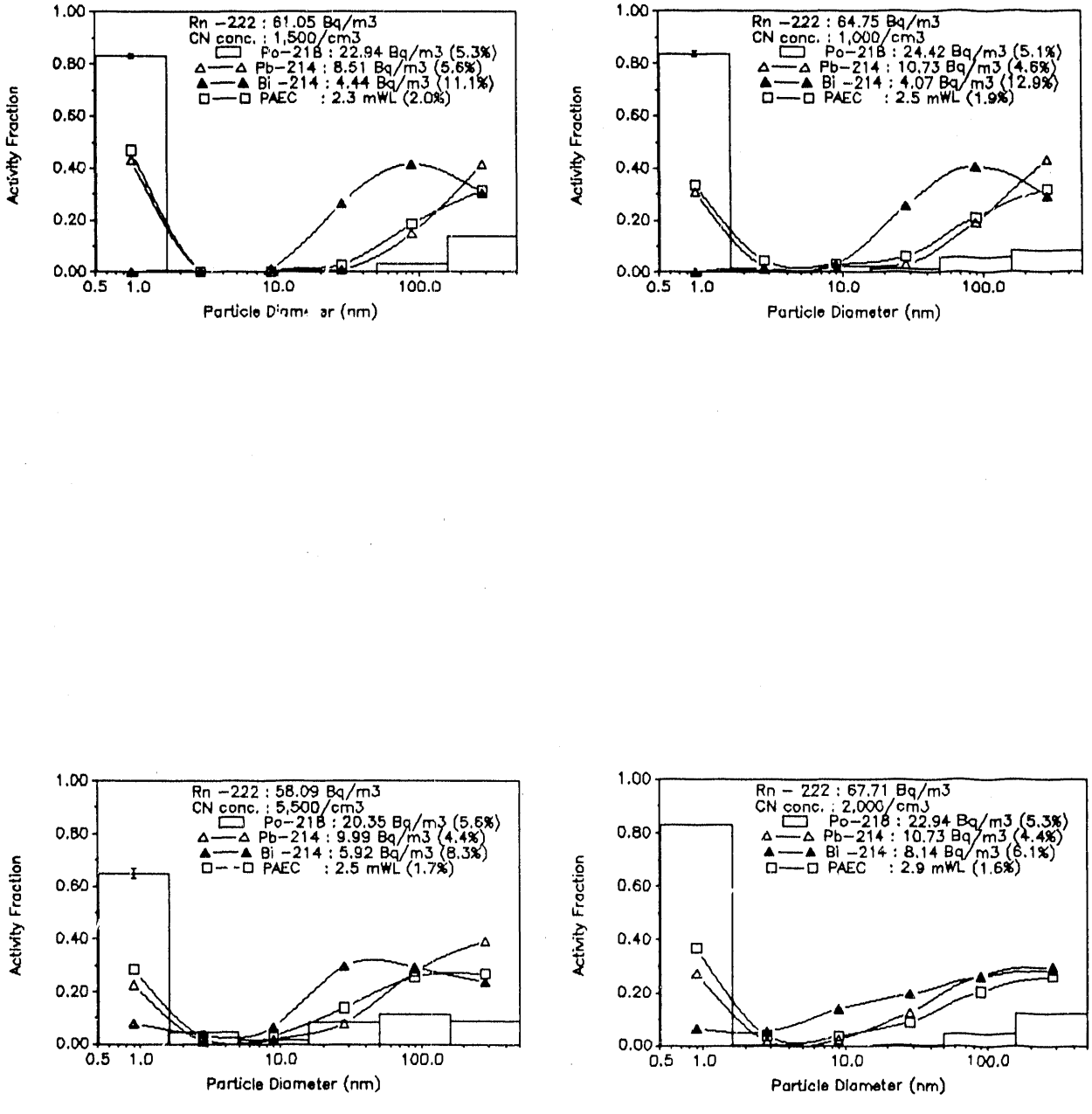

Figure 45 ^{218}Po, ^{214}Pb, and $^{214}Bi/^{214}Po$ activity size distributions measured with the air filtration system.

The average reductions in total ^{218}Po, ^{214}Pb, ^{214}Bi concentrations per Bq m^{-3} radon were approximately 15%, 50%, and 70%, respectively. The average reductions in PAEC per Bq m^{-3} radon were from 45% to 60% with average 25% increase in the "unattached" fraction of PAEC. However, the "unattached" ^{218}Po concentration increases in most cases with the air filtration system operating. These results are in general agreement with the evaluations HEPA filter by Hinds et al. (1983) and Maher *et al.* (1985). The increase in the "unattached" fraction of ^{218}Po, ^{214}Pb, and ^{214}Bi was in the range of 200% - 700% with average 75% reduction in PAEC by the filtration unit.

The average reductions in hourly dose rate per Bq m^{-3} radon (dose reductions) for males at sleep, rest, light work, and heavy work were 48%, 46%, 38%, and 32%, respectively; for females at rest and exercise, the dose reductions were 49% and 39%, respectively; for children age 10 at rest and exercise, the dose reductions were 47% and 40%, respectively; for children age 5 at rest and exercise, the dose reductions were 49% and 44%, respectively. For bronchial basal cell nuclei, the dose reductions for adult males at flowrates of 125 cm^3 s^{-1} and 833 cm^3 s^{-1} were 37% and 25%, respectively; for secretory cell nuclei, the dose reductions for adult males at flowrates of 125 cm^3 s^{-1} and 833 cm^3 s^{-1} were 37% and 26%, respectively. Although the "unattached" fraction dramatically increases when the air filtration system was used, the hourly dose rate per Bq m^{-3} radon was still reduced due to the large reduction in PAEC. The average dose reduction was 40%.

6.4.4 Conclusions

With the air filtration system operating, a bimodal size distribution of all three decay products was obtained with a major mode in the "cluster" fraction. More than 70% ^{218}Po activity was found in this size range. The "unattached" fraction of PAEC substantially increased to 60% - 85%. The equilibrium factor, F, decreased to the range of 0.10 - 0.35. Little activity of any radon decay products was found in the "attached" size range. These changes were related to particle removal by the air filtration system. The particle removal efficiency of the air filtration system was in the range of 40% - 70%. The attachment rate decreased even to 1 hr^{-1} with the higher deposition rate while the air filtration system was in use.

Under the typical conditions, the average reduction in PAEC per Bq m^{-3} radon was between 40% and 65% with 10% - 40% increase in the "unattached" fraction of PAEC. The same type of air filtration system was evaluated in a chamber by Kuennen and Roth (1989). They reported that the PAEC reduction was 84%. Continuous operation of the same type of air filtration system investigated by James et al. (1989) in another chamber found that PAEC was reduced by 60% to

90%. The resulting average reductions in hourly dose rate per Bq m^{-3} radon were between 20% and 40%. The same type of air filtration system was studied by James et al. (1989) where they found that the dose rate was reduced by 10% to 60%.

6.5 Background Conditions with the Electronic Air Cleaner

With the electronic air cleaner operating, the particle concentration in the living room of the Northford house was between 2,500 cm^{-3} and 4,000 cm^{-3}. Both conditions, with and without the electronic air cleaner had the same level of particle number concentrations. The results of the size distributions of radon decay products are as shown in Figure 46. The activity in the 0.9 nm size range was found to be 60% for ^{218}Po and 20% for ^{214}Pb and ^{214}Bi. The "unattached" fraction of ^{218}Po and PAEC was from 0.60 to 0.70 and ranged from 0.27 to 0.32, respectively. The equilibrium factor was in the range from 0.15 to 0.22. Approximately 10% of all three distributions was in the 1.5 - 15 nm size range. The remaining activity was attached to larger particles, 40% for ^{218}Po and 60% for ^{214}Pb and ^{214}Bi. With the electronic air cleaner operating, the size distributions of radon decay products are similar to those of the background conditions without any air cleaner. At the same time, the aerodynamic parameters shown in Table 10 were very similar both with and without the electronic air cleaner. This result may be due to the smaller removal efficiency of "attached" fraction with the electronic air cleaner than that of the air filtration system. The other reason is that the electronic air cleaner may produce particles to which radon decay products can attach. Rajala *et al.* (1986) found that the ESP could produce condensation nuclei. These nuclei were observable when no particle sources were present. The ozone generated by the corona discharge of the ESP could have an effect on the production of these submicron particles (Peyrous *et al.*, 1982). To understand whether the electronic air cleaner produces ozone, a continuous ozone monitor was operated at the same time as the electronic air cleaner. However, no ozone was detected. It may be explained by that any ozone produced by the electronic air cleaner was adsorbed by the activated charcoal filter before it could be detected by the monitor.

The average reductions in total ^{218}Po, ^{214}Pb, and ^{214}Bi concentrations per Bq m^{-3} radon were approximately 20%, 35%, and 45%, respectively. The average reductions in PAEC per Bq m^{-3} radon were between 25% and 40% with no significant increase in the "unattached" fraction. There were some reductions for the "unattached" ^{218}Po, ^{214}Pb, and ^{214}Bi concentration. These results are in general agreement with the evaluations of ESP by Hinds et al. (1983) and Maher et al. (1985). Their studies showed that the ESP reduced the ^{218}Po, ^{214}Pb, and ^{214}Bi concentrations and PAEC by 25%,

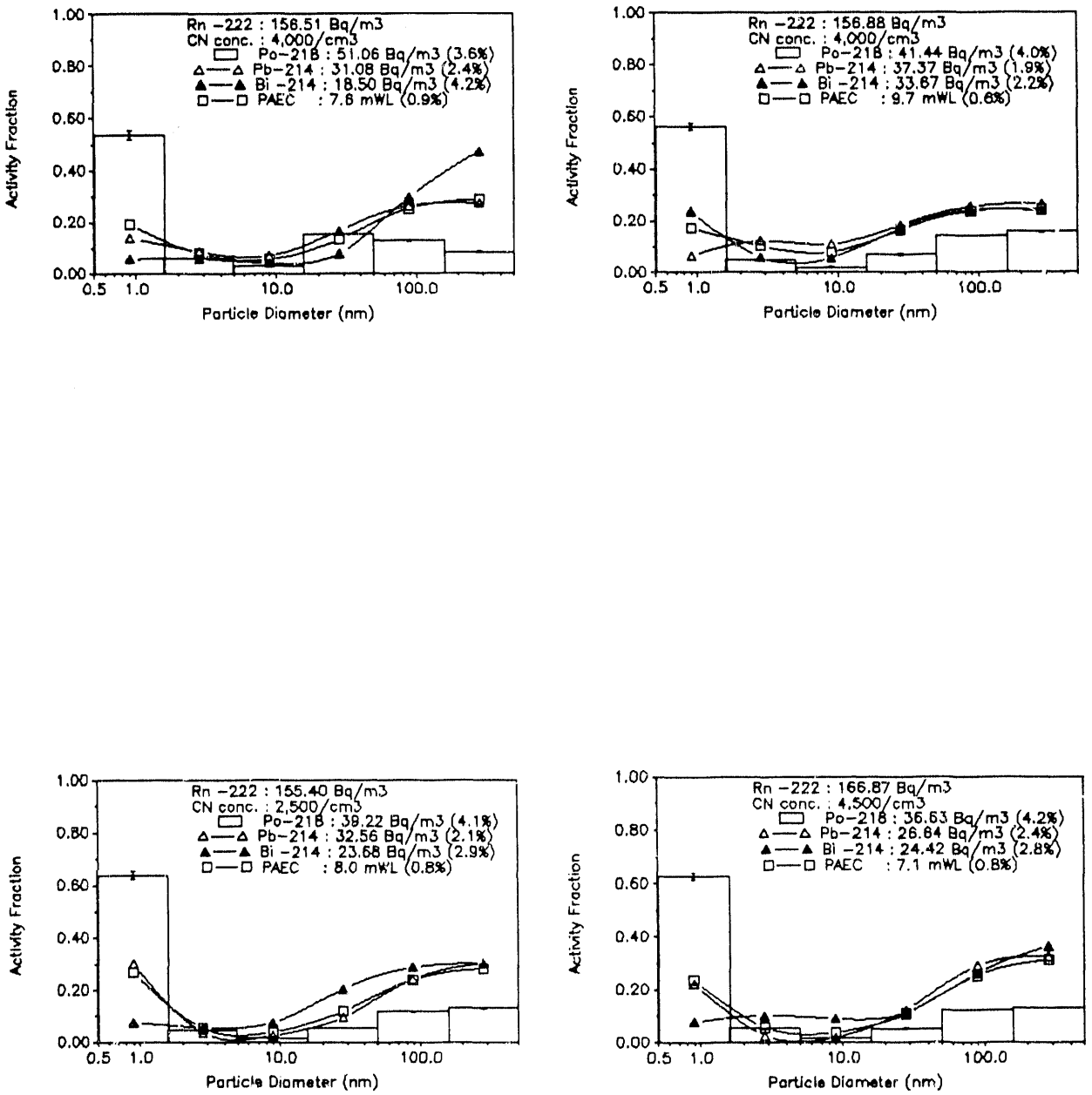

Figure 46 ^{218}Po, ^{214}Pb, and $^{214}Bi/^{214}Po$ activity size distributions measured with electronic air cleaner.

65%, 75%, and 65%, respectively. They also found a reduction in the concentration of "unattached" decay products and a much smaller PAEC reduction using the ESP. The reductions in hourly dose rate per Bq m^{-3} radon (dose reductions) for males at sleep, rest, light work, and heavy work were 22%, 22%, 18%, and 14%, respectively; for females at rest and exercise, the dose reductions were 23% and 18%, respectively; for children age 10 at rest and exercise, the dose reductions were 22% and 18%, respectively; for children age 5 at rest and exercise, the dose reductions were 24% and 22%, respectively. For bronchial basal cell nuclei, the dose reductions for adult males at flowrates of 125 cm^3 s^{-1} and 833 cm^3 s^{-1} were 17% and 10%, respectively; for secretory cell nuclei, the dose reductions for adult males at flowrates of 125 cm^3 s^{-1} and 833 cm^3 s^{-1} were 17%, 11%, respectively. Although the PAEC reductions are not so large, the hourly dose rate per Bq m^{-3} radon has decreased because the "unattached" fraction remained unchanged. The average dose reduction was 18%.

6.6 Influence of Particle Generation on the Background Conditions with the Air Filtration System

6.6.1 Candle Burning in the Princeton House

The influence of candle burning on the size distributions was investigated in the bedroom of the Princeton house and presented in Figures 47 and 48. During the candle burning, the particle concentration increased from 1,800 cm^{-3} to 60,000 cm^{-3}, then reached a steady state around 1,800 cm^{-3} by the second measurement. The activity of ^{218}Po, ^{214}Pb, and ^{214}Bi in the smallest size range was 65%, 50%, and 50%, respectively. The size distributions of ^{218}Po during the candle burning period both with and without the air filtration system were similar, both withn respect to the ^{218}Po cluster fraction and the size range of the "attached" mode. The "unattached" fraction of ^{218}Po and PAEC decreased from 0.93 to 0.73 and changed from 0.76 to 0.57, respectively. The equilibrium factor increased from 0.14 to 0.18. Approximately 15% of the activity in the 1.5 - 15 nm size range for ^{218}Po and ^{214}Pb was observed, but insignificant activity was observed for ^{214}Bi. For all three distributions, the "attached" mode peaked in the 15 - 150 nm size range. Because of effective particle removal by the air filtration system in the bedroom, the size distributions of the background, 55 minute, and 130 minute measurements were similar. The attachment rate increased to 4 hr^{-1} during candle burning, and back to 1 hr^{-1} after 55 and 130 minutes because of effective particle removal by the air filtration system. The smaller average diameter was observed 13 nm during candle burning, and back to 30 nm after 55 and 130 minutes compared with that of candle burning alone. The deposition rate of the "unattached" fraction did not change significantly with the air flitration system operating.

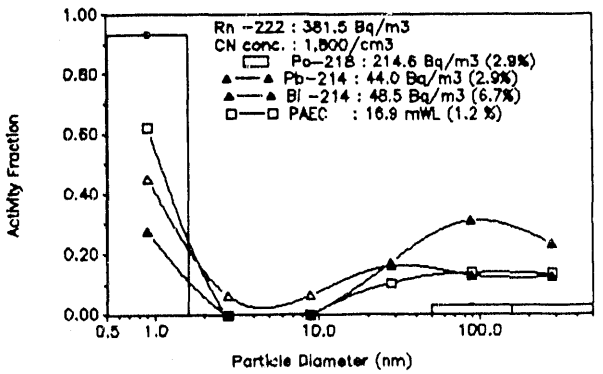

A: Background

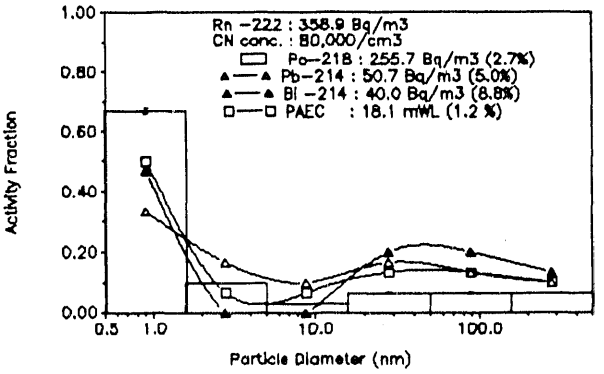

B: During candle burning

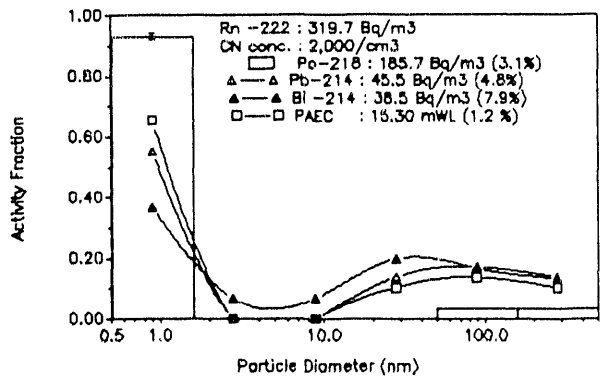

C: after 55 minutes

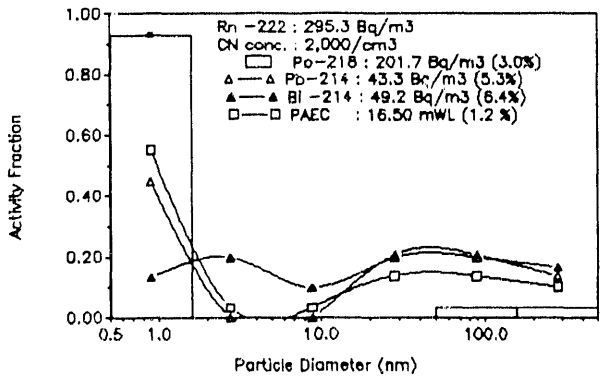

D: after 130 minutes

Figure 47 ^{218}Po, ^{214}Pb, and $^{214}Bi/^{214}Po$ activity size distributions measured under aerosol generated from candle burning in the bedroom with air filtration system. (a)

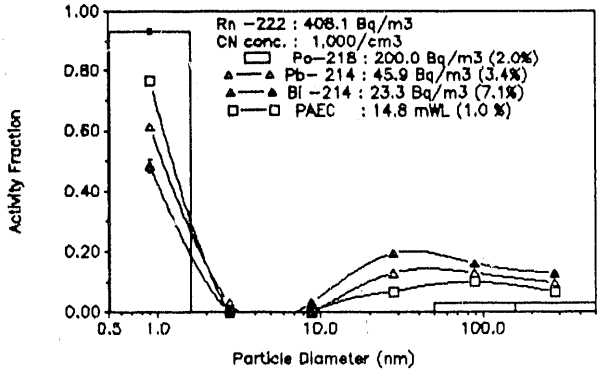

A: Background

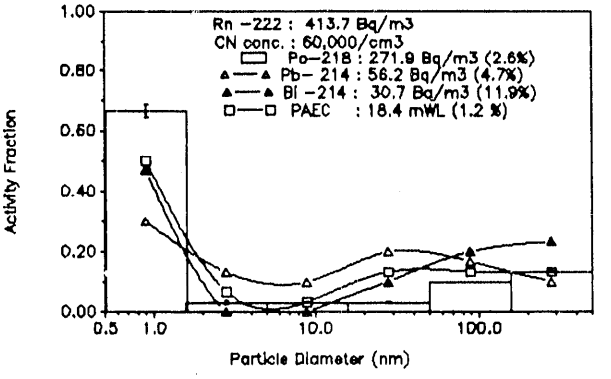

B: During candle burning

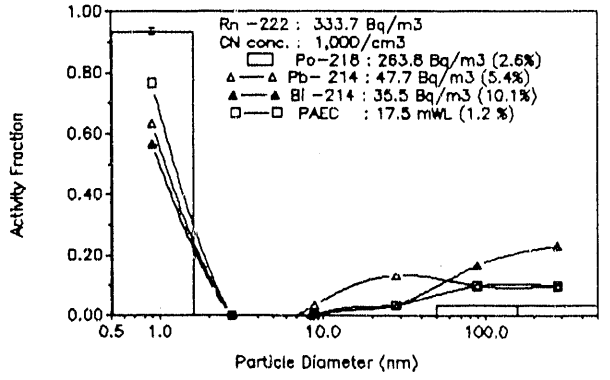

C: after 55 minutes

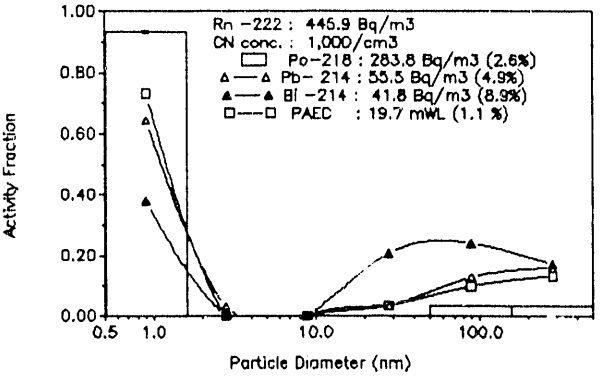

D: after 130 minutes

Figure 48 ^{218}Po, ^{214}Pb, and $^{214}Bi/^{214}Po$ activity size distributions measured under aerosol generated from candle burning in the bedroom with air filtration system. (b)

The summaries of aerodynamic parameters of radon decay products are presented in Table 18.

The reductions in PAEC per Bq m^{-3} radon were 54% with 40% increase in the "unattached" fraction of PAEC compared with that observed with candle burning alone. The conditions of two sets of experiments were quite similar. Thus, the hourly dose rates per Bq m^{-3} radon value were also similar. The average reductions in hourly dose rate per Bq m^{-3} radon for males at sleep, rest, light work, and heavy work were 20%, 18%, 6%, and 0%, respectively; for females at rest and exercise were 23% and 8%, respectively; for children age 10 at rest and exercise, the dose reductions were 22% and 9%; for children age 5 at rest and exercise, the dose reductions were 23%, and 15%, respectively. For bronchial basal cell, the dose increases for adult males at flowrates of 125 cm^3 s^{-1} and 833 cm^3 s^{-1} were 3% and 7%, respectively; for secretory cell, the dose reductions for adult males at flowrates of 125 cm^3 s^{-1} and 833 cm^3 s^{-1} were 6% and 6%, respectively. The average dose reduction was 12%.

6.6.2 Cigarette Smoldering in the Princeton House

During the interval that the two cigarettes were smoldered, the particle concentration in the bedroom of the Princeton house reached 60,000 cm^{-3}. The particle concentration returned to 1,800 cm^{-3} 60 minutes after cigarette smoldering was discontinuing. The activity of all three radon decay products in the 0.9 nm size range substantially decreased, to 10%, as shown in Figures 49 and 50. The remaining activity (80%) of all three radon decay products was in the 15 - 500 nm size range because of the higher attachment rate to cigarette particles. The "unattached" fraction of ^{218}Po and PAEC decreased from 0.93 to 0.13 and changed from 0.66 to 0.11, respectively. The equilibrium factor increased from 0.13 to 0.30. Generally, a bimodal size distribution was observed for all three decay products, with the major mode (80%) in the 15 - 500 nm size range and the minor mode (20%) in the 0.9 nm size range. The influences on all three decay products during the cigarette smoldering period were similar both with and without the air filtration system operating. After 60 and 135 minutes, the size distributions returned back to the background condition. This indicated effective particle removal in the bedroom. The only difference was slightly low "cluster" fraction of all three decay products by the 60-minute sample compared with background condition. The attachment rate increased from 1 hr^{-1} to 100 hr^{-1} during the particle generation period, and was down to 4 hr^{-1} by the 60 minute sample because of air filtration system removing particles. Thus, the average attachment diameter remained 60 nm. The deposition rate of the "unattached" fraction increased from 8 hr^{-1} to 12 hr^{-1} during the particle generation period as shown in Table 19.

Table 15 The measurements and calculation of X, d, $q^{(u)}$ and dose with candle burning by the air filtration system in Princeton House.

Aerosol Source Cleaner	Co (Bq/m^3)	Z ($10^3 cm^{-3}$)	f_1	f_p	F	PAEC (mWL)	X (hr^1)	d (nm)	$q^{(u)}$ (hr^{-1})	Dose($\mu Gyhr^{-1}/Bq/m^3$) M(s,r)M(l,h)	F(r,e)	C10(r,e) C5(r,e)	M(l,h) Basal	M(l,h) Secretory
(1)on (cleaner on for 4 hours)	477.3	1.8	0.931	0.533	0.14	18.1	1	30	19	6.4,7.8 20.6,38.1	6.4,20.1	7.3,20 8.4,14.5	6.2,29.8	10.5,48.8
on cleaner on for 5.5 hours)	381.5	1.8	0.933	0.621	0.164	16.9	1	30	11	7.8,9.5 26.3,49.8	7.6,25.5	8.8,25.8 10,17.8	7.9,40	13.5,65
on (during candle burning, cleaner on for 7 hours)	358.9	80	0.767	0.567	0.187	18.1	4	10	7	9.6,11.6 30,54.7	9.5,29.3	10.9,29.8 12.5,21.4	8.9,42.1	15.3,69.2
on (after 55 minutes)	319.68	2	0.931	0.655	0.177	15.3	1	26	10	8.8,10.7 29.8,56.6	8.6,28.9	9.9,29.3 11.3,20.1	9.9,45.4	15.3,74
on (after 130 minutes)	295.3	2	0.931	0.586	0.207	16.5	1	26	7	10.2,12.4 33,61.3	10.1,32.2	11.6,32.7 13.3,23.1	9.9,48	16.9,79
on (after 205 minutes)	315.61	2	0.933	0.666	0.190	16.2	0.9	24	7	9.8,11.9 32.7,61.6	9.6,31.7	11,32.2 12.6,22.3	9.8,48.8	16.7,80
(2)on (cleaner on for 4 hours)	428.5	1	0.967	0.833	0.136	15.7	0.46	26	7.5	8,9.9.0 28.1,53.8	7.5,27.1	8.9,27.4 10.2,18.6	8.4,43.5	14.4,70.6
on (cleaner on for 6 hours)	444.37	1	0.967	0.833	0.132	15.8	0.46	26	9.99	7.8,9.6 27.3,52.2	7.5,26.3	8.7,26.6 9.9,18.0	8.1,42.2	14,68.5
on (cleaner on for 8 hours)	408.11	1	0.934	0.767	0.131	14.8	0.96	36	11.9	7.5,9.2 25.9,49.5	7.3,25	8.4,25.4 9.6,17.3	7.8,40.0	13.3,65
on (cleaner on for 10 hours, during candle burning)	413.66	60	0.700	0.567	0.165	18.4	5.82	15	9.86	8.1,9.8 25.6,47.2	8.0,25.1	9.2,25.5 10.6,18.2	7.6,36.4	13.1,60
on (after 55 minutes)	333.7	1	0.936	0.767	0.194	17.5	0.93	35	3.77	10.7,13.1 37.2,71.2	10.4,35.9	11.9,36.4 13.7,24.7	11.1,57.4	19.1,93.4
on (after 130 minutes)	445.8	1	0.934	0.734	0.163	19.7	0.96	36	8.16	8.6,10.6 30.0,57.5	8.4,29.0	9.7,29.4 11.0,20.0	9.0,46.4	15.4,75.4

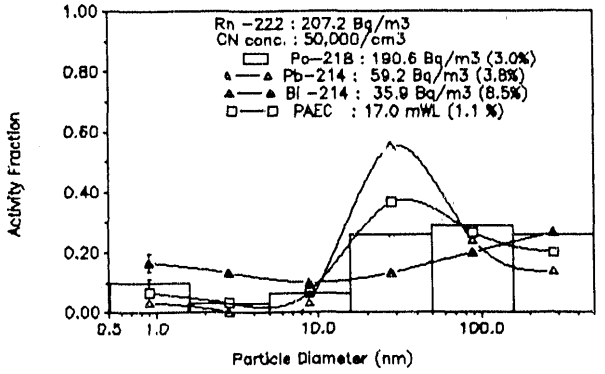

A: During Cigarette Smoldering

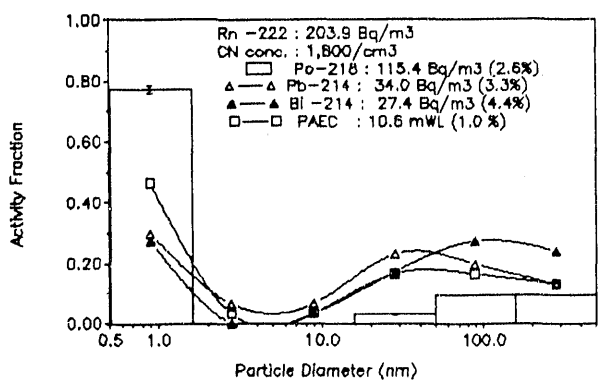

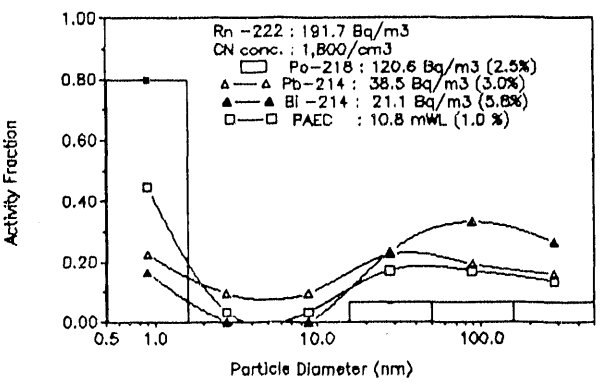

B: after 60 minutes

C: after 135 minutes

Figure 49 ^{218}Po, ^{214}Pb, and $^{214}Bi/^{214}Po$ activity size distributions measured under aerosol generated from cigarette smoke in the bedroom with air filtration system. (a)

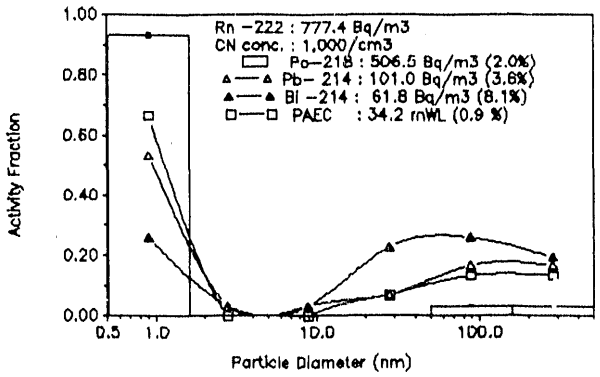

A: Background

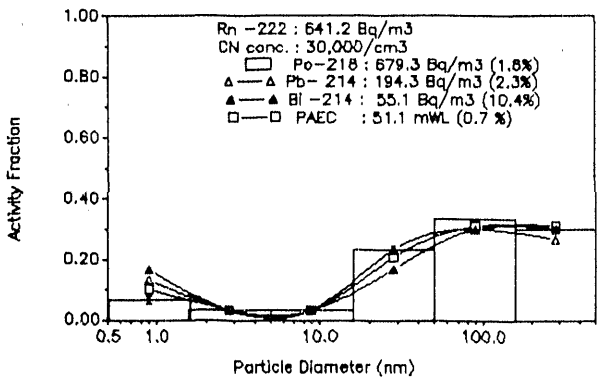

B: During cigarette smoldering

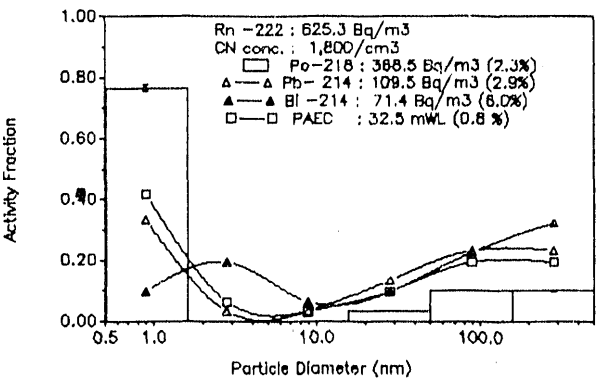

C: after 60 minutes

Figure 50 ^{218}Po, ^{214}Pb, and $^{214}Bi/^{214}Po$ activity size distributions measured under aerosol generated from cigarette smoke in the bedroom with air filtration system. (b)

Table 19 The measurements and calculation of X, d, $q^{(u)}$ and dose with cigarette smoidering by the air filtration system in Princeton House.

Aerosol Source Cleaner	Co (Bq/m^3)	Z ($10^3 cm^{-3}$)	f_1	f_p	F	PAEC (mWL)	X (hr^1)	d (nm)	$q^{(u)}$ (hr^{-1})	Dose($\mu Gyhr^{-1}/Bq/m^3$) M(s,r) M(l,h)	F(r,e)	C10(r,e) C5(r,e)	M(l,h) Basal	M(l,h) Secretory
(1)on (cleaner on for 4 hours, during cigarette smoke)	207.2	50	0.129	0.1	0.304	17.0	92	52	8	7.9,9.0 17.8,27.9	8.4,18.7	9.4,19.2 11,15.9	5.4,18.9	9.1,31.8
on (after 60 minutes)	203.9	1.8	0.774	0.5	0.193	10.6	4	60	13	8.6,10.3 27.0,49.6	8.5,26.4	9.7,26.9 11.2,19.2	8.1,38.7	13.8,63.4
on (after 135 minutes)	191.66	1.8	0.8	0.482	0.208	10.8	3	50	10	9.1,11.0 28.4,52.2	9.1,28.0	10.3,28.3 11.9,20.3	8.5,40.6	14.6,66.5
off (cleaner off for 3 hours)	385.91	3	0.467	0.161	0.428	44.6	15	90	6	9.8,11.4 25.6,43.6	10.1,25.9	11.3,26.5 13.2,20.5	7.8,31.8	13.2,53
(2)on (cleaner for 4 hours, background)	773.4	1	0.933	0.667	0.163	34.2	0.97	36	7.6	8.1,10.0 27.7,52.9	7.9,26.9	9.1,27.2 10.4,18.7	8.3,42.5	14.3,69.0
on (cleaner on for 5.5 hours, during cigarette smoke)	641.2	30	0.1	0.137	0.295	51.1	122	85	12.5	6.8,7.8 16.8,28.0	7.1,17.2	7.9,17.6 9.2,13.9	5.1,20	8.7,33.6
on (after 60 minutes)	625.3	1.8	0.767	0.483	0.192	32.5	4.12	61	12.1	8.3,10.0 25.9,47.4	8.2,25.4	9.4,25.8 10 8,18.5	7.7,36.5	13.2,60

The average reductions in PAEC per Bq m^{-3} radon were 25% during the particle generation period with the higher particle concentration, 68% after 60 minutes, and 60% after 135 minutes, compared with the PAEC observed with unfiltered cigarette smoke alone. The resulting hourly dose rates per Bq m^{-3} radon reductions were different for the two sets of experiments. In one set of the experiments, the hourly dose rate increased, while the second case had a reduced hourly dose rate. This result may be due to different degree of PAEC reductions with the air filtration system operating. For the case when the dose rate increased, the reduction in PAEC was much smaller (16%) with significantly increase of the "unattached" fraction (~10%). For the 60-minute measurements of the two sets of experiments, the average reductions in hourly dose rate per Bq m^{-3} radon for males at sleep, rest, light work, and heavy work were 26%, 23%, 3%, and -10%, respectively; for females at rest and exercise, the dose reductions were 32% and 8%, respectively; for children age 10 at rest and exercise were 28% and 9%, respectively; for children age 5 at rest and exercise, the dose reductions were 30% and 20%, respectively. For bronchial basal cell, the dose reductions for adult males at flowrates 125 $cm^3 s^{-1}$ and 833 $cm^3 s^{-1}$ were 33% and 13%, respectively; for secretory cell, the dose reductions for adult males at flowrates of 125 $cm^3 s^{-1}$ and 833 $cm^3 s^{-1}$ were 33% and 19%, respectively.

6.6.3 Vacuuming

6.6.3.1 Princeton House

The particle number concentration reached 40,000 cm^{-3} in the bedroom of the Princeton house during the vacuuming period. By the second measurement, the particle concentration declined to a steady state of 1,800 cm^{-3}. The results of the size distributions of radon decay products are presented in Figures 51 and 52 and the parameters describing the conditions in these experiments are given in Table 20. The activity in the smallest size range was observed to be 70% for ^{218}Po, and 30% for ^{214}Pb and ^{214}Bi. The equilibrium factor changed insignificantly. A moderate decrease in the "unattached" fraction during the vacuuming period was observed both with and without the air filtration system. A 25% increase in the activity of ^{218}Po in the 1.5 - 50 nm size range was observed due to the attachment of ^{218}Po to the small particles generated from vacuuming. A 30% increase in the 1.5 - 150 nm size range was also observed for all three radon decay products. The size distributions of the 60 and 130 minute measurements were very similar to the background condition. This result might be due to larger particle removal occurring in the bedroom and the lower attachment rate of aerosols from vacuuming for activity. The attachment rate increased from 1 hr^{-1}

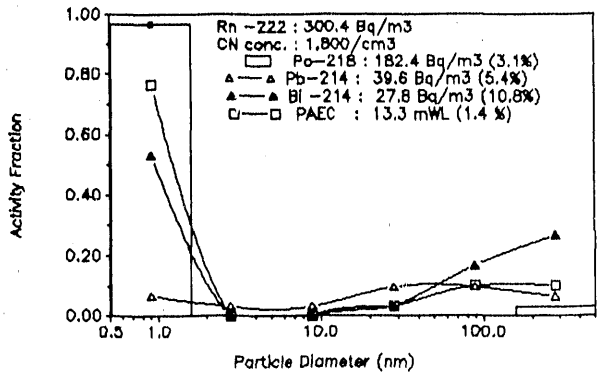

A: Background

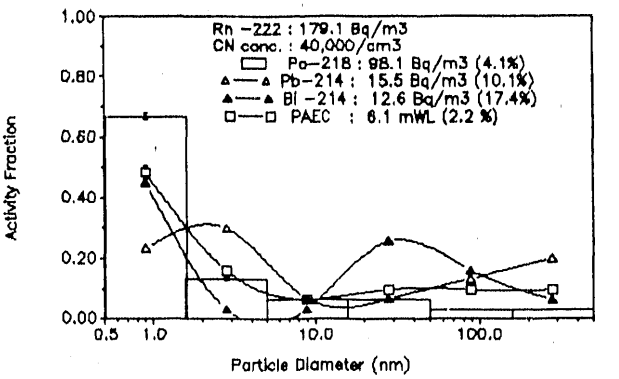

B: During the vacuuming

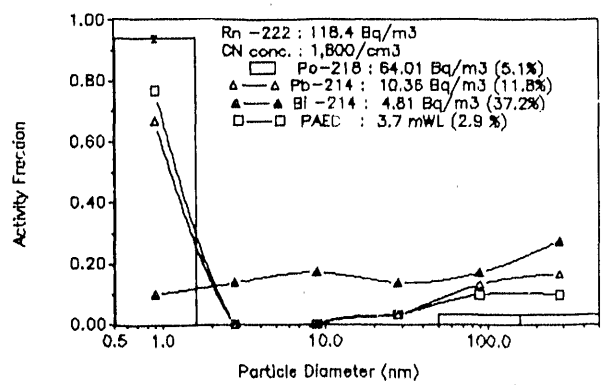

C: after 60 minutes

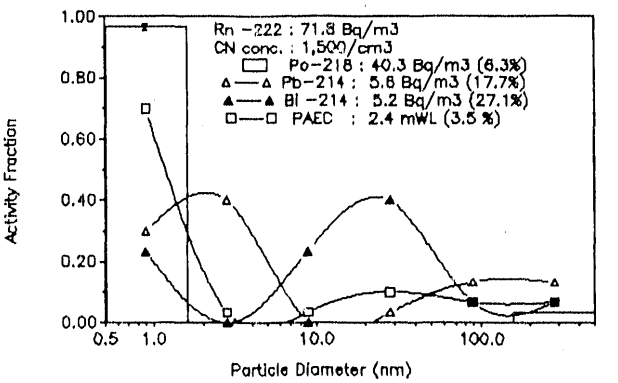

D: after 135 minutes

Figure 51 ^{218}Po, ^{214}Pb, and $^{214}Bi/^{214}Po$ activity size distributions measured under aerosol generated from vacuuming in the bedroom with air filtration system. (a)

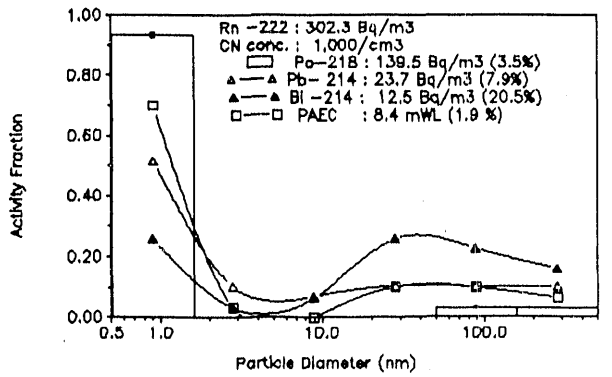

A: Background

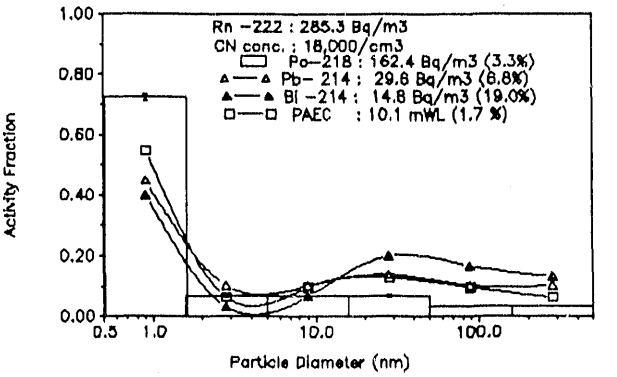

B: During the vacuuming

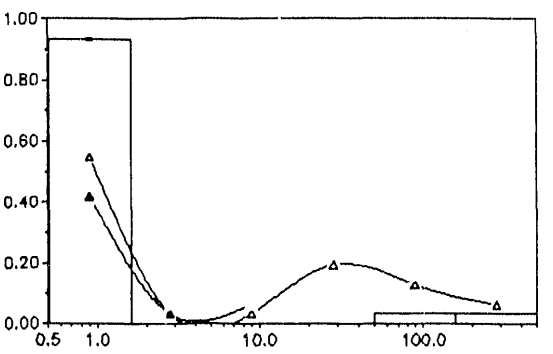

C: after 60 minutes

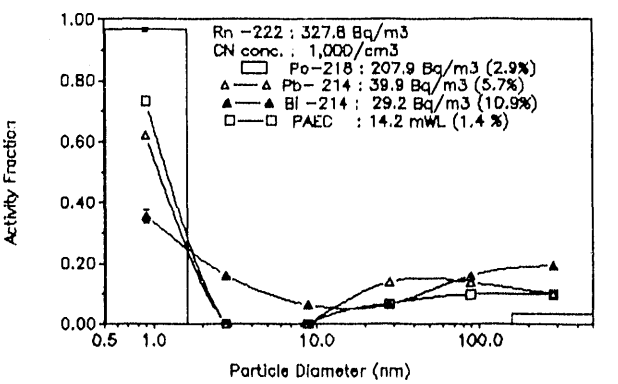

D: after 135 minutes

Figure 52 ^{218}Po, ^{214}Pb and $^{214}Bi/^{214}Po$ activity size distributions measured under aerosol generated from vacuuming in the bedroom with air filtration system. (b)

Table 20 The measurements and calculation of X, d, $q^{(u)}$ and dose with vacuuming by the air filtration system in Princeton house.

Aerosol Source Cleaner	Co (Bq/m^3) (10^3cm^{-3})	Z	f_1	f_p	F	PAEC (mWL)	X (hr^1)	d (nm)	$q^{(u)}$ (hr^{-1})	Dose($\mu Gyhr^{-1}/Bq/m^3$) M(s,r) M(l,h)	F(r,e)	C10(r,e) C5(r,e)	M(l,h) Basal	M(l,h) Secretory
(1)on (cleaner on for 6 hours)	322.64	1.8	0.967	0.828	0.159	13.8	0.4	18	9.4	8.9,11.2 32.5,62.3	8.7,31.3	10.2,31.6 11.8,21.4	9.6,50.2	16.7,81.8
on (cleaner on for 7.5 hours, background)	300.4	1.8	0.967	0.767	0.164	13.3	0.4	20	8.9	8.9,10.9 31.3,60.3	8.6,30.3	10.0,30.6 11.6,21.0	9.3,48.6	16.0,78.9
on (cleaner on 9.5 hours, during the vacuuming)	179.08	40	0.8	0.645	0.126	6.1	3.4	12	13.7	7.3,8.9 22.9,41.3	7.3,22.3	8.4,22.9 9.5,16.2	6.7,30.7	11.2,50.8
on (after 60 minutes)	118.4	1.8	0.937	0.767	0.115	3.7	0.9	26	12.1	5.9,7.6 21.9,42.2	5.9,21.1	6.7,21.9 7.6,14.3	6.7,33.8	11,55.7
on (after 135 minutes)	71.78	1.5	0.967	0.733	0.124	2.4	0.5	22	11	6.9,8.3 23.7,44.6	6.9,22.3	8.4,23.7 8.4,16.7	6.9,34.8	12.5,57.1
(2)on (background)	302.3	1	0.934	0.733	0.103	8.4	0.96	36	16.6	5.6,6.9 19.2,36.4	5.6,18.5	6.3,18.9 7.3,12.9	5.6,28.8	9.9,47.3
on (during the vacuuming)	285.27	18	0.793	0.612	0.131	10.1	3.54	17	12.7	7.4,8.8 22.8,41.7	7.4,22.4	8.4,22.8 9.5,16.5	6.7,32.2	11.6,52.9
on (after 60 minutes)	302.66	1	0.934	0.724	0.170	13.9	0.95	36	7.5	9.3,11.2 31.4,59.5	8.9,30.4	10.2,30.7 11.9,21.1	9.3,47.9	15.9,78
on (after 135 minutes)	327.82	1	0.967	0.733	0.160	14.2	0.46	26	7.9	8.5,10.4 29.6,56.4	8.2,28.7	9.4,28.9 11.0,19.8	8.8,45.5	14.9,74.1

to 3.5 hr^{-1} during the particle generation period, and decreased to 0.8 hr^{-1} after 60 and 135 minutes after the vacuuming was discontinued. The average diameter decreased from 30 nm to 15 nm during the particle generation period, and to 26 nm after 60 and 135 minutes after the end of vacuuming.

The average reduction in PAEC per Bq m^{-3} radon was 58% during the particle generation period, 59% by 60-minute measurment, and 50% by 135-minute measurement compared with the PAEC observed with vacuuming alone. There was a difference in the reductions of hourly dose rate per Bq m^{-3} radon between the measurements of the two sets of experiments during the vacuuming period. The difference in the size distributions, especially the 0.5 - 1.5 nm size range, was due to the different particle number concentration (one was 90,000 cm^{-3}, the other was 15,000 cm^{-3}). For the measurement with 90,000 cm^{-3} particle concentration, the hourly dose rate per Bq m^{-3} radon was much lower because of the significant decrease in the "unattached" fraction. For the 60-minute measurement, the reductions in hourly dose rate per Bq m^{-3} radon (dose reductions) for males at sleep, rest, light work, and heavy work were 31%, 28%, 21%, and 13%, respectively; for females at rest and exercise, the dose reductions were 34% and 20%, respectively; for children age 10 at rest and exercise, the dose reductions were 33% and 21%, respectively; for children age 5 at rest and exercise, the dose reductions were 34% and 27%, respectively. For bronchial basal cell, the dose reductions for adult males at flowrates of 125 $cm^3 s^{-1}$ and 833 $cm^3 s^{-1}$ were 18% and 7%, respectively; for secretory cell, the dose reductions for adult males at flowrates of 125 $cm^3 s^{-1}$ and 833 $cm^3 s^{-1}$ were 18% and 6%, respectively.

6.6.3.2 Northford House

With the air filtration system operating, the influence of vacuuming and clothes washing on the behavior of radon decay products in the living room of the Northford house is as shown in Figure 53. The vacuum was operated for 25 minutes. Ten minutes after vacuuming stopped, the particle concentration had increased from 1,500 cm^{-3} to 22,500 cm^{-3}. The activity of ^{218}Po in the 0.9 nm size range changed from 85% to 45%. The "unattached" fraction of ^{218}Po and PAEC decreased from 0.85 to 0.60 and changed from 0.50 to 0.35, respectively. The equilibrium factor, F, increased from 0.09 to 0.14. The remaining activity was dispersed over the 1.5 - 500 nm size range. The activity of ^{214}Pb and ^{214}Bi was evenly distributed over the whole size range (0.5 - 500 nm). This observation may be explained by (1) small particles were generated by the vacuum cleaner which have a lower attachment rate for activity, and (2) indoor particles were removed by the air filtration system. These size distributions of radon decay products were in good agreement with the measurements taken in the

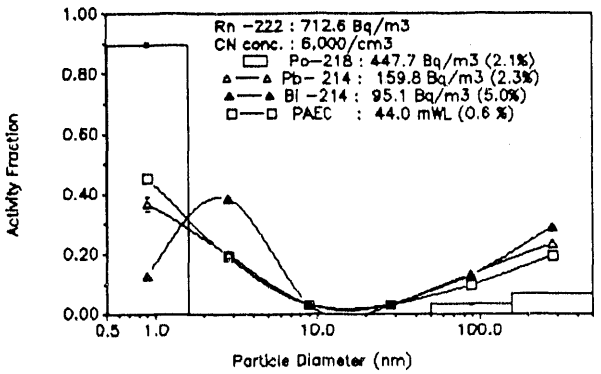

A: Background

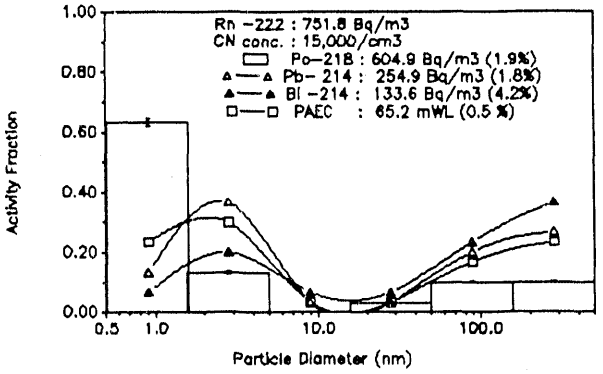

B: During the cooking

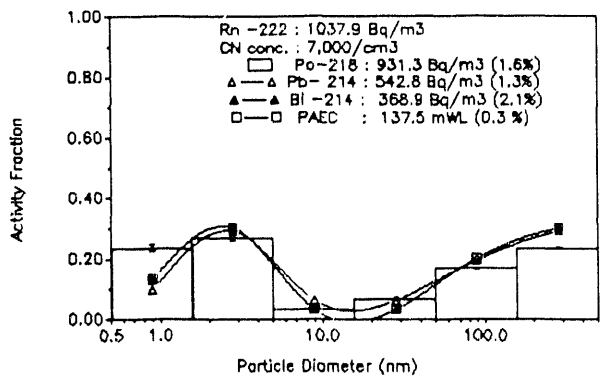

C: after 60 minutes

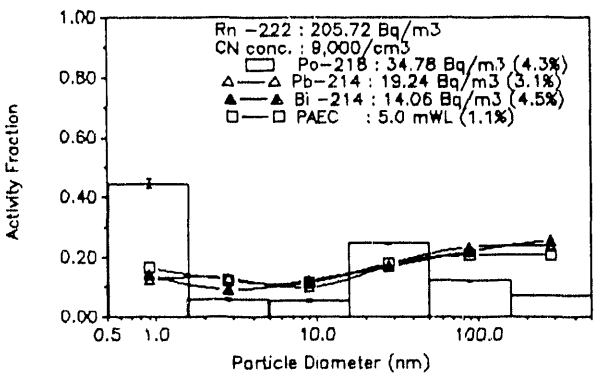

D: 100 minutes after vacuuming

Figure 53 ^{218}Po, ^{214}Pb, and $^{214}Bi/^{214}Po$ activity size distributions measured under aerosols generated from vacuuming with air filtration system.

Princeton house. However, the 100-minute measurement did not return to the background condition as it had in the Princeton house. The possible explanations are the addition of the washing machine as a particle source or the presence of an unidentified particle source. The attachment rate of approximately 7 hr^{-1} was higher than that observed in the Princeton house because of higher particle number concentration occurring in the Northford house. The larger average attachment diameter of 28 nm by the 10-minute measurement, and to 48 nm by the 100-minute measurement were obtained. The summaries of the aerodynamic parameters of radon decay products are presented in Table 14.

The reduction in PAEC per Bq m^{-3} radon was 54% with average 5% increase in the "unattach fraction of PAEC. The average the reductions in hourly dose rate per Bq m^{-3} radon (dose reductions) for males at sleep, rest, light work, and heavy work were 37%, 38%, 42%, and 46%, respectively; for females at rest and exercise, the dose reductions were 35% and 42%, respectively; for children age 10 at rest and exercise were 37% and 42%, respectively; for children age 5 at rest and exercise, the dose reductions were 37% and 40%, respectively. For bronchial basal cell nuclei, the dose reductions for adult males at flowrates of 125 cm^3 s^{-1} and 833 cm^3 s^{-1} were 44% and 50%, respectively; for secretory cell nuclei, the dose reductions for adult males at flowrates of 125 cm^3 s^{-1} and 833 cm^3 s^{-1} were 44% and 50%, respectively.

6.6.4 Cooking

6.6.4.1 Princeton House

During the cooking period in the kitchen, the particle number concentration was 100,000 cm^{-3} and 20,000 cm^{-3} in the kitchen and the bedroom of the Princeton house, respectively. The particle concentration declined to 5,000 cm^{-3} 135 minutes after cooking discontinued. The size distributions of radon decay products are as shown in Figures 54 and 55. The activity in the 0.9 nm size range was found to be 50% for ^{218}Po and 15% for ^{214}Pb and ^{214}Bi. The "unattached" fraction of ^{218}Po and PAEC decreased from 0.87 to 0.45 and reduced from 0.40 to 0.20. The equilibrium factor increased from 0.23 to 0.32. The fraction of all three distributions in the 1.5 - 5 nm size range was found to be 20%. Very little activity of all three radon decay products was in the 5 - 50 nm size range for all conditions. An increase from 20% to 50% in the 50 - 500 nm size range was observed for all three distributions. As a whole, a bimodal size distribution was observed. For ^{218}Po, the major mode was in "unattached" cluster size range. For ^{214}Pb and ^{214}Bi, the minor mode was in the 2.8 nm size range and the major mode was in the 280 nm size range. The size distributions of the second and third

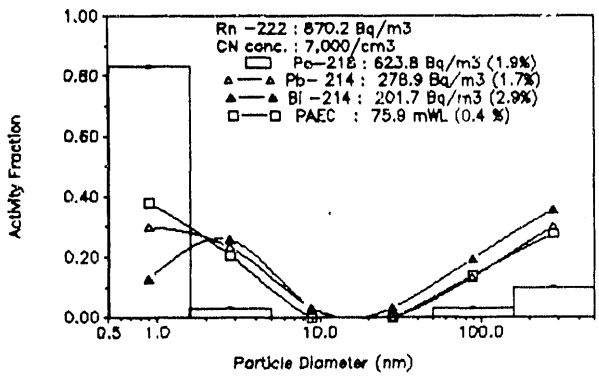

A: Background

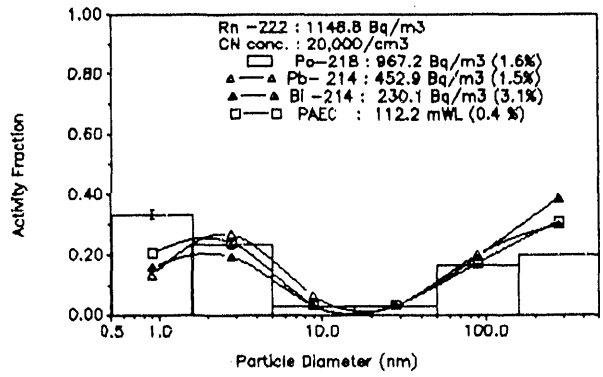

B: During the cooking

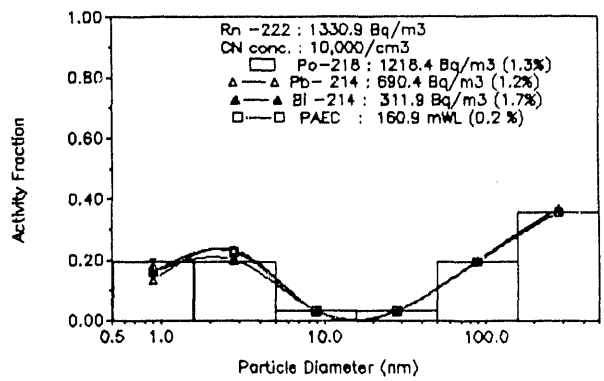

C: after 60 minutes

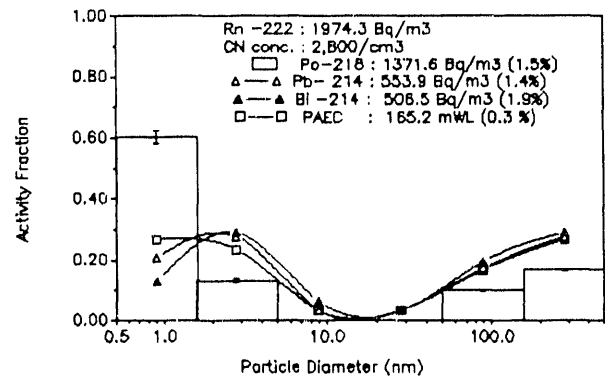

D: after 135 minutes

Figure 54 ^{218}Po, ^{214}Pb, and $^{214}Bi/^{214}Po$ activity size distributions measured under aerosol generated from cooking in the kitchen with air filtration system. (a)

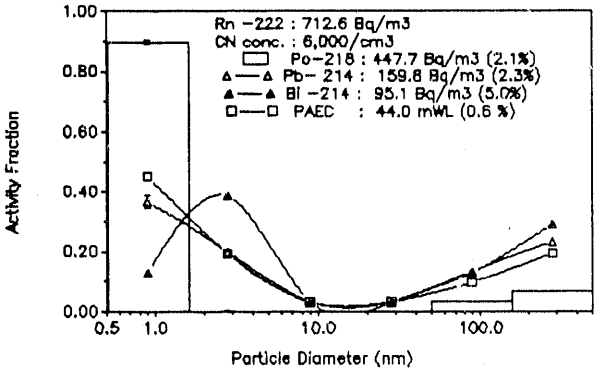

A: Background

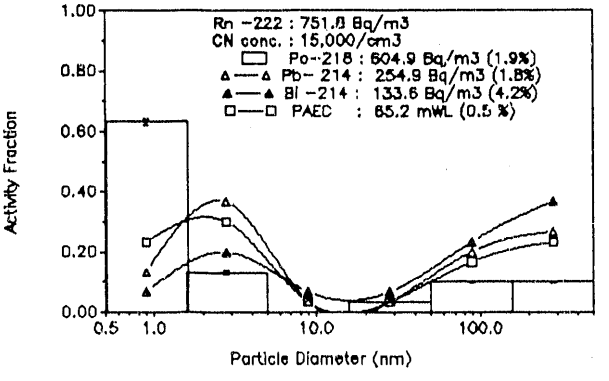

B: During the cooking

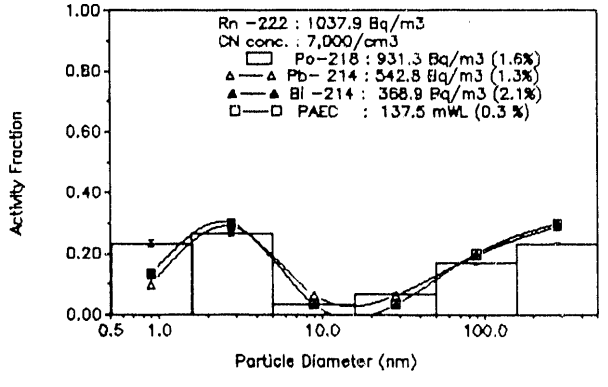

C: after 60 minutes

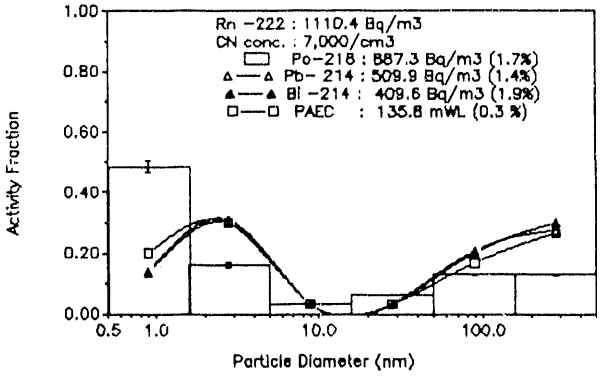

D: after 135 minutes

Figure 55 ^{218}Po, ^{214}Pb, and $^{214}Bi/^{214}Po$ activity size distributions measured under aerosol generated from cooking in the kitchen with air filtration system. (b)

measurements did not return to the background condition as did those of candle burning, cigarette smoldering, and vacuuming. A possible reason for this is that when the bedroom door was open, the particles transported from the kitchen entered the bedroom faster than the air filtration system could remove them. The attachment rate increased from 1.5 hr^{-1} to 6 hr^{-1} during the particl generation period, and to 10 hr^{-1} after 60 and 135 minutes after the end of cooking. At the same time, the average attachment diameter increased from 20 nm to 23 nm during the particle generation period, and to 52 nm after 60 and 135 minutes after the cooking stopped. The deposition rate of the "unattached" fraction decreased from 10 hr^{-1} to 4 hr^{-1}. The aerodynamic parameters of radon decay products are summarized in Table 21.

With the air filtration system operating, the reductions in PAEC per Bq m^{-3} radon were in the range of 17% - 56% (average 35%) compared with the PAEC per Bq m^{-3} radon observed with cooking alone. The reductions in the hourly dose rate per Bq m^{-3} radon were quite different between the two sets of experiments. The main reasons were (1) different levels of PAEC reductions by the air filtration system, (2) different background size distributions, especially the one with a minor mode in the 2.8 nm size range, and (3) the resulting size distributions were quite different, especially during the cooking period. By the 60 minute measurements, the average increases in hourly dose rate per Bq m^{-3} radon (dose increases) for males at sleep, rest, light work, and heavy work were 19%, 21%, 28%, and 31%, respectively; for females at rest and exercise, the dose increases were 15% and 26%, respectively; for children age 10 at rest and exercise, the dose increases were 17% and 26%, respectively; for children age 5 at rest and exercise, the dose increases were 17% and 21%, respectively. For bronchial basal cell, the average dose increases for adult males at flowrates of 125 cm^3 s^{-1} and 833 cm^3 s^{-1} were 22% and 28%, respectively; for secretory cell, the dose increases for adult males at flowrates of 125 cm^3 s^{-1} and 833 cm^3 s^{-1} were 24% and 29%, respectively.

6.6.4.2 Northford House

When only food preparation was being done in the kitchen of the Northford house, no influence the behavior of radon decay products was observed. The particle concentration increased from 4,000 cm^{-3} to 10,000 cm^{-3} five minutes before cooking was finished. The results of the size distributions of radon decay products are shown in Figure 56. A significant fraction in the 1.5 - 15 nm size range was observed for all three decay products. This result can be explained by that the particles larger than 20 nm were removed by the air filtration system. Therefore, the radon decay products in 1.5 - 15 nm have few indoor particles to attach to . The 115-minute measurement agrees,

Table 21 The measurements and calculation of X, d, $q^{(u)}$ and dose with cooking by the air filtration system in Princeton House.

Aerosol Source Cleaner	Co (Bq/m^3) (10^3cm^{-3})	Z	f_1	f_p	F	PAEC (mWL)	X (hr^1)	d (nm)	$q^{(u)}$ (hr^{-1})	Dose($\mu Gyhr^{-1}/Bq/m^3$) M(s,r) M(l,h)	F(r,e)	C10(r,e) C5(r,e)	M(l,h) Basal	M(l,h) Secretory
(1)on (cleaner on for 6 hours, background)	870.2	7	0.866	0.323	0.586	76	2.1	21	6	16.4,19.8 50.4,91.1	16.1,49.4	18.5,50.3 21.4,36.4	14.7,66.4	25.3,112.0
on (cleaner on for 7.5 hours, during the cooking)	1148.8	20	0.566	0.448	0.361	112	10	26	4.2	16.8,19.9 47.5,82.0	16.7,47.0	18.9,48.0 22.2,36.2	13.7,56.4	23.7,96.6
on (after 60 minutes)	1330.9	10	0.388	0.387	0.447	161	21	60	2.8	18.7,22.2 52.0,89.0	18.7,51.5	21.3,52.7 24.7,40.1	14.9,60	26,104
on (after 135 minutes)	1974.3	2.8	0.733	0.582	0.31	165	4.9	52	7.9	15.2,18.3 44.4,77.7	15.1,43.8	17.3,44.6 20.0,33.3	12.8,55.0	22.2,93
(2)on	1544.4	6	0.933	0.581	0.235	98.0	2.8	26	10	12.4,14.9 37.7,67.5	12.2,36.8	14.0,37.6 16.2,27.4	10.9,49.3	18.9,82.8
on	993.5	6	0.897	0.633	0.227	61.0	1.5	19	7.7	13.0,15.7 39.7,70.8	12.9,38.9	14.8,39.6 17.0,28.9	11.5,51.2	19.8,86.3
on (background)	712.6	6	0.897	0.646	0.228	44.0	1.5	19	8.8	12.9,15.6 40.1,72.4	12.8,39.2	14.6,39.9 17.0,28.8	11.6,53.5	20.2,89.5
on (during the cooking)	751.8	15	0.766	0.533	0.321	65.2	4.1	20	4.1	17.3,20.8 49.5,85.4	17.2,48.8	19.7,49.9 22.9,37.5	14.1,58.3	24.5,100
on (after 60 minutes)	1037.8	7	0.5	0.433	0.490	137	13	52	2.8	23.4,27.8 64.0,108.0	23.5,63.7	26.7,65.0 31.1,50.0	18.1,70.8	31.6,123
on (after 135 minutes)	1110.4	7	0.645	0.500	0.453	135	7.4	37	5.1	23.5,28.0 66.2,113.0	23.4,65.5	26.6,67.0 31.0,50.7	18.8,76.6	32.8,132

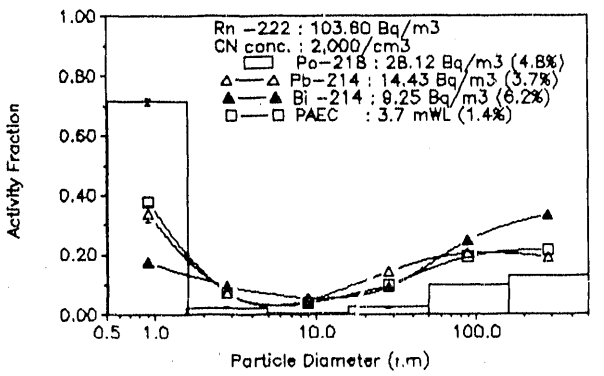

A: Background

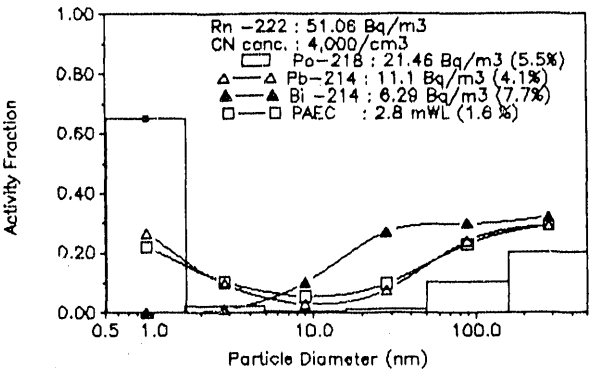

B: Food preparation

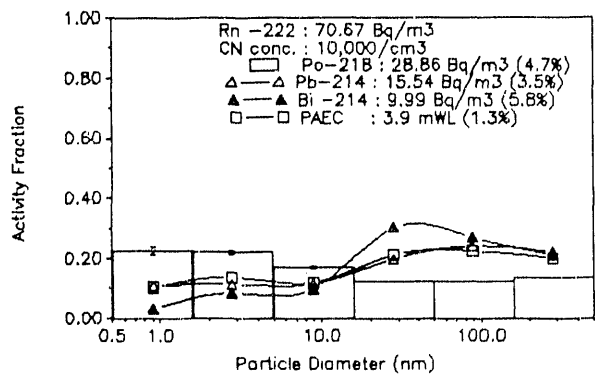

C: 5 minutes before cooking finished

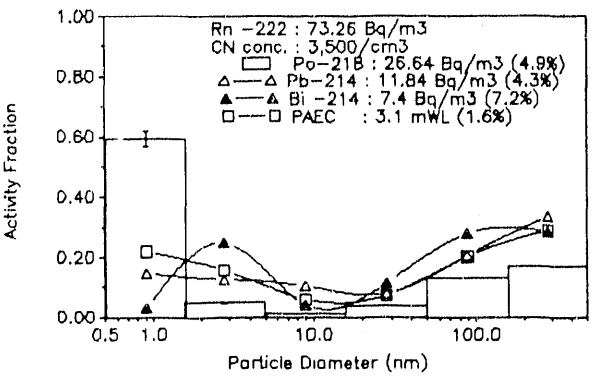

D: 115 minutes after cooking

Figure 56 ^{218}Po, ^{214}Pb, and $^{214}Bi/^{214}Po$ activity size distribution measured under aerosols generated by cooking with the air filtration system.

with respect to "cluster" fraction and "attached" mode, with the 135-minute size distributions taken in the Princeton house. The "unattached" fraction of ^{218}Po and PAEC was 0.45 and 0.24 during the active cooking period. The equilibrium factor was in the range of 0.20 to 0.25. The attachment rate was from 15 to 40 hr^{-1} with the average attachment diameter of 60 nm as shown in Table 16.

The average reduction in PAEC per Bq m^{-3} radon was 30% with the air filtration system operating. The average reductions in hourly dose rate per Bq m^{-3} radon (dose reductions) for males at sleep, rest, light work, and heavy work were 22%. 20%, 16%, and 14%, respectively; for females at rest and exercise, the dose reductions were 24% and 16%, respectively; for children age 10 at rest and exercise, the dose reductions were 22% and 22%, respectively; for children age 5 at rest and exercise, the dose reductions were 23% and 20%, respectively. For bronchial basal cell nuclei, the dose reductions for adult males at flowrates of 125 cm^3 s^{-1} and 833 cm^3 s^{-1} were 18% and 12%, respectively; for secretory cell nuclei, the dose reductions for adult males at flowrates of 125 cm^3 s^{-1} and 833 cm^3 s^{-1} were 17% and 12%, respectively.

6.6.5 Conclusion

The effects on the behavior of radon decay products during the particle generation period both with and without the air filtration system were very similar in terms of the ^{218}Po "cluster" fraction and the size range of the "attahed" mode. The size distributions of the follow-up measurements were similar to those of the background conditions because of the efficient particle removal of the air filtration system.

For candle burning, cigarette smoldering, and vacuuming occuring in the bedroom, the average reductions in PAEC per Bq m^{-3} radon by the filtration system were 60% with the air filtration operating in the bedroom. For cooking in the kitchen, the reduction in PAEC per Bq m^{-3} radon in the bedroom was much less, approximately 35%, with the filtration system operating in the bedroom. However, the hourly dose rate per Bq m^{-3} radon by James models (1989, 1990) strongly depends not only on total PAEC but also on the size distribution of PAEC. The reductions in hourly dose rate per Bq m^{-3} radon varied over a wide range, depending on the type of particles generated. For candle burning and vacuuming in the bedroom, the average reduction in hourly dose rate per Bq m^{-3} radon by the filtration system was 20% with the air filtration operating in the bedroom by the 60 minute measurement. For the cigarette smoldering in the bedroom and cooking in the kitchen, the reductions in dose per unit hour per Bq m^{-3} radon were quite different from the two sets of experiments. In a few cases, the hourly dose rate per Bq m^{-3} radon actually increased (20%) when

the bedroom when the air filtration system was operating in the bedroom. These increases can be explained not only by the difference in PAEC reductions but also by the different background and resulting size distributions.

6.7 Influence of Particle Generation on the Background Conditions with the Electronic Air Cleaner in the Northford House

6.7.1 Vacuuming

The influence of vacuuming on radon decay products with the electronic air cleaner was evaluated in the living room of the Northford house. The size distributions of radon decay products are as shown in Figure 57. The vacuum was in use for 10 minutes. During the vacuuming period, the particle concentration increased from 3,000 cm^{-3} to 12,000 cm^{-3}. The fraction of ^{218}Po in the 0.9 nm size range was 25%. Only 5% of the ^{218}Po activity was observed in the 1.5 to 50 nm size range. For ^{214}Pb and ^{214}Bi, 5% to 10% of the activity was found in 0.5 - 50 nm size range. The remainder of all three decay products had an "attached" mode approximately 28 nm. The changes in all three decay products with and without the electronic air cleaner were similar with respect to both the "unattached" fraction and "attached" mode. The attachment rate as shown in Table 14 was 31 hr^{-1} with the average particle attachment diameter of 45 nm during the particle generation period. The size distributions of the 100-minute measurement returned to the background condition more slowly than that without any air cleaner. The possible reasons are (1) the low particle removal efficiency of the electronic air cleaner, and (2) the shorter time interval between the beginning of the particle generation period and the second measurement, thus smaller deposition rate of radon decay products was observed.

The reduction in PAEC per Bq m^{-3} radon was 22% for the electronic air cleaner. During the vacuuming period, the dose reductions for males at sleep, rest, light work, and heavy work were 37%, 37%, 40%, and 41%, respectively; for females at rest and exercise, the dose reductions were 35% and 39%, respectively; for children age 10 at rest and exercise were 35% and 39%, respectively; for children age 5 at rest and exercise, the dose reductions were 36% and 37%, respectively. For bronchial basal cell nuclei, the dose reductions for adult males at flowrates of 125 $cm^3 s^{-1}$ and 833 $cm^3 s^{-1}$ were 40% and 42%, respectively; for secretory cell nuclei, the dose reductions for adult males at flowrates of 125 $cm^3 s^{-1}$ and 833 $cm^3 s^{-1}$ were 40% and 42%, respectively.

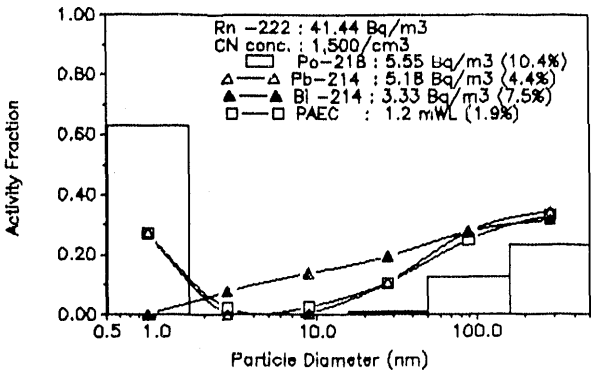

A: Background

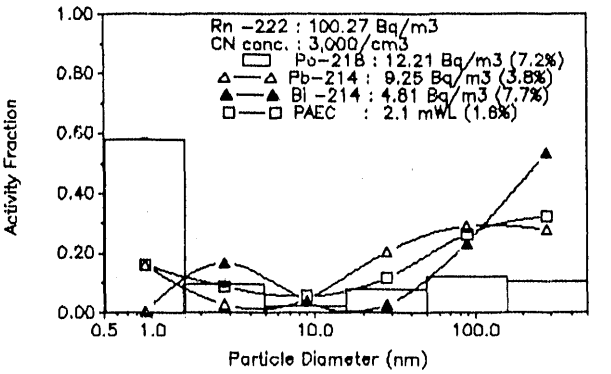

B: Background

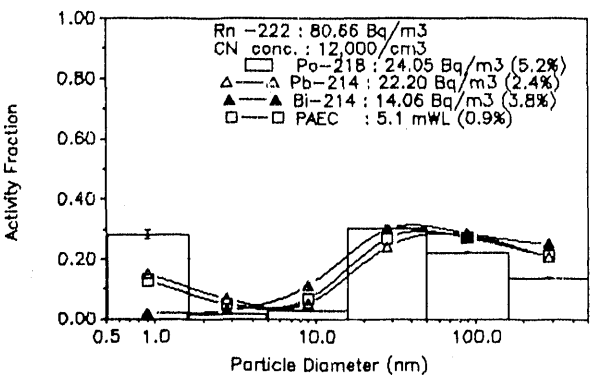

C: During the vacuuming

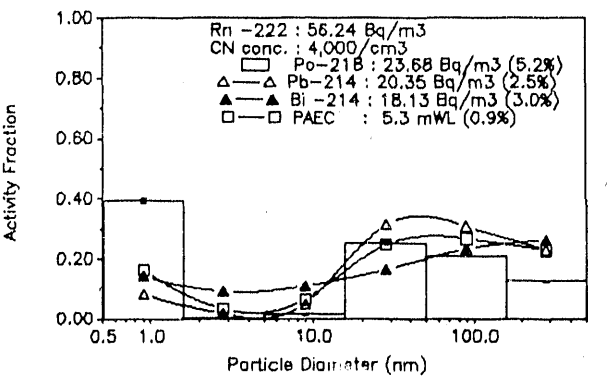

D: 100 minutes after vacuuming

Figure 57 ^{218}Po, ^{214}Pb, and $^{214}Bi/^{214}Po$ activity size distributions measured under aerosols generated from vacuuming with electronic air cleaner.

6.7.2 Cooking

When cooking started in the kitchen of the Northford house, a small change in the "attached" mode of radon decay products was observed. The particle number concentration rose from 4,000 cm^{-3} to 30,000 cm^{-3} forty minutes after cooking stopped. All three distributions as shown in Figure 58 appeared to have 10% activity in the smallest size range. Very little activity in any of the three distributions was in the 1.5 to 15 nm size range. The remaining activity of radon decay products was attached to the large indoor particles which ranged in the size from 15 to 500 nm. The "unattached" fraction of ^{218}Po and PAEC was 0.12 and 0.1 with the equilibrium factor, F, of 0.66. By the 140-minute measurement, the "unattached" fraction of ^{218}Po was lower than that by the 115-minute measurement with the air filter because of the lower particle removal efficiency of the electronic air cleaner. During the particle generation period, the size distributions of all three decay products both with and without the air cleaners were very similar in terms of the "unattached" fraction and the size range of the "attached" mode. The attachment rate was about 100 hr^{-1} during the cooking period. The average particle attachment diameter was 40 nm for the 40-minute measurement, and increased to 75 nm by the 140-minute measurement. The deposition rate of "unattached" fraction was in the range of 47 hr^{-1} as shown in Table 16. However, the time intervals for the background condition, active particle generation period, and the follow-up measurements were not the same with and without the air cleaners operating. Therefore, the differences in the size distribution of radon decay products may be influenced by this time interval differences.

The reduction in PAEC per Bq m^{-3} radon varied between -15% and 16%. The increase of PAEC may be related to larger "attached" fraction of radon decay products. Forty minutes after the end of the cooking, the dose reductions for males at sleep, rest, light work, and heavy work were 9%, 6%, -10%, and -21%, respectively; for females at rest and exercise, the dose reductions were 10% and -6%, respectively; for children age 10 at rest and exercise, the dose reductions were 10% and -6%, respectively; for children age 5 at rest and exercise, the dose reductions were 11% and 5%, respectively. For bronchial basal cell nuclei, the dose increases for adult males at flowrates of 125 $cm^3\ s^{-1}$ and 833 $cm^3\ s^{-1}$ were 12% and 40%, respectively; for secretory cell nuclei, the dose increases for adult males at flowrates of 125 $cm^3\ s^{-1}$ and 833 $cm^3\ s^{-1}$ were 12% and 35%, respectively. Therefore, there were increases in the dose at higher breathing rates.

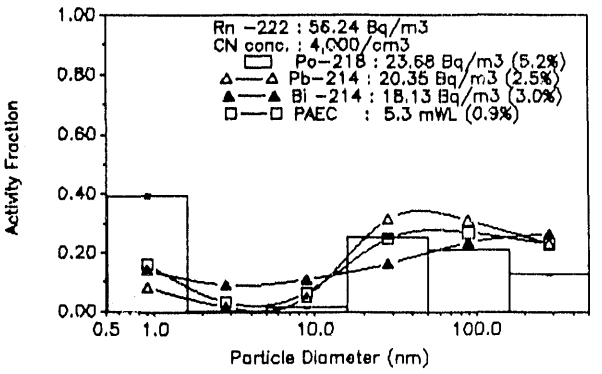

A: Background

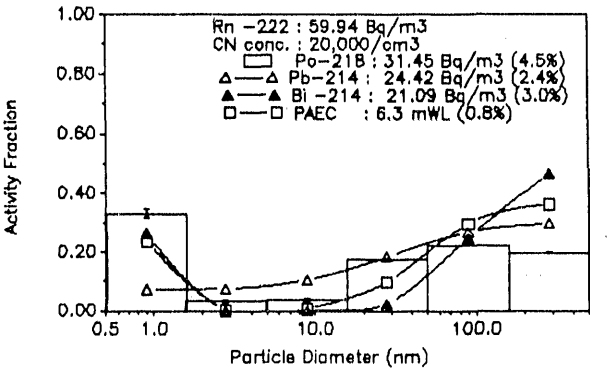

B: Cooking started

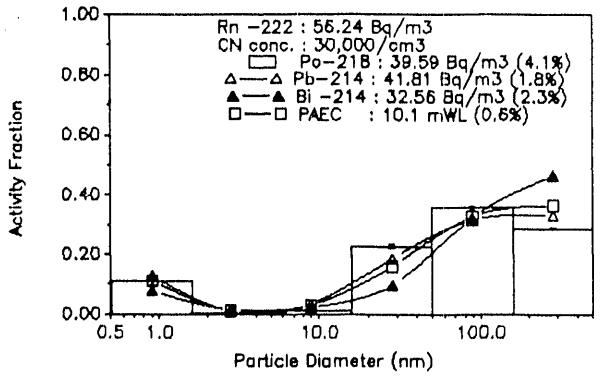

C: 40 minutes after cooking

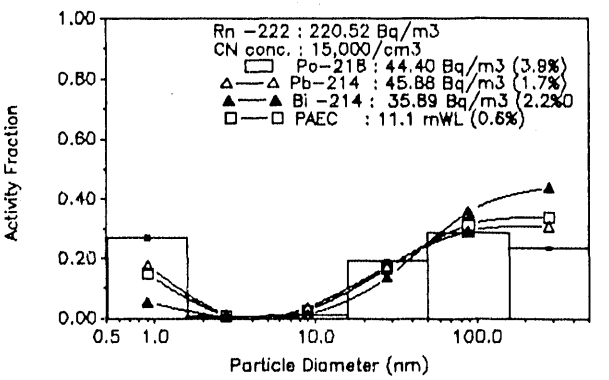

D: 140 minutes after cooking

Figure 58 ^{218}Po, ^{214}Pb, and $^{214}Bi/^{214}Po$ activity size distributions measured under aerosol generated from cooking with electronic air cleaner.

6.7.3 Clothes Washing and Drying

The influence on the behavior of radon decay products by the washing machine and clothes dryer was evaluated in the living room of the Northford house. The results of the size distributions of radon decay products are as shown in Figure 59. The washing machine and clothes dryer are new appliances and operated for an hour each. The particle concentration increase was not substantial and no change in the size distributions of radon decay products was observed in Table 22. It is conceivable that there are motors in each appliance and the heater in the clothes dryer that could generate particles. However, the results indicated that clothes washing and drying had no influence on radon decay products. The possible reason may be due to the fact that these two appliances are new and working very well.

6.7.4 Opening Door

The influence on radon decay products by opening the outside door was investigated in the Northford house. The results of the size distributions of radon decay products are as shown in Figure 60. The outside door was open for 20 minutes in order to obtain a high ventilation rate. Thirty minutes after initially opening the door, the particle concentration had increased to 10,000 cm^{-3}. The ^{218}Po distribution revealed very little activity in the 0.9 nm size range. All three distributions extended over the 1.5 - 500 nm size range. Most of the activity (70%) of the three decay products shifted to "attached" mode, due to a large number of outdoor particles entering the house.

6.7.5 Conclusion

With the electronic air cleaner, the size distributions of radon decay products were similar to those of background conditions without any air cleaner. A possible reason is that the particle removal efficiency of the electronic air cleaner is lower than that of the air filtration system. The "unattached" fraction of PAEC was between 12% and 32%. The equilibrium factor, F, was in the range of 0.15 - 0.66. The influence on the aerodynamic parmeters of radon decay products with the electronic air cleaner was insignificant. The reductions in PAEC per Bq m^{-3} radon were between 25% and 40% with average 18% dose reduction. During the vacuuming of the whole house, the reduction in PAEC per Bq m^{-3} radon was about 22% with average 38% dose reduction. For cooking in the kitchen, the PAEC and hourly dose rate per Bq m^{-3} radon increased in few cases.

Table 22 The measurements and calculation of X, d, $q^{(u)}$ and dose with clothes washing and drying in Northford house

Aerosol Source Cleaner	Co (Bq/m^3) (10^3cm^{-3})	Z	f_1	f_p	F	PAEC (mWL)	X (hr^1)	d (nm)	$q^{(u)}$ (hr^{-1})	Dose($\mu Gyhr^{-1}/Bq/m^3$) M(s,r) M(l,h)	F(r,e)	C10(r,e) C5(r,e)	M(l,h) Basal	M(l,h) Secretory
(1)Without air cleaner														
off (background)	2;0.2	5	0.538	0.255	0.169	9.6	11.6	60	72	6.4,7.5 16.5,27.5	6.6,16.7	7.4,17 8.6,13.4	4.9,18.9	8.4,32
off (during clothes washing)	129.5	17	0.502	0.256	0.294	10.3	13.5	35	24	11.7,13.6 29.7,49.1	11.9,30	13.4,30.6 15.7,24.2	8.8,33.5	15.1,56.9
off (30 minutes after clothes drying)	74.0	7	0.446	0.200	0.370	7.4	16.9	65	21.7	12.4,14.4 30.9,50.5	12.8,31.3	14.5,32.2 16.9,25.8	9.2,34	15.8,58.1
off (120 minutes after clothes drying)	105.1	12	0.366	0.188	0.243	6.9	23.5	50	49.4	7.0,8.2 17.9,30	7.3,18.2	8.2,18.6 9.5,14.6	5.4,20.8	9.2,35.2
(2)With electronic air cleaner														
on (background)	171.31	1.5	0.535	0.143	0.166	7.7	12	110	106	4.7,5.4 11.7,19.2	4.8,11.9	5.4,12.1 6.3,9.7	3,11.3	5.1,19.1
on (during clothes washing)	100.3	2.5	0.522	0.202	0.247	6.7	12	80	62	6.3,7.4 17.1,29.6	6.4,17.1	7.3,17.5 8.4,13.4	5.2,21.6	8.9,36.1
on (50 minutes after clothes drying)	82.9	2	0.440	0.165	0.263	5.9	17	130	86	6.4,7.5 16.3,27.4	6.5,16.5	7.4,16.9 8.6,13.3	4.9,19.2	8.4,32.4
on (160 minutes after clothes drying)	89.9	6	0.389	0.239	0.206	5.0	21	80	95	6.5,7.7 17.5,29.6	6.7,17.5	7.6,17.9 8.8,13.8	5.2,21	8.9,35.4

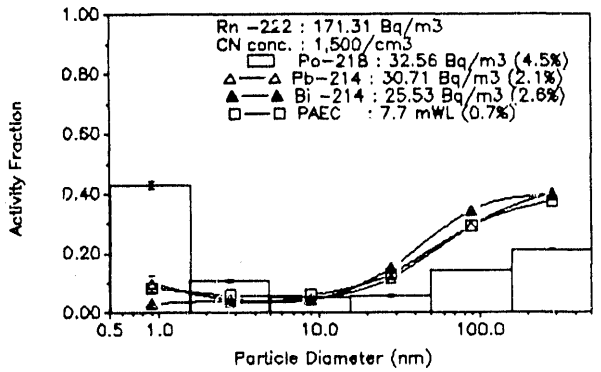

A: Background

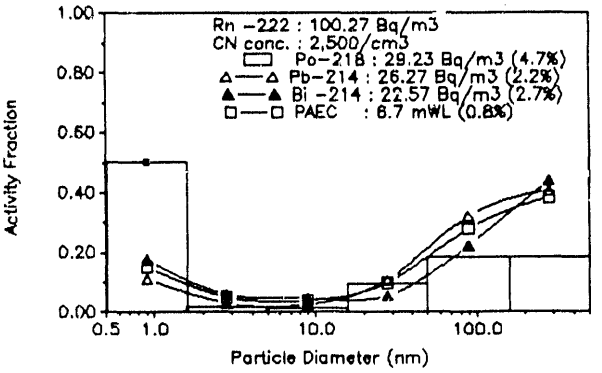

B: During clothes washing

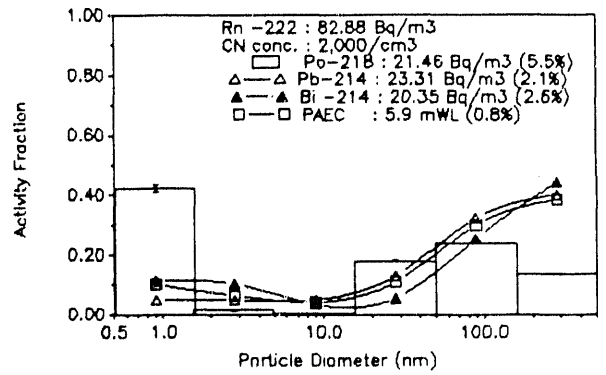

C: 50 minutes after clothes drying

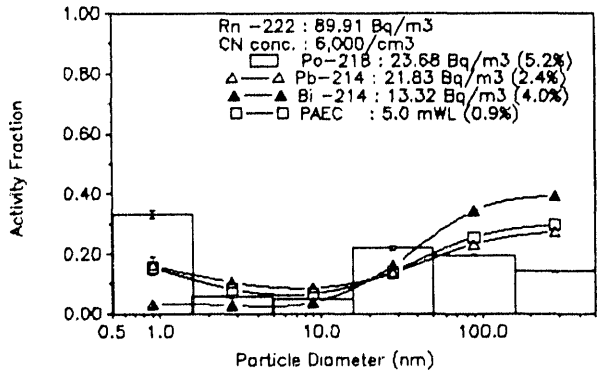

D: 160 minutes after clothes drying

Figure 59 ^{218}Po, ^{214}Pb, and $^{214}Bi/^{214}Po$ activity size distributions measured under aerosols generated from clothes washing and drying with electronic air cleaner.

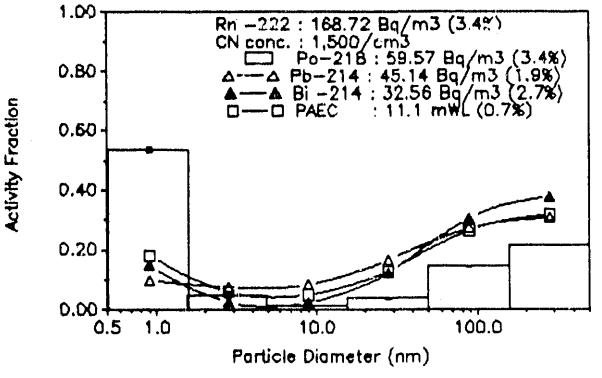

A: Background

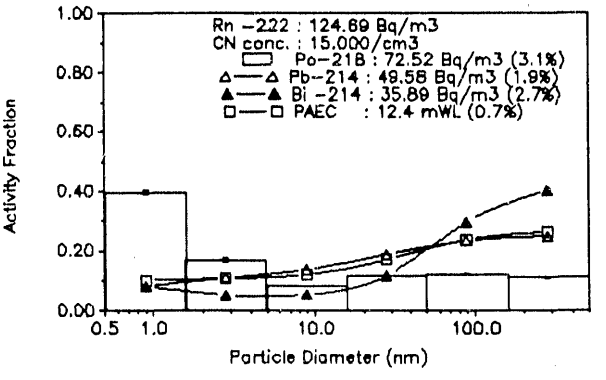

B: 20 minutes after cooking

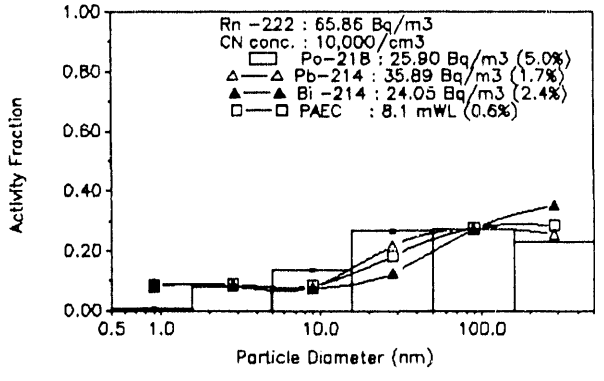

C: 30 minutes after door opening

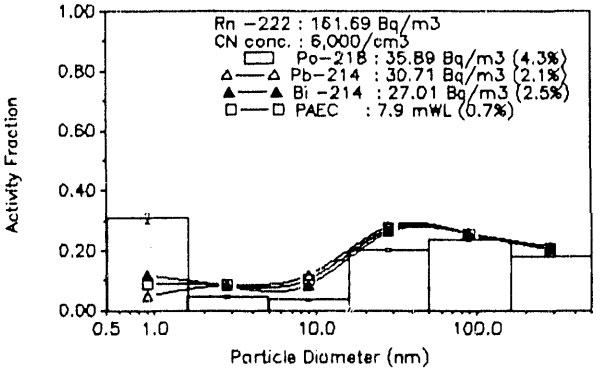

D: 180 minutes after door opening

Figure 60 ^{218}Po, ^{214}Pb, and $^{214}Bi/^{214}Po$ activity size distributions measured under aerosols generated from opening door with electronic air cleaner.

6.8 Estimated Yearly Dose Rate per Bq m^{-3} Radon

The yearly dose rate can be estimated using the average hourly dose rate per Bq m^{-3} radon ($mGyhr^{-1}$/Bq m^{-3}) in Table 23 by {(11.2)(8348)+(10.7)(365)+(9.8)(52)}(0.77)=75.3 $mGyyr^{-1}$/Bq m^{-3} for males and {(9.2)(8343)+(9.2)(365)+(9.2)(52)}(0.97)=78.1 $mGyyr^{-1}$/Bq m^{-3} for housewives. By the same principle, the yearly dose rate for children at age 10 are estimated as {(10.5)(8343)+(13)(365)+(10)(52)}(0.97)=90.1 $mGyyr^{-1}$/Bq m^{-3}, and {(12)(8343)+(12)(365)+(15.5)(52)}(0.97)=108.6 mGy yr^{-1}/Bq m^{-3} for children at age 5.

Table 23 Hourly dose rate per Bq m^{-3} radon (mGy hr^{-1}/Bq m^{-3}) of background condition, vacuuming, and cooking.

	Male	Female	Child 10	Child 5
Background	6.5 - 16.0 (11.2)	4.5 - 14.0 (9.2)	5 - 16 (10.5)	6 - 18 (12)
Cooking	9.5 - 12.0 (10.7)	8.5 - 10.0 (9.2)	9 - 17 (13)	11 - 20 (15.5)
Vacuuming	5.5 - 14.0 (9.8)	5.5 - 13.0 (9.2)	6 - 14 (10)	7 - 17 (12)

CHAPTER 7
CONCLUSIONS AND RECOMMENDATIONS

7.1 Conclusions

Field evaluations of two types of air cleaning systems were performed in three single-family houses. The three homes are located in the Springfield, PA, the Princeton, NJ, and the Northford, CT area. The two air cleaners evaluated in this study are a room-type air filtration system and an electronic air cleaner. The radon concentration, particle number concentration, and concentration and activity-weighted size distribution of radon decay products were measured in each house. Radon concentration was determined by a continuous radon monitor. A condensation nucleus counter was used to measure the particle number concentration. The concentration and activity-weighted size distribution of radon decay products were determined using a screen diffusion battery system with 6 sampler/detector units operated in parallel.

In the Springfield house, the experiments were performed in the basement. This first trial was made to check the measurement systems and make an initial comparison of size distributions of radon decay products both with and without the air filtration system operating. The influence of particles generated from a clothes dryer was also examined. In the Princeton house, several measurements were made in the living room and more than one hundred measurements in the master bedroom. The measurements were made both with and without the air filtration system operating. There were no occupants in the house during the measurements. The effect on the behaviors of radon decay products by different indoor particles was investigated. Particles were generated by running water in a shower, burning a candle, smoldering a cigarette, vacuuming, opening the bedroom door, and cooking. In the Northford house, the air filtration system and electronic air cleaner were continuously operated for one week, each. The occupants of this house lived in the way they usually live during these measurements. Realistic situations in the domestic environment were thus measured. Particles were produced from cooking, vacuuming, washing and drying clothes, and opening the outside door.

In 1987, the ICRP proposed 3 percent as the value of the "unattached" fraction for the bronchial dose calculations in the indoor environments. The "unattached" fraction of PAEC was between 7% and 20% in the basement of the Springfield house. This relatively low cluster fraction was due to the fact that the oil furnace had not been well maintained. The equilibrium factor was in the range of 0.13 - 0.19. Under typical conditions in the Princeton house, the "unattached" fraction of PAEC varied over a wide range; 7% - 40%. The equilibrium factor was

between 0.13 and 0.50. With additional particle sources such as smoldering a cigarette and cooking, the "unattached" fraction decreased to below 0.05. In the Northford house, the "unattached" fraction of PAEC varied from 25% to 45%. The equilibrium factor was in the range of 0.18 - 0.35. With the presence of additional aerosols from cooking, the "unattached" fraction decreased to 15%. However, these two terms ("unattached" fraction and equilibrium factor) were strongly dependent on the situation in the houses. However, these field measurements did suggest that ICRP underestimated the "unattached" fraction of radon decay products in the domestic environment. For "attached" aerosols, the AMD values (50 - 500 nm) obtained from the field measurements are the same order, as that suggested by ICRP (150 nm).

Under the typical conditions in the domestic environments, the size distribution of three decay products are bimodal. For the ^{218}Po size distributions, the major mode appears in the "cluster" fraction with the mid-point diameter of 0.9 nm. For ^{214}Pb and ^{214}Bi, the major mode is in the size range from 15 to 500 nm. This difference can be explained by the shorter half-life of ^{218}Po with fewer chances to attach to indoor particles. The "attached" fraction may be related to particles penetrating into the house from outdoor. With particles generated from candle burning and vacuuming, the decrease in the "unattached" fraction of ^{218}Po and PAEC was moderate (30% to 40%). An increase of three decay products in the 1.5 - 50 nm size range was observed. The size distribution of the follow-up measurement was similar to that of the background condition, with respect to both the ^{218}Po cluster fraction and the size range of the "attached" mode. This is due to a lower attachment rate and a higher deposition rate of these additional particles. Particles produced from cigarette smoldering and cooking had a higher attachment rate than those from candle burning and vacuuming. Therefore, most of the decay products shifted to "attached" mode and stayed for longer periods of time. With the air filtration system in use, a bimodal size distribution was observed for three decay products. The major mode was in the smallest size range, but little activity was observed in the "attached" mode because of effective particle removal by the air filtration system. The activity of ^{218}Po in the 0.9 nm size range was from 60% to 95%. The change on the size distributions of radon decay products during the active aerosol generation period both with and without the air filtration system was similar. While the electronic air cleaner was in use, the size distribution of radon decay products was similar to that of background condition without any air cleaner. The possible reason is that the particle removal efficiency of the electronic air cleaner is much lower than that of the air filtration system.

From the room model, the aerodynamic parameters of radon decay products were

calculated. The parameters are the attachment rate, the deposition rate of "unattached" fraction, and the average attachment diameter both with and without the air cleaners. The summaries of these parameters with the air filtration system (AFL) and electronic air cleaner (EAC) compared with the background condition (BK) are presented in Tables 24, 25, and 26. Aerosols generated from cigarette smoldering and cooking had larger attachment rate in the range of 100 hr^{-1}. On the other hand, the attachment rate of particles produced from candle burning and vacuuming is only 10 hr^{-1} with the average attachment diameter of 15 nm. With the air filtration in use, the attachment rate decreased to 1 hr^{-1} in the typical condition without any additional indoor particles. The electronic air cleaner insignificantly changed the aerodynamic parameters of radon decay products.

When the air filtration system was operating, the reductions in PAEC per Bq m^{-3} radon varied from 30% to 85% in the three houses. In the presence of additional particles, the reduction in PAEC was significantly lower. When the electronic air cleaner was operating, the PAEC reductions were in the range of 25% - 40%. However, the PAEC increased in a few cases during cooking. The summary of average reductions in PAEC per Bq m^{-3} radon in every situation by the air cleaners is shown in Table 27. By assuming the major indoor activities and using the calculated hourly dose rate per Bq m^{-3} radon, the estimated yearly dose rates are 75.3 $mGyyr^{-1}/Bq/m^3$ for male and 78.1 $mGyyr^{-1}/Bq/m^3$ for housewives. For child age 10 and 5, the yearly dose rates are 90.1 $mGyyr^{-1}/Bq/m^3$ and 108.6 $mGyyr^{-1}/Bq/m^3$, respectively. The reductions of hourly dose rate per Bq m^{-3} radon varied from 20% to 50% for the air filtration system and 10% to 25% for the electronic air cleaner. In a few cases with additional particles, both air cleaners did show increases in the hourly dose rate per Bq m^{-3} radon. The summaries of the average reductions in hourly dose rate per Bq m^{-3} radon by the air cleaners are presented in Table 28.

Table 24 Attachment rate (hr^{-1}) derived by room model at different conditions by the air cleaners.

	BK	Candle Burning	Cigarette Smoldering	Vacuuming	Cooking
BK	6-10	13	186	16	90
AFS	2	5	110	3	15
EAC	6-9	-	-	12	80

Table 25 Deposition rate (hr^{-1}) derived by room model at different conditions by the air cleaners.

	BK	Candle Burning	Cigarette Smoldering	Vacuuming	Cooking
BK	10-50	20	35	30	60
AFS	8-35	7-10	8-13	7-48	3-50
EAC	40-70	-	-	45	50

Table 26 Average attachment diameter (nm) derived by room model at different conditions by the air cleaners.

	BK	Candle Burning	Cigarette Smoldering	Vacuuming	Cooking
BK	50-90	15	110	35	80
AFS	20-30	10-15	85	15	60
EAC	45-60	-	-	45	75

Table 27 Average reductions in PAEC per Bq m^{-3} radon by the air cleaners.

	BK	Candle Burning	Cigarette Smoldering	Vacuuming	Cooking
AFS	45%-60%	54%	50%	56%	35%
EAC	25%-40%	-	-	22%	-15%-16%

7.2 Recommendations

Atomic Energy Control Board of Canada (AECB, 1979) proposed 0.02 WL as an indoor guideline level of radon decay products' concentrations. From the field measurements, the ratio between mWL and radon concentration (Bq m^{-3}) ranges from 0.05 to 0.15 depending the environments. At the same time, the average PAEC reductions of the air filtration system and the electronic air cleaner are 55% and 35%, respectively. Therefore, the maximum tolerant radon concentrations are 444 ± 222 Bq m^{-3} (20/0.1/0.45) with the air filtration system and 307 ± 150 Bq m^{-3} (20/0.1/0.65) with the electronic air cleaner. If radon concentration is below 666 Bq m^{-3} in the house, the use of an air filtration system is suggested to reduce radon risk to an acceptable level. The electronic air cleaner is recommended for use if the radon concentration ranges below 450 Bq m^{-3}. On the other hand, the effective mitigative method for radon concentration higher than 650 Bq m^{-3} may be a sub-slab ventilation to directly prevent radon entering the house.

Table 28 Summary of the average reductions in hourly dose rate per Bq m^{-3} radon by the air cleaners.

	BK	Candle Burning	Cigarette Smoldering	Vacuuming	Cooking
AFS	20%-40%	20%	15%	20%-40%	-20%-20%
EAC	20%	-	-	40%	-10%

REFERENCES

Abu-Jarad, F. and R.G. Sextro (1988) Reduction of radon progeny concentration in ordinary room due to a mixing fan, *Rad. Prot. Dosim.*, 24:507-511.

AECB (1977) *Criteria for Radioactive Clean-up in Canada*, Information Bulletin 77-2, Atomic Energy Control Board, Ottawa, April.

BEIR IV (1988) *Health Risks of Radon and Other Internally Deposited Alpha-Emitters*, Committee on the Biological Effects of Ionizing Radiations Board on Radiation Effects Research Commission on Life Sciences, National Research Council, National Academy Press, Washington, D.C.

Bigu, J. (1983) On the effect of a negative ion-generator and a mixing fan on the plate-out of radon decay products in a radon box, *Health Phys.*, 44:259-266.

Bigu, J. and M. Grenier (1984) On the effect of a negative ion-generator and a mixing fan on the attachment of thoron decay products in a thoron box, *Health Phys.*, 46:933-939.

Bigu, J. (1987) Plate-out of radon and thoron progeny on large surfaces, In radon and its decay products: occurrence, properties, and health effects. ed. P. K. Hopke (American Chemical Society, Washington, DC), 272-284.

Bowden, D.H. and F. Baldwin (1989) Measurement of the thickness of the bronchial epithelium; Research report INFO-0304, Atomic Energy Control Board, Ottawa, Ontario, Canada.

Cheng, Y.S.; Y. Yamada and H.C. Yeh (1988) Diffusional deposition of ultrafine aerosols in a human nasal cast, *J. Aerosol Sci.*, 19:741-751.

Cheng, Y.S. (1989) Deposition of thoron daughters in human head airways, Technical Exchange Meeting, Grand Junction, CO, September 18-19.

Cohen, B.C. (1987) Deposition of ultrafine particles in the human tracheobronchial tree, In *Radon and its Decay Products: Occurrence, Properties, and Health Effects*, ed. P. K. Hopke, American Chemical Society, Washington, DC, 475-486.

Egan, M.J. and W. Nixon (1985) A model of aerosol deposition in the lung for USA in inhalation dose assessments; *Radiat. Prot. Dosim.*, 11:5-17.

Egan, M.J.; W. Nixon; N.I. Robinson; A.C. James and R.F. Phalen (1989) Inhaled aerosol transport and deposition calculations for the ICRP Task group; *J. Aerosol Sci.*, 20:1301-1304.

EPA (1986) *A Citizen's Guide to Radon*, ODA-86-004, U.S. Environmental Protection Agency, Washington, DC.

EPA (1987) *Radon Reduction Methods (A Homeowner's Guide)*, 2nd edition, U.S. Environmental Protection Agency, Washington, DC.

EPA (1989) Current ORP Estimate of Annual Radon-Induced Lung Cancer Deaths in the General Population, memo dated August 17, 1989 from Margo Oge, Director, Radon Division, Office of Air and Radiation, U.S. Environmental Protection Agency, Washington, DC.

Findeisen, W. (1935) über das absetzen kleiner, in der luft suspendierrten teilchen in der menschlichen lunge bei der atmung, *Arch. Ges. Physiol.*, 23:857-860.

Frey, G.; P.K. Hopke and J. Stukel (1981) Effects of trace gases and water vapor on the diffusion coefficient of polonium-218, Scinece, 211:480-481.

Gastimeau, R.M.; P.J. Walsh and N. Underwood (1972) Thickness of bronchial epithelium with relation to exposure to radon, *Health Phys.*, 23:857-860.

George, A. C. and A.J. Breslin (1969) Deposition of radon daughters in humans exposed to uranium mine atmospheres, *Health Phys.*, 17:115-124.

George, A.C. (1972) Measurement of the uncombined fraction of radon daughters with wire screens, *Health Phys.*, 23:390-392.

George, A. C. and A.J. Breslin (1980) The distribution of ambient radon and radon daughters in residential buildings in New Jersey-New York area, in Natural radiation Environment III, USDOE, CONF-780422 (vol. 2). 1273-1293.

Gormley, P.C. and M. Kennedy (1949) Diffusion from a stream through a cylindrical tube, *Proc. R. Irish Acad. Sect.*, A52:163-169.

Hansen, J.E. and E.P. Ampaya (1975) Human air space, shape sizes, areas and volumes; *J. Appl. Physiol.*, 38:990-995.

Harley, N.H. and B.S. Pasternack (1972) Experimental absorption measurements applied to lung dose from radon daughters, *Health Phys.*, 23:771-782.

Harley, N.H. and B.S. Pasternack (1982) Environmental radon daughter alpha dose factors in a five-lobed human lung, *Health Phys.*, 42:789-799.

Hinds, W.C.; S.N. Rudnick; E.F. Maher and M.W. First (1982) Control of indoor radon decay products by air treatment devices, Paper 82-48.7, Air Pollution Control Association, Pittsburgh, PA.

Hinds, W.C.; S.N. Rudnick; E.F. Maher and M.W. First (1983) Control of indoor radon decay products by air treatment devices, *J. Air Pollut. Contr. Assoc.*, 33:134-136.

Hopke, P.K. (1986) Conceptual design of a system to characterize the radioactive ultrafine aerosol, in Indoor Radon, Air Pollution Control Association, Pittsburgh, PA.

Hopke, P.K.; M. Ramamurthi and E.O. Knutson (1990) Measurement of "unattached" fraction based on respiratory deposition, *Health Phys.* in press.

ICRP (1979) *Limits on Intakes of Radionuclide by Workers;* Annals of the ICRP, No 3/4.
ICRP (1987) *Lung Cancer Risk from Environmental Exposures to Radon Daughters*, Report of a Task Group, ICRP publication 50, International Commission on Radiological Protection, *Ann. of ICRP* 17(1).

Ingham, D.B. (1975) Diffusion of aerosols from a stream flowing through a cylindrical tube, *J. Aerosol Sci.*, 6:125-132.

Jacobi W. (1972) Activity and potential α-energy of ^{222}radon- and ^{220}radon-daughters in different air atmospheres, *Health Phys.*, 22:1163-1174.

Jacobi, W. and K. Eisfeld (1980) Internal dosimetry of radon-222, radon-220 and their short-lived daughters, GSF report S-626, Gesellschaft für Strahlen- und Umweltforschung, Munich-Neuherberg, West Germany.

James A.C.; G.F. Bradford and D.M. Howell (1972) Collection of unattached RaA atoms using wire gauge, *J. Aerosol Sci.*, 3:243-250.

James, A.C.; J.R. Greenhalgh and A. Birchall (1980) A Dosimetric Model for Tissues of the Human Respiratory Tract at Risk from Inhaled Radon and Thoron Daughters, in *Radiological Protection - Advances in Theory and Practice*, Proc. 5th Congress IRPA, Jerusalem, March 1980. Volume 2, Pergamon Press, Oxford, 1045-1048.

James, A.C.; W. Jacobi and F. Steinhausler (1982) *Respiratory Tract Dosimetry of Radon and Thorn Daughters : The State-of-the-Art and Implication for Epidemiology and Radiobiology*; In "Radiation Hazards in Mining: Control, Measurement and Medical Aspects" (Ed. M. Gomez). Soc. Mining Engrs., New York, 42-54.

James, A.C. (1984) Dosimetric approaches to risk assessment for indoor exposure to radon daughters, *Rad. Prot. Dosim.* 7:353-366.

James, A.C. (1988) Lung dosimetry, In: *Radon and its Decay Products in Indoor Air*, Nazaroff W.W. and A.V. Nero, eds. New York: Wiley-Interscience, 259-309.

James, A.C.; R.C. Roth; R.W. Kuennen and F.T. Cross (1989) The efficacy of a high efficiency room air treatment system in mitigating dose from radon decay products, presented at American Association of Aerosol Research meeting, Reno, NV.

Jonassen, N. (1982) Air filtration and radon daughter levels, *Environ. Int.*, 8:71-75.

Jonassen, N. (1983) The effect of electric fields on Rn-222 daughter products in indoor air, *Health Phys.*, 45:487-491.

Jonassen, N. (1984) Removal of radon daughters by filtration and electric fields, *Rad. Prot. Dosim.*, 7:407-411.

Jonassen, N. and J.P. McLaughlin (1984) Airborne radon daughters, behavior and removal, presented at The 3rd International Conference on Indoor Air Quality and Climate, Stockholm, August 1984.

Jonassen, N. and J.P. McLaughlin (1985) The reduction of indoor air concentrations of radon daughters without the use of ventilation, *Sci. Total Environ.*, 45:485-492.

Jonassen, N. and B. Jensen (1987) *Radon Daughter Levels in Indoor Air, Field Measurements*, Progress Report XI, Technical University of Denmark, Lyngby, Feb. 1987.

Jonassen, N. and B. Jensen (1988a) *Report on Test of NORAD Radon Daughter Removal System for Ion Systems, Inc.*, Report from the Technical University of Denmark, Lyngby, May 1988.

Jonassen, N. and B. Jensen (1988b) Modification of electric fields by space charges effects on airborne radon daughters, *Rad. Prot. Dosim.*, 24:497-501.

Jonassen, N. and B. Jensen (1988c) Removal of radon daughters by filtration and electrostatic plateout, *EPA 1988 Symposium on Radon and Radon Reduction Technology*, Denver, CO., Oct. 1988.

Jonassen, N. and B. Jensen (1989) *Radon Daughters in Indoor Air*, Final Report to Vattenfall, Technical University of Denmark, Lyngby, September 1989.

Kuennen, R.W. and R.C. Roth (1989) Reduction of radon working level by a room air cleaner, Paper No. 89-79.6, Air Pollution Control Association, Anaheim, CA.

Kulju, L.M.; M. Ramamurthi and P.K. Hopke (1986) The detection and measurement of the activity size distribution of ultrafine particles, Paper No. 86-40.6, Air Pollution Control Association, Pittsburgh, PA.

Lehtimäki, M.; G. Graeffe; K. Janka; V. Kulmala and M. Rajala (1984) On the behavior of radon daughters in indoor air, *Rad. Prot. Dosim.*, 7:165-168.

Lubin J.H. and J.D. Boice,Jr. (1989) Estimating Rn-induced lung cancer in the United States, *Health Phys.*, 3:417-427.

Maher, E.F. (1985) *The Control and Characterization of Radon Decay Products in Residences*, Doctoral dissertation, Department of Environmental Science and Physiology, School of Public Health, Harvard University, Boston, MA.

Maher, E.F. and N.M. Larid (1986) EM algorithm reconstruction of particle size distribution from diffusion battery data; *J Aerosol Sci.*, 16:557-570.

Maher, E.F.; S.N. Rudnick and D.W. Moeller (1987) Effective removal of airborne Rn decay products inside buildings, *Health Phys.*, 53:351-356.

Mercer, T.T. (1976) The effects of particle size on the escape of recoiling the RaB atoms from particulate surfaces, *Health Phys.*, 31:173-175.

Mercer, T.T.; M.L. Russell and J.D. Crapo (1989) Airway cell and nuclear depth distribution in human and rat lungs; *Health Phys.* (in press).

NCRP (1984) *Exposure from the Uranium Series with Emphasis on Radon and its Daughters*, NCRP report no. 77, National Council on Radiation Protection and Measurements, Bethesda MD.

Nazaroff, W.W. (1980) *A Residential Radon Daughter Monitor Based on Alpha Spectroscopy*, M. Eng. thesis, University of California, Berkeley.

Nazaroff, W.W., M.L. Boegel, C.D. Hollowell, and G.D. Roseme (1981) The use of mechanical ventilation with heat recovery for controlling radon and radon-daughter concentrations in houses, *Atmospheric Environ.*, 15:263-270.

NEA (1983) *Dosimetry Aspects of Exposure to Radon and Thoron Daughter Products*, Group of Experts Report, OECD Nuclear Energy Agency, Paris.

Nero, A.; M.B. Schwehr; W.W. Nazaroff and K.L. Revzan (1986) Distribution of airborne radon-222 concentrations in U.S. homes, Science, 234:992-997.

Nuclear Energy Agency (NEA), Dosimetry aspects of exposure to radon and thoron daughter products, NEA experts report, Pairs, 1983.

Olson, D.E.; G.A. Dart and G.F. Filley (1970) Pressure drop at fluid flow regime of air inspired into the human lung, *J. Appl. Physiol.*, 28:482-494.

Porstendörfer, J.; A. Wicke and A. Schraub (1978) The influence of exhalation, ventilation and deposition processes upon the concentration of radon (^{222}Rn), thoron (^{220}Rn) and their decay products in room air, *Health Phys.*, 34:465-473.

Porstendörfer, J. and T.T. Mercer (1978) Influence of nuclei concentration and humidity upon the attachment rate of atoms in the atmosphere, *Atmospheric Enviro.*, 12:2223-2228.

Porstendörfer, J.; G. Röbig and A. Ahmed (1979) Experimental determination of the attachment coefficients of atoms and ions on monodisperse aerosols, *J. Aerosol Sci.*, 10:21-28.

Porstendörfer, J. (1984) Behavior of radon daughter products in indoor air, *Rad. Prot. Dos.*, 7:107-113.

Porstendörfer, J, A. Reineking, and K.H. Becker (1987) Free fraction, attachment rates, and plate-out rates of radon daughters in houses, In *Radon and its Decay Products: Occurrence, Properties, and Health Effects*, ed. P.K. Hopke, American Chemical Society, Washington, DC. 285-300.

Rajala, M.; K. Janka; M. Lehtimäki; V. Kulmala; G. Graeffe and J. Keskinen (1985) The control of radon progeny by air treatment devices, *Sci. Total Environ.*, 45:493-498.

Rajala M.; K. Janka; M. Lehtimäki; V. Kulmala and G. Graeffe (1986) The influence of an electrostatic precipitator and a mechanical filter on Rn decay products, *Health Phys.*, 50:447-455.

Ramamurthi, M. (1989) The detention and measurement of the activity size distributions (dp > 0.5 nm) associated with radon decay products in indoor air, Ph.D. Thesis, University of Illinois, Urbana, IL.

Ramamurthi, M. and P.K. Hopke (1989) On improving the validity of wire screen "unattached" fraction Rn daughter measurements, *Health Phys.*, 56:189-194.

Ramamurthi, M; R. Strydom and P.K. Hopke (1990) Assessment of wire and tube peneration theories using a $^{218}PoO_x$ cluster aerosol, *J. Aerosol Sci.*, 21:203-211.

Ramamurthi, M and P.K. Hopke (1990) Simulation studies of reconstructions algorithms for the determination of optimum operating parameters and resolution of GRA systems (non-conventional diffusion batteries), *Aerosol Sci Technol.*(in press, vol12/#1).

Ramamurthi, M and P.K. Hopke (1990) An automated, semi-continuous system for measuring indoor radon progeny activity-weighted size distributions, d^p: 0.5-500 nm, *Aerosol Sci. Technol.* (paper under review).

Reineking, A.; K.H. Becker and J. Porstendörfer (1985) Measurements for the unattached fractions of radon daughters in houses, *Sci. Total Environ.*, 45:261-270.

Reineking, A. and J. Porstendörfer (1986) High-volume screen diffusion batteries and alpha-spectroscopy for measurement of the radon daughter activity size distributions in the environment, *J. Aerosol Sci.*, 17:873-879.

Reineking, A. and J. Porstendörfer (1989) The unattached fraction of the short-lived radon decay products in the indoor and outdoor environment, *Health Phys.*, (in press).

Rudnick, S.N.; W.C. Hinds; E.F. Maher and M. W. First (1983) Effect of plateout,air motion and dust removal on radon decay product concentration in a simulated residence, *Health Phys.*,45:463-470.

Stoute, J.R.D.; G.C.H. Groen and T.J.H. de Groot (1984) Characterisation of indoor atmospheres, *Rad. Prot. Dos.*, 7:159-163.

Strong, J.C. (1988) The size of attached and unattached radon daughters in room air, *J. Aerosol Sci.*, 19:1327-1330.

Strong, J.C. (1989) Design of NRPB activity size measurement system and results, presented at the Worshop on "Unattached" Fraction Measurements, University of ILlinois, IL, April 1989.

Swedjemark, G.A. (1983) The equilibrium factor, *Health Phys.*, 45:453-462.

Thomas, J.W. and L.E. Hinchliffe (1972) Filtration of 0.001 μm particles with wire screens, *J. Aerosol Sci.*, 3:387-393.

Tu, K.W. and E.O. Knutson (1984) Total deposition of ultrafine hydrophobic and hygroscopic aerosols in the human respiratory tract, *Aerosol Sci. Technol.*, 3:453-465.

Tu, K.W. and E.O. Knutson (1988) Indoor outdoor aerosol measurements for two residential buildings in New Jersey, *Aersosol Sci. Technol.*, 9:71-82.

Vanmarcke, H.; A. Janssens and F. Raes (1987) The behavior of radon daughters in the domestic environment, In *Radon and its Decay Products: Occurrence, Properties, and Health Effects*. Ed. P. K. Hopke, American Chemical Society, Washington, DC., 301-323.

Weibel, E.R. (1963) Morphometry of human lung, New York Academic Press.

Wrixon, A.D.; B.M.R. Green; R.R. Lomas; J.C.H. Miles; K.D. Cliff; E.A. Francis; C.M.H. Driscoll; A.C. James and M.C. O'Riordan (1988) Natural radiation exposure in U.K. Dwellings, NRPB Report NRPB-R190, Chilton, Didcot, Oxon.

Yeh, H.C. and G.M. Schum (1980) Models of human airways and their application to inhaled particle deposition, *Bull. Math. Biol.*, 42:461-480.

Yu, C.P.; C.K. Diu and T.T. Soong (1981) Statistical analysis of aerosol deposition in nose and mouth; *Am. Ind. Hyg. Assoc. J.*, 42:726-733.

Yu, C.P. and C.K. Diu (1982) A comparative study of aerosol deposition in different lung models; *Am. Ind. Hyg. Assoc. J.*, 43:54-65.

APPENDIX I
THE ACTIVITIES AND MEASUREMENTS IN THE SINGLE-FAMILY HOUSE IN SPRINGFIELD, PA

(a)Dec 13

10:01 The background measurements (12131001), (12131319), (12131521)

(b)Dec 15

0:19 The background measurements (12150019), (12150320), (12150621), (12150922)

11:00 Turn the air filtration system (air filter) on

14:57 The sample after 4-hour air filter running (12151457)

15:30 Turn air filter off

19:28 - 19:58 Clothes dryer operating for 30 minutes

19:28 The sample with clothes dryer running (12151928)

(c)Dec 17

10:00 Turn the air filter on

13:59 The sample after 4-hour air filter running (12171359)

17:00 The sample after 7-hour air filter running (12171700)

17:30 Turn the sir filter off

21:59 The sample with the air filter off for 4.5 hours (12172159)

(d)Dec 18

0:59 The background measurements (12180059), (12180400), (12180701), (12181001)

10:40 Turn the air filter on

13:01 The sample after 2.5-hour air filter running (12181301)

13:31 Turn the air filter off

16:04 The sample with the air filter off for 2.5 hours (12181604)

20:05 The sample with the air filter off for 6.5 hours (12182005)

(e)Dec 19

0:05 The background measurement (12190005)

12131001

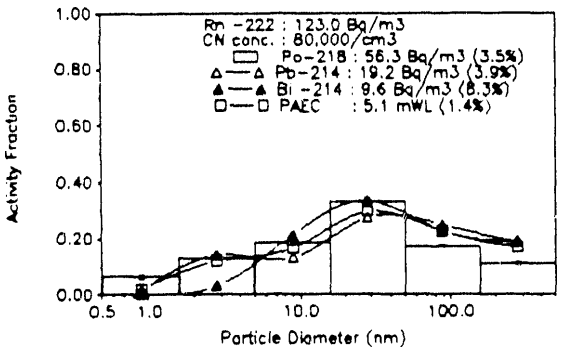

12131319

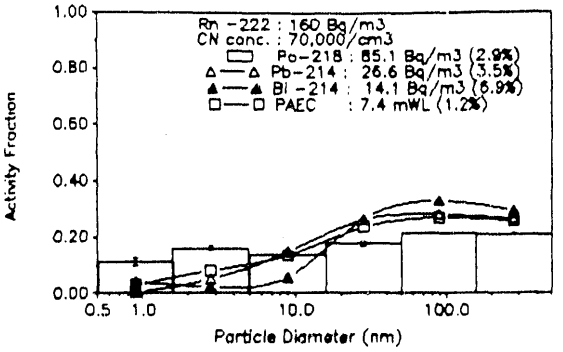

12131521

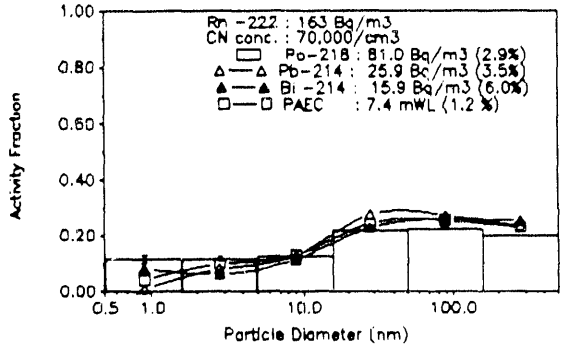

12150019

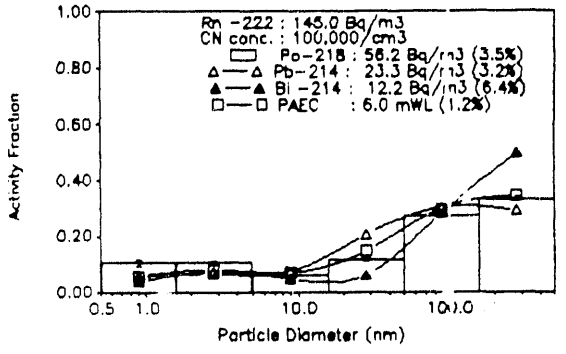

12150320

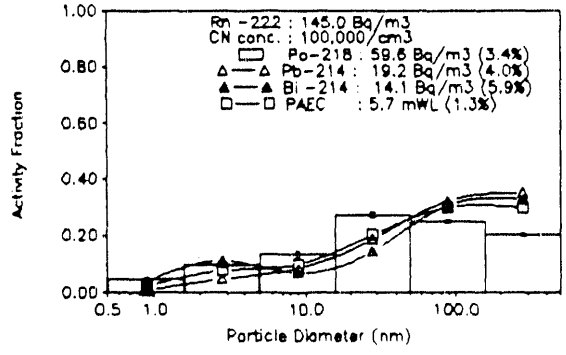

12150621

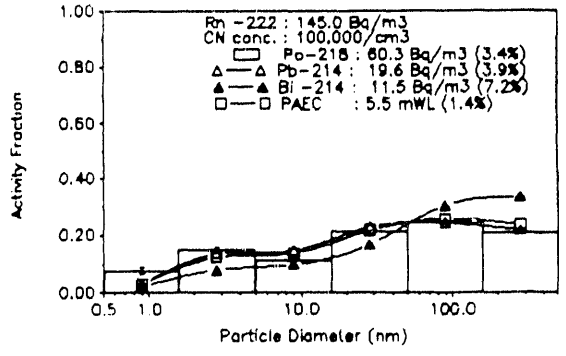

12150922

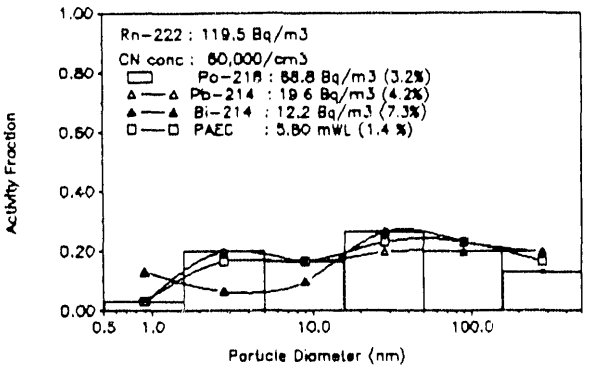

12151457

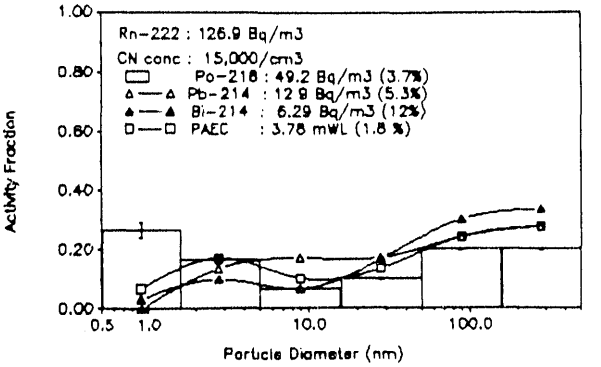

12151928

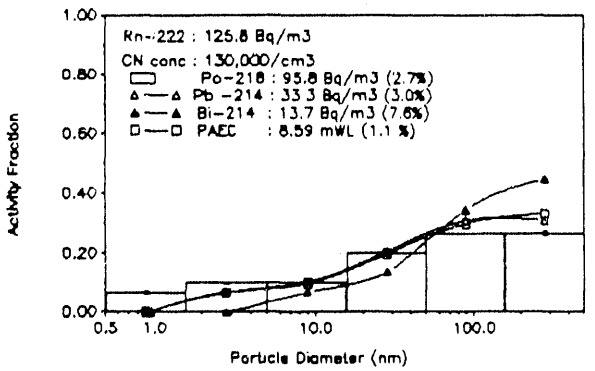

12171359

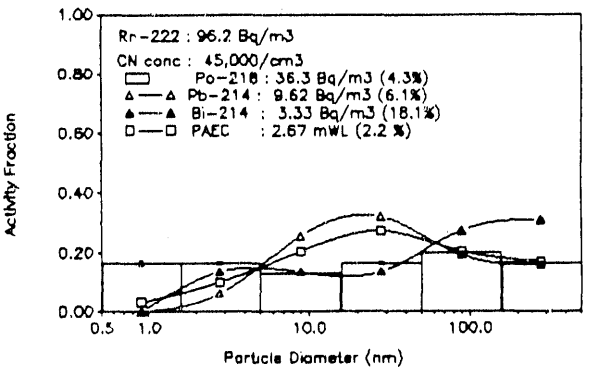

12171700

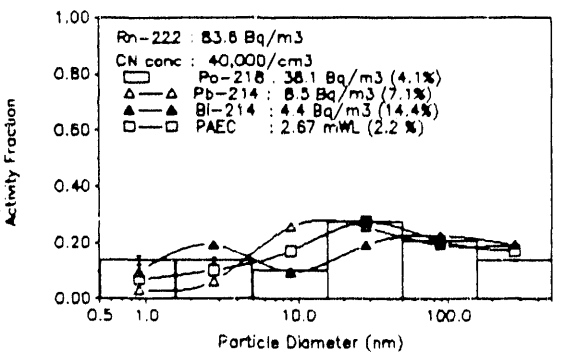

12172159

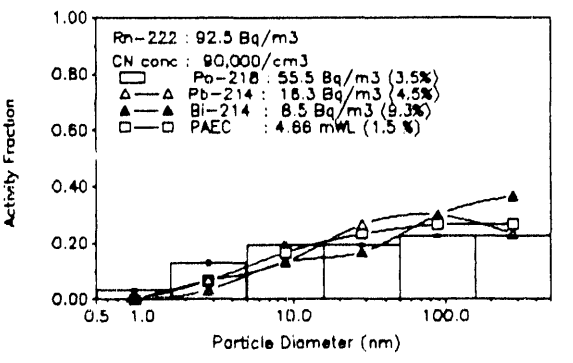

12180059

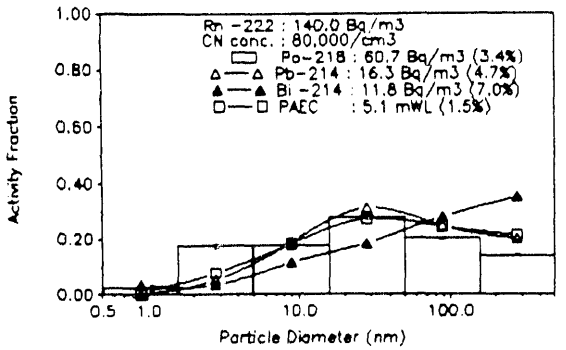

12180400

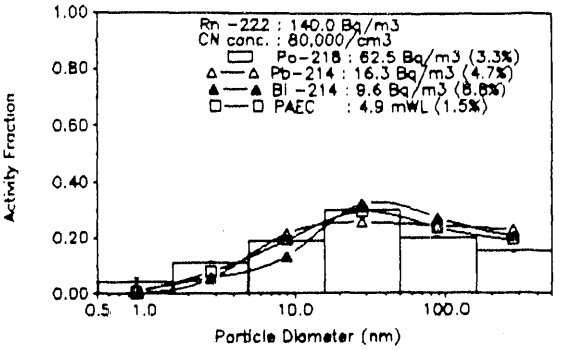

12180701

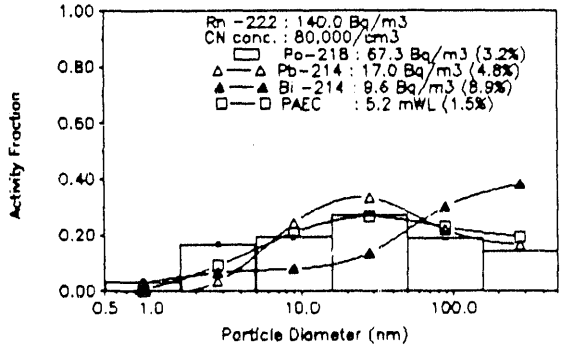

12181001

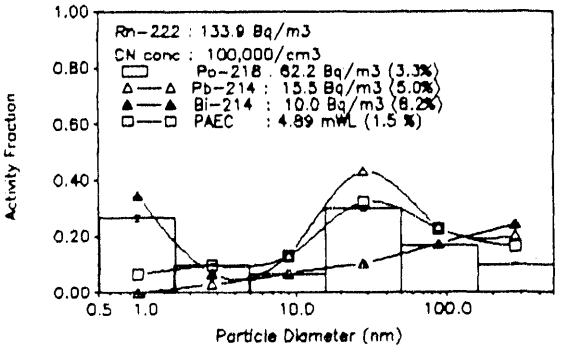

12181301

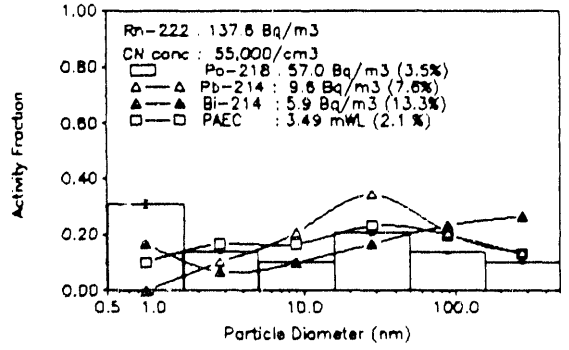

12181604

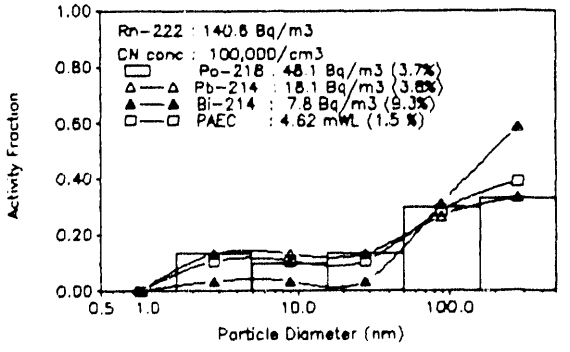

12182005

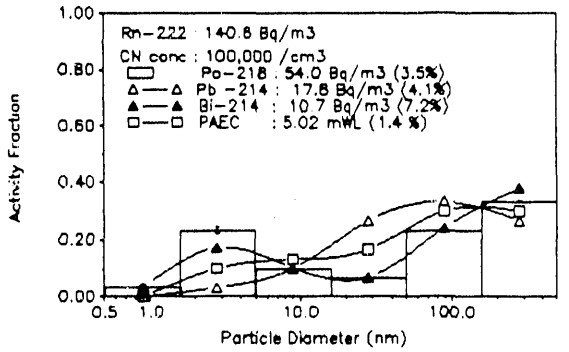

12190005

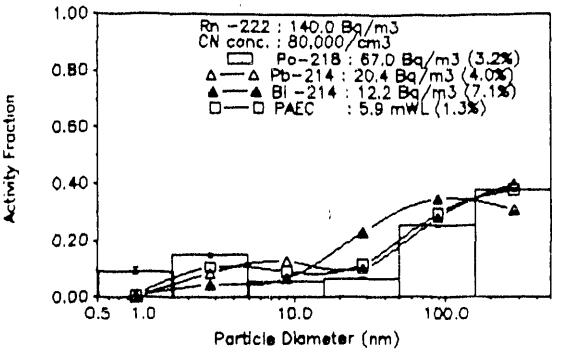

APPENDIX II

THE ACTIVITIES AND MEASUREMENTS IN THE SINGLE-FAMILY HOUISE IN PRINCETON, NJ

(a)Jan 17

Four measurements in the living room (1171530), (1171700), (1172045), (1172230)

(b)Jan 21

The following measurements were all made in the bedroom

The background conditions with the bedroom door open (1210007), (1210138), (1210309), (1210440), (1210611), (1210742)

8:42 Close the bedroom door

9:19 The sample after the door closed (1210919)

9:38 Turn the air filtration system (the filter) on and open door

11:38 The samples with the filter on and door opened (1211138), (1211309), (1211443)

15:03 Cleaner off and door closed

16:14 The samples with the filter off and door closed (1211614), (1211934), (1212105), (1212236)

(c)Jan 22

0:07 The samples with the filter off and door closed (1220007), (1220138), (1220309),(1220440)

6:00 - 6:20 Running water in a shower

6:00 - During the running water in a shower (1220600)

7:16 - 55 minutes after running water in a shower (1220716)

8:33 - 130 minutes after running water in a shower (1220833)

9:49 - More than 3 hours after running water in a shower (1220949), (1221105)

12:55 Turn the filter on

17:27 The sample after 5 hours with the filter on (1221727)

18:00 Turn the filter off

(d)Jan 23

4:40 The background condition with door closed and the filter off (1230440)

6:00 - 6:20 Candle burning

5:59 - During the candle burning period (1230559)

7:15 - 55 minutes after candle burning (1230715)

8:32 - 130 minutes after candle burning (1230832)

9:13 Turn the filter on

10:14 The background with the filter on (1231014), (1231130)

12:45 - 13:05 Candle burning

12:46 - During the candle burning period (1231246)

14:03 - 55 minutes after candle burning (1231403)

15:19 - 130 minutes after candle burning (1231519)

16:36 - 3.5 hours after candle burning (1231636)

23:16 Turn the filter off

(e)Jan 24

8:28 The background with door closed and the filter off (1240828)

9:40 - 10:00 Cigarette smoldering

9:44 - During the cigarette smoldering (1240944)

11:01 - 60 minutes after cigarette smoldering (1241101)

12:17 - 135 minutes after cigarette smoldering (1241217)

12:36 Turn the filter on

16:02 - 16:22 Cigarette smoldering

16:07 - During the cigarette smoldering (1241607)

17:26 - 60 minutes after cigarette smoldering (1241726)

18:57 - 135 minutes after cigarette smoldering (1241857)

19:12 Turn the filter off

22:17 The sample without the filter (1242217)

(f)Jan 25

1:19 The background without the filter (1250119), (1250420)

9:19 - 9:39 Vacuuming

9:24 - During the vacuuming (1250924)

11:04 - 60 minutes after vacuuming (1251104)

12:25 - 135 minutes after vacuuming (1251225)

12:40 Turn the filter on

16:58 The background with the filter on (1251658), (1251829), (1252000)

22:00 - 22:20 Vacuuming

22:04 - During the vacuuming (1252204)

(g) Jan 26

0:05 - 60 minutes after vacuuming (1260005)

1:22 - 135 minutes after vacuuming (1260122)

1:40 Turn the filter off and open door

2:53 The background with door opened and the filter off (1260253), (1260425), (1260556),(1260727)

8:55 - 9:15 Cooking in the kitchen

9:01 - During the cooking (1260901)

10:15 - 60 minutes after cooking (1261015)

11:30 - 135 minutes after cooking (1261130)

12:05 Turn the filter on

18:04 The background with the filter and door open (1261804)

19:30 - 19:50 Cooking

19:34 - During the cooking (1261934)

20:50 - 60 minutes after cooking (1262050)

22:08 - 135 minutes after cooking (1262208)

(h)Jan 27

0:39 The background with the filter on and door open (1270039), (1270310), (1270542)

7:53 - 8:13 Cooking in the kitchen

7:58 - During the cooking (1270758)

9:14 - 60 minutes after cooking (1270914)

10:31 - 135 minutes after cooking (1271031)

10:46 Turn the filter off

14:26 The background with door open and the filter off (1271426)

15:48 - 16:08 Cooking in the kitchen

15:53 - During the cooking (1271553)

17:10 - 60 minutes after cooking (1271710)

18:26 - 135 minutes after cooking (1271826)

18:41 Close the bedroom door

22:16 The background with the filter off and door closed (1272216)

(i)Jan 28

0:33 The background with the filter off and door closed (1280033), (1280249), (1280505), (1280721)

9:07 - 9:27 Cigarette smoldering

9:12 - during the cigarette smoldering (1280912)

10:28 - 60 minutes after cigarette smoldering (1281028)

11:45 - 135 minutes after cigarette smoldering (1281145)

12:00 Turn the filter on

16:00 The background with the filter on and door closed (1281600)

17:23 - 17:43 Cigarette smoldering

17:28 - During the cigarette smoldering (1281728)

18:45 - 60 minutes after cigarette smoldering (1281845)

(j)Jan 29

6:45 The background with the filter on and door closed (1290645)

8:33 - 8:53 Vacuuming

8:38 - During the vacuuming (1290838)

9:54 - 60 minutes after the vacuuming (1290954)

11:11 - 135 minutes after the vacuuming (1291111)

11:26 Turn the filter off

15:38 The background with the filter off and door closed (1291538)

17:08 - 17:28 Vacuuming

17:13 - During the vacuuming (1291713)

18:30 - 60 minutes after the vacuuming (1291830)

19:46 - 135 minutes after the vacuuming (1291946)

20:04 Turn the filter on

22:09 The background with the filter on and door closed (1292209)

(k)Jan 30

0:10 The background with the filter on and door closed (1300010), (1300211), (1300413)

6:05 - 6:25 Candle burning

6:05 - During the candle burning (1300605)

7:22 - 55 minutes after candle burning (1300722)

8:39 - 130 minutes after candle burning (1300839)

8:55 Turn the filter off

12:59 The background with the filter off and door closed (1301259)

14:23 -14:43 Candle burning

14:23 - During the candle burning (1301423)

15:40 - 55 minutes after candle burning (1301540)

16:57 - 130 minutes after candle burning (1301657)

1171530

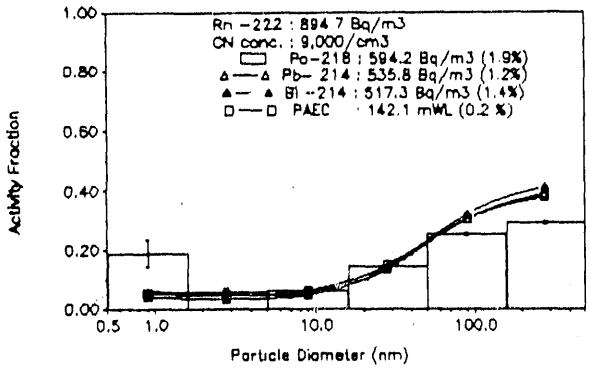

1171700

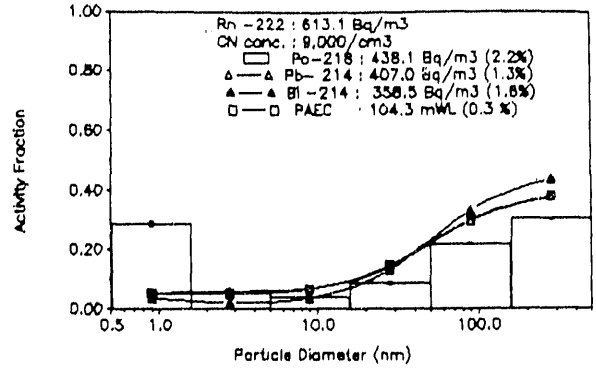

1172045

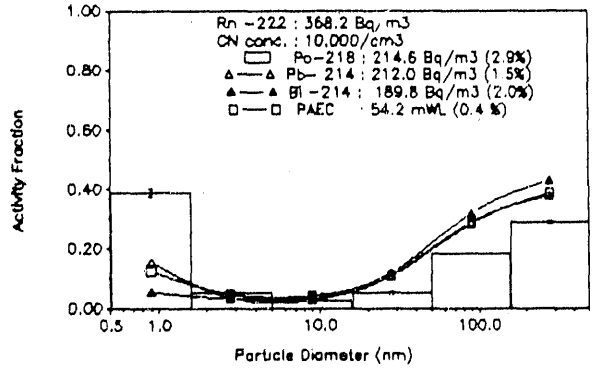

1172230

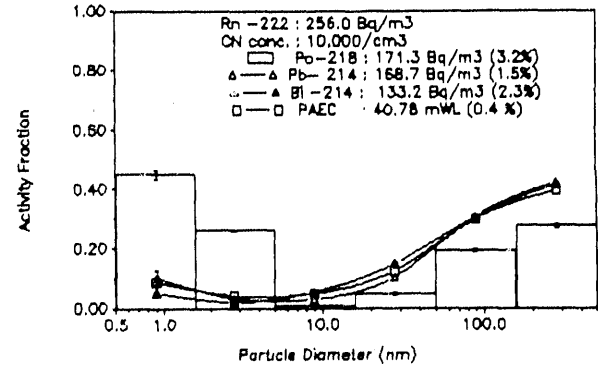

1210007

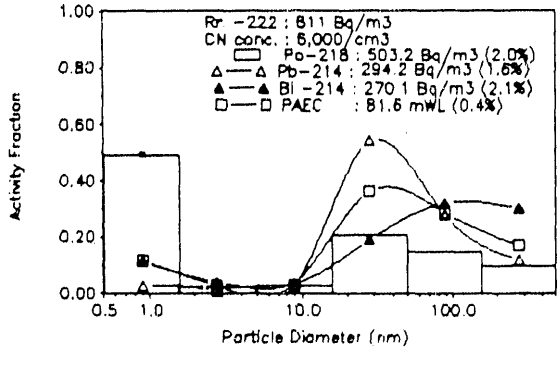

1210138

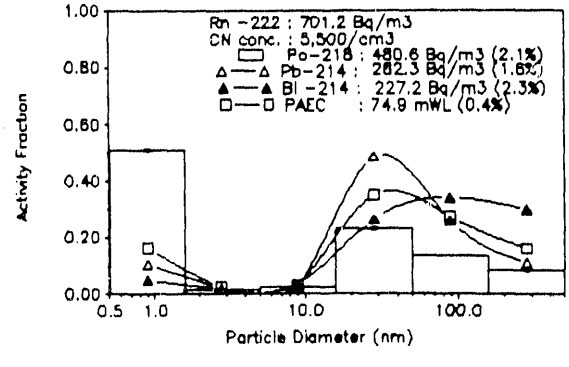

1210309

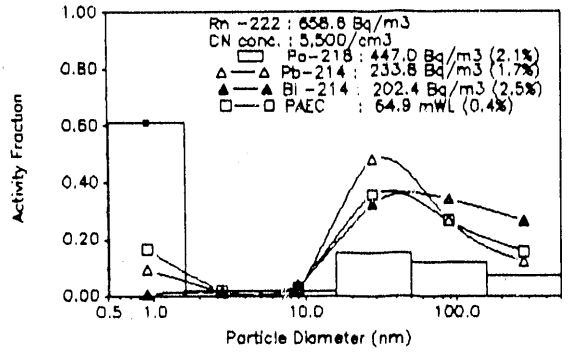

1210440

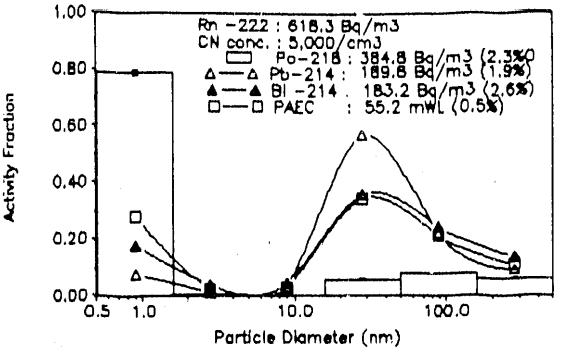

1210611

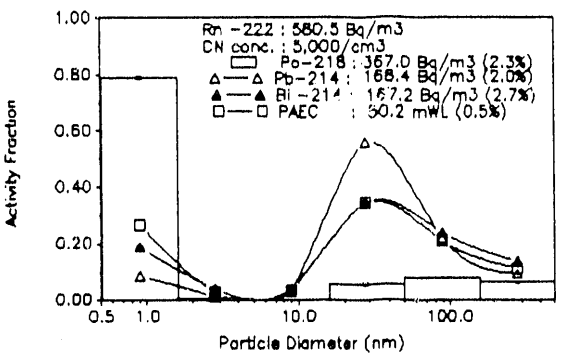

1210742

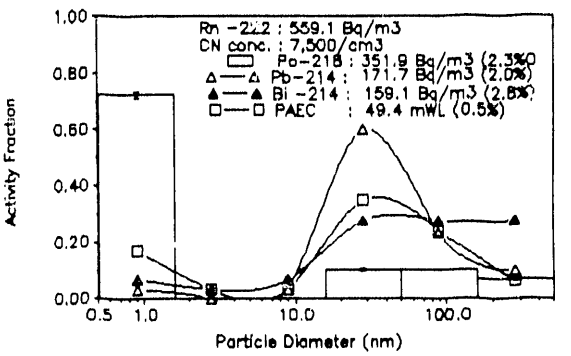

1210919

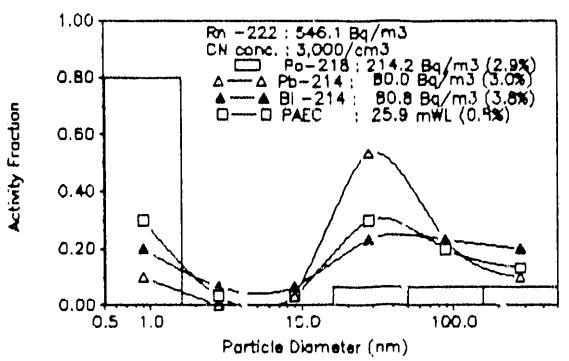

1211138

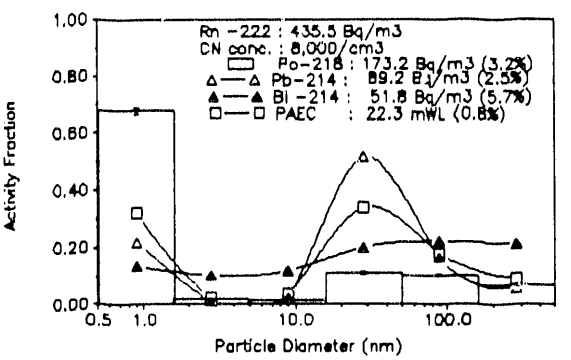

1211309

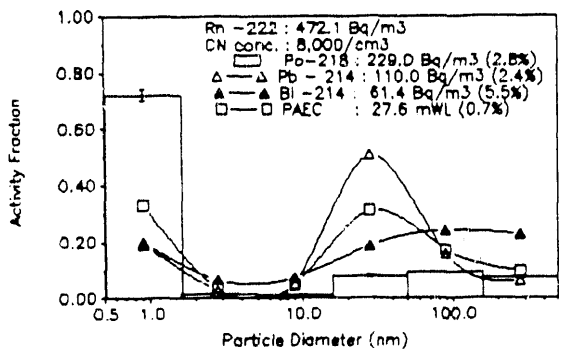

1211443

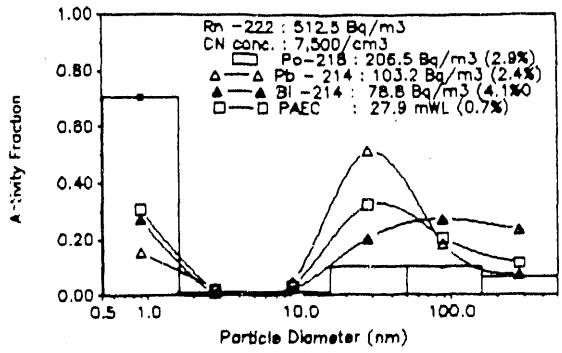

1211614

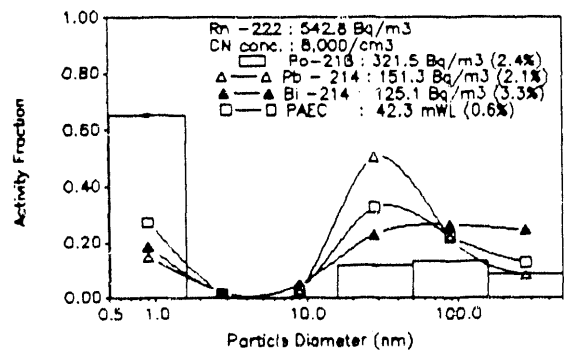

1211934

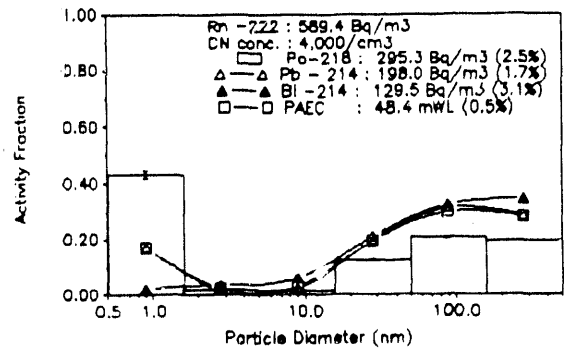

1212105

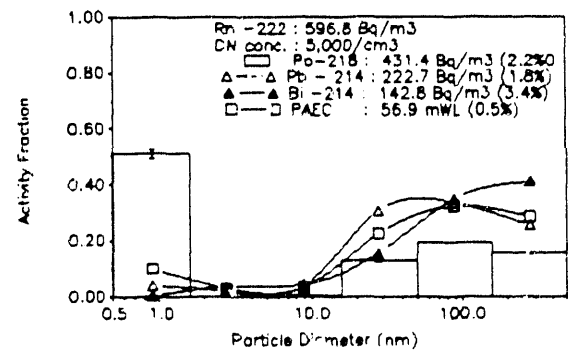

1212236

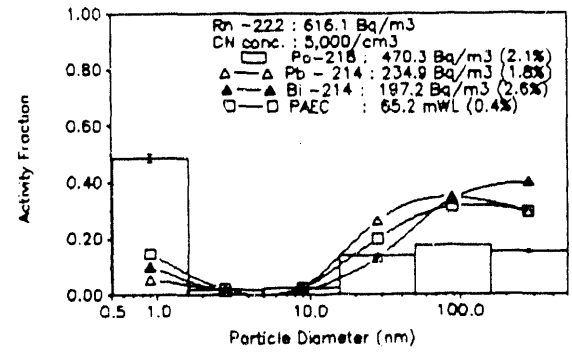

1220007

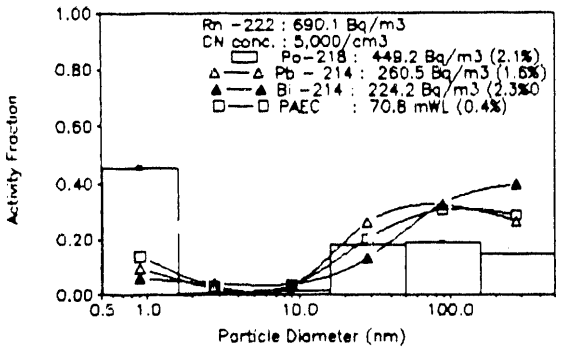

1220138

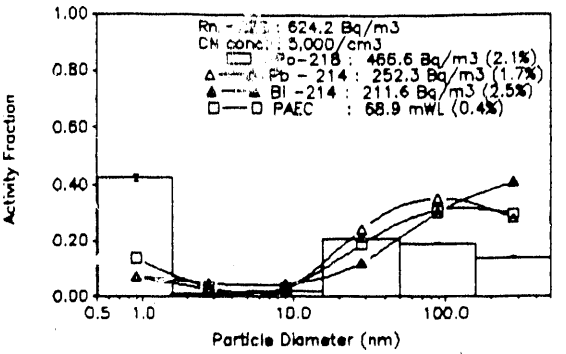

1220309

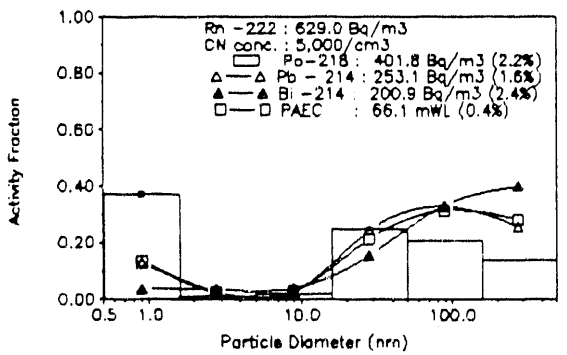

1220440

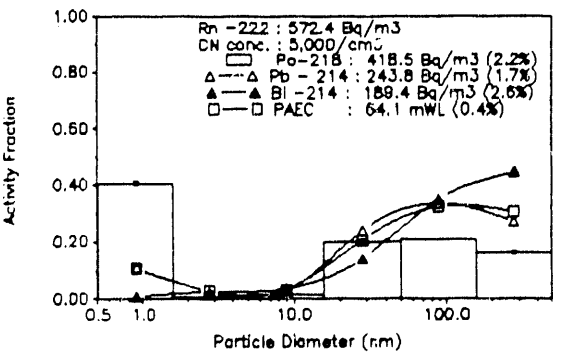

1220600

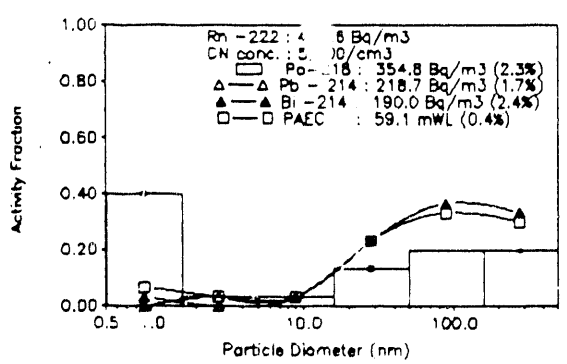

1220716

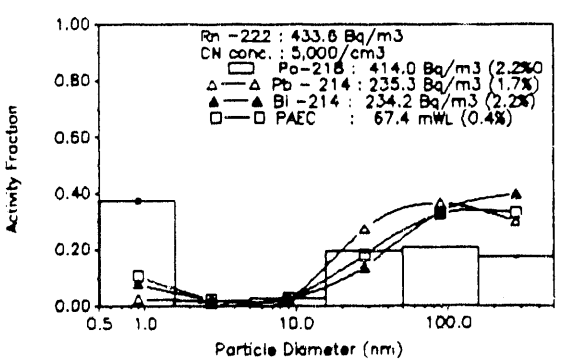

1220833

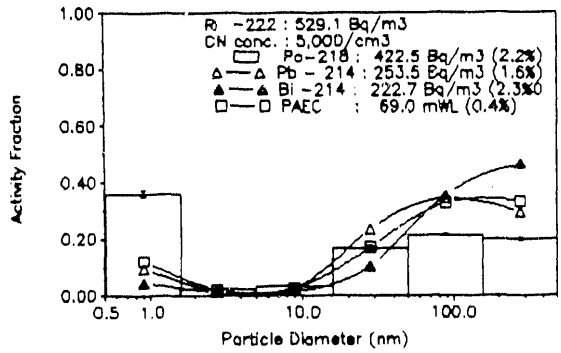

1220949

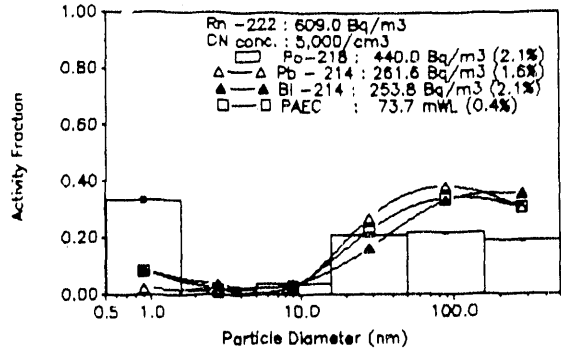

1221105

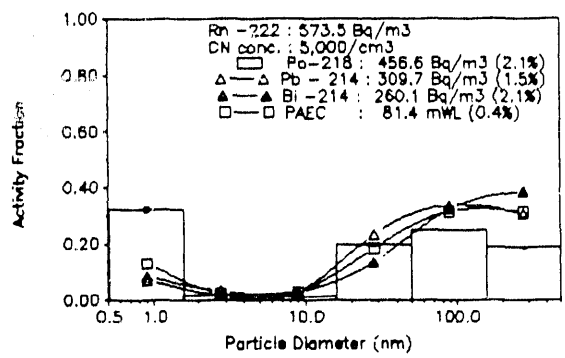

1221727

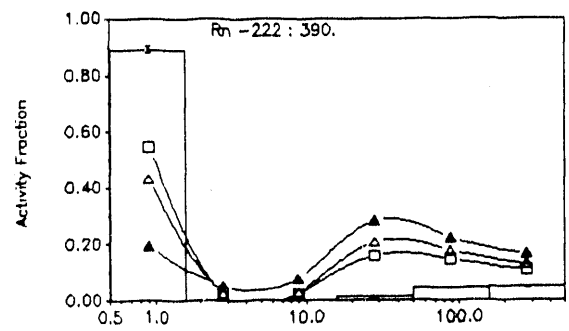

1230440

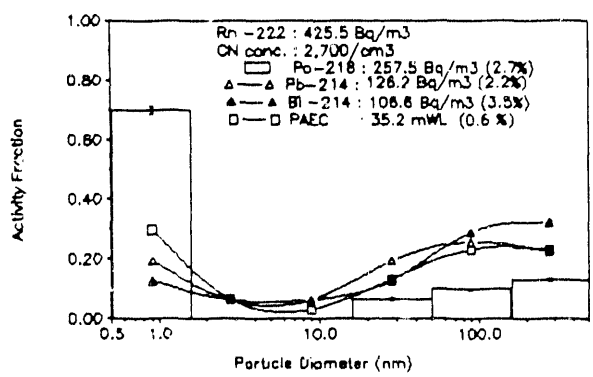

1230559

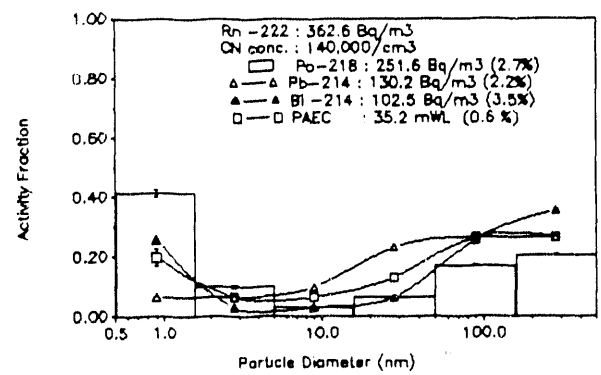

1230715

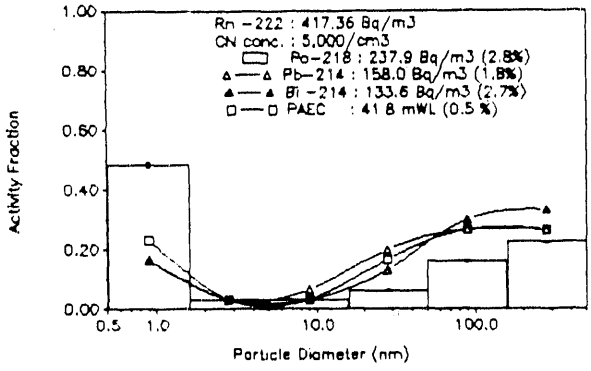

1230832

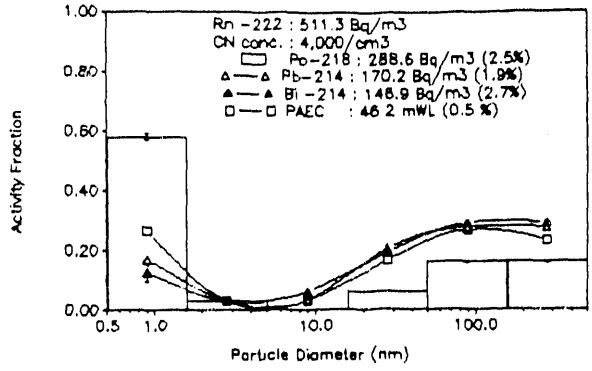

1231014

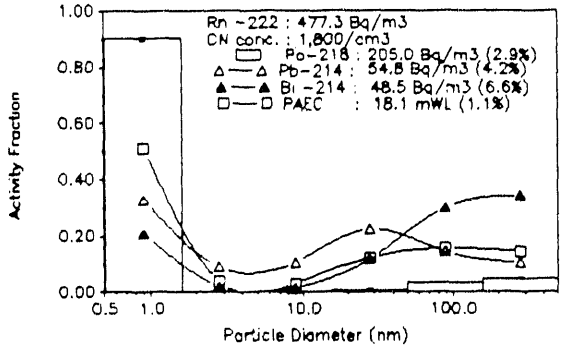

1231130

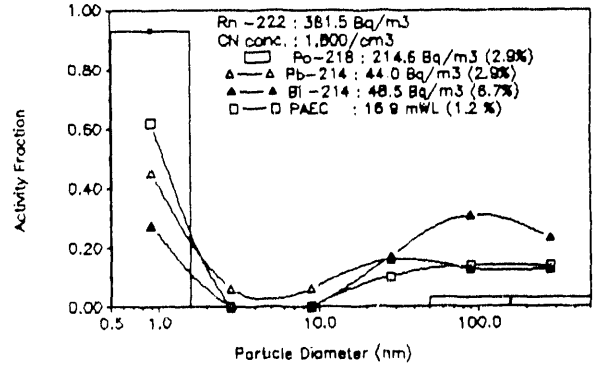

1231246

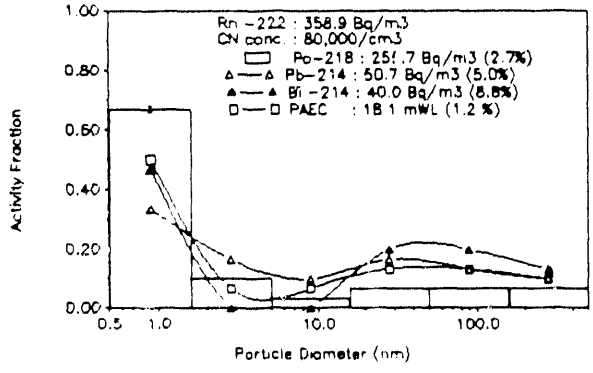

1231403

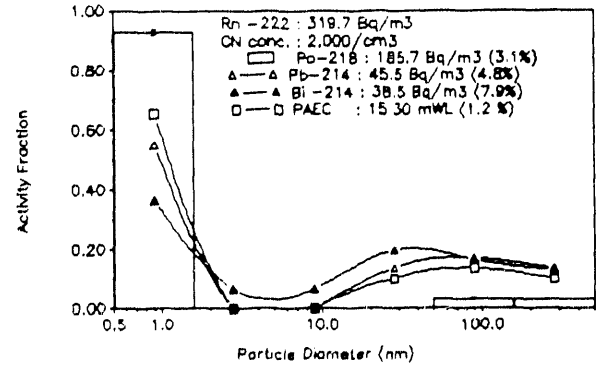

1231519

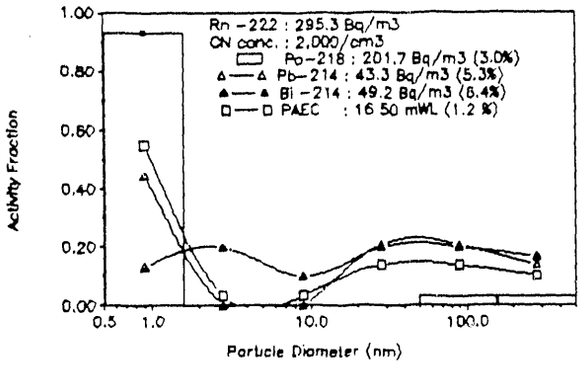

1231636

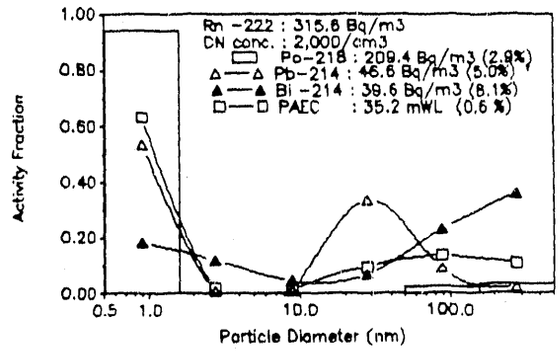

1240828

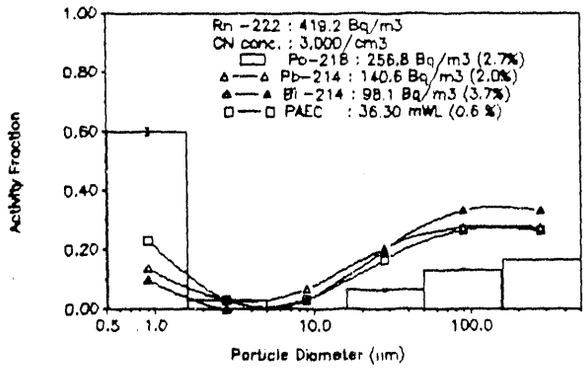

1240944

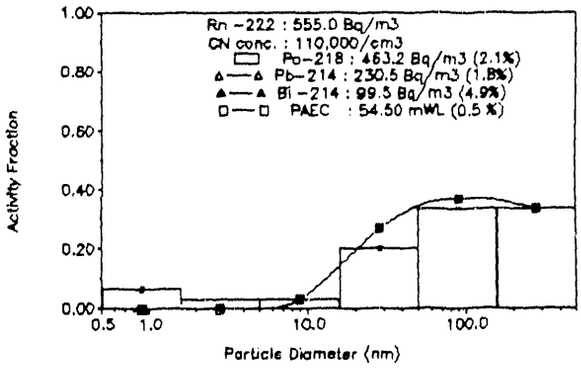

1241101

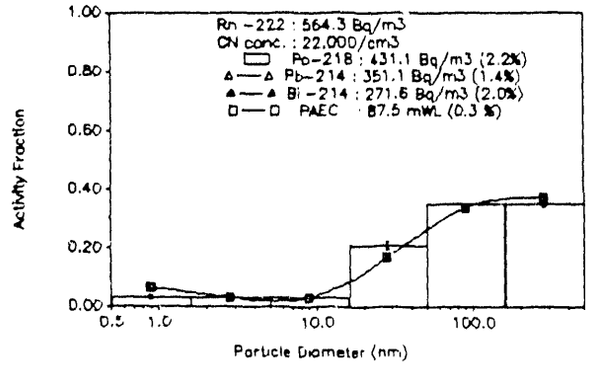

1241217

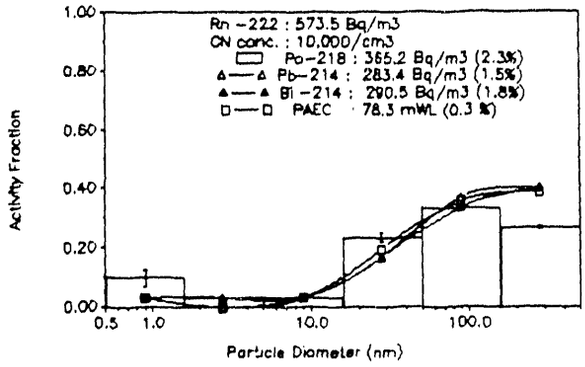

1241607

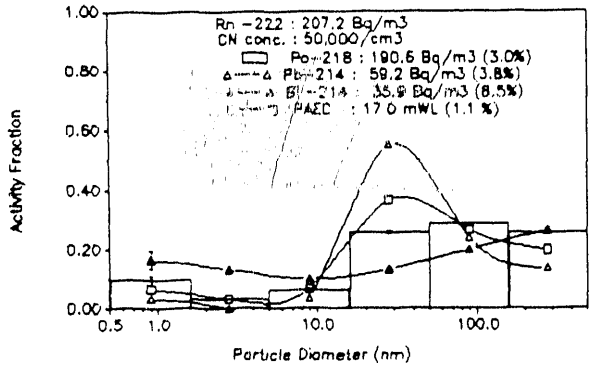

1241726

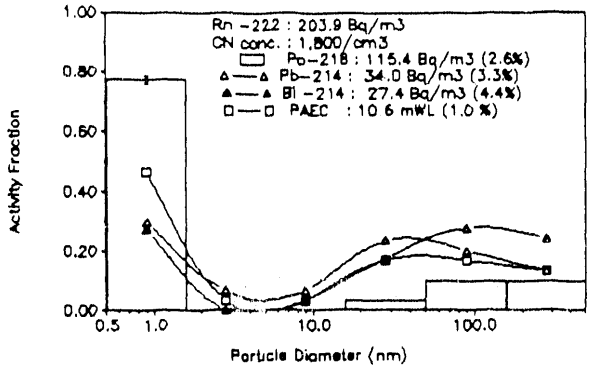

1241857

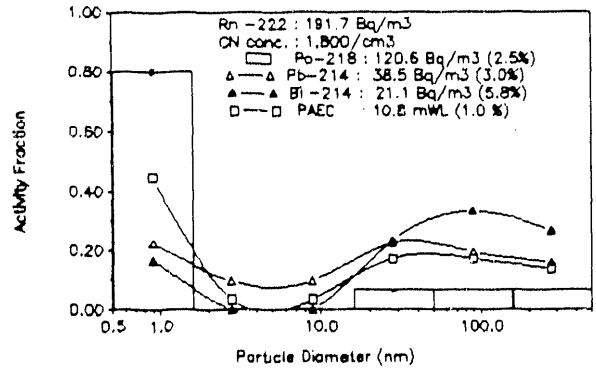

1242217

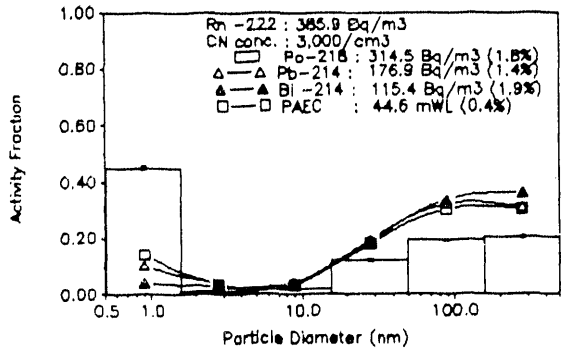

1250119

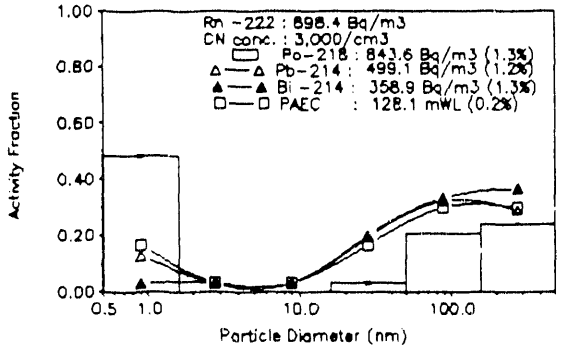

1250420

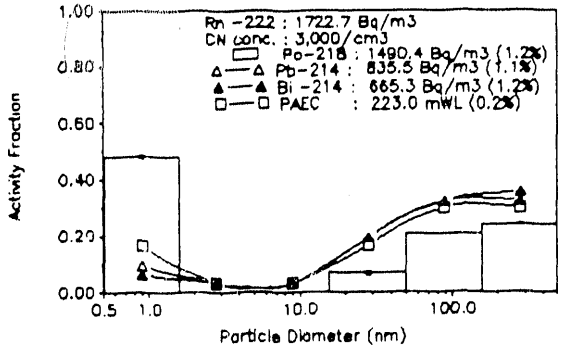

1250924

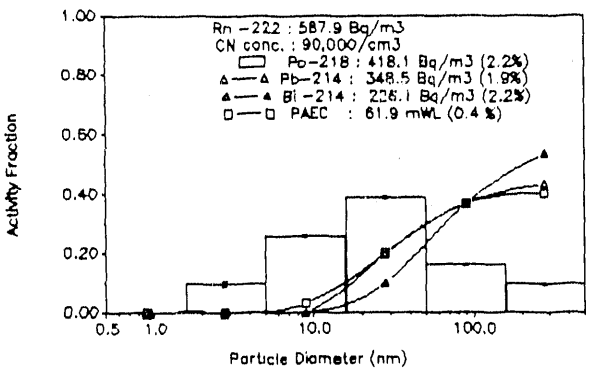

1251104

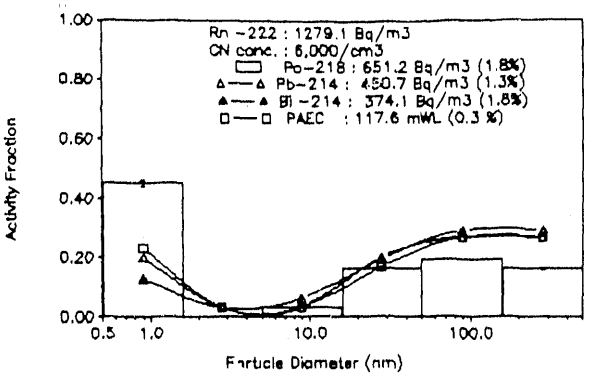

1251225

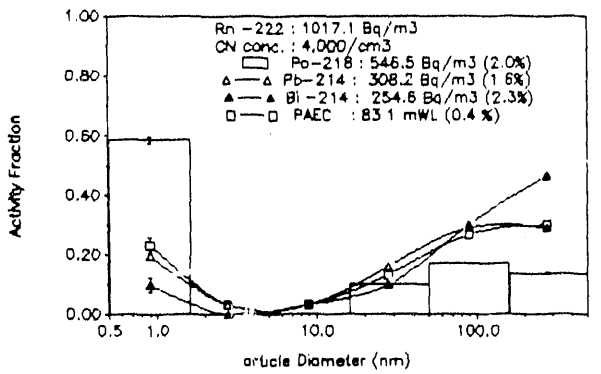

1251658

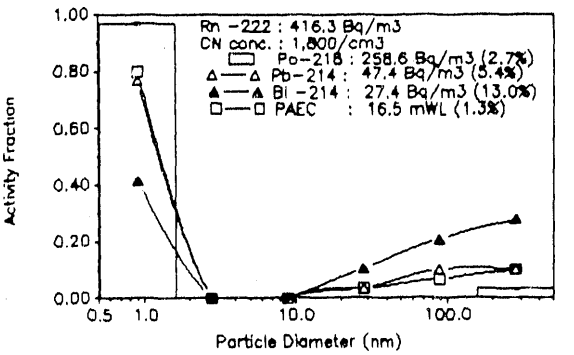

1251829

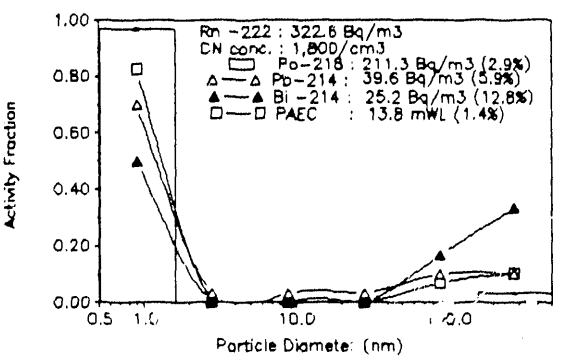

1252000

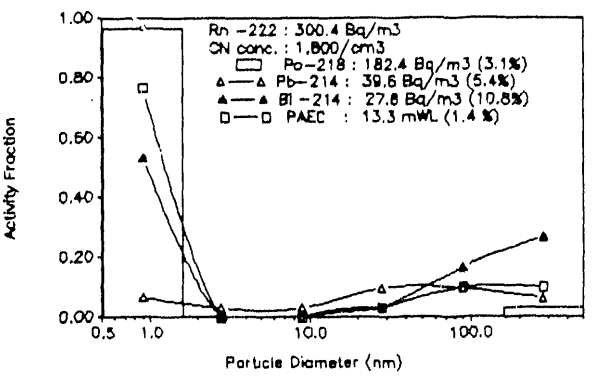

1252204

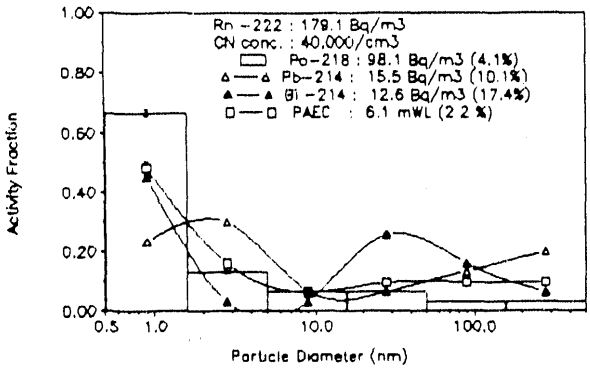

1260005

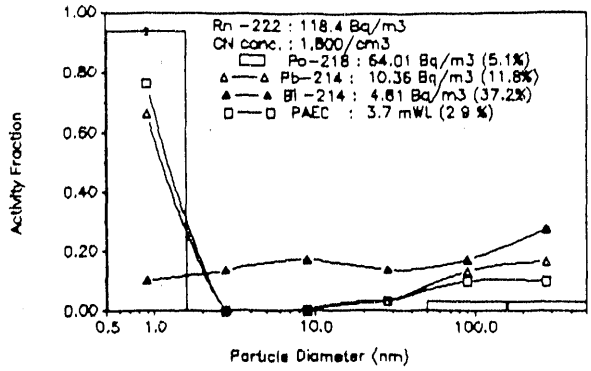

1260122

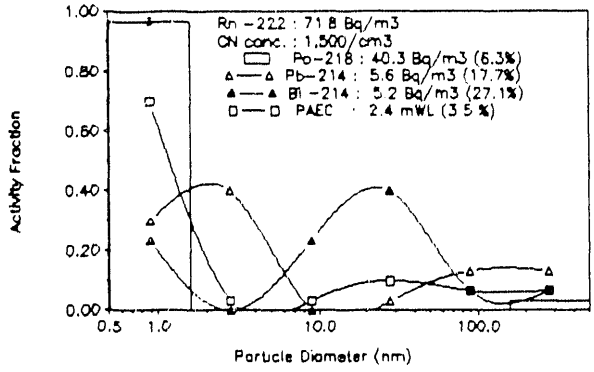

1260253

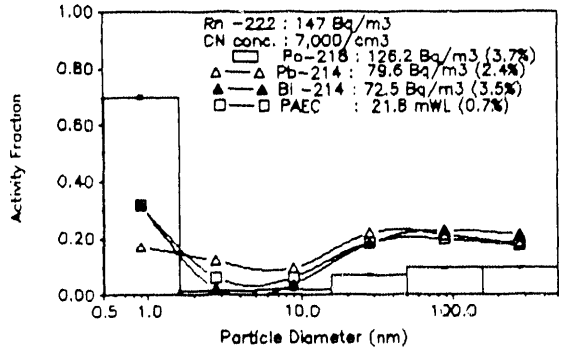

1260425

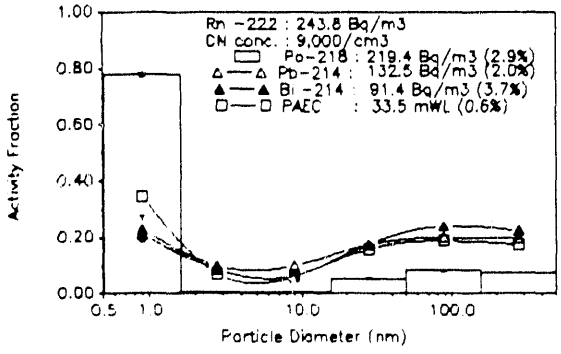

1260556

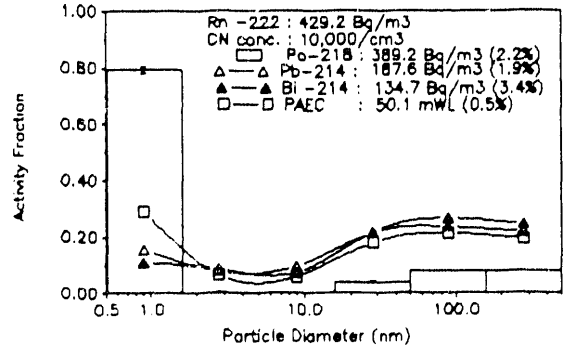

1260727

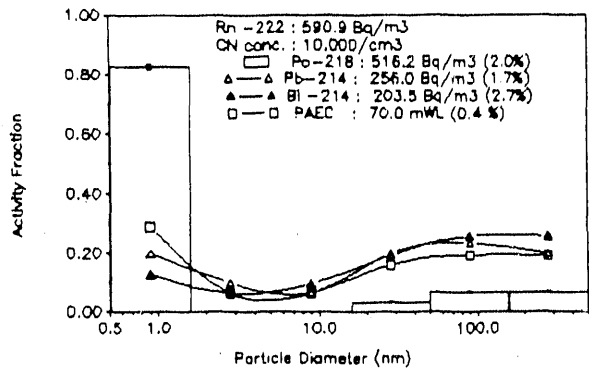

1260901

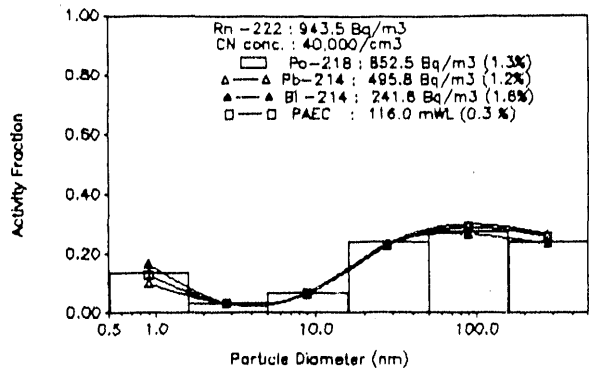

1261015

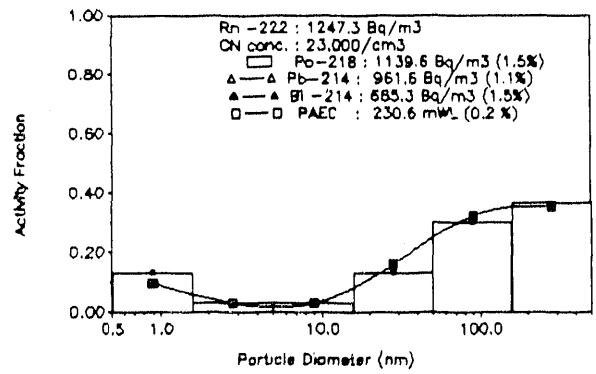

1261130

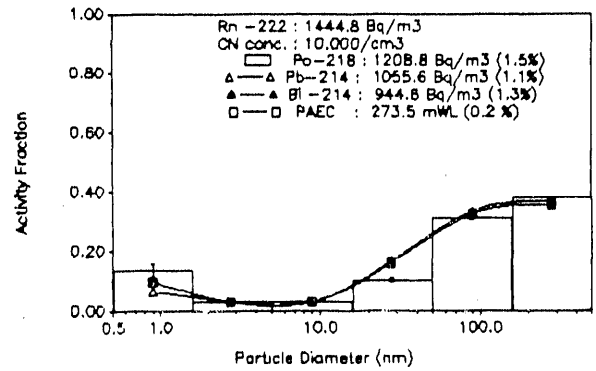

1261804

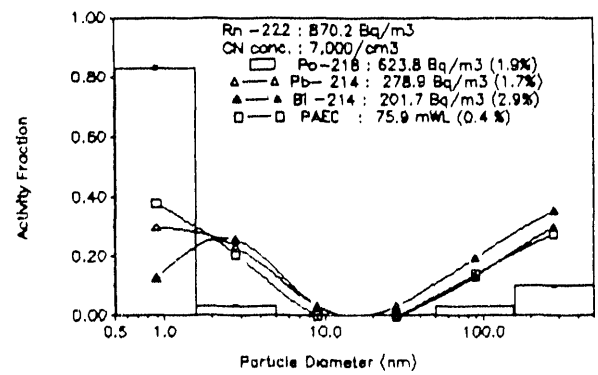

1261934

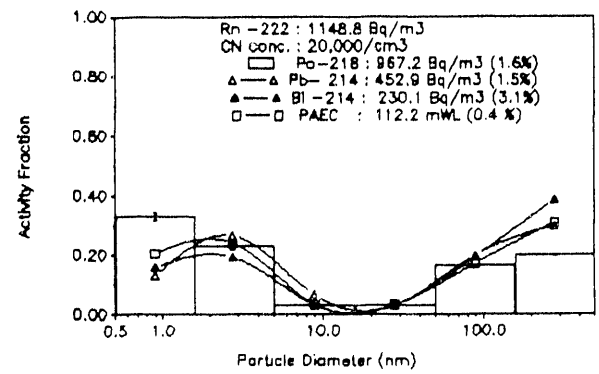

1262050

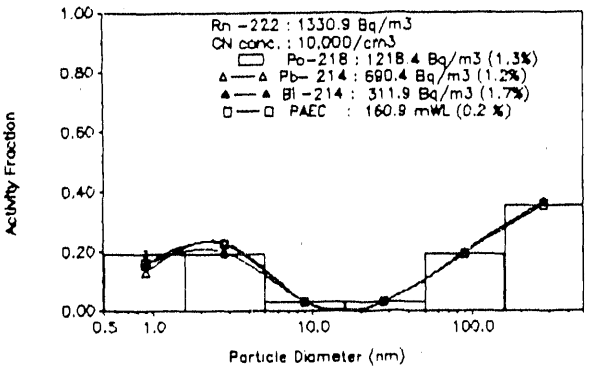

1262208

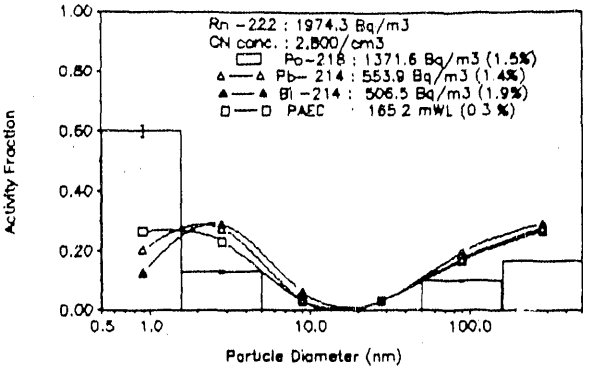

1270039

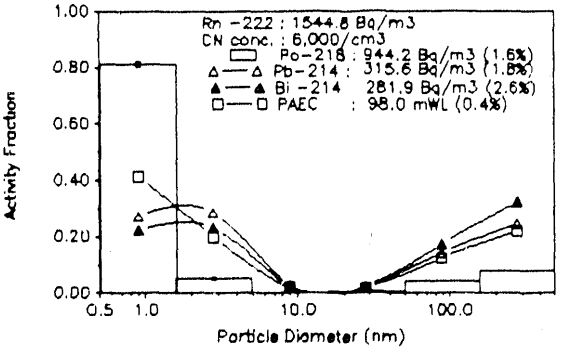

1270310

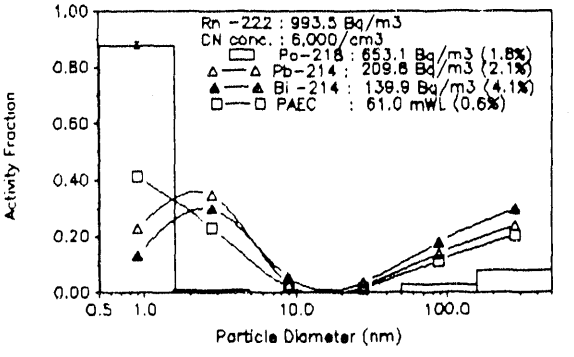

1270542

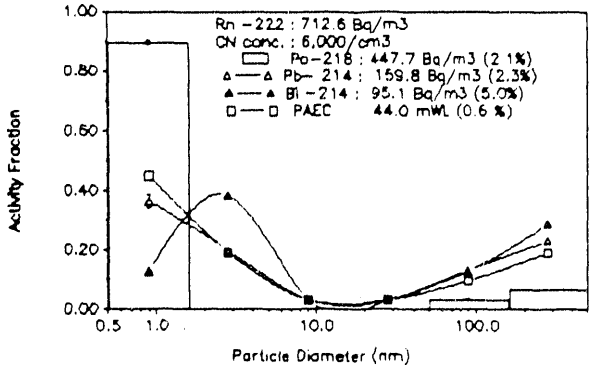

1270758

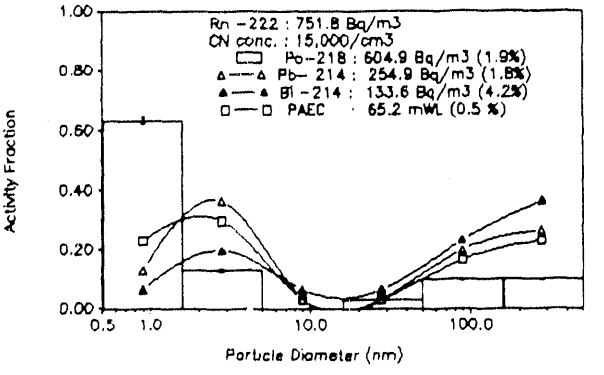

1270914

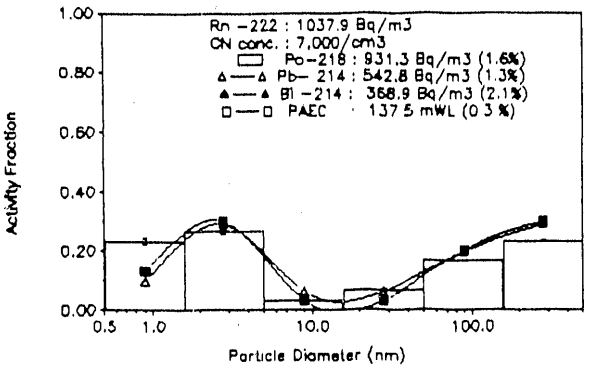

1271031

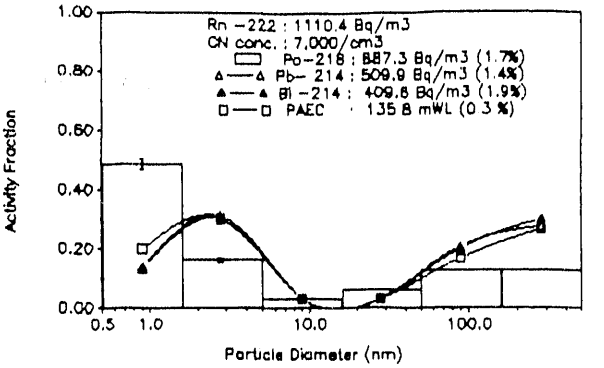

1271426

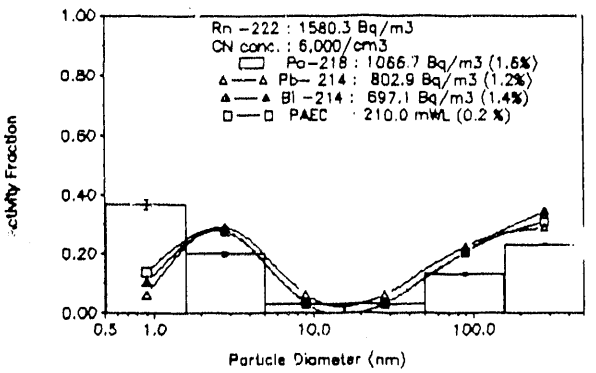

1271553

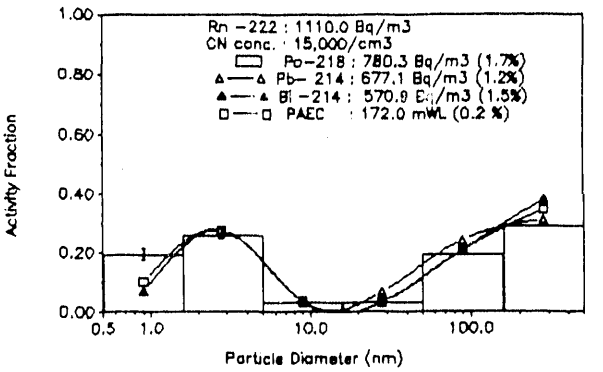

1271710

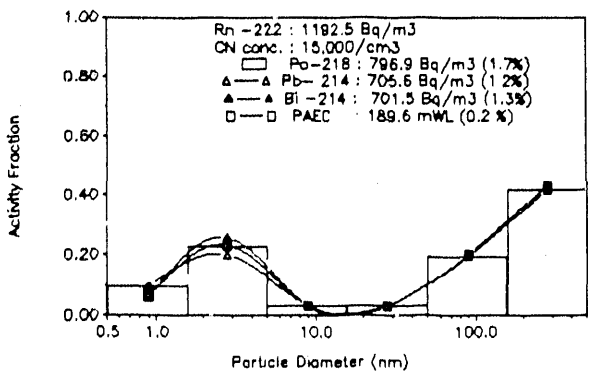

1271826

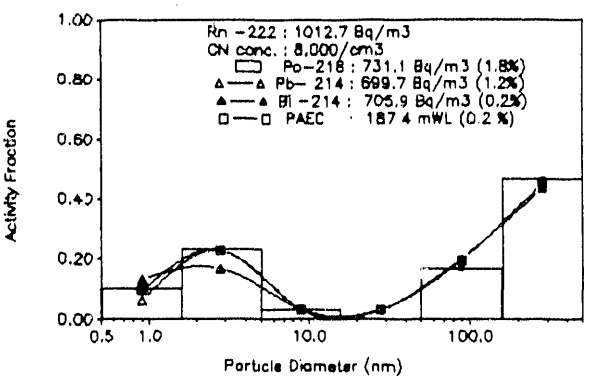

1272216

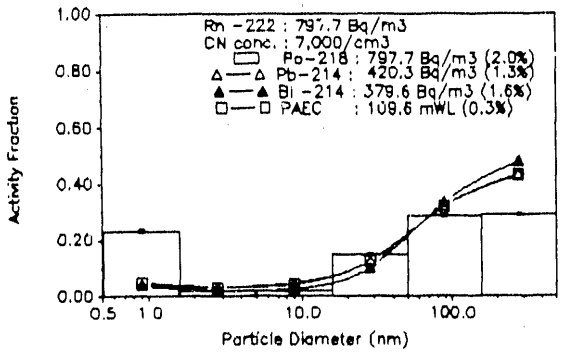

1280033

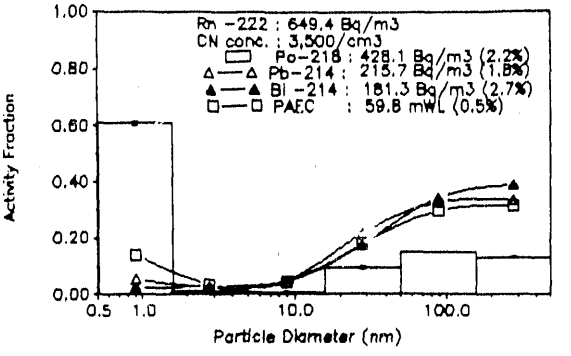

1280249

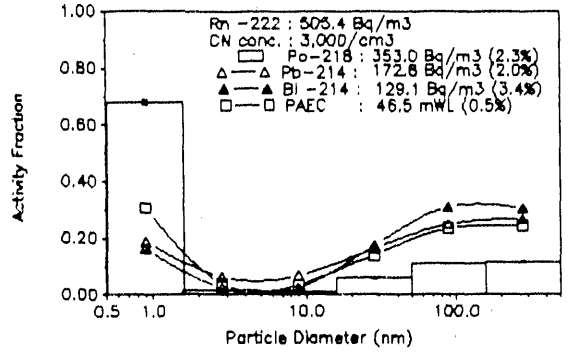

1280505

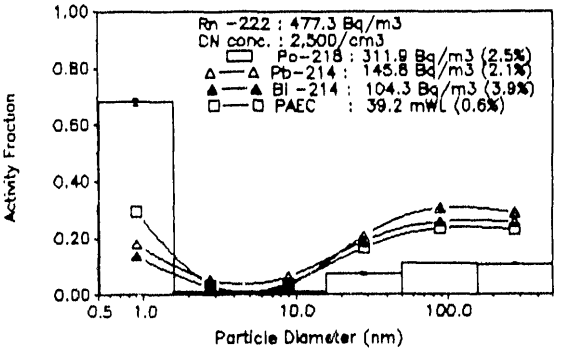

1280721

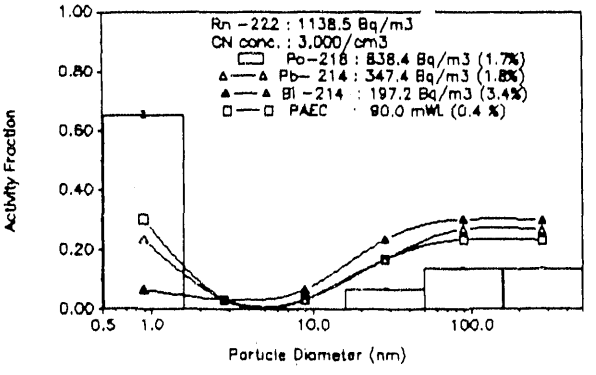

1280912

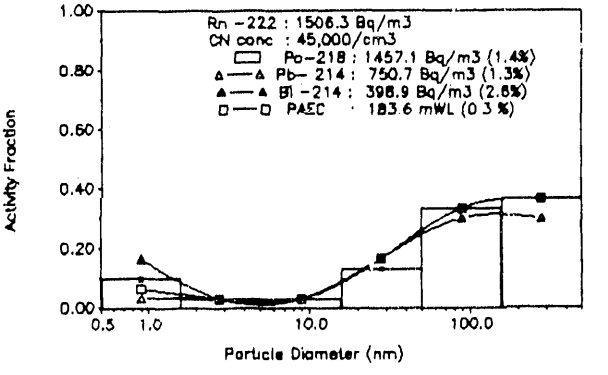

1281028

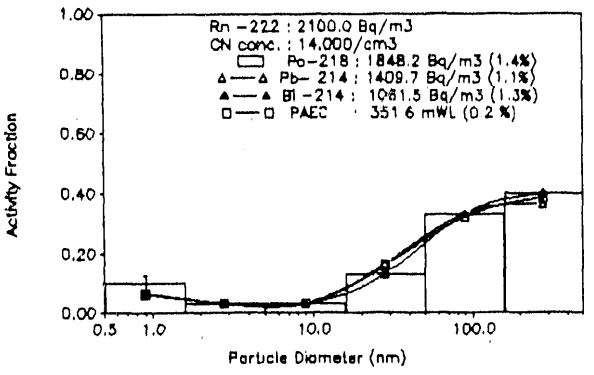

1281145

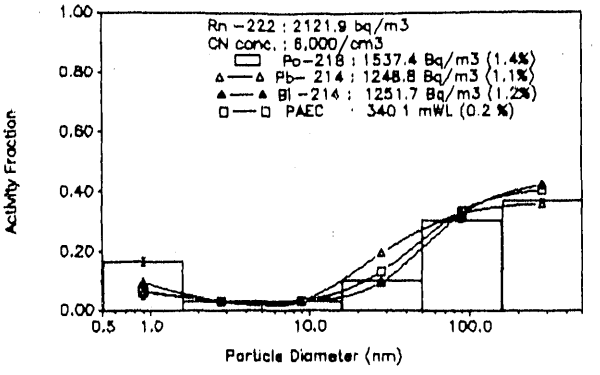

1281600

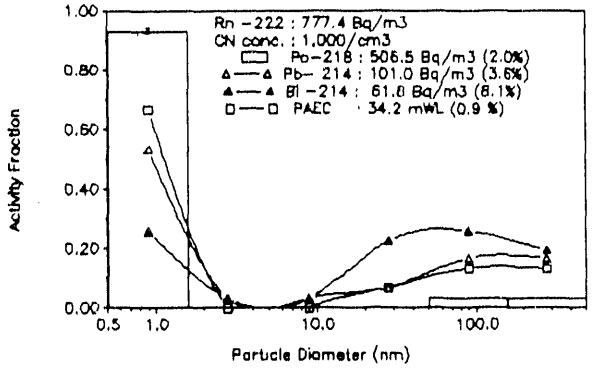

1281728

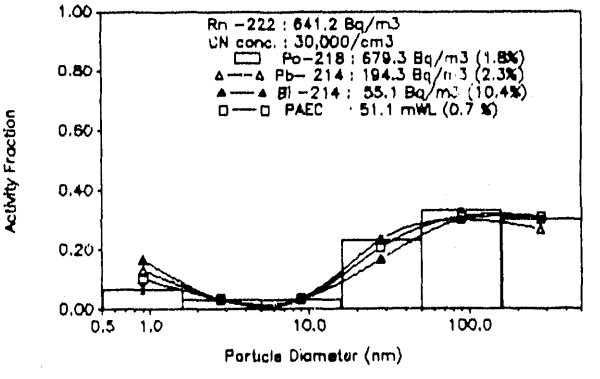

1281845

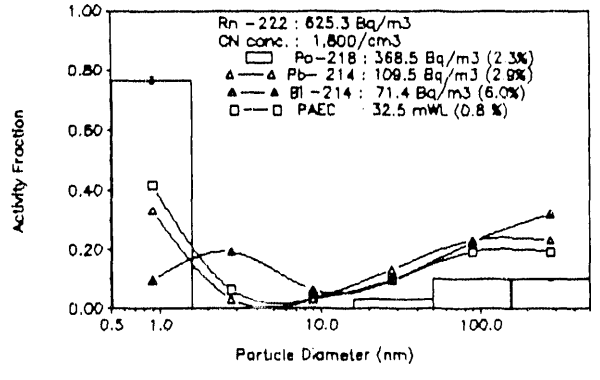

1290645

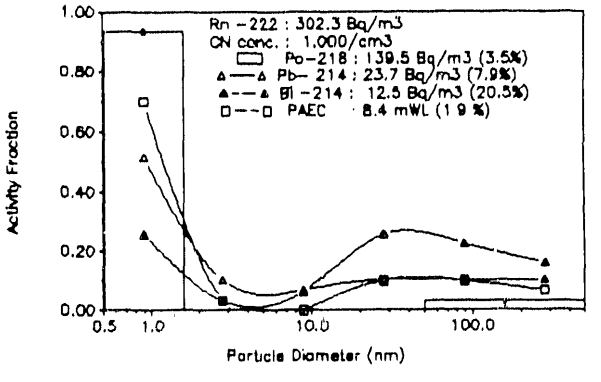

1290838

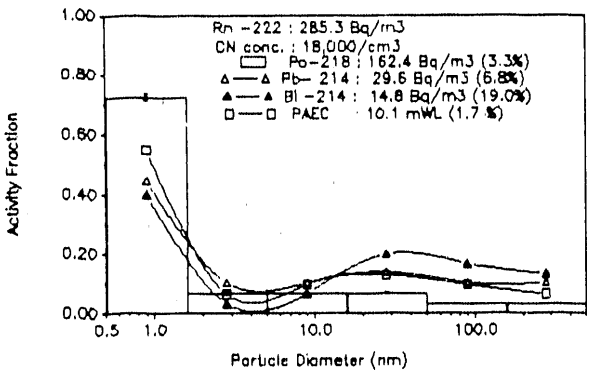

1290954

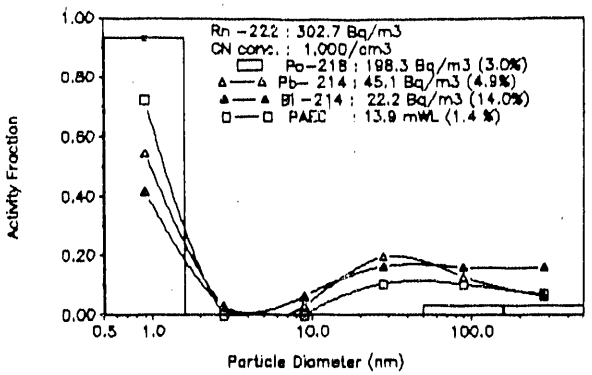

1291111

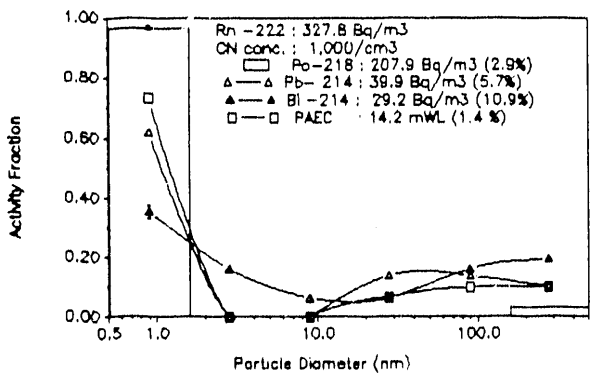

1291538

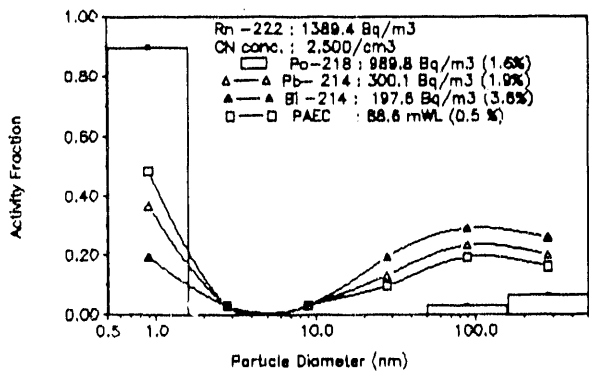

1291713

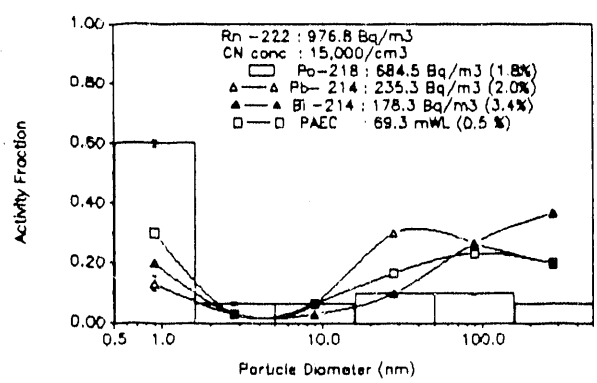

1291830

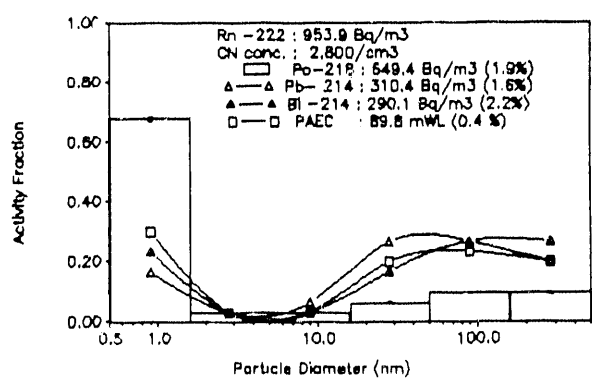

1291946

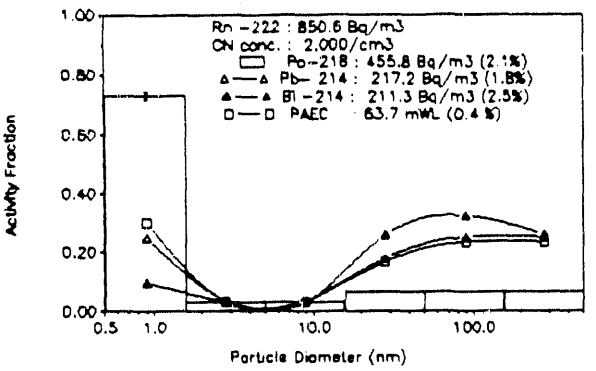

1292209

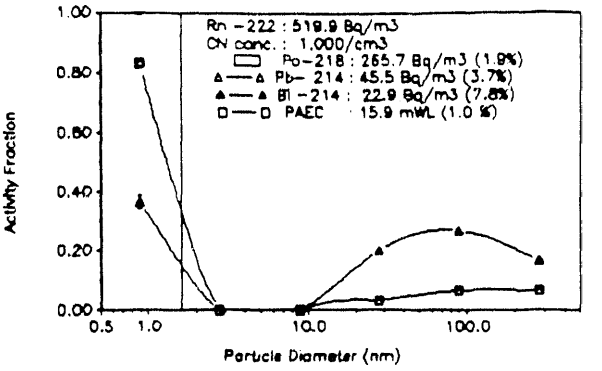

1300010

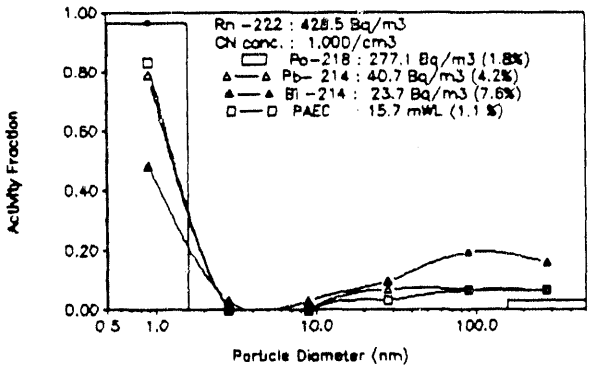

1300211

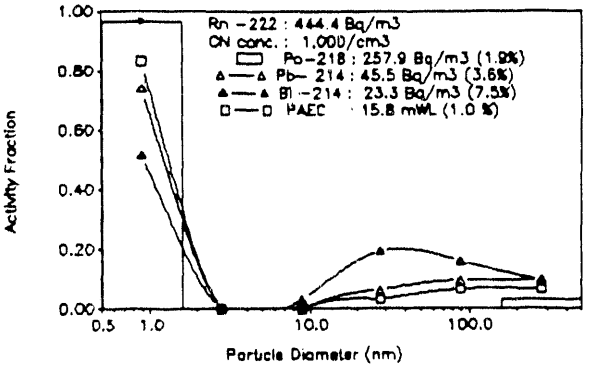

1300413

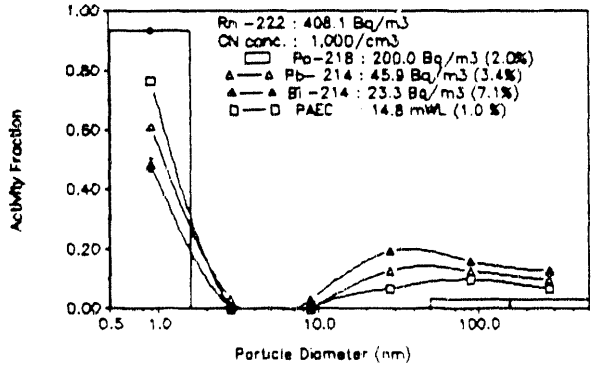

1300605

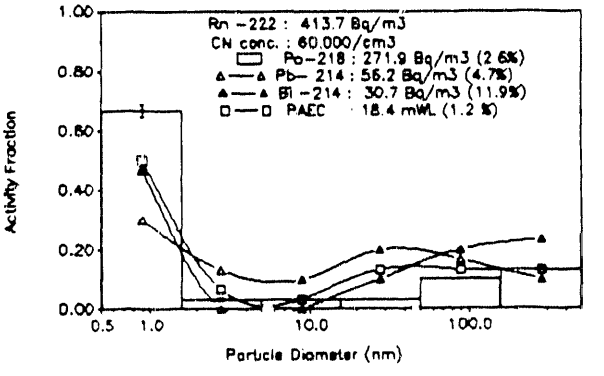

1300722

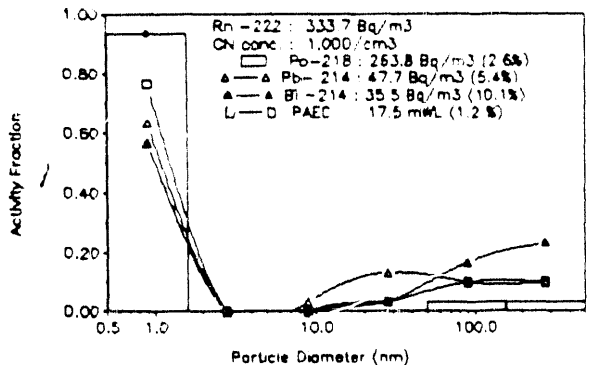

1300839

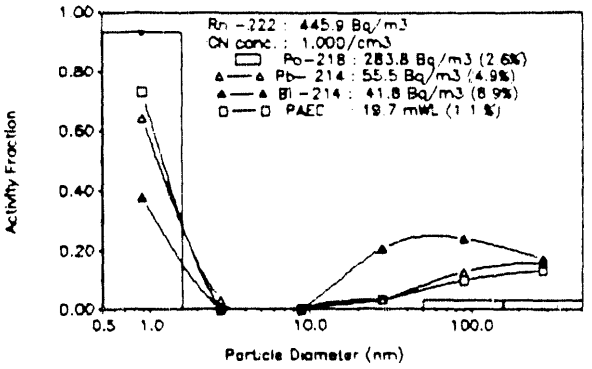

1301259

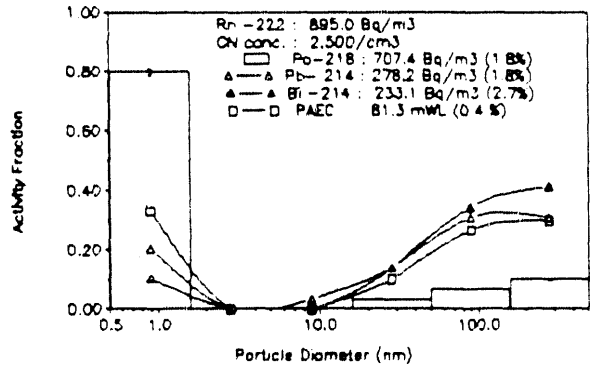

1301423

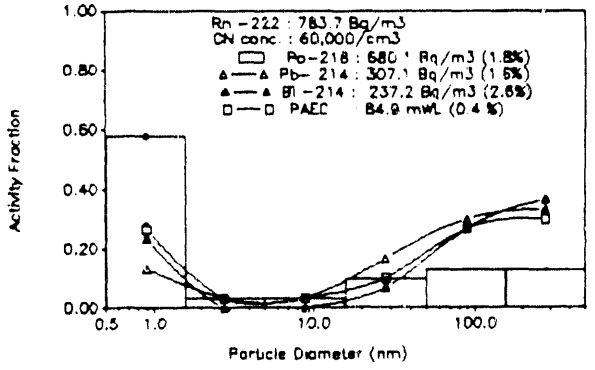

1301540

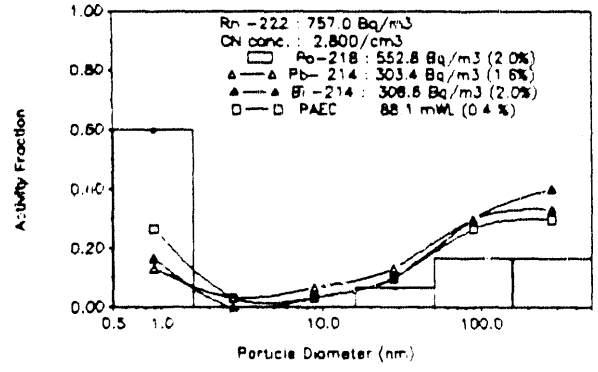

1301657

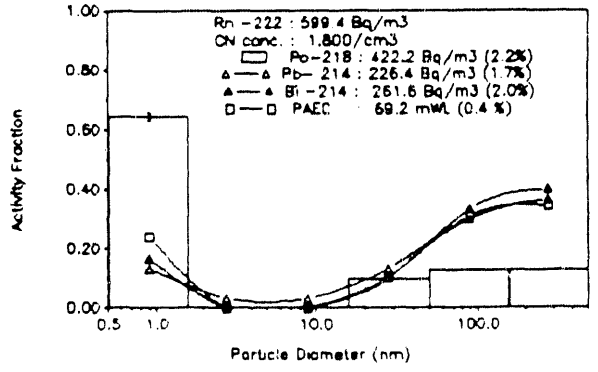

APPENDIX III

THE ACTIVITIES AND MEASUREMENTS IN THE SINGLE-FAMILY HOUSE IN NORTHFORD, CT

(a)March 21

9:02 The sample without the air filtration system (the filter) (3210902)

9:50 Turn on the filter

11:01 The sample before lunch (3211101)

12:30 - 13:30 Lunch

12:40 The sample during the lunch (3211240)

14:35 The sample after lunch (3211435)

16:51 The sample before dinner (3211651)

19:07 The sample before dinner (3211907)

19:15 - 19:45 Dinner preparation

19:45 - 20:20 Dinner time

(b)March 22

9:41 The sample in the morning (3220941)

11:42 The sample during lunch (3221142)

12:00 - 13:20 Lunch

13:42 The sample after lunch (3221342)

16:00 The sample during dinner preparation (3221600)

16:00 - 18:00 Dinner preparation

17:54 The sample after dinner preparation (3221754)

18:30 - 19:10 Dinner time

19:55 The sample after dinner finish (3221955)

(c)March 23

9:10 The sample in the morning (3230910)

11:21 The sample before lunch (3231121)

12:10 - 13:20 Lunch

12:40 - 12:50 Vacuuming

12:52 The sample during lunch and after vacuuming (3231252)

14:23 The sample after vacuuming (3231423)

15:55 The sample before dinner preparation (3231555)

17:30 - 18:20 Dinner preparation

17:55 The sample during dinner preparation (3231755)

18:20 - 18:45 Dinner time

19:41 The sample after dinner time (3231941)

(d)March 26

8:53 The sample in the morning (3260853)

10:30 The sample before vacuuming (3261030)

11:25 - 11:50 Vacuuming

11:50 - 12:40 Clothes washing

12:00 - 12:30 Lunch

12:01 The sample after vacuuming, during clothes washing and lunch (3261201)

13:33 The sample after lunch (3261333)

15:04 The sample before clothes drying (3261504)

16:45 - 17:58 Clothes drying

17:04 The sample during clothes drying (3261704)

18:35 - 18:52 Dinner preparation

18:50 The sample during dinner time (3261850)

18:55 - 19:20 Dinner time

20:36 The sample after dinner (3262036)

(e)March 27

9:22 The sample in the morning (3270922)

11:24 The sample before the lunch (3271124)

11:50 - 12:40 Lunch

13:02 The sample after lunch (3271302)

14:53 The sample in the afternoon (3271453)

16:44 The sample in the afternoon (3271644)

18:35 The sample before dinner preparation (3271835)

19:45 - 20:05 Dinner preparation

20:05 - 20:40 Dinner time

20:26 The sample during dinner time (3272026)

(f)March 28

8:55 The sample with the filter (3280855)

9:25 Turn off the filter

10:27 The sample without the filter (3281027)

11:50 - 12:40 Lunch

12:31 The sample during the lunch (3281231)

14:22 The sample after lunch (3281422)

16:13 The sample before candle burning (3281613)

18:28 The sample during the candle burning (3281828)

18:30 - 19:00 Candle burning for birthday party

18:30 - 21:30 Dinner time

(g)March 29

9:28 The sample in the morning (3290928)

11:06 The sample before lunch (3291106)

11:40 - 12:10 Dish washing and lunch

12:52 The sample after lunch (3291252)

15:10 The sample in the afternoon (3291510)

17:30 Dine out

18:01 The sample in the evening (3291801)

19:53 The sample at night (3291953)

(h)March 30

9:13 The sample before clothes washing (3300913)

9:55 - 10:45 Clothes washing

10:46 The sample after clothes washing and during clothes drying (3301046)

10:45 - 11:45 Clothes drying

12:18 The sample after clothes drying and during lunch (3301218)

12:20 -12:50 Lunch

13:52 The sample after lunch (3301352)

15:43 The sample before dinner cooking (3301543)

17:40 - 18:20 Dinner preparation

17:57 The sample during dinner preparation (3301757)

19:30 - 20:05 Dinner time

19:48 The sample during the dinner time (3301948)

(i)April 3

9:06 The sample in the morning (4030906)

10:47 The sample before lunch (4031047)

12:29 The sample during lunch (4031229)

12:30 - 13:40 Lunch

14:06 Cook hot soup

14:10 The sample during cooking the hot soup (4031410)

(j)April 4

8:58 The sample in the morning (4040858)

12:05 - 12:16 Vacuuming

12:27 The sample after vacuuming (4041227)

12:30 - 13:10 Lunch

14:28 The sample after lunch (4041428)

16:25 The sample during the first cooking (4041625)

16:35 - 16:45 The first cooking

18:26 The sample during the second cooking (4041826)

18:30 - 19:05 The second cooking

19:10 - 19:30 Dinner time

20:27 The sample after dinner (4042027)

(k)April 5

8:50 The sample in the morning without air cleaner (4050850)

9:00 - 9:10 Cooking potato

9:20 Turn on the electronic air cleaner (E P)

10:41 The sample after cooking and with ESP on (4051041)

12:33 The sample during lunch (4051233)

12:40 - 12:55 Lunch with four-minute cooking

14:24 The sample after cooking (4051424)

16:28 The sample before dinner preparation (4051628)

18:30 The sample during the dinner preparation (4051830)

18:30 - 19:00 Dinner preparation

19:00 - 19:40 Dinner time

20:31 The sample after dinner (4052031)

(l)April 6

9:07 The sample in the morning (4060907)

10:58 The sample during the lunch (4061058)

11:00 - 11:30 Lunch

12:50 The sample after lunch (4061250)

14:41 The sample in the afternoon (4061441)

17:58 The sample before dinner preparation (4061758)

19:05 - 19:35 Dinner preparation

19:35 - 19:55 Dinner time

19:59 The sample after dinner (4061959)

(m)April 9

8:44 The sample in the morning (4090844)

10:15 - 10:35 Dish washing and cooking

10:53 The sample before opening kitchen door (4091053)

11:30 - 11:50 Opening kitchen door

12:20 -13:00 Lunch

12:24 The sample during the lunch (4091224)

15:04 The sample after the lunch (4091504)

16:46 The sample in the afternoon (4091646)

18:27 The sample before dinner cooking (4091827)

19:02 - 19:30 Dinner cooking

19:30 - 20:00 Dinner time

20:08 The sample after dinner (4092008)

(n)April 10

9:02 The sample in the morning (4100902)

10:20 - 10:50 Clothes washing

10:34 The sample during the clothes washing (4101034)

10:55 - 11:50 Clothes drying

12:05 - 12:25 Lunch

12:41 The sample after clothes drying and lunch (4101241)

14:33 The sample in the afternoon (4101433)

16:24 The sample before dinner cooking (4101624)

18:05 - 18:50 Dinner cooking

18:15 The sample during the cooking (4101815)

19:05 - 19:45 Dinner time

20:07 The sample after dinner (4102007)

(o)April 11

8:48 The sample in the morning (4110848)

10:20 The sample before lunch (4101020)

12:10 - 12:40 Lunch

13:10 - 13:20 Vacuuming

13:20 The sample after vacuuming (4111320)

15:01 The sample before dinner preparation (4111501)

16:40 - 17:40 Dinner cooking

16:43 The sample during the cooking (4111643)

18:24 The sample after cooking (4111824)

19:30 - 20:15 Dinner time

20:05 The sample after dinner (4112005)

(p)April 12

9:27 The sample with ESP (4120927)

10:00 Turn ESP off

10:59 The sample after ESP off (4121059)

12:31 The sample without ESP (4121231)

3210902

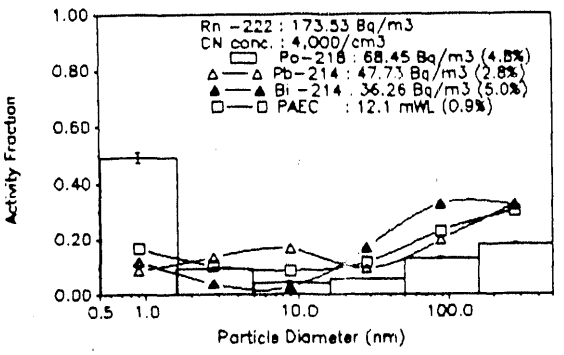

3211101

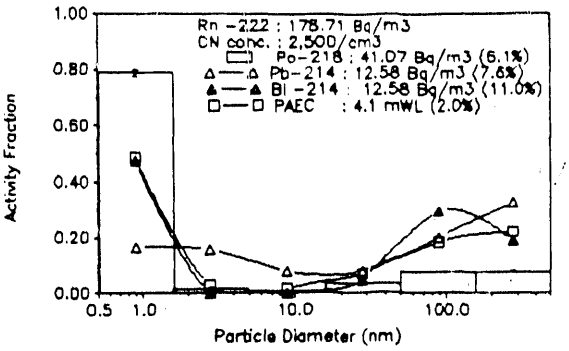

3211240

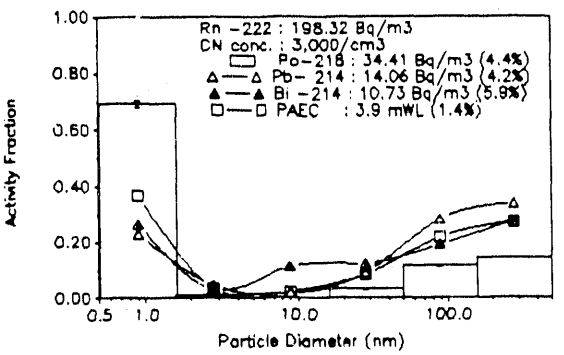

3211435

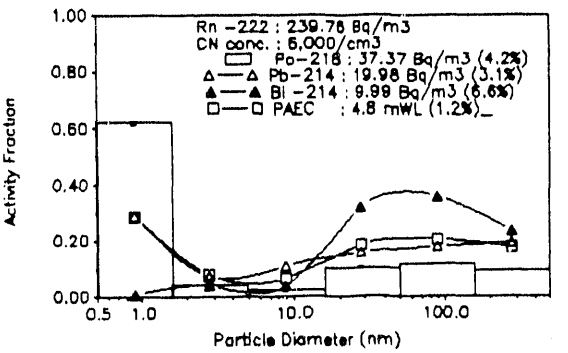

3211651

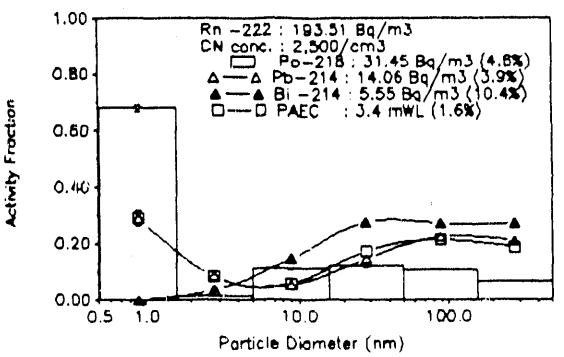

3211907

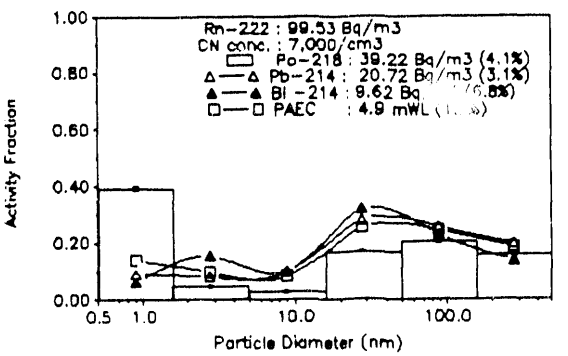

3220941

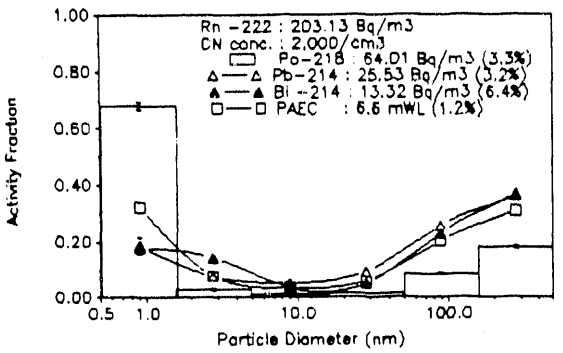

3221142

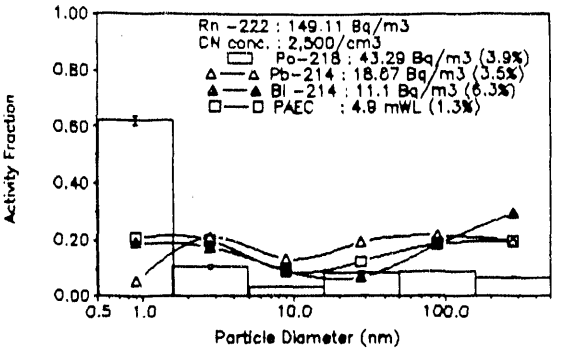

3221342

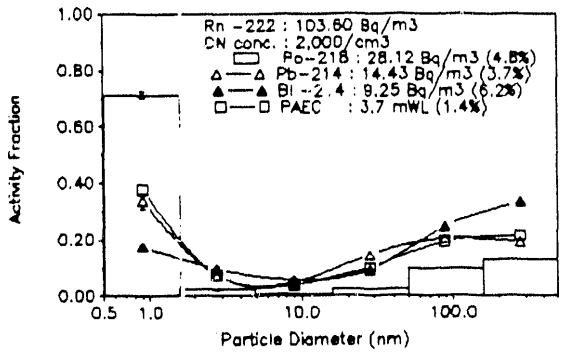

3221600

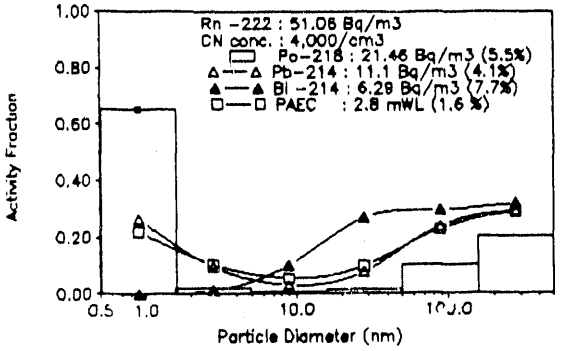

3221754

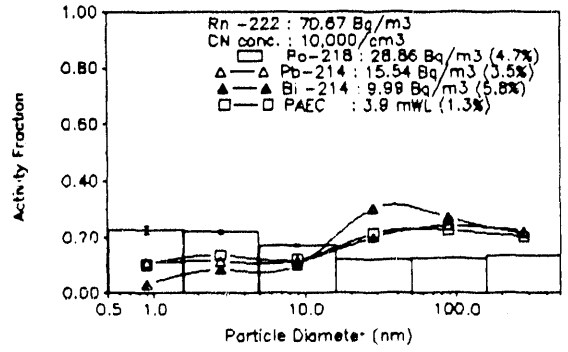

3221955

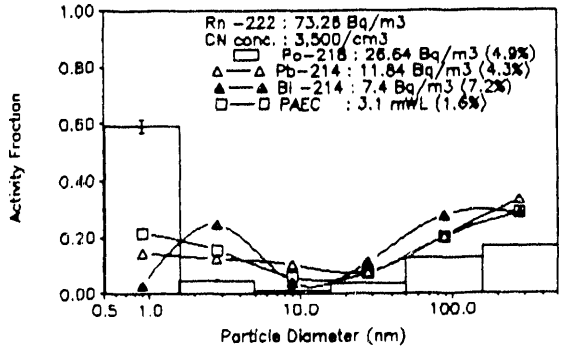

3230910

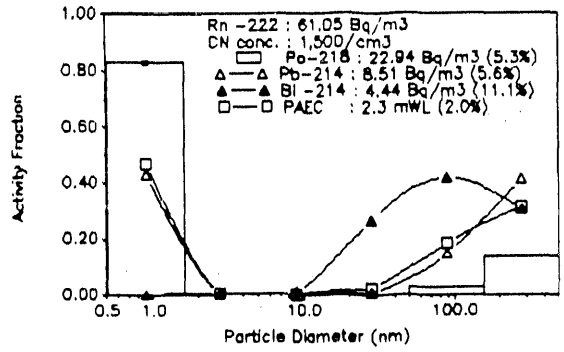

3231121

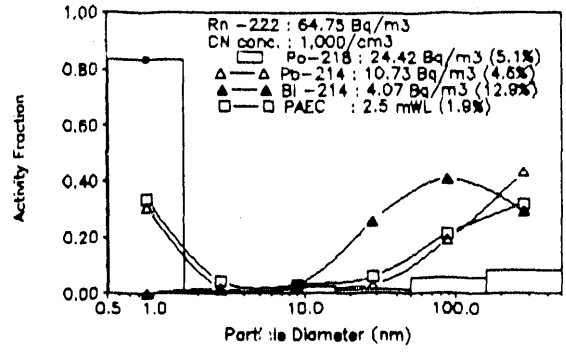

3231252

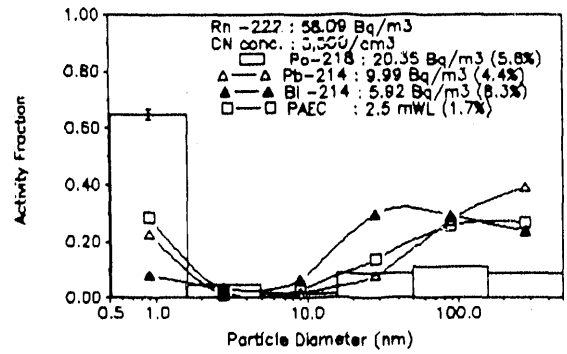

3231423

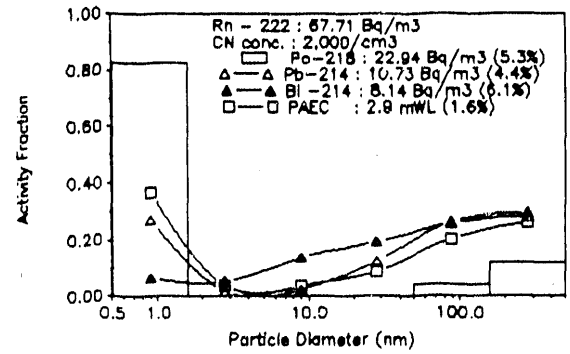

3231555

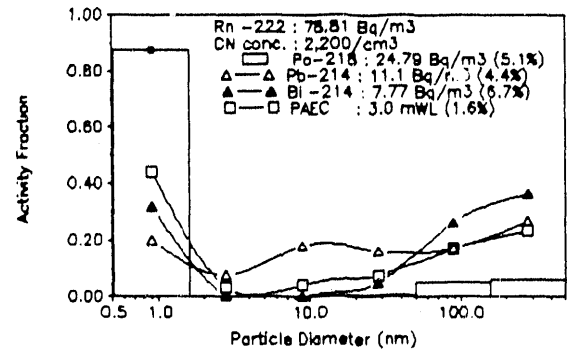

3231755

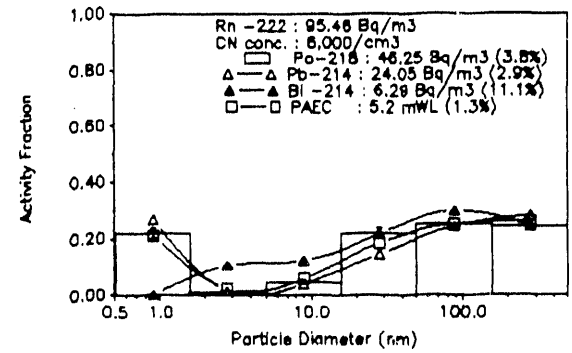

3231941

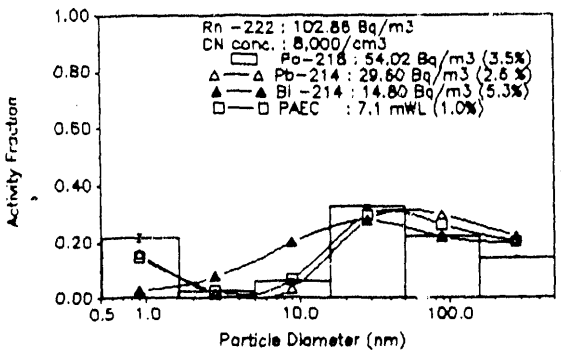

3260853

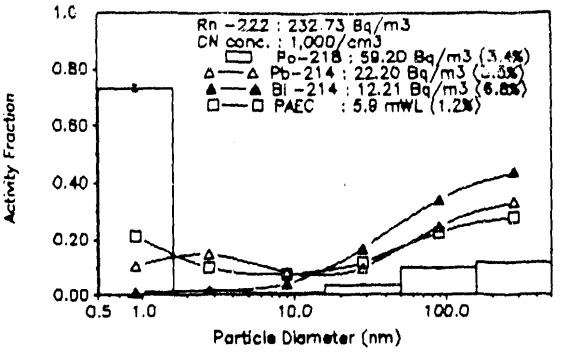

3261030

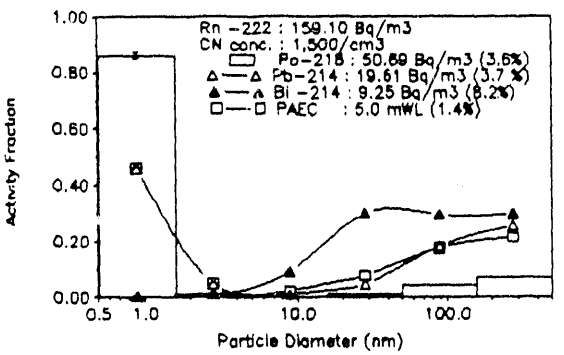

3261201

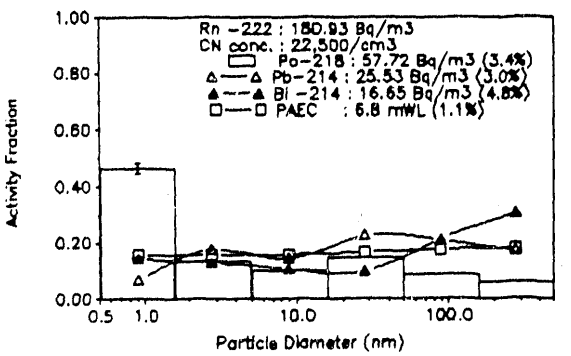

3261333

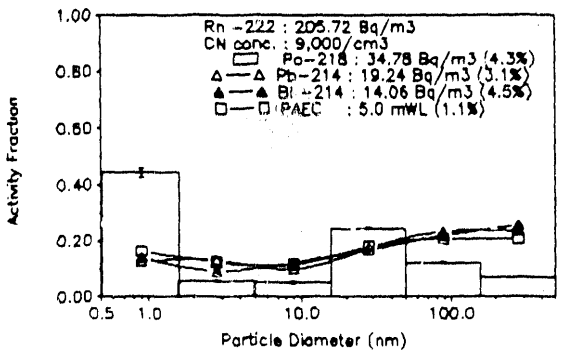

3261504

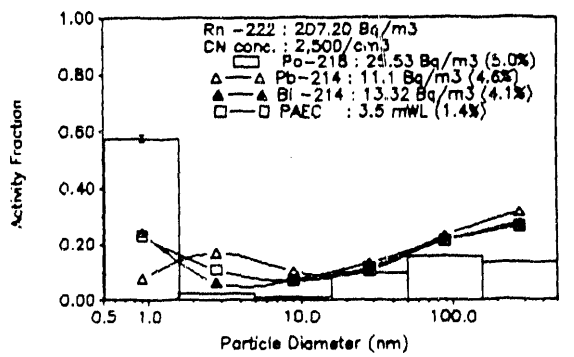

3261704

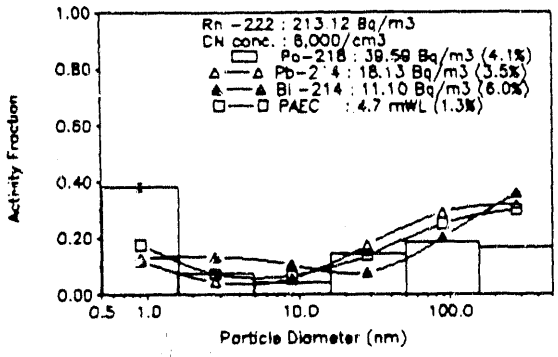

3261850

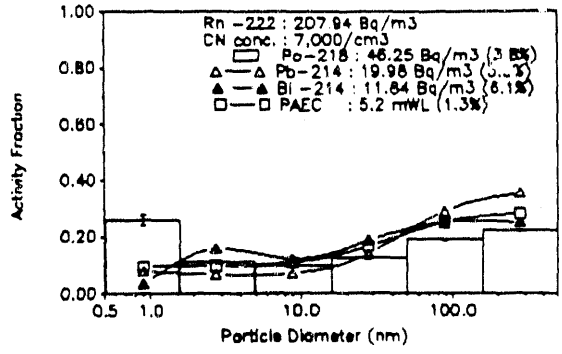

3262036

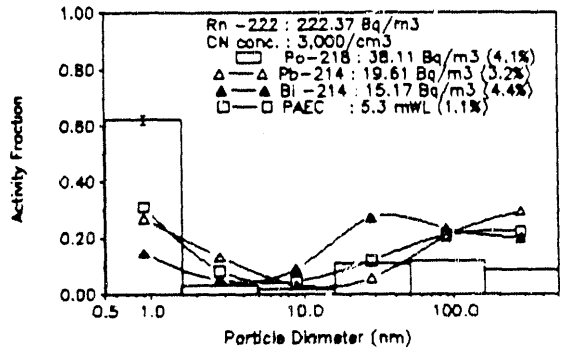

3270922

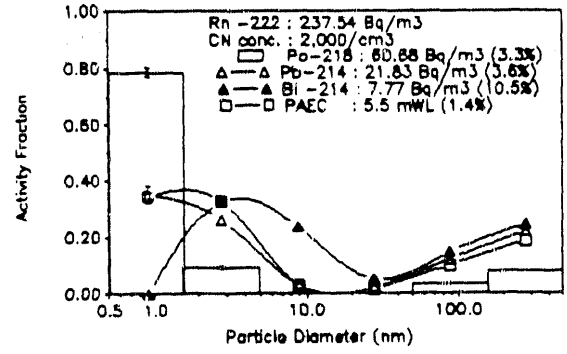

3271124

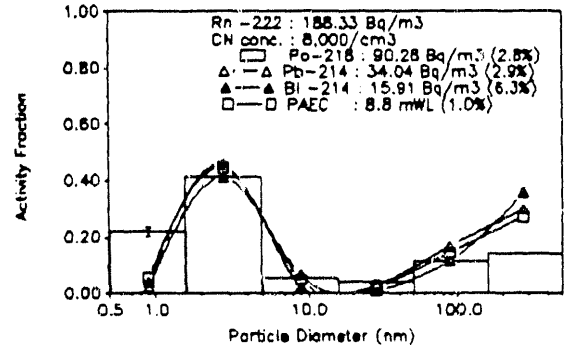

3271302

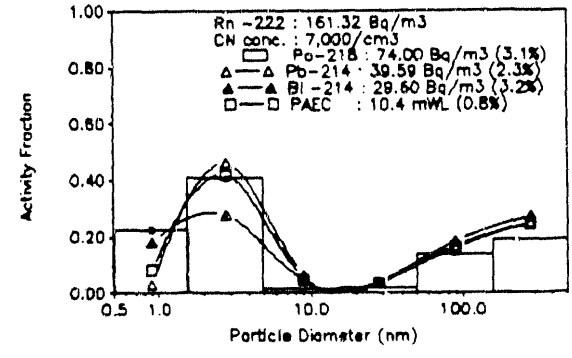

3271453

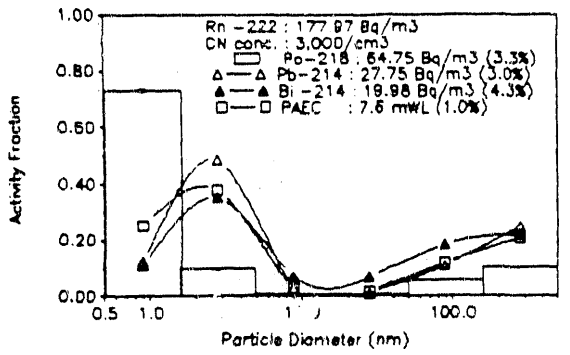

3271644

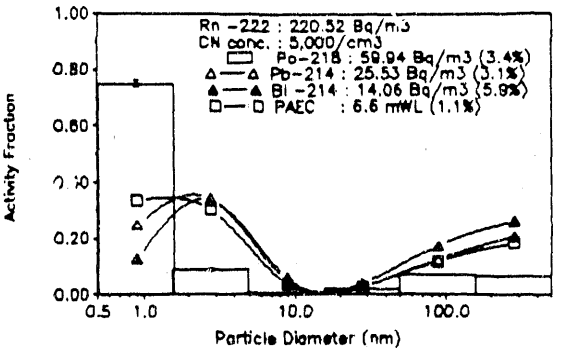

3271835

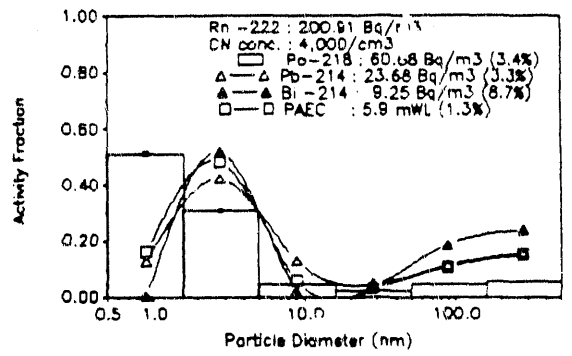

3272026

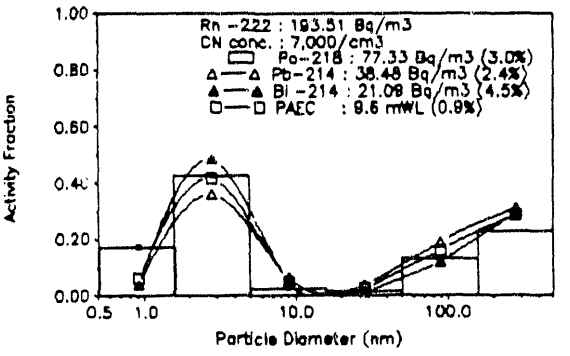

3280855

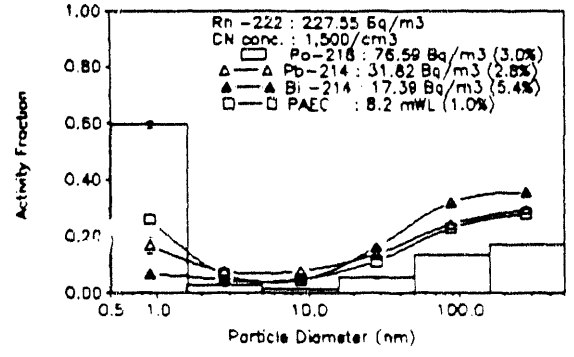

3281027

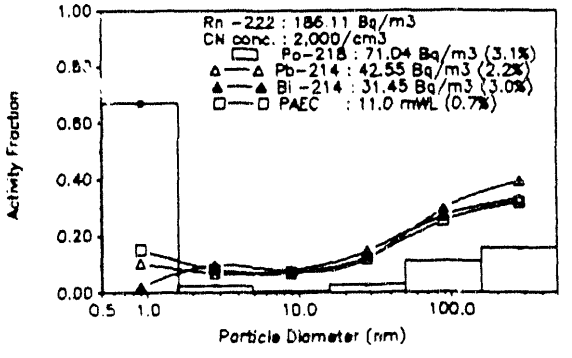

3281231

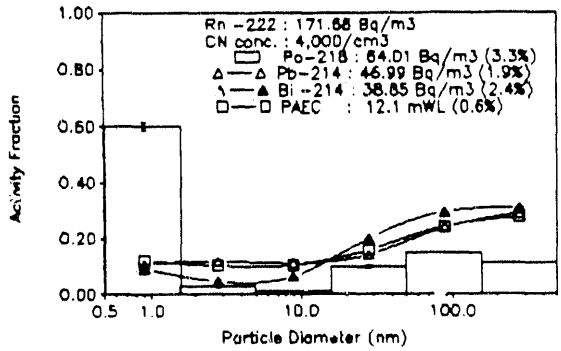

3281422

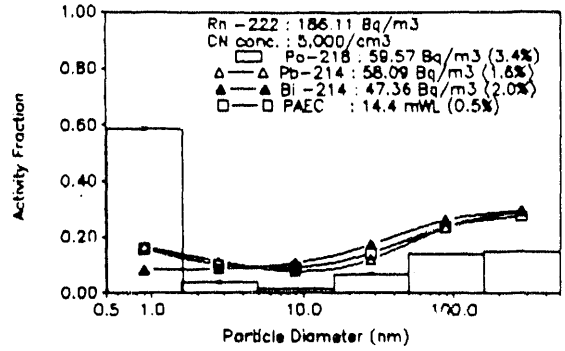

3281613

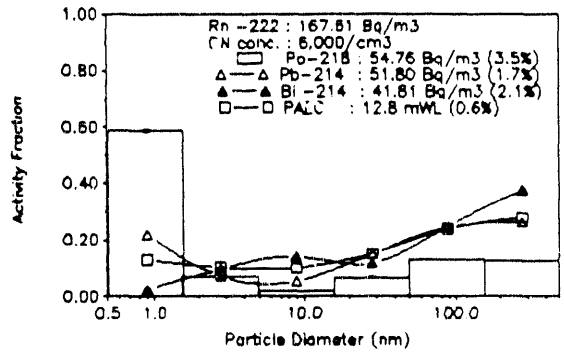

3281828

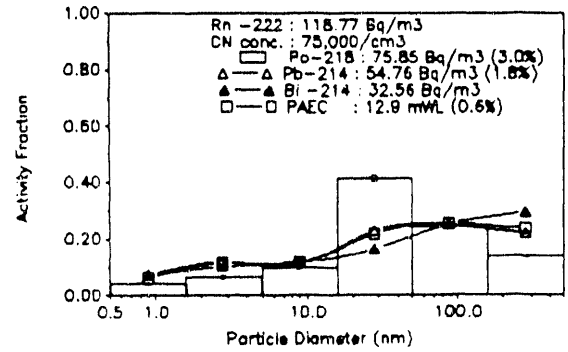

3290928

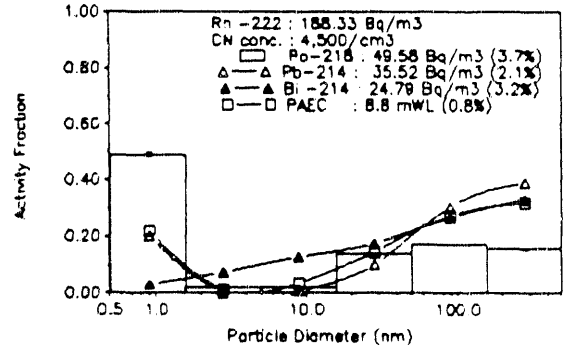

3291106

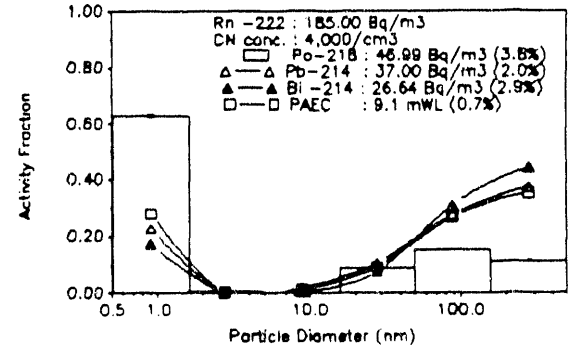

3291252

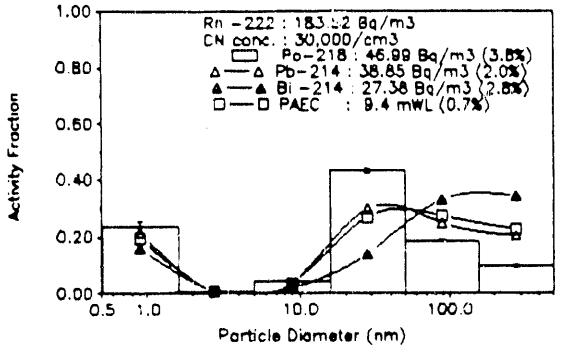

3291510

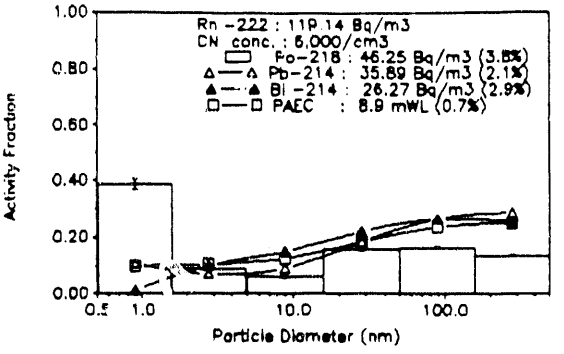

3291801

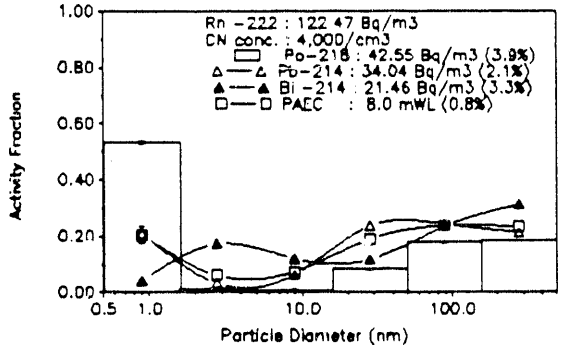

3291953

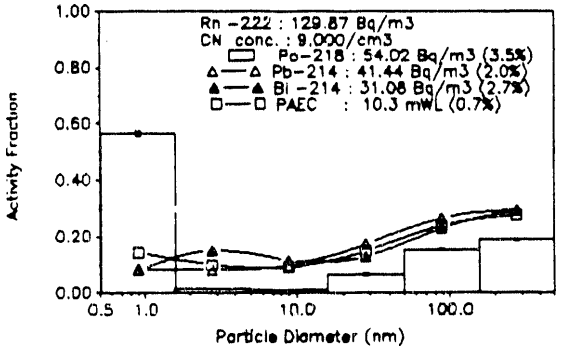

3300913

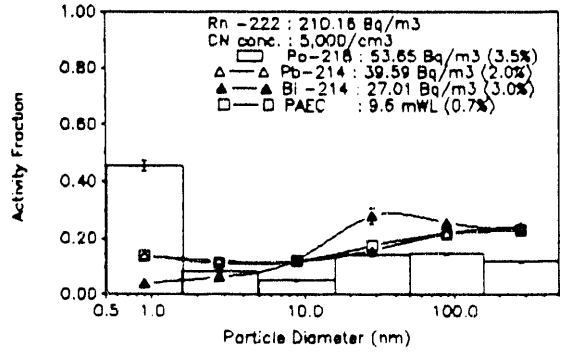

3301046

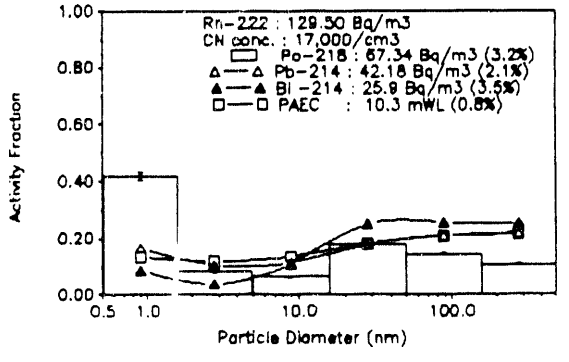

3301218

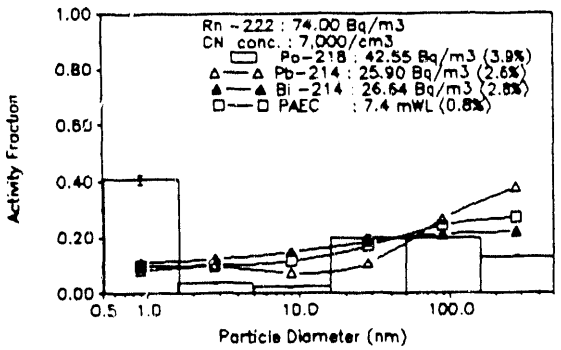

3301352

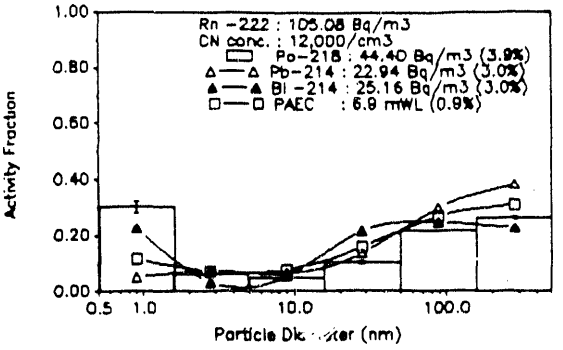

3301543

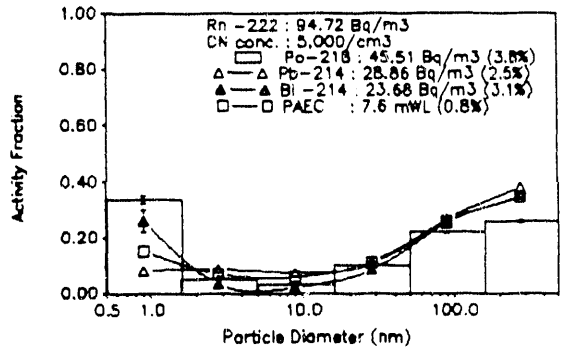

3301757

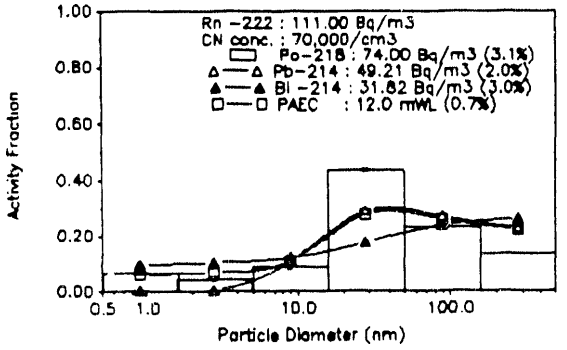

3301948

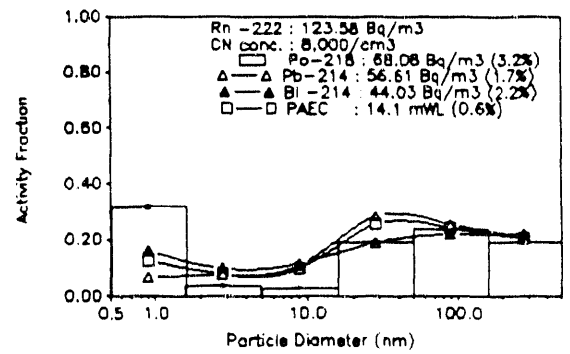

4030906

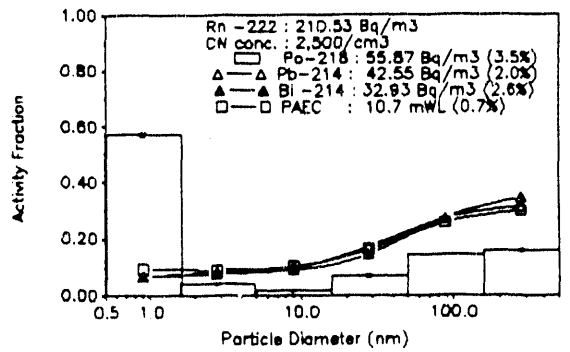

4031047

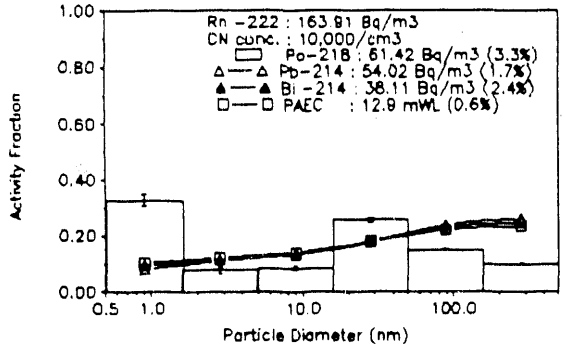

4031229

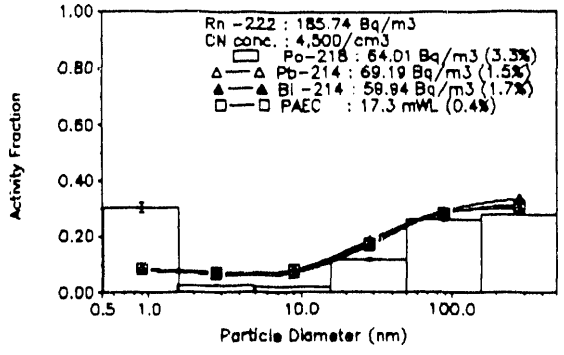

4031410

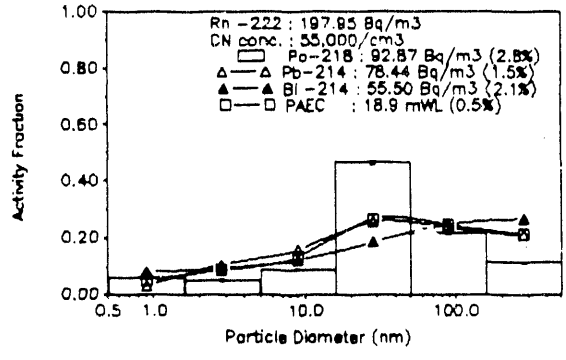

4040858

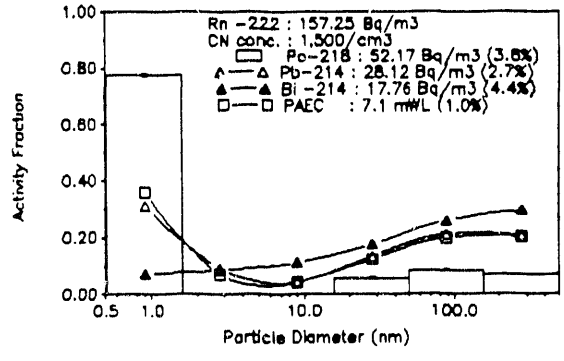

4041227

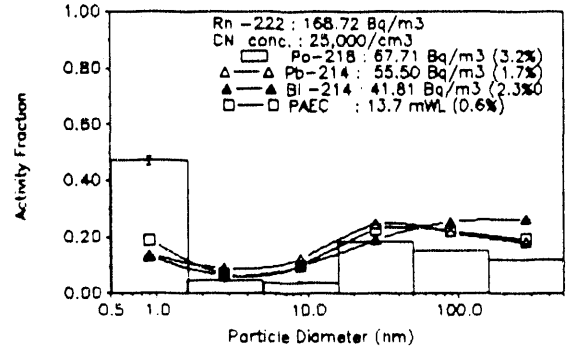

4041428

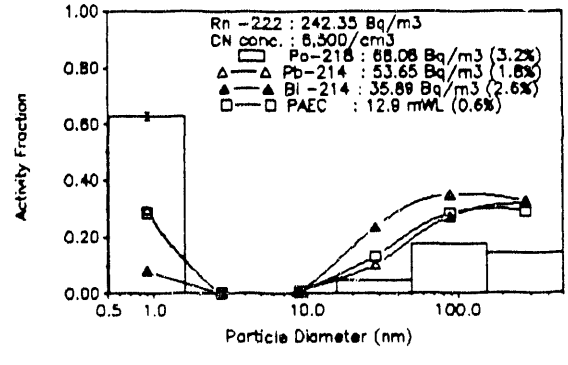

4041625

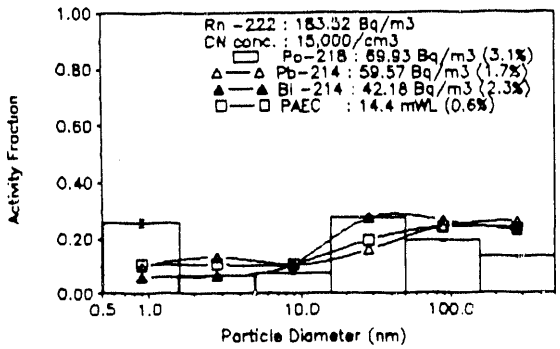

4041826

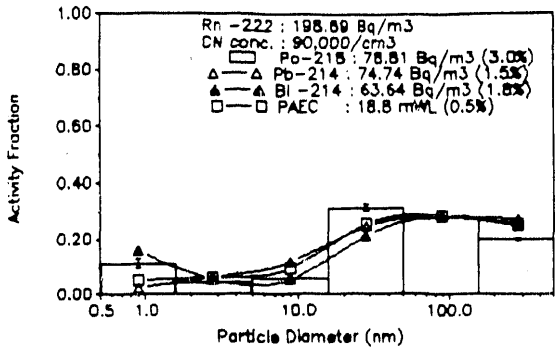

4042027

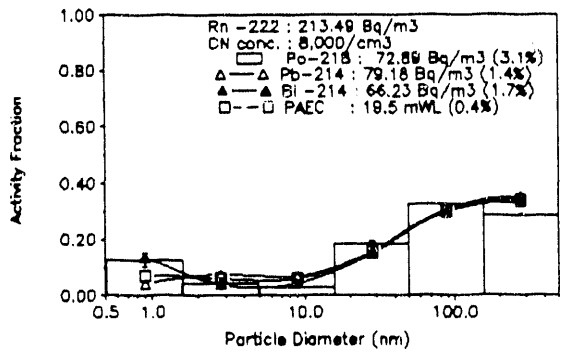

4050850

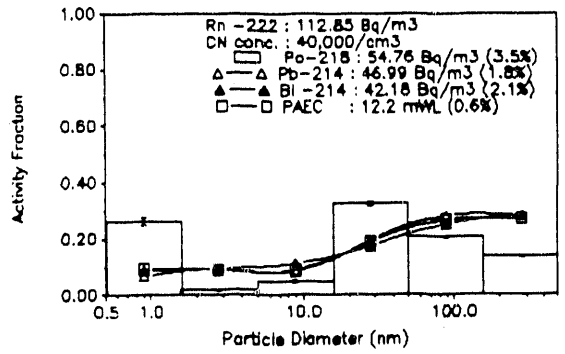

4051041

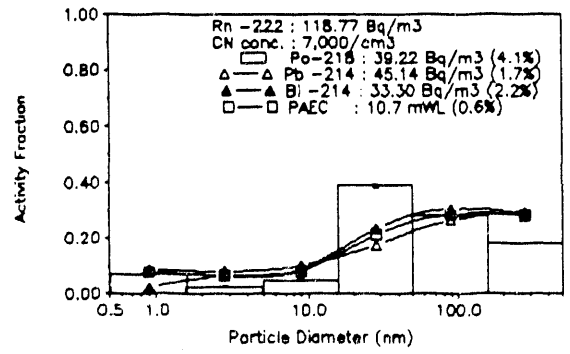

4051233

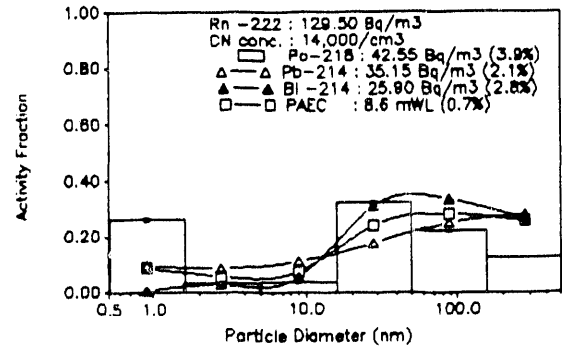

4051424

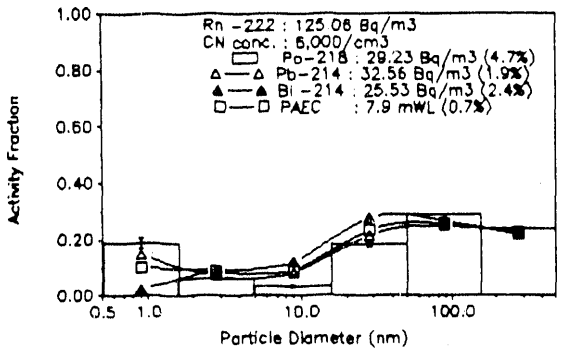

4051628

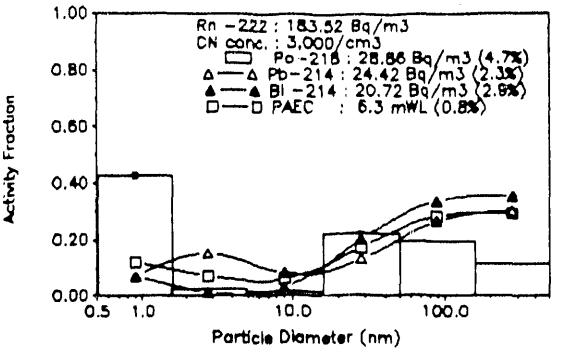

4051830

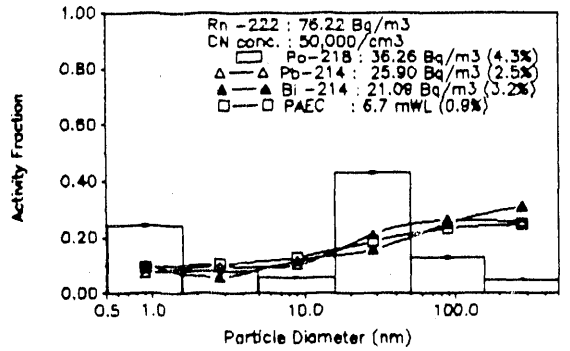

4052031

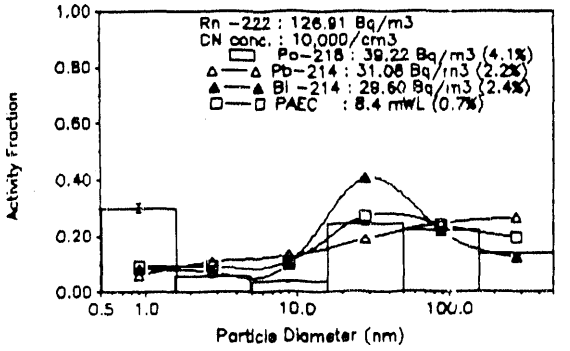

4060907

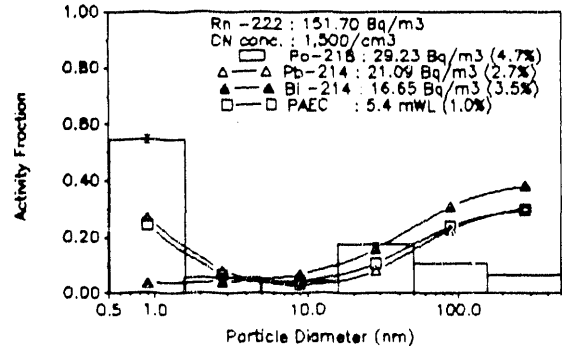

4061058

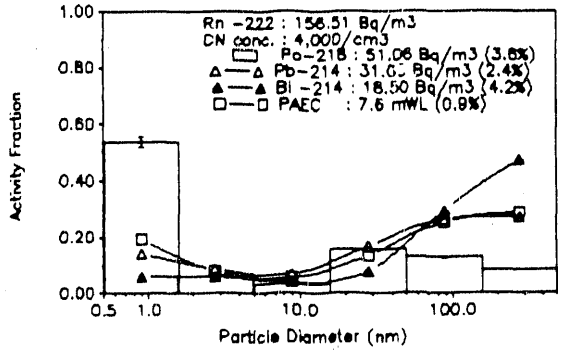

4061250

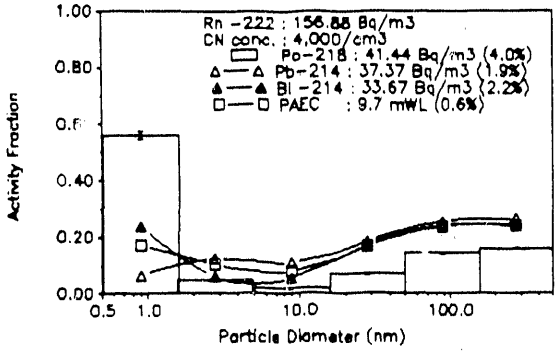

4061441

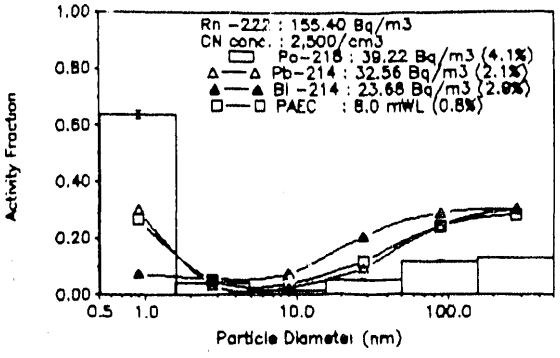

4061758

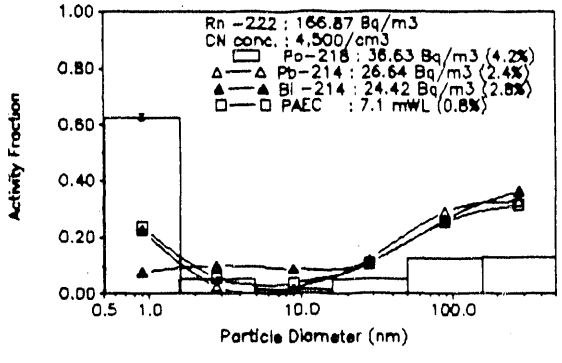

4061959

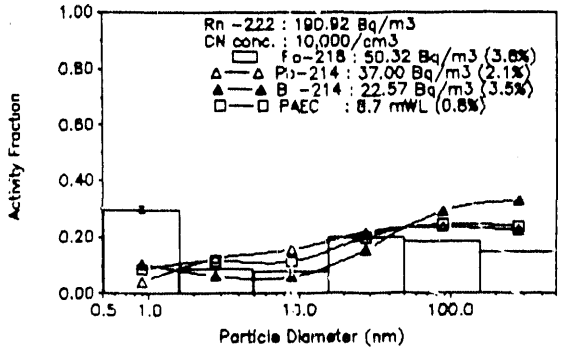

4090844

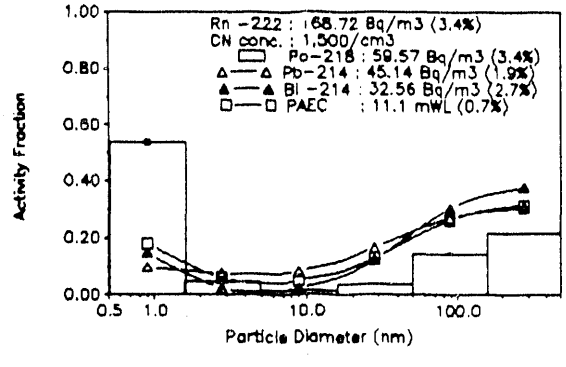

4091053

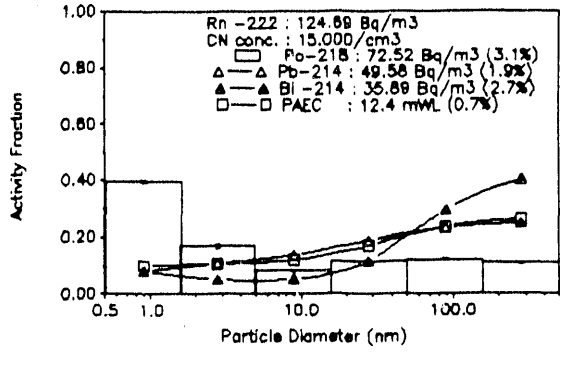

4091224

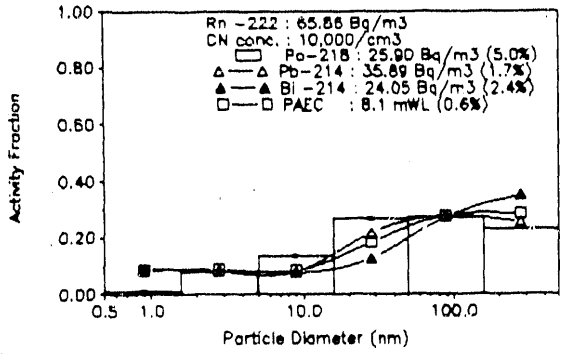

4091504

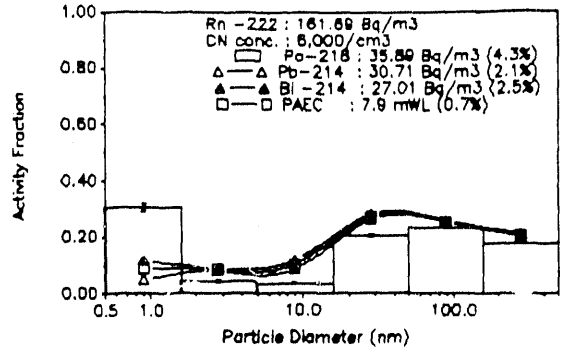

4091646

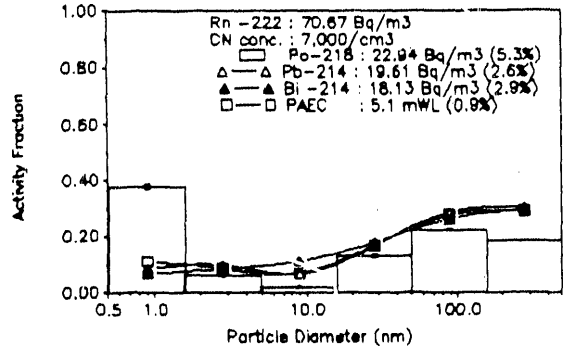

4091827

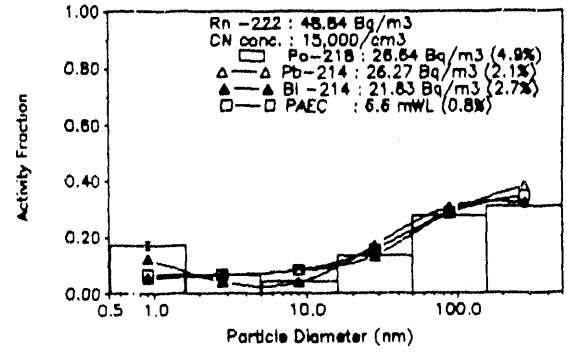

4092008

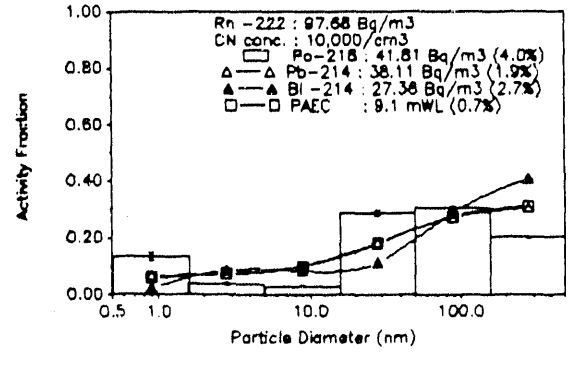

4100902

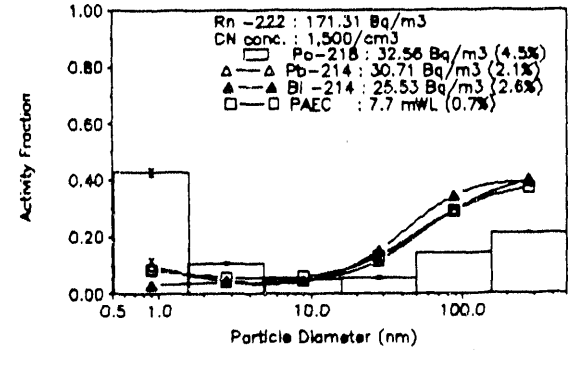

4101034

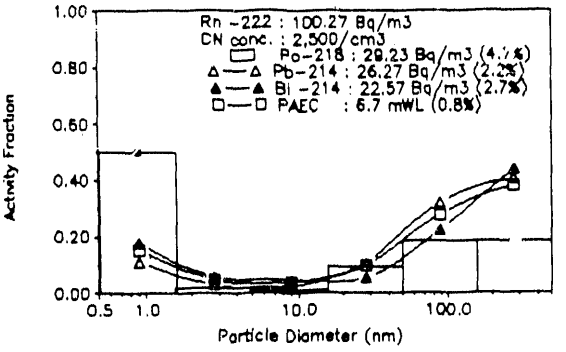

4101241

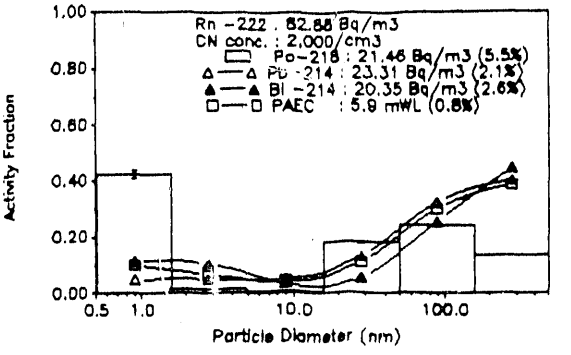

4101433

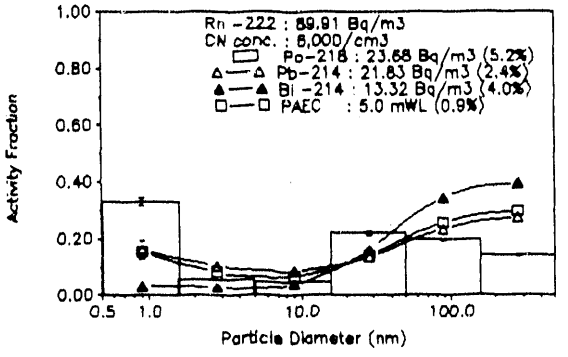

4101624

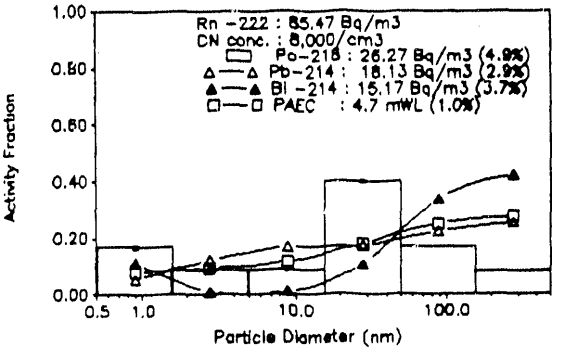

4101815

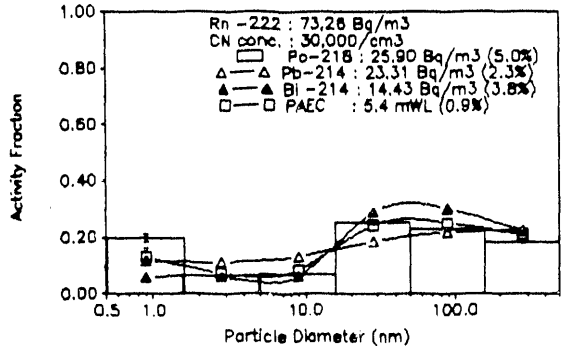

4102007

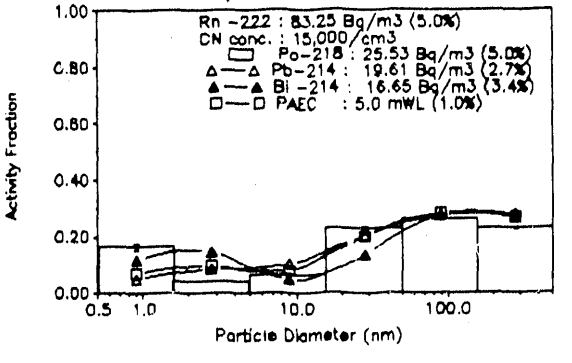

4110848

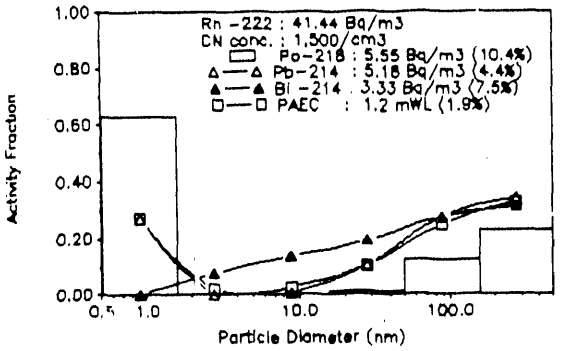

4111020

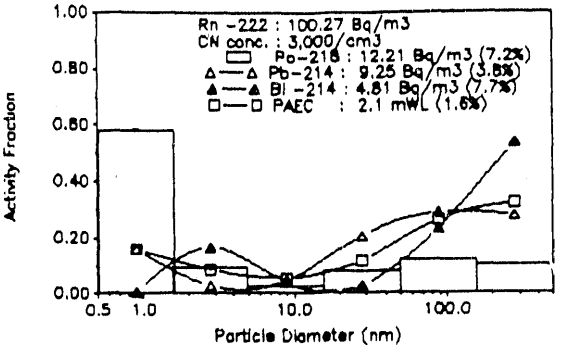

4111320

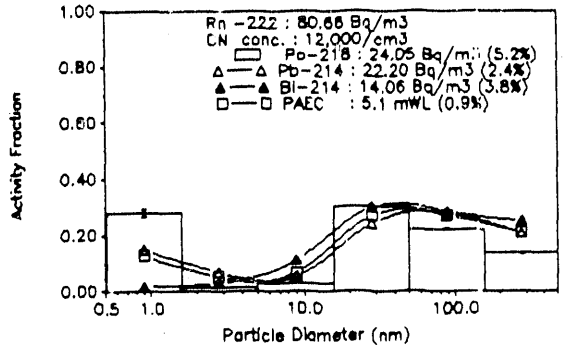

4111501

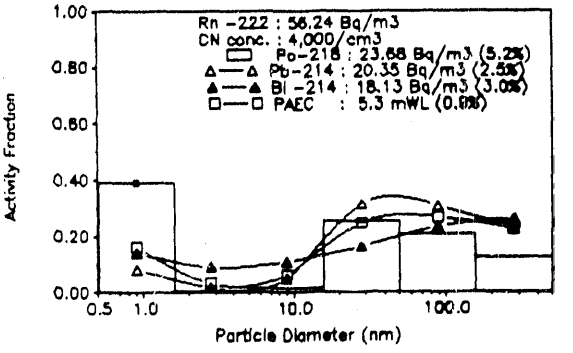

4111643

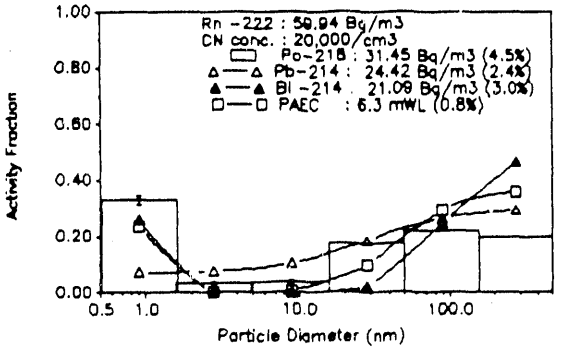

4111824

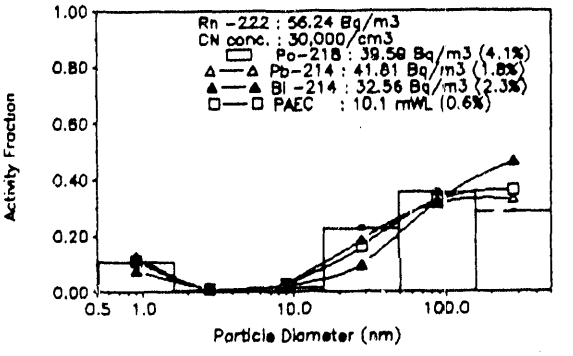

4112005

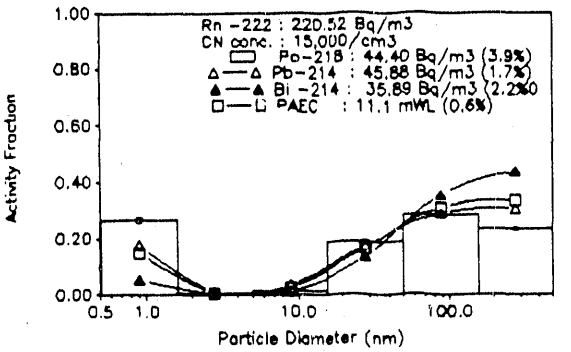

4120927

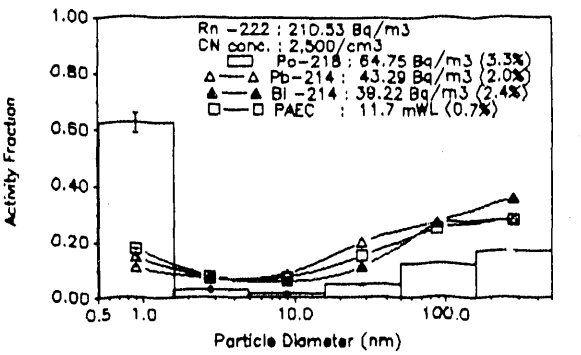

4121059

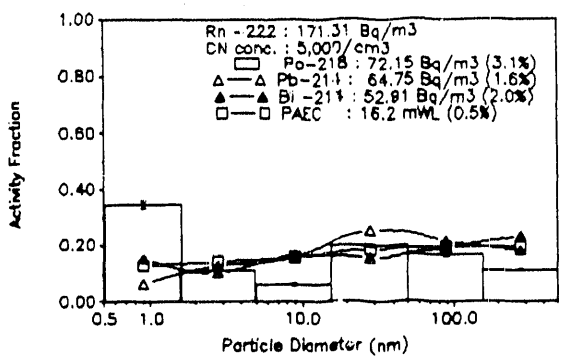

4121231

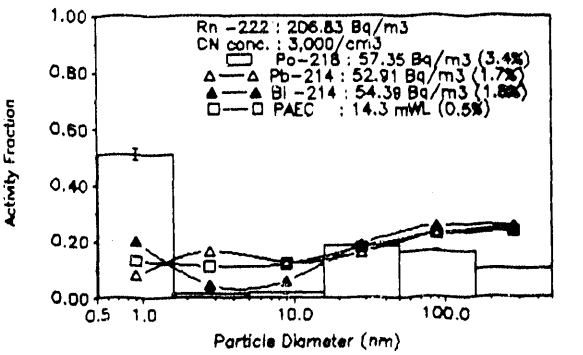

VITA

Chih-Shan Li was born on [redacted]

She received her Bachelor of Science degree in the Department of Chemical Engineering, National Taiwan University, Taipei, Taiwan in 1985. In the same year, she attended the Graduate School of Environmental Engineering at National Taiwan University and worked as a research assistant. She received her Master of Science degree from National Taiwan University in May 1987. She continued her graduate studies in Environmental Engineering in Civil Engineering program of the University of Illinois at Urbana-Champaign in August 1987, specializing in the Air Pollution area. From 1987 to 1989 she served as a research assistant for the Department of Civil Engineering and the University of Illinois Institute for Environmental Studies. In July 1989, she transferred to Clarkson University, Potsdam, NY. During her off-campus research in Potsdam, she performed field measurements in Princeton, NJ, Springfield, PA, and Northford, CT. Her immediate plan following graduation is to work in indoor air quality and environmental health as a post-doctoral research associate at John B. Pierce Foundation Laboratory, Center for the Health and the Environment, at Yale University School of Medicine.

END

DATE FILMED

12/31/90